# Testing Gravity with Black Holes


Oliver James Tattersall

St Peter's College

University of Oxford

A thesis submitted for the degree of

*Doctor of Philosophy*

Trinity 2019

# Abstract

## Testing Gravity with Black Holes

**Oliver J. Tattersall**

St Peter's College, University of Oxford

*Submitted for the degree of Doctor of Philosophy*
Trinity Term, 2019

In this thesis, I study the ways in which modified theories of gravity might be tested for using black holes. In particular, I focus on ways in which the gravitational waves emitted during the 'ringdown' of a perturbed black hole may be affected.

I will develop and demonstrate the use of a framework for analysing the evolution of perturbations in arbitrary modified gravity theories in both cosmological and black hole backgrounds. I will use this to show that the characteristic Quasi-normal mode (QNM) spectrum of frequencies for the gravitational waves emitted from a perturbed black hole may be altered even in the case that the background black hole is identical to a general relativistic black hole. This is purely due to the presence, and coupling to, additional gravitational degrees of freedom.

I will also explore the landscape of hairy black hole solutions in the wake of the multi-messenger observation of GW/GRB170817, and show that it is increasingly difficult to endow a black hole with scalar hair in modified gravity given the constraint that gravitational waves must propagate at the speed of light.

In addition, black hole perturbations in General Relativity are analysed, with analytic expressions for QNM frequencies calculated for scalar, vector, and gravitational perturbations to a slowly rotating Kerr-(Anti-)de Sitter black hole.

Finally, I will examine the specific case of black hole perturbations in Horndeski theory, demonstrating the qualitative difference in gravitational wave emission from a perturbed black hole in General Relativity and in Horndeski gravity. I will also forecast the detectability of such a modified gravitational wave signal, and estimate what constraints one might be able to place on fundamental parameters of Horndeski gravity through gravitational wave observations.

# Acknowledgements

First and foremost I would like to thank my supervisor, Pedro Ferreira, for his constant support and encouragement throughout the course of my DPhil. I could not have succeeded in Oxford without his enthusiasm and ambition for myself and my research.

I would also like to acknowledge the wider Oxford Astrophysics community for enjoyable and enlightening conversations throughout the past three years. In particular, I am thankful to Macarena Lagos for her help and collaboration when I was just starting my studies, and to the rest of the Cosmology group for their input over the years, and for welcoming me at Oxford.

My DPhil has taken me away from Oxford from time to time, and I would like to thank Professors Alessandra Buonanno and Emanuele Berti for hosting me for significant visits at the Albert Einstein Institute and at Johns Hopkins University respectively.

My time at Oxford would not have been nearly as fun without the friends I made here. To Oly, Jane, Dom, Carole, Fran, Nat, and to everyone else that made life in Oxford so memorable, thanks for all the great times.

To Ryan, Addie, Nick, Ellen, Lily, Nicky D, and to the countless others in London and farther afield that I've been lucky to call friends for years, thanks for everything. I can't wait for whatever comes next for us all.

I of course owe a huge debt to my family: my parents Andrew and Kathryn, my brother David, and sister-in-law Jen. I am eternally grateful for their unwavering love and support in all areas of my life, and for their encouragement in my pursuing a DPhil.

Finally, to Megan, to whom I owe everything. I never could have done this without you, nor would I have wanted to.

# Statement of Originality

I hereby declare that no part of this thesis has been submitted in support of another degree, diploma, or other qualification at the University of Oxford or other higher learning institute. The work in this thesis is based on material from the following publications, completed during the course of my time studying at the University of Oxford:

1. O. J. Tattersall, M. Lagos, P. G. Ferreira, *Phys. Rev. D* **96**, 064011 (2017)
2. O. J. Tattersall, P. G. Ferreira, M. Lagos, *Phys. Rev. D* **97**, 044021 (2018)
3. O. J. Tattersall, P. G. Ferreira, M. Lagos, *Phys. Rev. D* **97**, 084005 (2018)
4. O. J. Tattersall, P. G. Ferreira, *Phys. Rev. D* **97**, 104047 (2018)
5. O. J. Tattersall, *Phys. Rev. D* **98**, 104013 (2018)
6. O. J. Tattersall, P. G. Ferreira, *Phys. Rev. D* **99**, 104082 (2019)

I certify that the work in this thesis is entirely my own, with the following exceptions and clarifications:

**Chapter 2** is based on Paper 1, with the original draft of the paper prepared by me, and with subsequent editing by ML and PGF.

**Chapter 3** is based on Paper 2, with the original draft of the paper prepared by me, and with subsequent editing by ML and PGF.

**Chapter 4** is based on Paper 3, with the section focussing on Scalar-Tensor theories prepared by me, whilst the section focusing on other theories was shared by myself, PGF, and ML.

**Chapter 5** is based on Paper 5, which was entirely prepared by myself.

**Chapter 6** is based on Papers 4 and 6, with the original drafts prepared by me, and with subsequent editing by PGF.

# Contents

# Introduction

*"If one cannot see gravitation acting here, he has no soul"*

— Richard Feynman, *The Feynman Lectures on Physics*

## 1.1 Einstein's Theory

The phenomenon of gravity has captivated the minds and souls of physicists for centuries, including that of Richard Feynman as he remarked on "one of the most beautiful things in the sky - a globular star cluster" whilst teaching undergraduates [1]. From Isaac Newton's formulation of the inverse square law for the gravitational force [2], to the direct imaging of the shadow[1] of the black hole at the centre of M87 by the Event Horizon Telescope [3], the exploration of gravity and the way it shapes our universe has remained ever-present at the forefront of physical and astronomical research.

The cornerstone of our modern understanding of gravity, and one of the pillars upon which modern physics is based, is Albert Einstein's General Theory of Relativity [4] (GR). In his revolutionary work, first published in 1915, Einstein extended his Special Theory of Relativity [5] to describe gravity. In GR gravity is promoted from a force that exerts itself instantaneously over arbitrary distances (sitting uncomfortably at odds with Special Relativity's assertion that no signal can propagate faster than the speed of light in vacuum), to a geometrical phenomenon that appears due the dynamical, curved nature of the four dimensional spacetime that we call home.

The equations of motion that describe gravity in GR are known as the Einstein Field Equations (EFE), and are given by:

$$R_{\mu\nu} - \frac{1}{2} R g_{\mu\nu} = \frac{8\pi G}{c^4} T_{\mu\nu} - \Lambda g_{\mu\nu}. \tag{1.1}$$

[1] The shadow is formed due to photons emitted by radiating, accreting matter being gravitationally bent and captured at the event horizon of the black hole.

On the 'left hand side' of the eq. (1.1), $R_{\mu\nu}$ and $R$ are the Ricci tensor and scalar respectively associated with the four dimensional Riemannian metric $g_{\mu\nu}$, which describes the geometry of spacetime. On right 'right hand side', $T_{\mu\nu}$ describes all of the matter content of the universe (e.g. fluids, radiation), with $G$ and $c$ taking their usual meanings of Newton's Gravitational constant and the speed of light in vacuum respectively.

Finally, $\Lambda$ represents the enigmatic cosmological constant, whose introduction Einstein famously once called his "biggest blunder". This was because he originally introduced $\Lambda$ to ensure that a homogeneous and isotropic universe described by eq. (1.1) would be static in size; the discovery of Hubble and Lemaitre in the 1920s that the universe was expanding rendered $\Lambda$ obsolete in Einstein's eyes [6, 7]. Of course, almost exactly 70 years later, $\Lambda$ became relevant again as an explanation for the accelerating expansion of the universe as observed by the High-Z Supernova Search Team [8] and the Supernova Cosmology Project [9]. We will return to the subject of the accelerated expansion of the universe and the role of $\Lambda$ later in this chapter.

If one were to ignore the highly non-linear partial derivative nature of the left hand side of eq. (1.1), the EFE are beautiful in their simplicity. In the words of John Wheeler, "spacetime tells matter how to move; matter tells spacetime how to curve". Indeed, one can calculate with relative ease how a toy universe governed by eq. (1.1) might evolve given various matter components to make up $T_{\mu\nu}$. But some of the most beguiling solutions to eq. (1.1) arise when we consider a vacuum, with no matter at all.

## 1.2 Black Holes

In 1916, just over a month after Einstein announced GR to the world, Karl Schwarzschild found a spherically symmetric solution to eq. (1.1) describing the spacetime outside of a spherical mass, with $T_{\mu\nu} = 0 = \Lambda$ in that exterior region [10]. The Schwarzschild metric is given by:

$$g_{\mu\nu}dx^{\mu}dx^{\nu} = -\left(1-\frac{2M}{r}\right)dt^2 + \left(1-\frac{2M}{r}\right)^{-1}dr^2 + r^2 d\Omega^2 \tag{1.2}$$

where $M$ is the total spherical mass, whose exterior spacetime the metric describes, $t$ and $r$ are time and radial co-ordinates, and $d\Omega^2$ is the metric of the 2-sphere. We see that as $M \to 0$ we recover a flat Minkowski metric, whilst at $r = 0, 2M$ the metric seemingly becomes singular.

After work by Finkelstein in 1958 [11], we now recognise Schwarzschild's solution as describing a static and spherically symmetric black hole[2], possessing an event horizon at $r = 2M$ across which only one way travel to the centre of the black hole is possible - a point of no return. The apparent singular behaviour of the metric at $r = 2M$ can be shown to be merely a result of a poor choice of coordinates; on the other hand $r = 0$ really does describe a point at which the curvature diverges. This curvature singularity is hidden behind the event horizon, as no light (or any other signal, for that matter) can escape from within the horizon. The true nature of what lies 'behind the curtain' at the centre of black holes is a question that continues to occupy physicists.

Black holes are in many ways the simplest objects in GR, effective point masses, thought it wasn't until decades after Schwarzschild's original solution was published that astrophysical black holes were confirmed to exist. There is now, however, an embarrassment of observational evidence that black holes are real and abundant throughout the universe. The aforementioned Event Horizon Telescope has directly imaged the shadow of the black hole at the centre of the galaxy M87 [3], whilst observations of the proper motions of stars at the centre of our own Milky Way galaxy strongly suggests the presence of a supermassive black hole with a mass of $4.3 \times 10^6 M_\odot$ [15].

Among other observational signatures of black holes, however, the direct detection of gravitational waves emitted from binary black hole mergers by the Laser Interferometer Gravitational-wave Observatory (LIGO) and Virgo collaboration [16] is perhaps the most astounding.

## 1.3 Gravitational Waves

One of the more speculative[3] predictions that Einstein made using GR was the existence of gravitational waves, ripples of curvature in spacetime itself, propagating at the speed of light [17, 18]. It's these waves that mediate changes in the gravitational field, in much the same way that waves propagate through the electromagnetic field.

To illustrate these waves, one can imagine a small perturbation to a flat, empty spacetime such that $g_{\mu\nu} = \eta_{\mu\nu} + \varepsilon h_{\mu\nu}$, with $\varepsilon \ll 1$. We can then evaluate eq. (1.1) to $\mathcal{O}(\varepsilon)$ with this ansatz for the metric and find that, after choosing a suitable gauge[4], the metric

[2] Schwarzschild's solution has since been extended to describe black holes possessing angular momentum, electric charge, and to include the effects of a non-zero $\Lambda$ [12, 13, 14].

[3] At least at the time, due to their predicted faintness.

[4] This gauge is called, variously, the de Donder, Lorenz, or harmonic gauge. It is defined by choosing $\partial^\mu \bar{h}_{\mu\nu} = 0$

Figure 1.1: Diagram of the response of a ring of test particles to the two gravitational wave polarisations [19]

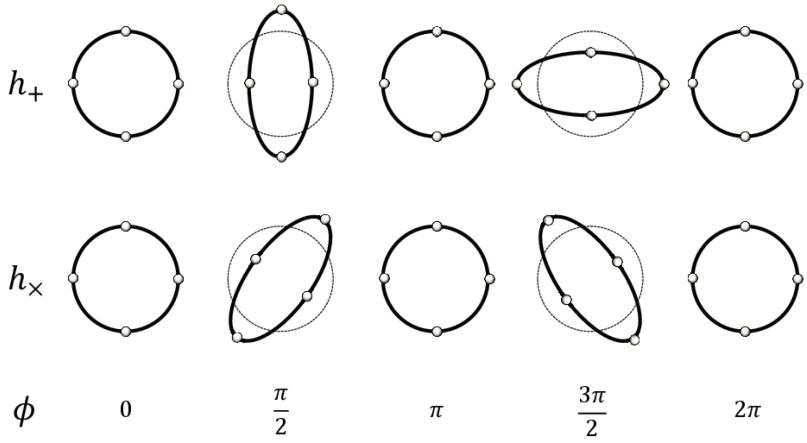


perturbation satisfies the wave equation

$$\Box \bar{h}_{\mu\nu} = 0, \tag{1.3}$$

where $\bar{h}_{\mu\nu} = h_{\mu\nu} - \frac{1}{2}\eta_{\mu\nu}h$ $h =, \eta^{\mu\nu}h_{\mu\nu}$, and $\Box = \eta^{\mu\nu}\partial_\mu\partial_\nu$ is the d'Alembertian wave operator. The solutions to this equation are plane waves with two polarisations travelling at the speed of light, and the effect of these waves as they pass by is to stretch and squeeze the very fabric of spacetime. Figure 1.1 shows the effect of these two polarisations of $h$, dubbed $h_+$ and $h_\times$, on a ring of test particles as the wave passes through.

This prediction of GR is not limited, however, solely to perturbations to a flat Minkowski background. On any (potentially curved) background perturbations to the metric can give rise to travelling waves, and they're in fact generated by any non-spherically symmetric motion of matter. We are bathed in gravitational radiation throughout our everyday lives, yet why don't we notice our surroundings being consistently stretched and squeezed around us? The answer is that spacetime is incredibly stiff, with one simple calculation [20] using dimensional analysis to estimate the 'Young's modulus' of spacetime with the combination

$$Y \sim \frac{c^2 f^2}{G} = 4.5 \times 10^{27} f^2 \text{ Pa}, \tag{1.4}$$

where $f$ is the frequency of the gravitational waves. For $f \sim 100Hz$ this leads to a 'stiffness' of spacetime around 20 orders of magnitude greater than that of steel. Clearly it takes a lot of energy to move spacetime even a minuscule amount, and either a massively energetic event or a remarkably sensitive detector would be required to observe such ripples in spacetime. In the end, it required both.

On the 14th of September 2015, gravitational waves completed a journey to Earth of about $1.4 \pm 0.6$ billion lightyears [21] from a distant merger of a binary black hole system

[22]. The system consisted of two black holes, respectively of masses 36 and 29 times the mass of the Sun, orbiting each other before merging to form a black hole with a mass 62 times the mass of our sun. In the process 3 solar masses of energy was emitted in the form of gravitational waves, briefly 'illuminating' the sky with more luminosity than every star and galaxy in the observable universe combined [23]. This huge outburst of energy had the effect of stretching the 4km long arms of the LIGO observatories by a distance equivalent to about $1/10,000$th of a proton, and ushered in the era of gravitational wave astronomy.

There have now been several detections of gravitational waves from binary black hole mergers [16], as well as those from a binary neutron star system [24], with each observation so far appearing to confirm all of the predictions of Einstein's GR [25]. But despite this, among numerous other experiments that validate the predictions of GR, there are reasons to question whether or not Einstein's theory is the final word on gravity.

## 1.4 Problems with General Relativity?

Einstein's theory of GR is currently the best description of gravity available to us, having survived over 100 years of testing [26]. It is widely accepted to be the correct description of gravity at Solar System scales, where not only do its predictions show remarkable agreement with astrophysical data, but precise measurements of phenomena such as light deflection around the Sun and perihelion shift of Mercury (among others) rule out many modifications to GR.

On the other hand, GR does not provide a complete or satisfactory description of gravity in all regimes. At high energies, unavoidable singularities arise during gravitational collapses and the so-called renormalization problem limits the analysis of quantum states [27]. Even in the classical regime, however, at low energies, there are questions as to GR's completeness at describing out universe.

The study of galaxy rotation curves reveals the outer stars of spiral galaxies to be orbiting with speeds much greater than those one would expect given the amount of visible matter contained within the galaxy [28]. In order to explain these observations within the framework of GR (and its Newtonian limit), one has to postulate the presence of huge amounts of 'dark matter' - a new component of the universe that interacts solely through gravity [29]. Dark Matter is now thought to constitute around 27% of the energy content of the universe, compared to just 5% for regular baryonic matter [30].

Even more troublingly, the accelerated expansion of the universe [8, 9] appears to be driven by an exotic form of matter with negative pressure, which constitutes around 68% of the energy content of the universe [30]. As mentioned above, the accelerated expansion

can be explained by GR through invoking a non-zero cosmological constant $\Lambda$, though the observed value of $\Lambda$ is around 120 orders of magnitude smaller than one might predict through calculations of the 'vacuum energy' from quantum field theory [31]. If one does not introduce a cosmological constant, we are instead left with another unknown exotic component of the universe, 'dark energy',with which to explain the observed accelerated expansion of the Universe [32].

The previous limitations suggest that, rather than introducing exotic dark components to the universe, GR may need modifications for both extreme energy regimes. Furthermore, modifications in the two regimes may be related as high energy corrections to GR might leak down to cosmological scales, showing up as low energy corrections. In order to modify GR, we can introduce additional gravitational fields (e.g. scalars or vectors) that interact with the metric $g_{\mu\nu}$ in non-trivial ways. For example, the famous Jordan-Brans-Dicke (JBD) model of gravity [33] promotes Newton's constant $G$ into a dynamical scalar field $\phi$, whose value can vary over space and time. We can compare the Einstein-Hilbert action of GR

$$S_{EH} = \int d^4x\sqrt{-g}\left(\frac{R}{16\pi G} + \mathscr{L}_M\right) \tag{1.5}$$

to that of JBD gravity

$$S_{JBD} = \frac{1}{16\pi}\int d^4x\sqrt{-g}\left(\phi R - \frac{\omega}{\phi}\partial_\mu\phi\,\partial^\mu\phi + 16\pi\mathscr{L}_M\right), \tag{1.6}$$

where in both cases the Lagrangian $\mathscr{L}_M$ contains all other matter components (including a potential cosmological constant term), to see the difference that introducing additional gravitational fields makes.

As mentioned above, in the weak field regime and on Solar System scales, modifications to GR are highly constrained [26]. On the other hand, strong field tests of gravity are only now being explored through gravitational wave observations of highly compact objects like black holes and neutron stars. There is thus room for novel tests of GR in the strong gravity regime [34, 35, 36, 37].

## 1.5 Black Hole Ringdown and Testing Gravity

The gravitational wave signal detected from a binary black hole merger (BBH), similar to that detected in September 2015 and described above, can be roughly split into three distinct sections: (i) the inspiral phase, where the two component black holes orbit each

Figure 1.2: Diagram of different stages of a BBH gravitational wave signal [49]

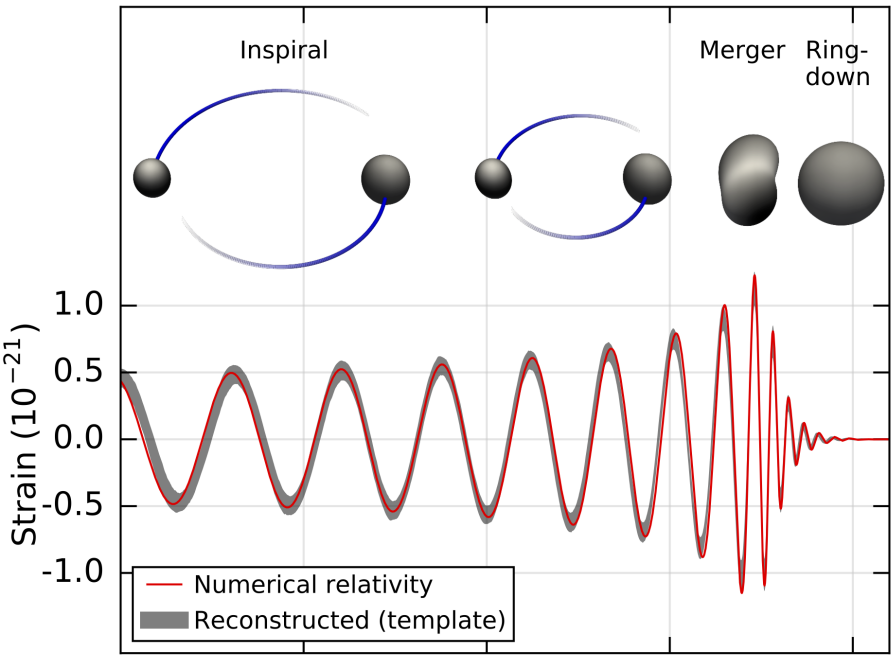


other with tighter and tighter orbits, as energy is lost from the system in the form of gravitational radiation; (ii) the merger phase, when the two black holes finally meet and chaotically merge into a single object; and (iii) the ringdown phase, where the highly perturbed remnant black hole relaxes to a steady state through the further emission of gravitational radiation. In (i), we can describe the system and the radiation emitted through the use of analytic 'post-Newtonian' expansion techniques [38], under the assumption that the characteristic internal velocity of the system is much smaller than $c$. In (ii), numerical relativity is required to solve for the highly nonlinear evolution of the metric as the two black hole spacetimes become one [39, 40, 41, 42, 43]. Finally, in (iii), perturbation theory can be used to analyse the remnant black hole as it relaxes [44, 45, 46, 47, 48]. Figure 1.2 illustrates the different phases of the signal with respect to the first direct detection of gravitational waves, GW150914 [49].

Of great interest to physicists and mathematicians alike is this final response of black holes to perturbations. Notably, perturbed black holes 'ring', emitting gravitational waves at a characteristic set of complex frequencies known as the quasi-normal mode (QNM) frequencies. These complex frequencies arise from solving the perturbed equations of motion for the black hole subject to boundary conditions such that the emitted waves are purely ingoing at the black hole horizon and purely outgoing at spatial infinity [44, 45, 46, 47, 48].

These QNM frequencies are dependent on the background properties of the black hole, acting like a 'fingerprint' for a given black hole. In fact, in GR black holes are believed to obey a series of 'no-hair theorems' that dictate that a black hole is uniquely described by its mass and angular momentum (assuming negligible electric charge) [50, 51, 52, 53, 54], and thus the Kerr black hole [12] is the most general description of an astrophysical black hole in GR.

We can define the complex QNM frequencies $\omega$ in terms of their real and imaginary parts, such that the observed gravitational wave strain $h$ is an exponentially damped sinusoid:

$$\omega_{\ell m} = 2\pi f_{\ell m} + i\tau_{\ell m}^{-1} \tag{1.7}$$

$$h_{\ell m} = A_{\ell m} e^{-t/\tau_{\ell m}} \sin\left(2\pi f_{\ell m} t + \phi_{\ell m}\right), \tag{1.8}$$

where $A$ and $\phi$ are an arbitrary amplitude and phase offset, respectively. Note that each term in the above equations are for a specific set of spherical harmonic indices $(\ell, m)$, as it is customary to analyse such systems through decomposition into spherical harmonics. We will cover this in more detail later in this thesis.

In GR, as described above, the $\omega_{\ell m}$ are functions solely of black hole mass $M$ and angular momentum $J$. Thus through a detection of two QNM frequencies in the ringdown signal of a gravitational wave event one can determine $M$ and $J$, and with a third frequency test the consistency of these values. This process is known as Black Hole Spectroscopy (BHS), and is expected to be possible in the near future with ground and space based gravitational wave observatories [37, 55, 56, 57, 58, 59, 60, 61].

Preliminary attempts at BHS with currently observed gravitational wave events appear to show consistency with the predictions of GR [25, 62], however future, more accurate observations of the ringdown provide the possiblity of testing gravity through exquisite measurements of QNM frequencies [63]. For whilst in GR the QNM spectrum is dependent on just two parameters, the presence of a cosmological constant, or a modification to the laws of gravity, can and will affect the spectrum of frequencies that a black hole will emit gravitational waves at. Thus the failure of consistency tests between QNM frequencies as described above would be a 'smoking gun' indication that the QNM spectrum is not as described by GR, and instead modifications to our theory of gravity should be considered (and indeed, can be tested).

When considering testing the predictions of ringdown emission between various theories of gravity, one can look for discrepancies induced either by: (a) a background black hole solution in a modified theory of gravity that differs from the standard GR description of black holes and/or by (b) a different dynamical evolution of gravitational waves with

respect to GR from the perturbed system, regardless of the properties of the background black hole. Much research has focussed on (a), looking for shifts in the GR QNM spectrum due to modifications to the background black hole; this has lead to a flurry of work on the generalised scalar-Gauss-Bonnet theory [64, 65, 66, 67, 68, 69, 70, 71, 72, 73, 74], among others [75, 76, 77, 78, 79, 80, 81, 82]. On the other hand, some work has focussed on case (b), where background black hole solutions are given by the same solutions as in GR, but the emitted gravitational wave signal is governed by modified equations of motion leading to modified emission [83, 84, 85]. This thesis will mostly focus on case (b).

The focus of this thesis will be on examining the ways in which the description and behaviour of black holes differs between GR and modified theories of gravity. In particular, how the ringdown signal and QNM spectrum of black holes may be affected by modifications to the underlying theory of gravity. Thus, with both present and future experiments, the predictions of GR can be compared and contrasted to those of alternative theories of gravity, allowing us to test gravity with black holes in a way not possible before.

## 1.6 Thesis Summary

In Chapter 2 I will present a fully covariant framework in which to study scalar, vector, and tensor cosmological perturbations in modified gravity theories, extending previous analysis into scalar perturbations. This framework will be presented in a theory agnostic manner, without specifying a single specific modified gravity theory, but rather considering wide classes of theories specified only by their field content. In this way large swathes of the cosmological modified gravity landscape can be analysed at once.

I will use the framework introduced in Chapter 2 to analyse perturbations to Schwarzschild black holes in modified gravity theories in Chapter 3. Again I will do this in a theory agnostic manner, and examine the ways in which generic modifications to gravity may affect the QNM spectrum of the ringdown signal of a perturbed Schwarzschild black hole.

Chapter 4 will focus on black hole solutions in modified gravity theories, and how constraints on the propagation speed of gravitational waves affects the landscape of 'hairy' black hole solutions. In Chapter 5, perturbations of a variety of classes of black holes in GR will be examined, and their QNM spectrum calculated analytically.

In Chapter 6, the specific case of black hole perturbations in Horndeski scalar-tensor gravity will be analysed. The QNM spectrum and ringdown signal of the perturbed black hole will be examined, with forecasts for parameter estimation errors with present and future experiments presented.

Finally, I will conclude with a summary of the research that has been undertaken throughout the production of this thesis. The ways in which the work presented here can aid tests of gravity with black holes will be discussed, as well as avenues of future research.

Chapters 2 and 3 are based largely on the work presented in [86] and [83] respectively. Chapters 4 and 5 are based on [87] and [88] respectively, whilst Chapter 6 is based on both [84] and [85].

Unless otherwise stated, throughout this thesis we will use natural units with $G = c = 1$, and the metric signature will be $(-,+,+,+)$. Indices using the Greek alphabet $(\alpha,\beta,...,\mu,\nu,...)$ will denote spacetime indices and run over coordinates 0-3, whilst Roman letters $(i,j,k,...)$ will denote spatial indices and run over coordinates 1-3.

# Chapter 2

# A covariant approach to parameterised cosmological perturbations

# Abstract

I present a covariant formulation for constructing general quadratic actions for cosmological perturbations, invariant under a given set of gauge symmetries for a given field content. This approach allows one to analyse scalar, vector and tensor perturbations at the same time in a straightforward manner. I apply the procedure to diffeomorphism invariant single-tensor, scalar-tensor and vector-tensor theories and show explicitly the full covariant form of the quadratic actions in such cases, in addition to the actions determining the evolution of vector and tensor perturbations. I will also discuss the role of the symmetry of the background in identifying the set of cosmologically relevant free parameters describing these classes of theories, including calculating the relevant free parameters for an axisymmetric Bianchi-I vacuum universe. This chapter is based on the research published in [86].

## 2.1 Introduction

In [89, 90] a method was proposed for constructing a general action, quadratic in the perturbed gravitational fields around a cosmological background, for general theories of gravity. Such an action depends on a finite number of free, time dependent, functions. It was shown that the presence of gauge symmetries leads to a number of Noether constraints which greatly restricts the number of free functions in such a way that the resulting action describes the most general gauge invariant action which is quadratic in the perturbed gravitational fields.

The method of [89, 90] was applied to an expanding Friedmann-Lemaitre-Robertson-Walker (FLRW) [7, 91, 92, 93, 94, 95, 96, 97] universe, using the Arnowitt-Deser-Misner (ADM) [98] variables as building blocks for the action. In this chapter I want to reach out and consider how one might construct a formalism which could be applied easily to a general background. The way is to consider a *fully covariant* method where we again use the power of the Noether constraints to impose the presence of gauge symmetries in the theory. Furthermore, by constructing actions which are fully covariant one can consider scalar, vector, and tensor type perturbations all in one go, as opposed to solely scalar perturbations, as in [89, 90]. In this chapter I will, as in [89, 90] focus on a homogeneous and isotropic, cosmological background. But throughout, I will discuss the main lessons which will allow us to consider more general background space-times. A key aspect of this chapter is that I will discuss the role that the symmetries of the background have and their interplay with gauge invariance. In doing so, I prepare the ground for more general analyses of linear perturbations in relativistic theories of gravity. In particular, in Chapter 3, I will apply the framework developed here to black hole perturbations.

*Outline:* In Section 2.2 I will describe the method proposed in [89, 90], now in covariant form, and use it to derive the action of a free massless spin-2 field propagating on Minkowski space, which corresponds to linearised GR. In Sections 2.3-2.5, I will derive the diffeomorphism-invariant quadratic actions of linear perturbations on a FLRW background for three families of theories of gravity: containing a single tensor field, a tensor field with a scalar field, and a tensor field with a vector field, respectively. The results of this chapter can thus be compared to those of [89] and [99]. In Section 2.6 I will discuss how the symmetries of the background impact the number of free functions characterising the resulting gravitational action. In particular, we will repeat the calculation of Section 2.3 with an axisymmetric Bianchi-I background [100]. In Section 2.7 I will discuss the results of this work and the method presented in this paper.

## 2.2 Covariant action approach

In this section I will describe the covariant method for constructing gauge invariant quadratic actions for linear perturbations and illustrate it by recovering linear general relativity in Minkowski space. The roles of the global symmetry of the background and the local gauge symmetry of the perturbations will be discussed also.

I will follow the same logic as in [89, 90] but using a covariant approach. The main steps of the method are summarised as follows:

1. For a given set of gravitational fields, choose a background and write a set of covariant projectors (a set of vectors and tensors) that foliate your space-time following the global symmetries of the background. Then, consider linear perturbations for each gravitational (and matter) field.

2. Construct the most general quadratic action[1] for the gravitational fields by writing all possible compatible contractions of the covariant background projectors and the linear perturbations. Introduce a free function of the background in front of each possible term and truncate the number of possible terms in the action by choosing a maximum number of derivatives.

3. Choose a desired gauge symmetry and impose local invariance of the quadratic action by solving a set of Noether constraints. The resulting action will be the most general quadratic gauge invariant action around a background with a given set of global symmetries.

We now proceed to illustrate the method by following each one of the previous step in the case of a single tensor gravitational field $g_{\mu\nu}$ (or metric) in vacuum with a diffeomorphism invariant action. In this case, the background will correspond to Minkowski space:

$$\bar{g}_{\mu\nu} = \eta_{\mu\nu}, \tag{2.1}$$

where the bar denotes the background value of the metric, and $\eta_{\mu\nu} = \text{diag}(-1,1,1,1)$ is the Minkowski metric. We know that this background has a global symmetry under the Poincare group, and thus we can describe the metric with only one projector, the tensor $\eta_{\mu\nu}$, that follows this symmetry. Hence, in this case, we do not need to make any particular foliation. Next, we consider linear perturbations and thus the full metric can be expressed as:

$$g_{\mu\nu} = \eta_{\mu\nu} + h_{\mu\nu}; \quad |h_{\mu\nu}| \ll |\eta_{\mu\nu}|, \tag{2.2}$$

[1] We consider quadratic actions in order to obtain equations of motion linear in the perturbed fields (assuming quadratic order terms in the equations of motion to be negligible).

where $h_{\mu\nu}$ is a linear perturbation, which can be a function of space and time.

We now follow step 2 and write the most general covariant quadratic action leading to second-order derivative equations of motion[2]. In this case, we can only have two different possible terms (modulo total derivatives):

$$S^{(2)} = \int d^4x \left[ \mathscr{A}^{\mu\alpha\beta\nu\gamma\delta} \bar{\nabla}_\mu h_{\alpha\beta} \bar{\nabla}_\nu h_{\gamma\delta} + \mathscr{B}^{\alpha\beta\gamma\delta} h_{\alpha\beta} h_{\gamma\delta} \right], \tag{2.3}$$

where $\bar{\nabla}_\mu$ are covariant derivatives with respect to the background metric, and the coefficients $\mathscr{A}$ and $\mathscr{B}$ are arbitrary tensors, functions of the background. These tensors must respect the symmetries of the background and hence be constructed with the tensor $\eta_{\mu\nu}$. Explicitly, the most general form these tensors can take is the following:

$$\begin{aligned} \mathscr{A}^{\mu\alpha\beta\nu\gamma\delta} =& c_3 \eta^{\mu\nu}\eta^{\alpha\beta}\eta^{\gamma\delta} + c_4 \eta^{\mu\alpha}\eta^{\nu\beta}\eta^{\gamma\delta} + c_5 \eta^{\mu\nu}\eta^{\alpha\gamma}\eta^{\beta\delta} + c_6 \eta^{\mu\gamma}\eta^{\nu\alpha}\eta^{\beta\delta}, \\ \mathscr{B}^{\alpha\beta\gamma\delta} =& c_1 \eta^{\alpha\beta}\eta^{\gamma\delta} + c_2 \eta^{\alpha\gamma}\eta^{\beta\delta}, \end{aligned} \tag{2.4}$$

where the coefficients $c_n$ are free functions of the background, i.e. constants in this case. We note that we have not actually written all the possible contractions in these tensors $\mathscr{A}$ and $\mathscr{B}$, but instead only those that are inequivalent after considering the contraction with the symmetric tensor perturbation $h_{\mu\nu}$ in the action in eq. (2.3).

If we separate each term of the action explicitly, the resulting most general quadratic action takes the following form:

$$\begin{aligned} S^{(2)} = \int d^4x \Big[ & c_1 h^2 + c_2 h_{\mu\nu} h^{\mu\nu} + c_3 \partial_\mu h \partial^\mu h + c_4 \partial_\mu h^{\mu\nu} \partial_\nu h + c_5 \partial_\mu h_{\nu\lambda} \partial^\mu h^{\nu\lambda} \\ & + c_6 \partial_\mu h_{\nu\lambda} \partial^\nu h^{\mu\lambda} \Big], \end{aligned} \tag{2.5}$$

where $h = \eta^{\mu\nu} h_{\mu\nu}$ and indices are lowered and raised with the background metric $\eta_{\mu\nu}$.

We now proceed to follow step 3, and we will impose symmetry under linear diffeomorphism invariance. Consider an infinitesimal coordinate transformation:

$$x^\mu \to x^\mu + \varepsilon^\mu; \quad |\varepsilon^\mu| \ll |x^\mu|, \tag{2.6}$$

where $\varepsilon^\mu$ is a linear perturbation that depends on space and time. Under this transformation the background stays the same but the gravitational perturbation field changes as:

$$h_{\mu\nu} \to h_{\mu\nu} + \partial_\mu \varepsilon_\nu + \partial_\nu \varepsilon_\mu. \tag{2.7}$$

[2]In principle, one could include terms in the action of higher derivative order in such a combination that the equations of motion remain second-order, but for simplicity we will restrict ourselves to actions which will explicitly lead to second-order equations.

If we wish our theory to be invariant under this coordinate transformations, then the variation of the action in eq. (2.5) with respect to the transformation in eq. (2.7) should vanish. After making suitable integrations by parts, we find that the variation of the action gives:

$$\delta_\varepsilon S^{(2)} = \int d^4x\, \varepsilon_\mu \Big[ -4c_2\partial_\nu h^{\mu\nu} - 4c_1\partial^\mu h + 2(c_4+c_6)\partial^\mu\partial^\nu\partial^\lambda h_{\nu\lambda} + 2(2c_5+c_6)\partial_\nu\Box h^{\mu\nu} + 2(2c_3+c_4)\partial^\mu\Box h\Big]. \tag{2.8}$$

For the action to be gauge invariant we need $\delta_\varepsilon S^{(2)}$ to vanish for arbitrary $\varepsilon^\mu$, and therefore the whole integrand to vanish. This leads to the following Noether identity:

$$-4c_2\partial_\nu h^{\mu\nu} - 4c_1\partial^\mu h + 2(c_4+c_6)\partial^\mu\partial^\nu\partial^\lambda h_{\nu\lambda} + 2(2c_5+c_6)\partial_\nu\Box h^{\mu\nu} + 2(2c_3+c_4)\partial^\mu\Box h = 0. \tag{2.9}$$

Since this must be satisfied off-shell, terms with different derivative structure must vanish independently, leading to the following set of Noether constraints:

$$c_1 = c_2 = 0,\ c_4 = -c_6 = -2c_3 = 2c_5. \tag{2.10}$$

These constraints are simple algebraic relations on the free coefficients $c_n$, and they ensure the action (2.5) is diffeomorphism invariant. Using our freedom to rescale the size of $h_{\mu\nu}$, we can set $-4c_4 = M_{Pl}^2$, the reduced Planck mass (squared), and write the resulting quadratic action as:

$$S^{(2)} = \int d^4x \frac{M_{Pl}^2}{4}\left[\frac{1}{2}\partial_\mu h\partial^\mu h - \partial_\mu h^{\mu\nu}\partial_\nu h - \frac{1}{2}\partial_\mu h_{\nu\lambda}\partial^\mu h^{\nu\lambda} + \partial_\mu h_{\nu\lambda}\partial^\nu h^{\mu\lambda}\right], \tag{2.11}$$

which we recognise as the quadratic expansion of the Einstein-Hilbert action about a Minkowski background [101].

## 2.3 Recovering general relativity in an expanding background

I will now apply the covariant method illustrated above around a homogeneous and isotropic background, in the case where the gravitational field content is given by a single tensor field and the action is invariant under linear coordinate transformations. In this case, we will need to explicitly couple a matter sector to the gravitational action in order to have a non-trivial background solution. For simplicity and concreteness, let us consider a scalar field $\varphi$ minimally coupled to the gravitational tensor field, although the structure of the final gravitational quadratic action will be valid for a general perfect fluid as well. The procedure

will give us a *general* parametrised gauge invariant gravitational action for cosmological perturbations, whereas the matter action is assumed to be known *a priori*.

We start by following step 1. We assume that the background is given by a spatially flat FLRW metric:

$$\bar{g}_{\mu\nu} = -dt^2 + a(t)^2 \delta_{ij} dx^i dx^j, \tag{2.12}$$

where $a(t)$ is the scale factor as a function of the physical time $t$. In order to describe this background in a covariant way, we make a 1+3 split and foliate the space-time with a time-like unit vector $u^\mu$, which induces orthogonal hypersurfaces with a spatial metric $\gamma_{\mu\nu}$ such that:

$$\gamma_{\mu\nu} = \bar{g}_{\mu\nu} + u_\mu u_\nu. \tag{2.13}$$

Thus $u^\mu$ and $\gamma_{\mu\nu}$ act as the projectors for this space-time. Specifically in this case, the time-like vector and spatial metric are given by:

$$u_\mu = (-1, \mathbf{0})_\mu, \tag{2.14}$$

$$\gamma_{ij} = a^2 \delta_{ij}, \tag{2.15}$$

$$\gamma_{\mu 0} = 0, \tag{2.16}$$

such that $\gamma_{\mu\nu}$ and $u_\mu$ are orthogonal to one another:

$$\gamma^{\mu\nu} u_\nu = 0. \tag{2.17}$$

A covariant 1+3 approach to cosmology has previously been developed [102] which shares similar projectors to the $u$ and $\gamma$ presented here. The strength of the formalism used in this paper, however, is that it can be readily utilised to split the background spacetime in different ways (e.g. see section 2.6 for a 1+1+2 split). Further differences between the two formalisms are discussed in appendix B.1.

We now add a matter scalar field $\varphi$, whose background must also be homogeneous and isotropic and hence can only be a function of time:

$$\bar{\varphi} = \bar{\varphi}(t). \tag{2.18}$$

Next, we consider linear perturbations in the metric and matter field so the full perturbed fields are given by:

$$\begin{aligned} g_{\mu\nu} &= \bar{g}_{\mu\nu} + h_{\mu\nu}; \quad |h_{\mu\nu}| \ll |\bar{g}_{\mu\nu}|, \\ \varphi &= \bar{\varphi}(t) + \delta\varphi; \quad |\delta\varphi| \ll |\bar{\varphi}|. \end{aligned} \tag{2.19}$$

We now move onto step 2 and construct the most general quadratic gravitational action. As in Section 2.2, the most general action quadratic in $h_{\mu\nu}$ with up to second order equations of motion can be written as:

$$S_G^{(2)} = \int d^4x a^3 \left[ \mathscr{A}^{\mu\nu\alpha\beta} h_{\mu\nu} h_{\alpha\beta} + \mathscr{B}^{\mu\nu\alpha\beta\delta} \bar{\nabla}_\delta h_{\mu\nu} h_{\alpha\beta} + \mathscr{C}^{\mu\nu\alpha\beta\kappa\delta} \bar{\nabla}_\kappa h_{\mu\nu} \bar{\nabla}_\delta h_{\alpha\beta} \right], \tag{2.20}$$

where the coefficients $\mathscr{A}$, $\mathscr{B}$, and $\mathscr{C}$ are tensors depending on the background. Notice that here we have added a tensor with five indices $\mathscr{B}^{\mu\nu\alpha\beta\delta}$, which we ignored in the previous section as in Minkowski space this tensor would be constant and hence the second term in eq. (2.20) would correspond to a boundary term. Also, for future convenience we have defined the tensors in action (2.20) with a factor $a^3$ in front.

We now write the most general form that the tensors $\mathscr{A}$, $\mathscr{B}$, and $\mathscr{C}$ can have respecting the symmetries of the background. In this case, they can be constructed using the projectors, the time-like unit vector $u^\mu$ and the spatial metric $\gamma_{\mu\nu}$, in the following way:

$$\mathscr{A}^{\mu\nu\alpha\beta} = A_1 \gamma^{\mu\nu}\gamma^{\alpha\beta} + A_2 \gamma^{\mu\alpha}\gamma^{\nu\beta} + A_3 \gamma^{\mu\nu} u^\alpha u^\beta + A_4 \gamma^{\mu\alpha} u^\nu u^\beta + A_5 u^\mu u^\nu u^\alpha u^\beta, \tag{2.21}$$

$$\mathscr{B}^{\mu\nu\alpha\beta\delta} = B_1 \gamma^{\delta\alpha}\gamma^{\nu\beta} u^\mu + B_2 \gamma^{\alpha\beta}\gamma^{\nu\delta} u^\mu + B_3 \gamma^{\mu\nu} u^\alpha u^\beta u^\delta + B_4 \gamma^{\mu\delta} u^\nu u^\alpha u^\beta, \tag{2.22}$$

$$\begin{aligned}
\mathscr{C}^{\mu\nu\alpha\beta\kappa\delta} = {} & C_1 \gamma^{\mu\nu}\gamma^{\alpha\beta}\gamma^{\kappa\delta} + C_2 \gamma^{\mu\alpha}\gamma^{\nu\beta}\gamma^{\kappa\delta} + C_3 \gamma^{\mu\nu}\gamma^{\alpha\kappa}\gamma^{\beta\delta} + C_4 \gamma^{\mu\kappa}\gamma^{\alpha\beta}\gamma^{\nu\delta} \\
& + (C_5 \gamma^{\mu\nu}\gamma^{\alpha\beta} + C_6 \gamma^{\mu\alpha}\gamma^{\nu\beta}) u^\kappa u^\delta + (C_7 \gamma^{\mu\nu}\gamma^{\kappa\delta} + C_8 \gamma^{\mu\kappa}\gamma^{\nu\delta}) u^\alpha u^\beta \\
& + C_9 \gamma^{\alpha\beta} u^\mu u^\nu u^\kappa u^\delta + C_{10} \gamma^{\kappa\delta} u^\alpha u^\beta u^\mu u^\nu + (C_{11} \gamma^{\kappa\delta}\gamma^{\beta\nu} + C_{12} \gamma^{\kappa\beta}\gamma^{\delta\nu}) u^\mu u^\alpha \\
& + (C_{13} \gamma^{\alpha\beta}\gamma^{\nu\delta} + C_{14} \gamma^{\alpha\nu}\gamma^{\delta\beta}) u^\mu u^\kappa + C_{15} \gamma^{\mu\alpha} u^\nu u^\beta u^\kappa u^\delta + C_{16} \gamma^{\mu\kappa} u^\nu u^\beta u^\alpha u^\delta \\
& + C_{17} u^\mu u^\alpha u^\nu u^\beta u^\kappa u^\delta,
\end{aligned} \tag{2.23}$$

where, as in the previous section, we have only defined the set of tensors that lead to distinct terms in the quadratic action[3]. Here, the coefficients $A_i$, $B_i$, and $C_i$ are arbitrary scalar functions of the background, and hence of time. We note that the tensors $\mathscr{A}$, $\mathscr{B}$, and $\mathscr{C}$ could come from the background metric $\bar{g}_{\mu\nu}$ and its derivatives to arbitrary order. Hence, we are restricting the number of derivatives allowed for the perturbations $h_{\mu\nu}$, but not for the background.

From equations (2.21)-(2.23) we can see how less symmetric backgrounds can lead to a larger number of free parameters in the gravitational action. Whereas in Minkowski the action in step 2 had only 6 free constant parameters, in a homogeneous and isotropic background we find 26 free functions of time. As we shall see later, we will also find more

[3]Whilst in principle one should symmetrise over the indices of $\mathscr{A}$, $\mathscr{B}$, and $\mathscr{C}$ in order to obtain the most general tensors, the additional symmetrised terms do not contribute any new terms to the action so they have been ommited.

Noether constraints in this section, and so the total gauge invariant action will have only one extra free parameter compared to the Minkowski case.

Having obtained an explicit expression for the coefficients in eq. (2.20), we proceed to step 3. We want the total action (gravity and matter) to be linearly diffeomorphism invariant. Specifically, we will impose gauge invariance in the gravitational action (2.20) coupled to the matter action of a minimally coupled scalar field without a potential:

$$S_M = -\int d^4x\sqrt{-g}\left(\frac{1}{2}\bar{\nabla}_\mu\varphi\bar{\nabla}^\mu\varphi\right). \tag{2.24}$$

If we expand this action to quadratic order in the linear perturbations given in eq. (2.19) we get:

$$\begin{aligned} S_M^{(2)} = -\int d^4x\, a^3 \Bigg[&\frac{1}{4}\left(\frac{1}{2}h^2 - h_{\mu\nu}h^{\mu\nu}\right)\left(\frac{1}{2}\bar{g}^{\mu\nu}\bar{\nabla}_\mu\bar{\varphi}\bar{\nabla}_\nu\bar{\varphi}\right) \\ &+\frac{1}{2}h\left(-\frac{1}{2}h^{\mu\nu}\bar{\nabla}_\mu\bar{\varphi}\bar{\nabla}_\nu\bar{\varphi}\bar{g}^{\mu\nu}\bar{\nabla}_\mu\delta\varphi\bar{\nabla}_\nu\bar{\varphi}\right) \\ &-h^{\mu\nu}\bar{\nabla}_\mu\delta\varphi\bar{\nabla}_\nu\bar{\varphi} + \frac{1}{2}\bar{g}^{\mu\nu}\bar{\nabla}_\mu\delta\varphi\bar{\nabla}_\nu\delta\varphi + \frac{1}{2}h\,h^{\mu\nu}\bar{\nabla}_\mu\bar{\varphi}\bar{\nabla}_\nu\bar{\varphi}\Bigg], \end{aligned} \tag{2.25}$$

where we have defined the trace $h = h_{\mu\nu}\bar{g}^{\mu\nu}$. The matter action also leads to the following background equation of motion:

$$\bar{\nabla}_\mu\bar{\nabla}^\mu\bar{\varphi} = 0. \tag{2.26}$$

In principle we could have different fields sourcing the matter content of our FRW universe, however we do not expect different minimally coupled sources to affect our results greatly. As we will see, it is simply the matter energy density $\dot{\bar{\varphi}}^2$ that appears in our results for the Noether constraints.

We want the total quadratic action to be linearly diffeomorphism invariant. In this case, the metric perturbation will transform as the Lie derivative of the background metric along an infinitesimal coordinate transformation vector $\varepsilon^\mu$. That is,

$$h_{\mu\nu} \to h_{\mu\nu} + \bar{\nabla}_\mu\varepsilon_\nu + \bar{\nabla}_\nu\varepsilon_\mu. \tag{2.27}$$

In addition, the matter scalar perturbation will transform as:

$$\delta\varphi \to \delta\varphi + \varepsilon^\mu\bar{\nabla}_\mu\bar{\varphi}. \tag{2.28}$$

The total action given by the combination of (2.20) and (2.25) can now be varied to find the Noether identities. Schematically, an infinitesimal variation of the total action can be written as:

$$\hat{\delta}S_T^{(2)} = \hat{\delta}S_G^{(2)} + \hat{\delta}S_M^{(2)} = \int d^4x\left[\mathscr{E}^{\mu\nu}\hat{\delta}h_{\mu\nu} + \mathscr{E}_\varphi\hat{\delta}(\delta\varphi)\right], \tag{2.29}$$

where $\hat{\delta}$ denotes a function variation, and $\mathscr{E}^{\mu\nu}$ with $\mathscr{E}_\varphi$ denote the equations of motion of the perturbation fields $h_{\mu\nu}$ and $\delta\varphi$, respectively. We now consider the functional variation of the action when the perturbation fields transform under the gauge symmetry, as in equations (2.27) and (2.28). After making suitable integrations by parts we find:

$$\hat{\delta}_\varepsilon S_T^{(2)} = \int d^4x \left[-2\bar{\nabla}_\nu \left(\mathscr{E}^{\mu\nu}\right) + \mathscr{E}_\varphi \bar{\nabla}^\mu \bar{\varphi}\right] \varepsilon_\mu, \tag{2.30}$$

where we have used the fact that $\mathscr{E}^{\mu\nu}$ is a symmetric tensor. For the total action to be gauge invariant we impose $\hat{\delta}_\varepsilon S_T^{(2)} = 0$, which leads to four Noether identities given by each one of the components of the bracket in eq. (3.14). From these Noether identities we can read a number of Noether constraints that will relate the values of the free parameters $A_i$, $B_i$ and $C_i$ of the quadratic gravitational action. In order to read off the Noether constraints easily, we rewrite the Noether identities solely in terms of the projectors $u^\mu$ and $\gamma_{\mu\nu}$, by eliminating all covariant derivatives of the background using the equations in Appendix B.1. For instance, we will rewrite the covariant derivative of the background matter field as:

$$\bar{\nabla}_\mu \bar{\varphi} = -u_\mu \dot{\bar{\varphi}}, \tag{2.31}$$

where an overdot represents a derivative with respect to the physical time. In this way, due to the fact that $\gamma_{\mu\nu}$ and $u^\mu$ are orthogonal, any perturbation field contracted with tensors having different $u$ index structure, for example, must vanish independently. Through this process, the following Noether constraints are obtained for the $A_i$, $B_i$, and $C_i$:

$$\begin{aligned}
&A_1 = -\frac{\dot{\bar{\varphi}}^2}{16},\ A_2 = \frac{1}{8}(\dot{\bar{\varphi}}^2 + 32H^2C_5 + 32H\dot{C}_5),\ A_3 = \frac{1}{8}(-\dot{\bar{\varphi}}^2 + 32H\dot{C}_5),\\
&A_4 = \frac{1}{4}(\dot{\bar{\varphi}}^2 + (32H^2 - 16\dot{H})C_5 + 32H^2\dot{C}_5),\ A_5 = \frac{1}{16}(-\dot{\bar{\varphi}}^2 - 96H^2C_5),\\
&B_1 = 4HC_5 + 4\dot{C}_5,\ B_3 = -B_4 = 4HC_5,\\
&C_1 = -C_2 = -(C_5 + H^{-1}\dot{C}_5),\ C_3 = -C_4 = 2C_5 - 2H^{-1}\dot{C}_5,\\
&2C_6 = C_8 = -C_7 = C_{11} = -C_{12} = -2C_5,\ C_{13} = -C_{14} = -4C_5,\\
&B_2 = C_{15} = C_{16} = C_{17} = C_9 = C_{10} = 0.
\end{aligned} \tag{2.32}$$

In addition, we also obtain a constraint on the background quantities:

$$\dot{H} = \frac{\dot{\bar{\varphi}}^2}{16C_5}. \tag{2.33}$$

We note that this equation has a similar form to the Friedmann equation if we identify $-8C_5 = M^2$, with the exception that $M$ is a free function of time here, as opposed to the

constant Planck mass. We find that the number of free parameters in the action is reduced from 26 to only one. We note that the background also has one free function $a$ ($\bar{\varphi}$ is not considered free as it is related to $a$ through (2.26)), and that $a$ and $M$ are related through eq. (2.33). Hence the entire model (background and perturbations) is described using one free function. Explicitly, we find the total quadratic action to be given by:

$$S_T^{(2)} = \int d^4x a^3 M^2 \left[ \mathscr{L}_{EH} - (3H^2 + \dot{H}) \frac{1}{8} \left( h^2 - 2h_{\mu\nu} h^{\mu\nu} \right) + \frac{d \log M^2}{d \log a} \mathscr{L}_+ \right] + S^{(2)}_{M,\delta\varphi}, \tag{2.34}$$

where we have defined the lagrangian $\mathscr{L}_{EH}$ to be the quadratic Taylor expansion in the metric perturbations of the Einstein Hilbert lagrangian $\frac{1}{2}\sqrt{-g}R$, whilst $\mathscr{L}_+$ represents terms which are beyond general relativity. $S^{(2)}_{M,\delta\varphi}$ represents those terms in the quadratic matter action (given by eq. (2.25)) that depend on $\delta\varphi$. Those terms which are quadratic in $h_{\mu\nu}$ have been incorporated into the other terms of eq. (2.34). The Lagrangians $\mathscr{L}_{EH}$ and $\mathscr{L}_+$ are given by:

$$\begin{aligned}
\mathscr{L}_{EH} =& \frac{1}{8} \bar{\nabla}_\mu h \bar{\nabla}^\mu h - \frac{1}{4} \bar{\nabla}_\mu h^{\mu\nu} \bar{\nabla}_\nu h - \frac{1}{8} \bar{\nabla}_\mu h^{\mu\lambda} \bar{\nabla}_\nu h^\nu_\lambda + \frac{1}{4} \bar{\nabla}_\mu h_{\nu\lambda} \bar{\nabla}^\nu h^{\mu\lambda} \\
&+ \frac{1}{4} h^{\mu\rho} (h^{\nu\sigma} \bar{R}_{\rho\nu\mu\sigma} - h^{\nu\rho} \bar{R}_{\mu\nu}) + \frac{1}{16} \bar{R} (h^2 - 2h_{\mu\nu} h^{\mu\nu}) + \frac{1}{4} \bar{R}_{\mu\nu} (2h^\mu_\sigma h^{\sigma\nu} - h h^{\mu\nu}),
\end{aligned} \tag{2.35}$$

and

$$\begin{aligned}
\mathscr{L}_+ =& -\frac{1}{2} H^2 h_{\mu\nu} h^{\mu\nu} - \frac{1}{8} h^2 - 2H^2 h^\sigma_\mu h_{\nu\sigma} u^\mu u^\nu - \frac{3}{4} H^2 h h_{\mu\nu} u^\mu u^\nu - \frac{7}{4} H^2 h_{\mu\nu} h_{\sigma\lambda} u^\mu u^\nu u^\sigma u^\lambda \\
&- \frac{1}{8} \bar{\nabla}_\mu h^{\sigma\lambda} \bar{\nabla}_\nu h_{\sigma\lambda} u^\mu u^\nu - \frac{1}{4} H h^\nu_\mu u^\mu \bar{\nabla}_\nu h + \frac{1}{8} \bar{\nabla}_\mu h \bar{\nabla}_\nu h u^\mu u^\nu + \frac{1}{8} \bar{\nabla}_\mu h \bar{\nabla}^\mu h \\
&- \frac{1}{2} H h^{\nu\sigma} u^\mu \bar{\nabla}_\sigma h_{\mu\nu} - \frac{1}{4} \bar{\nabla}_\mu h \bar{\nabla}^\sigma h_{\nu\sigma} u^\mu u^\nu + \frac{1}{4} \bar{\nabla}_\mu h^{\mu\nu} \bar{\nabla}^\sigma h_{\nu\sigma} - \frac{1}{4} \bar{\nabla}_\mu h \bar{\nabla}_\nu h^{\mu\nu} \\
&- \frac{1}{2} H h_{\mu\rho} u^\mu u_\nu u^\sigma \bar{\nabla}_\sigma h^{\nu\rho} - \frac{1}{4} H h_{\mu\nu} u^\mu u^\nu u^\sigma \bar{\nabla}_\sigma h - \frac{1}{4} u^\mu u^\nu \bar{\nabla}_\nu h_{\mu\sigma} \bar{\nabla}^\sigma h \\
&+ \frac{1}{4} u^\mu u^\nu \bar{\nabla}_\sigma h \bar{\nabla}^\sigma h_{\mu\nu} - \frac{1}{8} \bar{\nabla}_\sigma h_{\mu\nu} \bar{\nabla}^\sigma h^{\mu\nu} - \frac{3}{4} H h_{\mu\rho} u^\mu u^\nu u^\sigma \bar{\nabla}^\rho h_{\nu\sigma} \\
&+ \frac{1}{4} u^\mu u^\nu \bar{\nabla}^\sigma_{\mu\sigma} \bar{\nabla}^\rho h_{\nu\rho} + \frac{1}{4} H h_{\mu\nu} u^\mu u^\nu u^\sigma \bar{\nabla}^\rho h_{\sigma\rho} + \frac{1}{2} u^\mu u^\nu \bar{\nabla}_\nu h_{\mu\sigma} \bar{\nabla}_\rho h^{\sigma\rho} \\
&- \frac{1}{4} u^\mu u^\nu \bar{\nabla}_\sigma h_{\mu\nu} \bar{\nabla}_\rho h^{\sigma\rho} - \frac{1}{4} u_\mu u^\nu \bar{\nabla}_\rho h_{\nu\sigma} \bar{\nabla}^\rho h^{\mu\sigma} - \frac{1}{2} H h_{\mu\nu} u^\mu u^\nu u^\sigma u^\rho u^\lambda \bar{\nabla}_\lambda h_{\sigma\rho} \\
&+ \frac{1}{4} u^\mu u^\nu u^\sigma u^\rho \bar{\nabla}_\sigma h_{\mu\nu} \bar{\nabla}^\lambda h_{\rho\lambda} - \frac{1}{4} u^\mu u^\nu u^\sigma u^\rho \bar{\nabla}_\rho h_{\sigma\lambda} \bar{\nabla}^\lambda h_{\mu\nu},
\end{aligned} \tag{2.36}$$

where $\bar{R}$, $\bar{R}_{\mu\nu}$ and $\bar{R}_{\rho\nu\mu\sigma}$ are the Ricci scalar, Ricci tensor and Riemann tensor for the background metric, respectively. We note that contrary to [89] these actions are explicitly written in a covariant form and, under the standard SVT decomposition, they give the

evolution of scalar, vector and tensor perturbations all at once. As we will see next, this action propagates one physical scalar degree of freedom (d.o.f) , and two tensor d.o.f, and therefore we associate this model with that of a massless graviton coupled to a matter scalar field.

Let us first consider scalar perturbations. In this case, we can choose the Newtonian gauge and hence write the perturbed metric as:

$$h_{\mu\nu} = -2\Phi u_\mu u_\nu - 2\Psi\gamma_{\mu\nu}, \tag{2.37}$$

where $\Phi$ and $\Psi$ are the two gravitational potentials describing the scalar perturbations. After making suitable integrations by parts, (2.34) can be shown to be equal to the action given by eq. (3.33) in [89], which indeed propagates one physical scalar d.o.f.

Next, we write the action for vector perturbations. We calculate (2.34) in a gauge such that [99] the perturbed metric takes the following form:

$$h_{\mu\nu} = -u_\mu \gamma^\lambda_\nu N_\lambda - u_\nu \gamma^\lambda_\mu N_\lambda, \tag{2.38}$$

where $N_\lambda$ is a transverse vector that describes the vector perturbations of the metric and satisfies $N_\mu u^\mu = \partial_i N^i = 0$. The resultant action for vector perturbations is given by:

$$S_v^{(2)} = \int d^4x \, \frac{1}{a}\frac{M^2}{8}\left(\partial_i N_j + \partial_j N_i\right)^2. \tag{2.39}$$

From here we see that $N_i$ is an auxiliary field, i.e. does not have time derivatives and hence it does not represent a physical propagating d.o.f. As expected then, there are no physical vector perturbations propagating.

Finally, for tensor perturbations we can write the perturbed metric as:

$$h_{\mu\nu} = a^2 \gamma_{\mu\alpha}\gamma_{\nu\beta} e^{\alpha\beta}, \tag{2.40}$$

where $e^{\alpha\beta}$ describes the tensor perturbations which are traceless and transverse, that is, $e^\mu{}_\mu = 0$ and $\partial^i e_{ij} = 0$, respectively. In this case we find the gravitational action to be:

$$S_t^{(2)} = \int d^4x a^3 \frac{M^2}{8}\left((\dot{e}_{ij})^2 - \frac{1}{a^2}\left(1 + \frac{d\log M^2}{d\log a}\right)(\partial_k e_{ij})^2\right). \tag{2.41}$$

From here we see that $e_{ij}$ is a dynamical field that in principle has 6 d.o.f, but due to the transverse and traceless conditions, it propagates only two physical d.o.f, that we associate to the two polarisations of massless graviton.

Whilst it may be unsettling to recover a time-dependent effective Planck mass $M(t)$, we interpret this as arising from the unknown evolution of $a(t)$ and its relation to $M$ through

eq. (2.33). If we fix the background evolution of $a$ to correspond to GR then in turn we require $M = M_{Pl}$ so that eq. (2.33) corresponds to the Friedmann equation, and thus we recover general relativity coupled minimally to a matter scalar field. Indeed, from the final action in eq. (2.34), we see that when the mass is constant the contribution from $\mathscr{L}_+$ vanishes and the combination of $(3H^2 + \dot{H})$ contributes only as an integration constant that can be interpreted as the cosmological constant. This can be explicitly shown by integrating eq. (2.33) and combining the resulting solution with the matter background eq. (2.26). This interpretation is consistent with the result of using the Friedmann equations *a priori* to evaluate $(3H^2 + \dot{H})$ with a potential-less scalar field. Thus the correct quadratic expansion of the Einstein-Hilbert action with cosmological constant (i.e. general relativity) is recovered in the case of a constant $M$.

## 2.4 Scalar-Tensor theories

Having studied the case of a single-tensor perturbation on a cosmological background, we now construct the most general gravitational action for cosmological perturbations of a tensor and a scalar field, that leads to second order equations of motion and is linearly diffeomorphism invariant [103, 104]. We follow the covariant procedure as in the previous section, but with the addition of a gravitational scalar field $\chi$:

$$\chi = \bar{\chi}(t) + \delta\chi; \quad |\delta\chi| \ll |\bar{\chi}|, \tag{2.42}$$

where $\bar{\chi}$ is the background value of the field, which we assumed to be time-dependent only to comply with the global symmetries of the background, and $\delta\chi$ is a linear perturbation non-minimally coupled to the metric $g_{\mu\nu}$ and its perturbation, $h_{\mu\nu}$. Since we have the same homogeneous and isotropic background as in the previous section, we also use the 1+3 split of space-time with the time-like vector $u^\mu$ and the spatial metric $\gamma_{\mu\nu}$.

We move onto step 2 and write down the most general scalar-tensor gravitational action as:

$$\begin{aligned} S_G^{(2)} = \int d^4x a^3 \Big[ & \mathscr{A}^{\mu\nu\alpha\beta} h_{\mu\nu} h_{\alpha\beta} + \mathscr{B}^{\mu\nu\alpha\beta\delta} \bar{\nabla}_\delta h_{\mu\nu} h_{\alpha\beta} + \mathscr{C}^{\mu\nu\alpha\beta\kappa\delta} \bar{\nabla}_\kappa h_{\mu\nu} \bar{\nabla}_\delta h_{\alpha\beta} \\ & + A_\chi (\delta\chi)^2 + \mathscr{A}_\chi^{\mu\nu} \delta\chi h_{\mu\nu} + \mathscr{B}_\chi^{\mu\nu\delta} h_{\mu\nu} \bar{\nabla}_\delta \delta\chi + \mathscr{C}_\chi^{\mu\nu} \bar{\nabla}_\mu \chi \bar{\nabla}_\nu \chi \\ & + \mathscr{D}_\chi^{\mu\nu\delta\kappa} \bar{\nabla}_\kappa \delta\chi \bar{\nabla}_\delta h_{\mu\nu} \Big], \end{aligned} \tag{2.43}$$

where the $\mathscr{A}$, $\mathscr{B}$, and $\mathscr{C}$ are the same as those given by (2.21)-(2.23). We see that we also have two new tensors describing the self-interactions of the scalar field and three for the interactions between the scalar and tensor fields. These new tensors are arbitrary functions of

the background, and hence must follow the background symmetry and can be constructed solely from the projectors $u^\mu$ and $\gamma_{\mu\nu}$. Similarly as in the previous section, we proceed to write down the most general forms these five new tensors can take:

$$\mathscr{A}_\chi^{\mu\nu} = A_{\chi 1} u^\mu u^\nu + A_{\chi 2}\gamma^{\mu\nu} \tag{2.44}$$

$$\mathscr{B}_\chi^{\mu\nu\delta} = B_{\chi 1} u^\mu u^\nu u^\delta + B_{\chi 2} u^\delta \gamma^{\mu\nu} + B_{\chi 3} u^\mu \gamma^{\delta\nu} \tag{2.45}$$

$$\mathscr{C}_\chi^{\mu\nu} = C_{\chi 1} u^\mu u^\nu + C_{\chi 2}\gamma^{\mu\nu} \tag{2.46}$$

$$\begin{aligned}\mathscr{D}_\chi^{\mu\nu\delta\kappa} = {} & D_{\chi 1} u^\mu u^\nu u^\delta u^\kappa + D_{\chi 2} u^\mu u^\nu \gamma^{\kappa\delta} + D_{\chi 3} u^\kappa u^\delta \gamma^{\mu\nu} + D_{\chi 4} u^\mu u^\kappa \gamma^{\delta\nu} + D_{\chi 5}\gamma^{\mu\nu}\gamma^{\kappa\delta} \\ & + D_{\chi 6}\gamma^{\mu\kappa}\gamma^{\nu\delta},\end{aligned} \tag{2.47}$$

while $A_\chi$ is a scalar and hence simply considered to be free function of time. Here, each of the coefficients $A_{\chi n}$, $B_{\chi n}$, $C_{\chi n}$, and $D_{\chi n}$ are free functions of time as well. We see that we have 14 additional free functions due to the inclusion of the scalar field $\chi$.

We now follow step 3. Similarly as before, we add matter and consider a scalar field $\varphi$ minimally coupled to the metric $g_{\mu\nu}$. The matter quadratic action is given by eq. (2.25) and we must impose linear diffeomorphism invariance of the total action (gravity with matter). While the metric and matter perturbations transform as in eq. (2.27)-(2.28) under an infinitesimal coordinate transformation, the new scalar field transforms as:

$$\delta\chi \to \delta\chi + \varepsilon^\mu \bar{\nabla}_\mu \bar{\chi}. \tag{2.48}$$

The total action given by the combination of (2.43) and the matter action (2.25) can now be varied under the gauge transformation. As in Sections 2.2 and 2.3, we obtain a number of Noether constraints by enforcing independent terms in the Noether identities to vanish. We find 36 Noether constraints through this process, the full list of which can be found in Appendix A.1. Hence, the final action only depends on four free parameters that we name $M$, $\alpha_B$, $\alpha_K$, $\alpha_T$, following the notation of [99]. The relation between these four final parameters and the parameters in eq. (2.43) are given in Appendix A.1.

Analogously to the previous section, we can write the final total gauge-invariant action as the matter action plus the quadratic expansion of the Einstein-Hilbert action given in eq. (2.35) plus an additional Lagrangian $\mathscr{L}_{\chi+}$ containing terms involving the perturbed scalar $\delta\chi$ and the free functions $M$, $\alpha_B$, $\alpha_K$, $\alpha_T$:

$$S_T^{(2)} = \int d^4x\, a^3 M^2 \left[\mathscr{L}_{EH} - \left(3H^2 + \dot{H}\right)\frac{1}{8}\left(h^2 - 2h_{\mu\nu}h^{\mu\nu}\right) + \mathscr{L}_{\chi+}\right] + S^{(2)}_{M,\delta\varphi}, \tag{2.49}$$

where $\mathscr{L}_{EH}$ is given by (2.35) whilst $\mathscr{L}_{\chi+}$ is given by eq. (A.11) in appendix A.

Once again, having obtained a form for the fully covariant diffeomorphism invariant action, we can study the scalar, vector, and tensor actions separately. As expected, we will

see that this action propagates two physical scalar d.o.f (one from matter and one from the gravitational scalar $\chi$), in addition to two tensor d.o.f.

The scalar action can be calculated by expressing the metric perturbation $h_{\mu\nu}$ in terms of the standard cosmological perturbation variables $\Phi$, $\Psi$, $E$, and $B$. After making suitable integrations by parts and the field redefinition of the perturbed gravitational scalar $\delta\chi \to \bar{\chi}\delta\chi$, the action in eq. (2.49) can be shown to be equal to the action given by eq. (4.15) in [89], which indeed propagates two physical scalar d.o.f.

For vector perturbations, we again use the decomposition given by (2.38) in the unitary gauge where $\delta\chi = 0$. The resultant action for vector perturbations is then given by:

$$S_v^{(2)} = \int d^4x \frac{1}{a}\frac{M^2}{8}\left(\partial_i N_j + \partial_j N_i\right)^2. \tag{2.50}$$

As in the previous section, this action does not propagate any physical vector perturbations.

Finally, for tensor perturbations, using the decomposition given by (2.40), we find that the resultant action is given by:

$$S_t^{(2)} = \int d^4x a^3 \frac{M^2}{8}\left((\dot{e}_{ij})^2 - \frac{(1+\alpha_T)}{a^2}(\partial_k e_{ij})^2\right). \tag{2.51}$$

which propagates two physical d.o.f. We emphasise that both of the results (2.50) and (2.51) are in agreement with those of [99, 105].

The results of Section 2.3 can be recovered by setting the three $\alpha$ parameters to the following values:

$$\alpha_B = 0,\ \alpha_K = 0,\ \alpha_T = \frac{d\log M^2}{d\log a}. \tag{2.52}$$

In this case we get that

$$\mathscr{L}_{\chi+} = \frac{d\log M^2}{d\log a}\mathscr{L}_+, \tag{2.53}$$

and we recover the Friedmann equation (2.33) from the Noether constraint given in eq. (A.9), and as result all the interactions between the metric and $\delta\chi$ and the self-interactions of $\delta\chi$ vanish.

Now that we have identified the relevant free parameters characterising scalar-tensor gravity theories, it is possible to identify the physical effects of each one of them, and constrain them with observations. Indeed, as explained in [105] $M$ is a generalised Planck mass, $\alpha_T$ induces a tensor speed excess, $\alpha_K$ is a kineticity term determining the kinetic energy of the gravitational scalar $\delta\chi$, and $\alpha_B$ is a braiding term that induces kinetic mix between the perturbed metric and gravitational scalar, and thus contributes to the kinetic energy of $\delta\chi$ indirectly, through backreaction with gravity. All these parameters can be constrained with current cosmological data with numerical codes such as the ones given

in [106, 107], and hence we can find the family of such modified gravity theories that are compatible with cosmological data. As expected, observational constraints are compatible with the GR values of $\alpha_T = \alpha_K = \alpha_B = 0$ and constant $M$, and strongly disfavour large deviations from these values [108].

## 2.5 Vector-Tensor theories

In this section we construct the most general diffeomorphism invariant quadratic action for linear cosmological perturbations when the gravitational fields are given by a metric $g_{\mu\nu}$ and a vector field $\zeta^\mu$ (see [109, 110] for Einstein-Aether and generalized Einstein-Aether and [111] for generalized Proca theories). Similarly as the previous sections, we add a matter scalar field $\varphi$ minimally coupled to the metric only.

We again follow the covariant procedure for a homogeneous and isotropic background. The perturbed metric and matter field are given by eq. (2.19), and now we add a gravitational vector field:

$$\zeta^\mu = \bar{\zeta}(t)u^\mu + \delta\zeta^\mu; \quad |\delta\zeta^\mu| \ll |\bar{\zeta}u^\mu| \tag{2.54}$$

where $\bar{\zeta}$ is the background value of the field, which must be a function of time only and proportional to $u^\mu$ due to the symmetries of the background. Here, $\delta\zeta^\mu$ is a linear perturbation and is a function of space and time.

We now follow step 2 and, due to the global background symmetries, we use the 3+1 split of space-time as in the previous sections, giving us the time-like vector $u^\mu$ and the spatial metric $\gamma_{\mu\nu}$ as the projectors to describe our background metric. We write the most general gravitational action which is quadratic in the perturbation fields $h_{\mu\nu}$ and $\delta\zeta^\mu$ and lead to a maximum of second-order derivatives in the equations of motion:

$$\begin{aligned} S_G^{(2)} = \int d^4x a^3 \Big[ & \mathscr{A}^{\mu\nu\alpha\beta} h_{\mu\nu} h_{\alpha\beta} + \mathscr{B}^{\mu\nu\alpha\beta\delta} \bar{\nabla}_\delta h_{\mu\nu} h_{\alpha\beta} + \mathscr{C}^{\mu\nu\alpha\beta\kappa\delta} \bar{\nabla}_\kappa h_{\mu\nu} \bar{\nabla}_\delta h_{\alpha\beta} \\ & + \mathscr{A}_{\zeta^2}^{\mu\nu} \delta\zeta_\mu \delta\zeta_\nu + \mathscr{A}_{h\zeta}^{\mu\nu\lambda} \delta\zeta_\lambda h_{\mu\nu} + B_\zeta u^\mu \gamma^{\nu\lambda} \delta\zeta_\mu \bar{\nabla}_\nu \delta\zeta_\lambda + \mathscr{B}_\zeta^{\mu\nu\lambda\kappa} h_{\mu\nu} \bar{\nabla}_\kappa \delta\zeta_\lambda \\ & + \mathscr{C}_\zeta^{\mu\nu\kappa\delta} \bar{\nabla}_\kappa \delta\zeta_\mu \bar{\nabla}_\delta \delta\zeta_\nu + \mathscr{D}_\zeta^{\mu\nu\lambda\kappa\delta} \bar{\nabla}_\kappa \delta\zeta_\lambda \bar{\nabla}_\delta h_{\mu\nu} \Big]. \end{aligned} \tag{2.55}$$

The tensors $\mathscr{A}$, $\mathscr{B}$, and $\mathscr{C}$ are the same as those given by (2.21)-(2.23). The new tensors describing self interactions of the vector field and interactions between the vector and tensor

fields are given by:

$$\mathscr{A}^{\mu\nu}_{\zeta^2} = A_{\zeta 1} u^\mu u^\nu + A_{\zeta 2}\gamma^{\mu\nu} \tag{2.56}$$

$$\mathscr{A}^{\mu\nu\lambda}_{h\zeta} = A_{\zeta 3} u^\mu u^\nu u^\lambda + A_{\zeta 4}\gamma^{\mu\nu}u^\lambda + A_{\zeta 5} u^\mu \gamma^{\nu\lambda} \tag{2.57}$$

$$\begin{aligned}\mathscr{B}^{\mu\nu\lambda\kappa}_{\zeta} = {} & B_{\zeta 1} u^\mu u^\nu u^\lambda u^\kappa + B_{\zeta 2} u^\mu u^\nu \gamma^{\lambda\kappa} + B_{\zeta 3} u^\kappa u^\lambda \gamma^{\mu\nu} + B_{\zeta 4} u^\mu u^\lambda \gamma^{\kappa\nu} + B_{\zeta 5} u^\mu u^\kappa \gamma^{\nu\lambda} \\ & + B_{\zeta 6}\gamma^{\mu\nu}\gamma^{\lambda\kappa} + B_{\zeta 7}\gamma^{\mu\kappa}\gamma^{\nu\lambda}\end{aligned} \tag{2.58}$$

$$\begin{aligned}\mathscr{C}^{\mu\nu\kappa\delta}_{\zeta} = {} & C_{\zeta 1} u^\mu u^\nu u^\kappa u^\delta + C_{\zeta 2} u^\mu u^\nu \gamma^{\kappa\delta} + C_{\zeta 3} u^\kappa u^\delta \gamma^{\mu\nu} + C_{\zeta 4} u^\mu u^\kappa \gamma^{\nu\delta} + C_{\zeta 5}\gamma^{\mu\nu}\gamma^{\kappa\delta} \\ & + C_{\zeta 6}\gamma^{\mu\kappa}\gamma^{\nu\delta}\end{aligned} \tag{2.59}$$

$$\begin{aligned}\mathscr{D}^{\mu\nu\lambda\kappa\delta}_{\zeta} = {} & D_{\zeta 1} u^\mu u^\nu u^\lambda u^\kappa u^\delta + D_{\zeta 2} u^\lambda u^\kappa u^\delta \gamma^{\mu\nu} + D_{\zeta 3} u^\lambda u^\mu u^\nu \gamma^{\kappa\delta} + D_{\zeta 4} u^\lambda u^\mu u^\kappa \gamma^{\delta\nu} \\ & + D_{\zeta 5} u^\mu u^\nu u^\delta \gamma^{\kappa\lambda} + D_{\zeta 6} u^\mu u^\kappa u^\delta \gamma^{\nu\lambda} + D_{\zeta 7} u^\lambda \gamma^{\mu\nu}\gamma^{\kappa\delta} + D_{\zeta 8} u^\lambda \gamma^{\mu\kappa}\gamma^{\delta\nu} \\ & + D_{\zeta 9} u^\mu \gamma^{\nu\kappa}\gamma^{\delta\lambda} + D_{\zeta 10} u^\kappa \gamma^{\mu\nu}\gamma^{\delta\lambda} + D_{\zeta 11} u^\kappa \gamma^{\mu\delta}\gamma^{\nu\lambda} + D_{\zeta 12} u^\mu \gamma^{\nu\lambda}\gamma^{\kappa\delta},\end{aligned} \tag{2.60}$$

with each of the coefficients $A_{\zeta n}$, $B_{\zeta n}$, $C_{\zeta n}$, and $D_{\zeta n}$ being free functions of time, in addition to the scalar $B_\zeta$. We note that we have gained 31 additional free functions due to the inclusion of the vector field $\zeta^\mu$.

We now follow step 3. As before, the total action is given by the combination of the quadratic gravitational action in eq. (2.55) and the quadratic matter action in eq. (2.25). We must now impose linear diffeomorphism invariance of the total action under a coordinate transformation given by (2.6). The metric and matter perturbations transforming as in eq. (2.27)-(2.28), whilst the new vector field transforms as:

$$\delta\zeta^\mu \to \delta\zeta^\mu + \bar{\xi} u^\nu \bar{\nabla}_\nu \varepsilon^\mu - \varepsilon^\nu \bar{\nabla}_\nu (\bar{\xi} u^\mu). \tag{2.61}$$

As in the previous sections, by varying the total action under infinitesimal gauge transformations, we obtain four Noether identities which in turn lead to a number of Noether constraints. For vector-tensor theories we obtain 47 Noether constraints, the full list of which can be found in Appendix B.4. Therefore, the final action has 10 free parameters (arbitrary functions of time): $C_{\zeta 2}$-$C_{\zeta 6}$, $D_{\zeta 4}$, $D_{\zeta 7}$, $D_{\zeta 9}$, and $C_5$. Similarly as before, we define an effective mass of the vector-tensor action and its running as:

$$M^2 = -8C_5 + 2(C_{\zeta 5} + C_{\zeta 6})\bar{\xi}^2, \quad \alpha_M = \frac{d\log M^2}{d\log a}. \tag{2.62}$$

Analogously to (2.34) and (2.49), the total final gauge-invariant action can be written as the matter action plus the quadratic expansion of the Einstein-Hilbert action (2.35) plus an additional Lagrangian $\mathscr{L}_{\zeta_+}$ containing terms involving the perturbed vector $\delta\zeta^\mu$ and involving the 10 free parameters:

$$S^{(2)}_T = \int d^4x a^3 M^2 \left[\mathscr{L}_{EH} - (3H^2 + \dot{H})\frac{1}{8}\left(h^2 - 2h_{\mu\nu}h^{\mu\nu}\right) + \mathscr{L}_{\zeta_+}\right] + S^{(2)}_{M,\delta\varphi}. \tag{2.63}$$

We do not present $\mathscr{L}_{\zeta_+}$ in its entirety here due to the excessive length of the expression. However, having obtained a form for the fully covariant diffeomorphism invariant action, we can study the actions for scalar, vector, and tensor type perturbations separately. For scalar perturbations, we proceed as in the previous sections and, in addition, decompose the vector perturbation $\delta\zeta^\mu$:

$$\delta\zeta^\mu = \left(Z_0 - \bar{\zeta}\Phi\right) u^\mu + \gamma^{\mu\nu}\partial_\nu Z_1, \tag{2.64}$$

where $Z_0$ and $Z_1$ are the two scalar perturbations. We decompose the time perturbation of the vector field as in eq. (2.64) so that the field $\Phi$ appears explicitly as an auxiliary field (i.e. without that derivatives) in the final action for scalar perturbations. After making suitable integrations by parts, (2.63) can be shown to be equal to the following action:

$$\begin{aligned}
S_s^{(2)} = \int d^4x\, a^3 \Big( & T_{\Phi^2}\Phi^2 + T_{\partial^2\Phi^2}\partial_i\Phi\partial^i\Phi + T_{\dot{\Psi}^2}\dot{\Psi}^2 + T_{\partial^2\Psi^2}\partial_i\Psi\partial^i\Psi + T_{\Phi\Psi}\Phi\Psi + T_{\Phi\dot{\Psi}}\Phi\dot{\Psi} \\
& + T_{\partial\Phi\partial\Psi}\partial_i\Phi\partial^i\Psi + T_{Z_0\Phi}Z_0\Phi + T_{\dot{Z}_0\Phi}\dot{Z}_0\Phi + T_{\partial Z_0\partial\Phi}\partial_i Z_0\partial^i\Phi + T_{Z_0\Psi}Z_0\Psi \\
& + T_{\dot{Z}_0\Psi}\dot{Z}_0\Psi + T_{\dot{Z}_0\dot{\Psi}}\dot{Z}_0\dot{\Psi} + T_{\partial Z_0\partial\Psi}\partial_i Z_0\partial^i\Psi + T_{Z_0^2}Z_0^2 + T_{\dot{Z}_0^2}\dot{Z}_0^2 + T_{\partial^2 Z_0^2}\partial_i Z_0\partial^i Z_0 \\
& + T_{\partial\dot{Z}_0\partial Z_1}\partial_i\dot{Z}_0\partial^i Z_1 + T_{\partial Z_0\partial Z_1}\partial_i Z_0\partial^i Z_1 + T_{\partial\Phi\partial Z_1}\partial_i\Phi\partial^i Z_1 + T_{\partial\Phi\partial\dot{Z}_1}\partial_i\Phi\partial^i\dot{Z}_1 \\
& + T_{\dot{\Psi}\dot{Z}_1}\dot{\Psi}\dot{Z}_1 + T_{\partial\Psi\partial Z_1}\partial_i\Psi\partial^i Z_1 + T_{\partial\dot{\Psi}\partial Z_1}\partial_i\dot{\Psi}\partial^i Z_1 + T_{\partial^2 Z_1^2}\partial_i Z_1\partial^i Z_1 + T_{\partial^2\dot{Z}_1^2}\partial_i\dot{Z}_1\partial^i\dot{Z}_1 \\
& + T_{\partial^4 Z_1^2}\partial_i\partial_j Z_1\partial^i\partial^j Z_1\Big)
\end{aligned} \tag{2.65}$$

where we have defined 27 auxiliary coefficients $T$, one for each interaction term, which are not independent and instead can all be expressed in terms of the 10 free parameters. We do not give the explicit form of the $T$ coefficients here for brevity's sake, but a dictionary relating the $T$ parameters to the 10 remaining free functions is given in Appendix A.2. As shown in Appendix A.2, this action for scalar perturbations in fact depends only on 9 different combinations of the 10 free parameters, and hence by observing the cosmological effect of these perturbations we can only constrain these 9 combinations. We also note that the result found here is a subclass of that one in [89], where it was found that the action for scalar perturbations depended indeed on 10 combinations of free parameters instead of 9. The difference lies in the fact that in this paper we have imposed gauge invariance of the full covariant fields, and hence for scalar *and* vector perturbations (tensor perturbations are gauge independent in this case), whereas in [89] the gauge invariance was imposed only on scalar perturbations. Vector perturbations lead to additional Noether constraints, one of which relates the 10 free parameters found in [89] and thus reduces the action for scalar perturbations to the one presented in this paper.

As explained in [89], one might naively expect this action to propagate at most two physical scalar d.o.f, namely, a potential helicity-0 mode of a massive vector and the matter

field. However, we find that this action propagates three physical scalar d.o.f described by $\Psi$, $Z_0$ and $Z_1$, while $\Phi$ is an auxiliary field. Since we do not have the full non-linear completion of these models, at this level it is not possible to identify with certainty where the third scalar comes from, but it is likely to represent an unstable mode called Boulware-Deser ghost [112], which can typically appear in modified gravity theories unless the field interactions are restricted to particular forms (see for instance [113, 111, 103, 114]). In our case, it is possible to avoid such mode, by an appropriate choice of the free parameters. Indeed, inspired by the Generalised Proca theory [111], which describes the ghost-free action of a massive vector field non-minimally coupled to a metric, we can fix two free parameters, namely $C_{\zeta 2} = 0$ and $D_{\zeta 4} = \bar{\zeta} C_{\zeta 4}$, and make the kinetic terms of $Z_0$ vanish, in which case $Z_0$ becomes an auxiliary field and action (2.65) propagates only two physical scalar d.o.f described by $\Psi$ and $Z_1$.

For vector perturbations, we use the decomposition given by (2.38) for $h_{\mu\nu}$. The following decomposition of $\delta\zeta^\mu$ into a divergence-less spatial vector $Z^\mu$ is used:

$$\delta\zeta^\mu = \left(\delta Z_\nu - \bar{\zeta} N_\nu\right)\gamma^{\mu\nu}, \tag{2.66}$$

where we have decomposed the vector perturbation in this way so that the field $N_\nu$ appears explicitly as an auxiliary field in the final action. The resultant action for vector perturbations is given by:

$$S_v^{(2)} = \int d^4x a^3 \left[ T_{\partial^2 N^2} \frac{1}{a^4} \partial_i N_j \partial_i N_j + T_{\partial N \partial \delta Z} \frac{1}{a^4} \partial_i N_j \partial_i \delta Z_j + T_{\delta Z^2} \delta Z_i \delta Z^i + T_{\delta \dot{Z}^2} \delta \dot{Z}_i \delta \dot{Z}^i \right.$$
$$\left. + T_{\partial^2 \delta Z^2} \frac{1}{a^4} \partial_i \delta Z_j \partial_i \delta Z_j \right]. \tag{2.67}$$

Again, we have defined intermediate coefficients $T$, one for each interaction term, and they are related to the 10 free parameters ad shown in Appendix A.2. In the appendix we also show that there are only 5 independent combinations of the free parameters this action depends on, and hence, if vector perturbations leave any signature, we can at best constrain these 5 combinations. We note that this action has two vector fields $N_i$ and $\delta Z_i$, though $N_i$ appears as an auxiliary field (i.e. without time derivatives). Thus there is only one physical vector field propagating, which has two d.o.f that we associate to two helicities $\pm 1$ of a vector field[4].

For tensor perturbations, again using the decomposition given by (2.40), we find the following action:

$$S_t^{(2)} = \int d^4x a^3 \frac{M^2}{8} \left( (\dot{e}_{ij})^2 - \frac{(1+\alpha_T)}{a^2} (\partial_k e_{ij})^2 \right), \tag{2.68}$$

[4]Remember that these are in addition to a third degree of freedom associated with the massive vector field which is accounted for in the scalar action.

which propagates one physical tensor field, and hence two d.o.f. Here we have defined the parameter $\alpha_T$ to represent the speed excess of gravitational waves in vector-tensor gravity, analogously to eq. (2.51):

$$\alpha_T = \alpha_M - \frac{1}{HM^2}\left(4\dot{C}_{\zeta 5}\bar{\zeta}^2 + 4C_{\zeta 5}\bar{\zeta}\left(H\bar{\zeta} + 2\dot{\bar{\zeta}}\right) + 2\dot{D}_{\zeta 9}\bar{\zeta} - 2D_{\zeta 7}\dot{\bar{\zeta}} + 2D_{\zeta 9}\left(H\bar{\zeta} + \dot{\bar{\zeta}}\right)\right). \tag{2.69}$$

We emphasise that the results shown in this section for vector and tensor perturbations have never been shown before, as the work on [89] focused only on scalar perturbations. Here we have found that the structure of the action for tensor perturbations is the same as that one for scalar-tensor theories as there are no extra tensor fields involved in the model, and can help constrain only one of the 10 free parameters of the model. However, the action for vector perturbations is quite different to that one for scalar-tensor theories, as vector-tensor theories propagate one physical vector field, whose potential signatures could help constrain at most 5 of the 10 free parameters of the model.

Finally, we mention that the results of Section 2.3 can be recovered by setting the free parameters to the following values:

$$\begin{aligned} C_{\zeta 2} =& C_{\zeta 2} = C_{\zeta 3} = C_{\zeta 4} = C_{\zeta 5} = C_{\zeta 6} = 0 \\ D_{\zeta 4} =& D_{\zeta 7} = D_{\zeta 9} = 0. \end{aligned} \tag{2.70}$$

In which case, we find that:

$$M^2 = -8C_5,\ \alpha_T = \alpha_M,\ \mathscr{L}_{\zeta_+} = \alpha_M \mathscr{L}_+. \tag{2.71}$$

Similarly to the case of scalar-tensor theories, it should be possible to identify the physical effects associated to each one of the 10 free parameters found for vector-tensor theories, in addition to theoretical and numerical constraints on them. Up to date, such analysis has been done for the special case of Generalised Proca theories [115, 116, 117, 118], but the parametrised action presented in this section is more general and its further analysis will be left for future work.

## 2.6 The role of global symmetries and the number of free parameters

For each case considered so far, we have found that a finite number of free constants or functions can parametrise a general class of linearized theories. The number of free functions, or parameters, that come out of the Noether constraints will depend on the field

content but also, crucially, on what we are assuming about the background space-time. So, for example, we found that on Minkowski space, the result was one free constant which lead us to the massless Fierz-Pauli action – linearized general relativity. But when we repeated the calculation on an expanding background and assumed a $3+1$ split, we found one free *function* of time, $M^2(t)$ which is more general than the linearized general relativity on an expanding background. To understand why this is so, we need to look at the role that global symmetries play in the procedure.

Global symmetries are symmetries of the background, which are independent of the local gauge symmetries of the perturbations; we can have gauge invariance around a background with any symmetry. For instance, as shown in [89], we can have linearly diffeomorphism invariant actions in Lorentz-breaking theories such as Einstein-Aether. For this reason, we must enforce both types of symmetries – gauge and global – *independently*. While from the covariant action approach it is clear that Noether constraints enforce gauge symmetries, we clarify that making the appropriate choice of background projectors to construct the most general action in step 2 will enforce global symmetries of the background.

### 2.6.1 Considering Minkowski again

In order to illustrate this key point, let us go back to the quadratic action for a single tensor (or metric) in Minkowski space-time, shown in Section 2.2. We found that if we construct the most general action in step 2 using the a single projector $\eta_{\mu\nu}$ the final diffeomorphism invariant action does not have any free parameters. Let us now repeat the calculation but now assuming a $3+1$ split of the space-time, and hence using the projectors $u^\mu$ and $\gamma_{\mu\nu}$ to construct the most general action in step 2. In such a case the coefficients $\mathscr{A}$ and $\mathscr{B}$ in eq. (2.4) would be replaced by the expressions given in eq. (2.21) and (2.23). At this point we can already see that there are many more free parameters in this action, compared to the six parameters in eq. (2.4). After following step 3, and imposing linear diffeomorphism invariance, the resulting action is the following:

$$\begin{aligned} S^{(2)} = \int d^4x \Bigg[ & \left( \frac{1}{2}\partial_\mu h \partial^\mu h - \partial_\mu h^{\mu\nu}\partial_\nu h - \frac{1}{2}\partial_\mu h_{\nu\lambda}\partial^\mu h^{\nu\lambda} + \partial_\mu h_{\nu\lambda}\partial^\nu h^{\mu\lambda} \right) \\ & + \alpha \left( \frac{1}{2}u^\mu u^\nu \partial_\mu h^{\alpha\beta}\partial_\nu h_{\alpha\beta} - \frac{1}{2}u^\mu u^\nu \partial_\mu h \partial_\nu h + 2u^\mu u^\nu \partial_\nu h^\lambda_\mu \partial_\lambda h - u^\mu u^\nu \partial_\lambda h_{\mu\nu}\partial^\lambda h \right. \\ & \left. - u^\mu u^\nu \partial_\lambda h^\lambda_\mu \partial_\rho h^\rho_\nu - 2u^\mu u^\nu \partial_\nu h_{\mu\lambda}\partial_\rho h^{\lambda\rho} + u^\mu u^\nu \partial_\lambda h_{\mu\nu}\partial_\rho h^{\lambda\rho} + u^\mu u^\nu \partial_\rho h_{\nu\lambda}\partial^\rho h^\lambda_\mu \right) \Bigg], \end{aligned} \tag{2.72}$$

where we have again redefined the perturbation $h_{\mu\nu}$ to eliminate an overall free factor in the action, and $\alpha$ is an arbitrary constant. Unlike the action in eq. (2.11), here we find one

free parameter $\alpha$ that multiplies terms involving the time-like vector $u^\mu$. We emphasise that to obtain this action we have indeed used that $u^\mu$ and $\gamma_{\mu\nu}$ are those of a Minkowski metric, and hence the difference in the two actions does not come from the possibility that the background metric of eq. (2.72) is more general than the one previously used. The difference is due to the fact that in arriving at (2.72) we have not respected the global symmetries of the background space-time. As our background metric is Minkowski, our action cannot contain any Poincare symmetry breaking terms such as $u^\mu$. Therefore, to obtain the correct action for linear perturbations around Minkowski we must impose the background symmetry and enforce $\alpha$ to vanish. In this way we recover our previous result.

From this example we conclude that it is a consistency condition to construct the quadratic action for perturbations using projectors that preserve the global background symmetries. This is because the general tensors of step 2 $\mathscr{A}$, $\mathscr{B}$, $\mathscr{C}$, etc, can only come from the background fields, and hence they must preserve the same global symmetries.

### 2.6.2 Axisymmetric Bianchi-I

We can explore the role that the global symmetries of the background play further by constructing the most general diffeomorphism-invariant quadratic gravitational action in an anisotropic universe. For the background, we will consider an axisymmetric Bianchi-I model [100, 119, 120], such that the line element is given by:

$$ds^2 = -dt^2 + a(t)^2 dx^2 + b(t)^2 \left(dy^2 + dz^2\right). \tag{2.73}$$

Unlike the case of an isotropic universe, anisotropic universes permit dynamic vacuum solutions (e.g. the Kasner models in GR [121]); for simplicity we will consider such an anisotropic vacuum universe here. In this case, the right set of projectors to be chosen are those from a 1+1+2 split of space-time. Thus we now define three projectors: a time-like vector $u^\mu$, a space-like vector $x^\mu$, and a space-like tensor $\gamma_{\mu\nu}$ such that the background metric is expressed as:

$$\bar{g}_{\mu\nu} = -u_\mu u_\nu + x_\mu x_\nu + \gamma_{\mu\nu}. \tag{2.74}$$

The projectors $u^\mu$, $x^\mu$, and $\gamma_{\mu\nu}$ are non trivial due to the dynamical nature of the background. Explicitly, they are given by:

$$u_\mu = (-1, \mathbf{0})_\mu, \tag{2.75}$$

$$x_\mu = (0, a, 0, 0)_\mu, \tag{2.76}$$

$$\gamma_{ij} = b^2 \delta_{ij}, \tag{2.77}$$

$$\gamma_{\mu 0} = \gamma_{\mu 1} = 0, \tag{2.78}$$

where $i, j$ now run over coordinates 2 and 3 such that $u^\mu$, $x^\mu$, and $\gamma_{\mu\nu}$ are mutually orthogonal. Having chosen a set of projectors in accordance with step 1 of the method outlined throughout this paper, we can now move onto step 2 and write the most general quadratic action leading to second-order derivative equations of motion. This action can be written as:

$$S_G^{(2)} = \int d^4x\, a\, b^2 \left[ \mathscr{D}^{\mu\nu\alpha\beta} h_{\mu\nu} h_{\alpha\beta} + \mathscr{E}^{\mu\nu\alpha\beta\delta} \bar{\nabla}_\delta h_{\mu\nu} h_{\alpha\beta} + \mathscr{F}^{\mu\nu\alpha\beta\kappa\delta} \bar{\nabla}_\kappa h_{\mu\nu} \bar{\nabla}_\delta h_{\alpha\beta} \right], \tag{2.79}$$

where the tensors $\mathscr{D}$, $\mathscr{E}$, and $\mathscr{F}$ are given in Appendix A.3. The action given by eq. (2.79) depends on 122 free functions of time, a large increase from the 26 free functions that were needed in Section 2.3. We additionally have 2 free functions of time from the background - the scale factors $a$ and $b$.

Having obtained our most general quadratic action for the anisotropic Bianchi-I background, we can now proceed to step 3 and impose diffeomorphism invariance on the action (2.79), with the metric transforming as in eq. (2.27). As in the previous sections of this chapter, we obtain a number of Noether constraints that reduce the number of free parameters present in our theory from 124 (122 from eq. (2.79) and 2 from the background) to one free function of time $M^2$ and two constants $c_1$ and $c_2$ (a full list of the Noether constraints can be found in Appendix A.3), whilst a relation between the two scale factors $a$ and $b$ is also found. The final gauge invariant action is given in Appendix A.3. $M^2$ and $c_1$ arise from the 122 free parameters in the action (2.79), whilst $c_2$ is an integration constant which comes from the relation found between the two scale factors:

$$H_1 = \frac{c_2}{H_2} - \frac{1}{2} H_2, \tag{2.80}$$

where we have defined $H_1 = \frac{\dot{a}}{a}$ and $H_2 = \frac{\dot{b}}{b}$. By setting $c_2 = 0$ we find that $H_1 = -\frac{1}{2} H_2$. This relation corresponds to the non-trivial Kasner solution for an axisymmetric vacuum universe in General Relativity [121, 122, 123]:

$$ds^2 = -dt^2 + t^{-\frac{2}{3}} dx^2 + t^{\frac{4}{3}} \left( dy^2 + dz^2 \right). \tag{2.81}$$

We can further set $M^2 = -4c_1 = M_{Pl}^2$ and, after making some integrations by parts on the remaining terms, recover the exact Kasner solution (i.e. the quadratic expansion of the Einstein-Hilbert action about the background given by eq. (2.81)):

$$S^{(2)}_{GR} = \int d^4x\, t\, M^2 \left[ -\frac{1}{9t^2} h_{\mu\nu} h^{\mu\nu} + \frac{1}{9t^2} h^2 - \frac{1}{3t^2} h^{\alpha}_{\mu} h_{\nu\alpha} u^{\mu} u^{\nu} + \frac{1}{3t^2} h^{\alpha}_{\mu} h_{\nu\alpha} x^{\mu} x^{\nu} \right.$$
$$+ \frac{1}{3t^2} h h_{\mu\nu} u^{\mu} u^{\nu} - \frac{1}{3t^2} h h_{\mu\nu} x^{\mu} x^{\nu} + \frac{2}{3t^2} h_{\mu\nu} h_{\alpha\beta} u^{\mu} u^{\alpha} x^{\nu} x^{\beta}$$
$$- \frac{2}{3t^2} h_{\mu\nu} h_{\alpha\beta} u^{\mu} u^{\nu} x^{\alpha} x^{\beta} + \frac{1}{8} \bar{\nabla}_{\mu} h \bar{\nabla}^{\mu} h + \frac{1}{4} \bar{\nabla}_{\mu} h^{\mu\alpha} \bar{\nabla}^{\nu} h_{\nu\alpha} - \frac{1}{4} \bar{\nabla}^{\mu} h \bar{\nabla}^{\nu} h_{\mu\nu}$$
$$\left. - \frac{1}{8} \bar{\nabla}_{\alpha} h_{\mu\nu} \bar{\nabla}^{\alpha} h^{\mu\nu} \right]. \tag{2.82}$$

Thus, as in Section 2.3, the correct general relativistic solution can be found by a specific choice for the remaining free parameters in our theory. Unlike the resulting gauge invariant action found in 2.3, however, the action found for an axisymmetric Bianchi-I vacuum universe depends not only on a free function of time $M^2$ (as well as the background scale factor $a$), but also on two constants $c_1$ and $c_2$. This increased number of parameters in the final theory is a result of the reduced symmetry of our background space-time (from a homogenous and isotropic FLRW space-time to an anisotropic axisymmetric Bianchi-I space-time).

As we have seen in the previous examples, the symmetry of the background plays a crucial role on determining the final number of relevant free parameters in the quadratic action for perturbation. In general, the less symmetric the background, the more free parameters we will get (or at least the same number). As we have seen, we impose a given background symmetry by choosing the appropriate basis of background vectors and tensors that respect the symmetry, and construct the most general action in step 2 using that basis. Doing this is crucial for consistency as the coefficients of this general action (such as $\mathscr{A}^{\mu\nu\alpha\beta\gamma\delta}$ and $\mathscr{B}^{\alpha\beta\gamma\delta}$) can only come from the background fields and their derivatives, and hence they must respect the same symmetries.

## 2.7 Conclusion

In this chapter I have presented a covariant approach for constructing quadratic actions for linear perturbations, for a given set of fields, background global symmetries, and gauge local symmetries. I have discussed the relevance in distinguishing gauge and global symmetries and the role they play in the final construction of quadratic actions of perturbations.

The approach presented in this chapter is divided in 3 steps. In step 1 we choose the background on which perturbations propagate. This background will usually have a certain set of global symmetries, i.e. rigid symmetries that do not depend on space and time. For instance, if the background is Minkowski the global symmetries will be given by the

Poincare group, but if the background is FLRW, the symmetries are spatial rotations and translations (isotropy and homogeneity, respectively). In step 2 we construct the most general quadratic action for perturbations that lead to a chosen maximum number of derivatives in the equations of motion. This general action will have free coefficient multiplying the different possible quadratic interaction terms of the perturbation fields. These coefficients come from the background fields and their derivatives, and hence they must satisfy the same global symmetries of the background in order to be consistent. Therefore, the background symmetries play a crucial role in step 2. We achieve this consistency by choosing an appropriate basis of background projectors to use to write the general coefficients of the general quadratic action. Finally, in step 3, we impose that the general action of step 2 is invariant under certain local gauge transformations and, hence, in this step gauge symmetries are the ones playing a crucial role. We impose gauge symmetries by finding the relevant set of Noether identities associated to the symmetry and enforcing that they vanish. This leads to a set of relations between the free coefficients of the quadratic action in such a way that the final action is invariant under the desired local symmetries.

The covariant action approach presented in this chapter is general and systematic and we have shown how it can be applied to cosmology to construct general parametrised actions linear perturbations for different families of modified gravity models: scalar-tensor and vector-tensor diffeomorphism invariant theories. Since gauge invariance has been imposed on the covariant set of perturbation fields, we have hence made scalar and vector perturbations gauge invariant, and we have presented their corresponding actions in this chapter. In the case of scalar-tensor theories, we have recovered the same well-known result of previous works, but for vector-tensor theories we have extended the results of [89] and found that the action for scalar perturbations depends on 9 free parameters instead on 10, once gauge invariance on vector perturbations is imposed. We have also shown explicitly the action for vector and tensor perturbations, which are found to depend only on 5 and 1 free parameters, respectively. These results highlight the fact that scalar perturbations are essential for constraining modified gravity as they are the ones containing the most information on the free parameters, but the search of signatures in tensor or vector modes could be used complementary to improve constraints on some of the free parameters.

The power of this method is that it is agnostic of the fine detail of a 'full' non-linear theory (other than the field content), and can be applied to any type of background, with the example of an axisymmetric Bianchi-I vacuum model given explicitly. In particular, it can be applied to non-cosmological backgrounds such a black hole space-time of various forms and guises, linking cosmological tests to tests on astrophysical scales. Indeed, in Chapter 3 the framework developed in this chapter will be applied to Schwarzshild black

holes, in an attempt to determine the most general set of linear perturbations for a given field content which will play a role in black hole ringdown, and those which will affect the QNM spectrum of perturbed black holes in modified gravity.

# Chapter 3

# General theories of linear gravitational perturbations to a Schwarzschild Black Hole

# Abstract

The framework developed in Chapter 2 is used to analyse the structure of linear perturbations about a spherically symmetric background in different families of gravity theories, and hence study how QNMs of perturbed black holes may be affected by modifications to GR. We restrict ourselves to single-tensor, scalar-tensor and vector-tensor diffeomorphism-invariant gravity models in a Schwarzschild black hole background. We show explicitly the full covariant form of the quadratic actions in such cases, which allow us to then analyse odd parity (axial) and even parity (polar) perturbations simultaneously in a straightforward manner. This chapter is based on the research published in [83].

## 3.1 Introduction

The recent detection of gravitational waves (GW) from the merger of black hole binaries by the LIGO/Virgo collaboration [16] has opened a new window of physics that will allow us to test gravity in completely new regimes [25]. While GR enjoys great success and accuracy in the weak field regime around the Solar System, and in the arena of strongly self gravitating systems such as radio pulsars [124], the highly dynamical strong field regime around merging black holes (and other compact objects) was previously unobserved [59]. This situation is changing and with the accumulation of data from new black hole mergers, in addition to the plans of future observatories such as eLISA, KAGRA, and the Einstein Telescope, we will be able to impose precise observational constraints in new regimes by analysing the evolution of GW signals.

The black hole remnant resulting from the merger of two black holes is, initially, highly deformed. It subsequently settles down to a quiescent state by emitting gravitational radiation - dubbed the 'ringdown'. In GR, this process is described as the final black hole 'shedding hair' and can be characterized by two parameters: the black hole's mass and angular momentum (assuming negligible electric charge). The fact that black holes in GR have 'no hair' has become one of the cornerstone results of modern gravity [55, 57, 125, 58, 126, 127, 128, 129]. In extensions to GR the situation is different. The final state, the black hole remnant, may have additional structure or hair or it might not. But the structure of the GW signal could carry information about the underlying theory of gravity, even if the final equilibrium state is a black hole which is indistinguishable from those found in GR (for example Schwarzschild or Kerr). Thus, the characterisation of the ringdown might allow us to discriminate between GR and alternative theories of gravity [130].

Over the past decade, a set of numerical algorithms have been established to characterise the ringdown in terms of quasi-normal modes [47]. A number of consistency checks have been proposed for testing the no-hair hypothesis by comparing the values of the dominant and sub-dominant quasinormal modes; as a by product, it should be possible to read off the spin and mass of the final black hole [56]. The errors and the associated signal-to-noise ratio of such procedures have been studied in detail [131, 132, 133] and it has been shown that it should be possible to find accurate constraints on black hole parameters from future data.

There has been some attempts at exploring the ringdown process in specific extensions of GR. The evolution equations have been analysed for Jordan-Brans-Dicke gravity [134,

135], for scalar-tensor theories with non-minimal derivative couplings [76], for Einstein-Dilaton-Gauss-Bonnet gravity [64], for TeVeS models [136], and for Dynamical Chern-Simons gravity [137, 138], to mention but a few. But it is fair to say that the literature is far from complete and comprehensive. With the advent of black hole spectroscopy it is timely to start exploring extensions of General Relativity more thoroughly with the hope that future data might allow us to place stringent constraints on such modifications.

The study of the ringdown process through the quasi-normal modes involves the analysis of linear perturbations around a stationary black hole [47]. By studying the structure of the evolution equations, subject to a particular set of boundary conditions, one is able to determine frequencies and damping scales which contain a wealth of information. The problem is entirely analogous to that of analysing deviations from homogeneity on a cosmological spacetime (such as a Friedman-Robertson-Walker universe) [139]. There, one uses a set of basis functions tailored to homogeneous and isotropic spacetime and studies their evolution and spatial morphology. Comparing to cosmological observations one is then able to extract information about, for example, the expansion of the universe, the densities of the different energy components and the statistical properties of the initial conditions.

Given the similarities between the study of quasi-normal modes and cosmological perturbations, it would make sense to explore whether techniques developed for cosmology might be applied to the study of black hole physics. The focus of this chapter will be to show that the method developed for constructing general quadratic theories of gravity in the context of cosmological linear perturbation theory in Chapter 2 can also be used to develop families of perturbed actions around black hole spacetimes. In doing so, it is possible to develop a formalism for quasi-normal modes in general theories of gravity. By constraining quasi-normal modes, we will be able to constrain the free functions present in the quadratic actions presented in this chapter, and therefore extensions to General Relativity. Key to this construction is that the actions considered here are built with a minimal set of assumptions and, as a result, should cover a wide range of models in the space of non-linear gravitational theories.

The focus of this chapter will be on linear perturbations. For simplicity and clarity, we will restrict ourselves to a Schwarzschild background although the method we present should be applicable to Kerr or more exotic black holes arising in extensions of GR. This restriction merits a brief discussion. The most straightforward extension to GR is the addition of a non-minimally coupled scalar field – scalar-tensor gravity theories. It is well established that a wide range of scalar-tensor theories have no hair and thus settle down to Schwarzschild or Kerr black holes [140]. However it is possible to construct hairy black

holes in scalar-tensor theories [141]. The same can be said of theories where the extra gravitational degree of freedom is a 4-vector: for example generalized Proca theories [142, 143]. In this chapter, the extensions to GR we will consider involve either an extra scalar or vector field and given that these theories have regimes with a Schwarzschild solution, we are justified in restricting ourselves to having it as the background space time.

This chapter will be structured as follows: In Sections 3.2-3.4, we will derive the diffeomorphism-invariant quadratic actions of linear perturbations on a Schwarzschild background for three families of theories of gravity: containing a single-tensor field, a tensor field with a scalar field, and a tensor field with a vector field, respectively. In each case we will derive the equations of motion for odd parity (axial) and even parity (polar) type perturbations. In Section 5.5 I will discuss the results of this work and the method presented in this chapter.

Throughout this chapters, indices using the greek alphabet ($\mu$, $\nu$, $\lambda$...) will continue denote space-time indices and run over coordinates 0-3. Capital Roman letters ($A$, $B$, $C$...) will denote angular indices and run over coordinates 2-3.

## 3.2 Single-tensor theories on a Schwarzschild background

In this section we apply the framework developed and illustrated in Chapter 2 for analysing perturbations around a spherically symmetric background. In particular, we consider the case when the gravitational field content is given by a single tensor field and construct the most general quadratic action around a stationary and static black hole background, that is invariant under linear coordinate transformations and has second-order derivative equations of motion.

We start by following step 1. We assume that the background is given by the Schwarzschild metric:

$$ds^2 = \bar{g}_{\mu\nu} dr^\mu dr^\nu = -f dt^2 + f^{-1} dr^2 + r^2 d\theta^2 + r^2 \sin^2\theta d\phi^2, \tag{3.1}$$

where we have used spherical coordinates and defined $f = 1 - \frac{2M}{r}$, where $M$ is the mass of the central black hole. In order to describe this background in a covariant way, we foliate the spacetime according to the background symmetries. We make a 1+1+2 split and define a time-like unit vector $u^\mu$ and a space-like vector $r^\mu$, which induces orthogonal hypersurfaces with a spatial metric $\gamma_{\mu\nu}$ such that:

$$\gamma_{\mu\nu} = \bar{g}_{\mu\nu} + u_\mu u_\nu - r_\mu r_\nu. \tag{3.2}$$

Thus, $u^\mu$, $r^\mu$ and $\gamma_{\mu\nu}$ act as the projectors for this spacetime. Specifically in this case, projectors are given by:

$$u_\mu = (-f^{\frac{1}{2}}, \mathbf{0})_\mu, \tag{3.3}$$

$$r_\mu = (0, f^{-\frac{1}{2}}, 0, 0)_\mu, \tag{3.4}$$

$$\gamma_{AB} = r^2 \Omega_{AB}, \tag{3.5}$$

$$\gamma_{\mu 0} = \gamma_{\mu 1} = 0, \tag{3.6}$$

where $\mathbf{0}$ is a 3D zero vector, and $\Omega_{AB}$ is the metric on the unit 2-sphere. These projectors are mutually orthogonal to one another:

$$\gamma^{\mu\nu} u_\nu = 0; \quad \gamma^{\mu\nu} r_\nu = 0; \quad u^\mu r_\mu = 0. \tag{3.7}$$

We now move onto step 2 and construct the most general quadratic gravitational action. As in Section 2.2, the most general action quadratic in $h_{\mu\nu}$ with up to second order equations of motion can be written as:

$$S_G^{(2)} = \int d^4x r^2 \sin\theta \left[ \mathscr{A}^{\mu\nu\alpha\beta} h_{\mu\nu} h_{\alpha\beta} + \mathscr{B}^{\mu\nu\alpha\beta\delta} \bar{\nabla}_\delta h_{\mu\nu} h_{\alpha\beta} + \mathscr{C}^{\mu\nu\alpha\beta\kappa\delta} \bar{\nabla}_\kappa h_{\mu\nu} \bar{\nabla}_\delta h_{\alpha\beta} \right], \tag{3.8}$$

where the coefficients $\mathscr{A}$, $\mathscr{B}$, and $\mathscr{C}$ are tensors depending on the background. Notice that here, unlike the action in Section 2.2, we have a tensor with five indices $\mathscr{B}^{\mu\nu\alpha\beta\delta}$, which we previously ignored as it only contributes to the action as a boundary term in a Minkowski background. Also, for future convenience we have defined the tensors in action (3.8) with a factor $r^2 \sin\theta$ in front.

We now write the most general form that the tensors $\mathscr{A}$, $\mathscr{B}$, and $\mathscr{C}$ can have respecting the symmetries of the background. In this case, they can be constructed using the three relevant projectors $u^\mu$, $r^\mu$, and $\gamma_{\mu\nu}$, in the following way:

$$\begin{aligned}
\mathscr{A}^{\mu\nu\alpha\beta} = {} & A_1 \gamma^{\mu\nu}\gamma^{\alpha\beta} + \gamma^{\mu\nu}\left(A_2 u^\alpha u^\beta + A_3 r^\alpha r^\beta + A_4 u^\alpha r^\beta\right) \\
& + \gamma^{\mu\alpha}\left(A_5 \gamma^{\nu\beta} + A_6 u^\nu u^\beta + A_7 r^\nu r^\beta + A_8 u^\nu r^\beta\right) \\
& + u^\mu u^\nu \left(A_9 u^\alpha u^\beta + A_{10} r^\alpha r^\beta + A_{11} u^\alpha r^\beta\right) + r^\mu r^\nu \left(A_{12} r^\alpha r^\beta + A_{13} r^\alpha u^\beta\right) \\
& + A_{14} u^\mu r^\nu u^\alpha r^\beta,
\end{aligned} \tag{3.9}$$

$$\begin{aligned}
\mathscr{B}^{\mu\nu\alpha\beta\delta} = {} & \gamma^{\mu\nu}\gamma^{\alpha\delta}\left(u^\beta B_1 + r^\beta B_2\right) + \gamma^{\mu\delta}\gamma^{\nu\alpha}\left(u^\beta B_3 + r^\beta B_4\right) \\
& + \gamma^{\mu\nu}\left(u^\alpha u^\beta u^\delta B_5 + r^\alpha r^\beta r^\delta B_6 + u^\alpha r^\beta u^\delta B_7 + u^\alpha r^\beta r^\delta B_8 + r^\alpha r^\beta u^\delta B_9 \right. \\
& \left. + u^\alpha u^\beta r^\delta B_{10}\right) + \gamma^{\mu\delta}\left(u^\nu u^\alpha u^\beta B_{11} + r^\nu r^\alpha r^\beta B_{12} + u^\nu u^\alpha r^\beta B_{13} + r^\nu u^\alpha r^\beta B_{14}\right.
\end{aligned}$$

$$
\begin{aligned}
&+u^\nu r^\alpha r^\beta B_{15}+r^\nu u^\alpha u^\beta B_{16}\Big)+\gamma^{\mu\alpha}\left(u^\nu r^\beta u^\delta B_{17}+u^\nu r^\beta r^\delta B_{18}\right)\\
&+r^\mu r^\nu u^\alpha u^\beta\left(r^\delta B_{19}+u^\delta B_{20}\right)+r^\mu r^\nu r^\alpha u^\beta r^\delta B_{21}+u^\mu u^\nu u^\alpha r^\beta u^\delta B_{22}\\
&+r^\mu r^\nu r^\alpha u^\beta u^\delta B_{23}+u^\mu u^\nu u^\alpha r^\beta r^\delta B_{24},
\end{aligned}
\tag{3.10}
$$

$$
\begin{aligned}
\mathscr{C}^{\mu\nu\alpha\beta\kappa\delta} &= C_1\gamma^{\mu\nu}\gamma^{\alpha\beta}\gamma^{\kappa\delta}+C_2\gamma^{\mu\alpha}\gamma^{\nu\beta}\gamma^{\kappa\delta}+C_3\gamma^{\mu\nu}\gamma^{\alpha\kappa}\gamma^{\beta\delta}+C_4\gamma^{\mu\kappa}\gamma^{\alpha\beta}\gamma^{\nu\delta}\\
&+\left(C_5\gamma^{\mu\nu}\gamma^{\alpha\beta}+C_6\gamma^{\mu\alpha}\gamma^{\nu\beta}\right)u^\kappa u^\delta+\left(C_7\gamma^{\mu\nu}\gamma^{\kappa\delta}+C_8\gamma^{\mu\kappa}\gamma^{\nu\delta}\right)u^\alpha u^\beta\\
&+C_9\gamma^{\alpha\beta}u^\mu u^\nu u^\kappa u^\delta+C_{10}\gamma^{\kappa\delta}u^\alpha u^\beta u^\mu u^\nu+\left(C_{11}\gamma^{\kappa\delta}\gamma^{\beta\nu}+C_{12}\gamma^{\kappa\beta}\gamma^{\delta\nu}\right)u^\mu u^\alpha\\
&+\left(C_{13}\gamma^{\alpha\beta}\gamma^{\nu\delta}+C_{14}\gamma^{\alpha\nu}\gamma^{\delta\beta}\right)u^\mu u^\kappa+C_{15}\gamma^{\mu\alpha}u^\nu u^\beta u^\kappa u^\delta+C_{16}\gamma^{\mu\kappa}u^\nu u^\beta u^\alpha u^\delta\\
&+C_{17}u^\mu u^\alpha u^\nu u^\beta u^\kappa u^\delta+\left(C_{18}\gamma^{\mu\nu}\gamma^{\alpha\beta}+C_{19}\gamma^{\mu\alpha}\gamma^{\nu\beta}\right)r^\kappa r^\delta\\
&+\left(C_{20}\gamma^{\mu\nu}\gamma^{\kappa\delta}+C_{21}\gamma^{\mu\kappa}\gamma^{\nu\delta}\right)r^\alpha r^\beta+C_{22}\gamma^{\alpha\beta}r^\mu r^\nu r^\kappa r^\delta+C_{23}\gamma^{\kappa\delta}r^\alpha r^\beta r^\mu r^\nu\\
&+\left(C_{24}\gamma^{\kappa\delta}\gamma^{\beta\nu}+C_{25}\gamma^{\kappa\beta}\gamma^{\delta\nu}\right)r^\mu r^\alpha+\left(C_{26}\gamma^{\alpha\beta}\gamma^{\nu\delta}+C_{27}\gamma^{\alpha\nu}\gamma^{\delta\beta}\right)r^\mu r^\kappa\\
&+C_{28}\gamma^{\mu\alpha}r^\nu r^\beta r^\kappa r^\delta+C_{29}\gamma^{\mu\kappa}r^\nu r^\beta r^\alpha r^\delta+C_{30}r^\mu r^\alpha r^\nu r^\beta r^\kappa r^\delta\\
&+\gamma^{\mu\nu}\left(C_{31}\gamma^{\alpha\beta}r^\kappa u^\delta+C_{32}\gamma^{\alpha\kappa}u^\beta r^\delta+C_{33}\gamma^{\alpha\kappa}u^\delta r^\beta+C_{34}\gamma^{\kappa\delta}r^\alpha u^\beta\right)\\
&+\gamma^{\mu\alpha}\left(C_{35}\gamma^{\nu\beta}u^\kappa r^\delta+C_{36}\gamma^{\kappa\delta}r^\nu u^\beta\right)\\
&+\gamma^{\mu\kappa}\left(C_{37}\gamma^{\alpha\delta}r^\nu u^\beta+C_{38}\gamma^{\nu\delta}r^\alpha u^\beta+C_{39}\gamma^{\nu\alpha}r^\beta u^\delta+C_{40}\gamma^{\nu\alpha}u^\beta r^\delta\right)\\
&+\gamma^{\mu\nu}\left(r^\alpha r^\beta u^\kappa u^\delta C_{41}+u^\alpha u^\beta r^\kappa r^\delta C_{42}+r^\alpha u^\beta r^\kappa u^\delta C_{43}\right)\\
&+\gamma^{\kappa\delta}\left(u^\mu u^\nu r^\alpha r^\beta C_{44}+r^\mu u^\nu r^\alpha u^\beta C_{45}\right)\\
&+\gamma^{\mu\kappa}\left(u^\nu r^\alpha r^\beta u^\delta C_{46}+r^\nu u^\alpha u^\beta r^\delta C_{47}+u^\nu u^\alpha r^\beta r^\delta C_{48}+r^\nu u^\alpha r^\beta u^\delta C_{49}\right)\\
&+\gamma^{\mu\alpha}\left(r^\nu r^\beta u^\kappa u^\delta C_{50}+u^\nu u^\beta r^\kappa r^\delta C_{51}+u^\nu r^\beta u^\kappa r^\delta C_{52}\right)+u^\mu u^\nu u^\alpha r^\beta\gamma^{\kappa\delta}C_{53}\\
&+\gamma^{\mu\nu}\left(u^\alpha u^\beta u^\kappa r^\delta C_{54}+u^\alpha r^\beta u^\kappa u^\delta C_{55}\right)\\
&+\gamma^{\mu\kappa}\left(u^\nu u^\alpha r^\beta u^\delta C_{56}+u^\nu u^\alpha u^\beta r^\delta C_{57}+r^\nu u^\alpha u^\beta u^\delta C_{58}\right)\\
&+\gamma^{\mu\alpha}\left(u^\nu u^\beta u^\kappa r^\delta C_{59}+u^\nu r^\beta u^\kappa u^\delta C_{60}\right)+r^\mu r^\nu r^\alpha u^\beta\gamma^{\kappa\delta}C_{61}\\
&+\gamma^{\mu\nu}\left(r^\alpha r^\beta r^\kappa u^\delta C_{62}+r^\alpha u^\beta r^\kappa r^\delta C_{63}\right)\\
&+\gamma^{\mu\kappa}\left(r^\nu r^\alpha u^\beta r^\delta C_{64}+r^\nu r^\alpha r^\beta u^\delta C_{65}+u^\nu r^\alpha r^\beta r^\delta C_{66}\right)\\
&+\gamma^{\mu\alpha}\left(r^\nu r^\beta r^\kappa u^\delta C_{67}+r^\nu u^\beta r^\kappa r^\delta C_{68}\right)+u^\mu u^\nu u^\alpha u^\beta r^\kappa u^\delta C_{69}\\
&+r^\mu u^\nu u^\alpha u^\beta u^\kappa u^\delta C_{70}+r^\mu r^\nu r^\alpha r^\beta r^\kappa u^\delta C_{71}+u^\mu r^\nu r^\alpha r^\beta r^\kappa r^\delta C_{72}\\
&+u^\mu u^\nu u^\alpha u^\beta r^\kappa r^\delta C_{73}+r^\mu u^\nu u^\alpha u^\beta r^\kappa u^\delta C_{74}+r^\mu r^\nu u^\alpha u^\beta u^\kappa u^\delta C_{75}
\end{aligned}
$$

$$
\begin{aligned}
&+ r^\mu u^\nu r^\alpha u^\beta u^\kappa u^\delta C_{76} + r^\mu r^\nu r^\alpha r^\beta u^\kappa u^\delta C_{77} + u^\mu r^\nu r^\alpha r^\beta u^\kappa r^\delta C_{78} \\
&+ u^\mu u^\nu r^\alpha r^\beta r^\kappa r^\delta C_{79} + u^\mu r^\nu u^\alpha r^\beta r^\kappa r^\delta C_{80} + u^\mu r^\nu r^\alpha r^\beta u^\kappa u^\delta C_{81} \\
&+ u^\mu u^\nu r^\alpha r^\beta u^\kappa r^\delta C_{82} + u^\mu r^\nu u^\alpha r^\beta u^\kappa r^\delta C_{83} + u^\mu u^\nu u^\alpha r^\beta r^\kappa r^\delta C_{84}, \qquad (3.11)
\end{aligned}
$$

where, as in the previous section, we have only defined the set of tensors that lead to distinct terms in the quadratic action[1]. Here, the coefficients $A_n$, $B_n$, and $C_n$ are arbitrary scalar functions of the background, and hence of radius. We note that the tensors $\mathscr{A}$, $\mathscr{B}$, and $\mathscr{C}$ could come from the background metric $\bar{g}_{\mu\nu}$ and its derivatives to arbitrary order. Hence, we are restricting the number of derivatives allowed for the perturbations $h_{\mu\nu}$, but not for the background. We comment here that, in using only the projectors $u^\mu, r^\mu$, and $\gamma^{\mu\nu}$, we have implicitly restricted ourselves to studying theories that do not include parity violation. To study such theories, for example Chern-Simons theories of gravity [144], we would also have to use the four dimensional Levi-Civita tensor $\varepsilon^{\mu\nu\alpha\beta}$ when constructing our background tensors.

From equations (3.9)-(3.11) we can see how less symmetric backgrounds can lead to a larger number of free parameters in the gravitational action. Whereas with a Minkowski background in section 2.2 the action in step 2 had only 6 free constant parameters, in a spherically symmetric background we find 122 free functions of radius. As we shall see later, we will also find more Noether constraints in this section, and so the total gauge invariant action will have only one extra free parameter compared to the Minkowski case.

Having obtained an explicit expression for the coefficients in eq. (3.8), we proceed to step 3. We want the total quadratic action to be linearly diffeomorphism invariant. In this case, the metric perturbation will transform as the Lie derivative of the background metric along an infinitesimal coordinate transformation vector $\varepsilon^\mu$. That is,

$$
h_{\mu\nu} \to h_{\mu\nu} + \bar{\nabla}_\mu \varepsilon_\nu + \bar{\nabla}_\nu \varepsilon_\mu, \qquad (3.12)
$$

where again $\varepsilon_\mu$ is an arbitrary gauge parameter. The action given by eq. (3.8) can now be varied to find the Noether identities. Schematically, an infinitesimal variation of the total action can be written as:

$$
\delta S_G^{(2)} = \int d^4x \left[ \mathscr{E}^{\mu\nu} \delta h_{\mu\nu} \right], \qquad (3.13)
$$

where $\delta$ denotes a functional variation, and $\mathscr{E}^{\mu\nu}$ is the equations of motion of the perturbation field $h_{\mu\nu}$. We now consider the functional variation of the action when the perturbation

[1] Whilst in principle one should symmetrise over the indices of $\mathscr{A}$, $\mathscr{B}$, and $\mathscr{C}$ in order to obtain the most general tensors, the additional symmetrised terms do not contribute any new terms to the action so they have been ommited.

field transform as in eq. (3.12). After making suitable integrations by parts we find:

$$\delta_\varepsilon S_T^{(2)} = \int d^4x \left[-2\bar{\nabla}_\nu \left(\mathscr{E}^{\mu\nu}\right)\right] \varepsilon_\mu, \tag{3.14}$$

where we have used the fact that $\mathscr{E}^{\mu\nu}$ is a symmetric tensor. For the total action to be gauge invariant we impose $\delta_\varepsilon S_T^{(2)} = 0$, which leads to four Noether identities given by each one of the components of the bracket in eq. (3.14). From these Noether identities we can read a number of Noether constraints that will relate the values of the free parameters $A_n$, $B_n$ and $C_n$ of the quadratic gravitational action. In order to read off the Noether constraints easily, we rewrite the Noether identities solely in terms of the projectors $u^\mu$, $r^\mu$ and $\gamma_{\mu\nu}$, by eliminating all covariant derivatives of the background using the equations in Appendix B.1. For instance, we will rewrite the covariant derivative of a function $G$ as:

$$\bar{\nabla}_\mu G = f^{\frac{1}{2}} r_\mu \frac{\partial G}{\partial r}. \tag{3.15}$$

In this way, due to the fact that the projectors are mutually orthogonal, any perturbation field contracted with different projectors or different index structure must vanish independently. Through this process, we obtain 120 Noether constraints for the coefficients $A_n$, $B_n$, and $C_n$ (see Appendix B.2). Thus, we are left with only two free parameters: a free function of $r$, $C_1$, and a constant, $C_{41}$. In fact, we find that all terms which depend on the parameter $C_1$ cancel in the final action, thus leaving the action dependent only on the constant $C_{41}$. We can thus write the total *gauge invariant* action as:

$$S_G^{(2)} = \int d^4x\, r^2 \sin\theta\, M_{Pl}^2\, \mathscr{L}_{EH}, \tag{3.16}$$

where we have chosen $C_{41} = -\frac{1}{4}M_{Pl}^2$, with $M_{Pl}$ being the reduced Planck mass, in order to describe modifications from GR. The Lagrangian $\mathscr{L}_{EH}$ is the quadratic expansion of the Einstein-Hilbert action, i.e. $\frac{1}{2}\sqrt{-g}R$, and is given by eq. (2.35).

Having found the most general gauge invariant quadratic action for a single tensor field on a Schwarzschild background, we can now find the equations of motion for different types of perturbations. Due to the spherical symmetry of the background, perturbations can be decomposed into tensor spherical harmonics and classified in terms of their parity: either odd (axial) or even (polar) [145, 146]. As our action is gauge invariant, we are free to choose a convenient gauge for our calculations. We will work in the Regge-Wheeler gauge

[145], in which our odd and even perturbations take the following form [145, 146]:

$$h^{odd}_{\mu\nu,\ell m} = \begin{pmatrix} 0 & 0 & h_0(r)B^{\ell m}_\theta & h_0(r)B^{\ell m}_\phi \\ 0 & 0 & h_1(r)B^{\ell m}_\theta & h_1(r)B^{\ell m}_\phi \\ sym & sym & 0 & 0 \\ sym & sym & 0 & 0 \end{pmatrix} e^{-i\omega t}, \tag{3.17}$$

$$h^{even}_{\mu\nu,\ell m} = \begin{pmatrix} H_0(r)f & H_1(r) & 0 & 0 \\ sym & \frac{H_2(r)}{f} & 0 & 0 \\ 0 & 0 & K(r)r^2 & 0 \\ 0 & 0 & 0 & K(r)r^2\sin\theta \end{pmatrix} Y^{\ell m} e^{-i\omega t}, \tag{3.18}$$

where *sym* indicates a symmetric entry, $B^{\ell m}_\mu$ is the odd parity vector spherical harmonic and $Y^{\ell m}$ is the standard scalar spherical harmonic, as described in [147, 148][2]:

$$B^{\ell m}_\theta = -\frac{1}{\sin\theta}\frac{\partial}{\partial\phi}Y^{\ell m}, \quad B^{\ell m}_\phi = \sin\theta\frac{\partial}{\partial\theta}Y^{\ell m}. \tag{3.19}$$

Here, the amplitude of linear perturbations is described by the functions $h_i$, $H_i$ and $K$. The properties of tensor spherical harmonics and of the Schwarzschild spacetime are explored in great length in [147, 148]; the calculations of those papers were used throughout the calculations made here. We have also assumed a time dependence of $e^{-i\omega t}$ for our perturbations, due to the static nature of the background spacetime[3]. Furthermore, spherical harmonic indices will be omitted from now on, with each equation assumed to hold for a given $\ell$ (we will find that the equations of motion are independent of $m$, which is unsurprising due to the spherical symmetry of the background). In general, the metric perturbation will then be represented by a sum over $\ell$, $m$, and $\omega$ of the modes.

Clearly eq. (3.16) shows that we have recovered the correct quadratic expansion of GR for single tensor theories of gravity. It will, however, be instructive for later sections to proceed with the full analysis of the equations of motion derived from the action given by eq. (3.16).

### 3.2.1 Odd parity perturbations

We will first consider odd parity perturbations, where $h_{\mu\nu}$ is given by eq. (3.17). We find the following two Euler-Lagrange equations upon varying eq. (3.16) with respect to $h_0$ and

[2]Note there are slight differences in convention between the definitions of tensorial spherical harmonics used in [147] and [148]).

[3]The case of $\omega = 0$, i.e. for purely static perturbations, is interesting for the study of Tidal Love Numbers [149, 150, 151] and the tidal deformation of black holes in modified theories of gravity [78]. This study lies outside the scope of this thesis, however.

$h_1$, respectively:

$$\frac{d^2h_0}{dr^2} + i\omega\frac{dh_1}{dr} + i\omega\frac{2h_1}{r} - \frac{h_0}{r^2}f^{-1}\left(\ell(\ell+1) - \frac{4M}{r}\right) = 0, \tag{3.20}$$

$$f^{-1}\left(2i\omega\frac{h_0}{r} - i\omega\frac{dh_0}{dr} + \omega^2 h_1\right) - \frac{h_1}{r^2}(\ell+2)(\ell-1) = 0. \tag{3.21}$$

Multiplying eq. (3.20) by $-i\omega$ and taking the $r$ derivative of eq. (3.21) and substituting, we find:

$$-i\omega h_0 = f\frac{d}{dr}(h_1 f). \tag{3.22}$$

Using eq. (3.22) to eliminate $h_0$ from eq. (3.21), we arrive at the famous Regge-Wheeler equation [145]:

$$\frac{d^2Q}{dr_*^2} + \left[\omega^2 - V_{RW}(r)\right]Q = 0, \tag{3.23}$$

where we have introduced the Regge-Wheeler function $Q$ and the tortoise coordinate $r_*$ [145] such that:

$$Q = h_1\frac{f}{r}, \tag{3.24}$$

$$dr_* = f^{-1}dr, \tag{3.25}$$

whilst the potential $V_{RW}(r)$ is given by

$$V_{RW} = \left(1 - \frac{2M}{r}\right)\left(\frac{1}{r^2}\ell(\ell+1) - \frac{6M}{r^3}\right). \tag{3.26}$$

Figure 3.1 shows the value of $V_{RW}$ plotted for varying $\ell$ for a black hole with $M = 1/2$ (such that the horizon is at $r = 1$).

### 3.2.2 Even parity perturbations

For even parity perturbations, where $h_{\mu\nu}$ is given by eq. (3.18), four Euler-Lagrange equations are found upon varying eq. (3.16) with respect to $H_0$, $H_1$, $H_2$, and $K$. After a series of straightforward, but lengthy, manipulations, the following set of equations is found:

$$\frac{dK}{dr} + \frac{r-3M}{r(r-2M)}K - \frac{1}{r}H_0 + \frac{1}{2}\frac{\ell(\ell+1)}{i\omega r^2}H_1 = 0, \tag{3.27}$$

$$\frac{dH_0}{dr} + \frac{r-3m}{r(r-2M)}K - \frac{r-4M}{r(r-2M)}H_0 + \left[\frac{i\omega r}{r-2M} + +\frac{1}{2}\frac{\ell(\ell+1)}{i\omega r^2}\right]H_1 = 0, \tag{3.28}$$

$$\frac{dH_1}{dr} + \frac{i\omega r}{r-2M}K + \frac{i\omega r}{r-2M}H_0 + \frac{2M}{r(r-2M)}H_1 = 0, \tag{3.29}$$

Figure 3.1: Regge-Wheeler potential $V_{RW}$ as a function of $r$ for varying $\ell$, with $M = 1/2$.

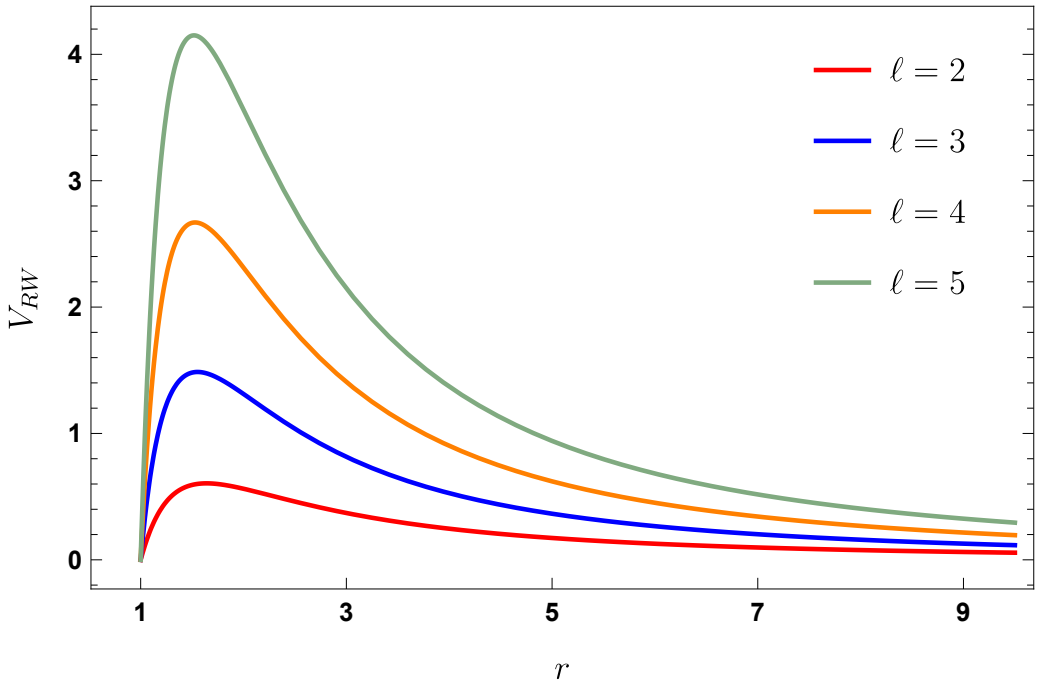


which satisfy the following algebraic identity:

$$\left[\frac{6M}{r}+(\ell+2)(\ell-1)\right]H_0-\left[(\ell+2)(\ell-1)-\frac{2\omega^2r^3}{r-2M}+\frac{2M(r-3M)}{r(r-2M)}\right]K \\ -\left[2i\omega r+\frac{\ell(\ell+1)M}{i\omega r^2}\right]H_1=0, \tag{3.30}$$

and the relation $H_0 = H_2$ is also found. We can make the following field redefinitions, as described in [152], to rewrite $K$ and $H_1$ in terms of the Zerilli function $\psi(r)$ (with a relation for $H_0$ also found):

$$\begin{aligned} K =& g_1(r)\psi+\left(1-\frac{2M}{r}\right)\frac{\partial\psi}{\partial r}, \\ H_1 =& -i\omega\left(g_2(r)\psi+r\frac{\partial\psi}{\partial r}\right), \\ H_0 =& \frac{\partial}{\partial r}\left[\left(1-\frac{2M}{r}\right)\left(g_2(r)\psi+r\frac{\partial\psi}{\partial r}\right)\right]-K, \end{aligned} \tag{3.31}$$

where we have introduced:

$$g_1(r) = \frac{\lambda(\lambda+1)r^2+2\lambda Mr+6M^2}{r^2(\lambda r+3M)},\ g_2(r) = \frac{\lambda r^2-3\lambda Mr-3M^2}{(r-2M)(\lambda r+3M)}, \tag{3.32}$$

Figure 3.2: Zerilli potential $V_Z$ as a function of $r$ for varying $\ell$, with $M = 1/2$.

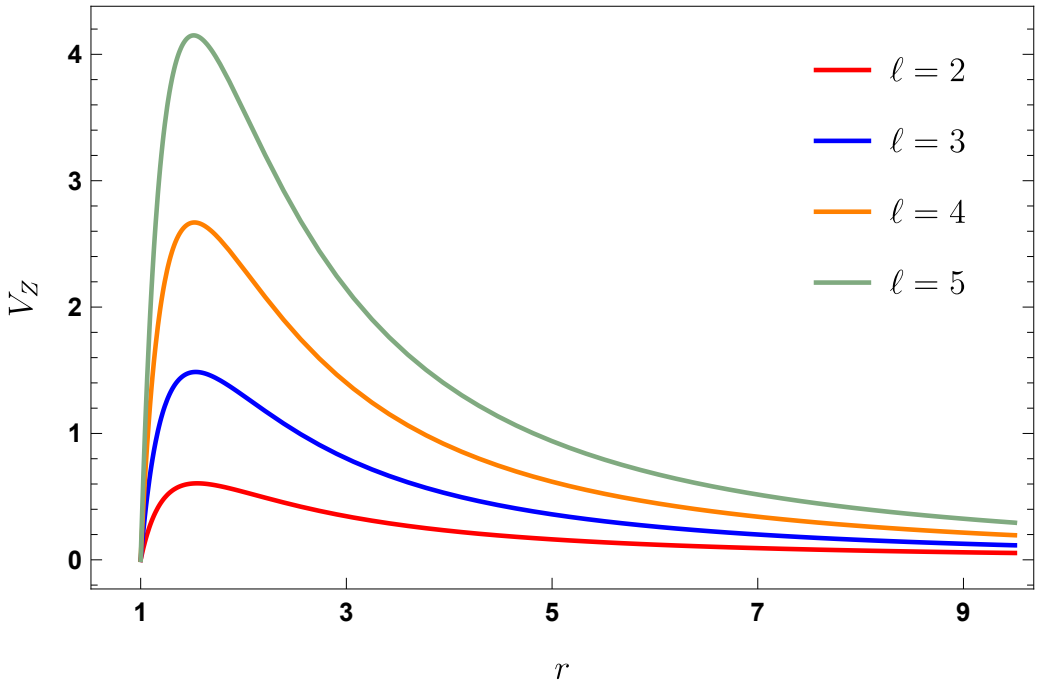


and $2\lambda = (\ell+2)(\ell-1)$. After making the substitutions given by eq. (3.31) in eq. (3.30), we find a single equation determining the evolution of perturbations, the familiar Zerilli equation [153]:

$$\frac{d^2\psi}{dr_*^2} + \left[\omega^2 - V_Z(r)\right]\psi = 0, \tag{3.33}$$

where the potential $V_Z(r)$ is given by

$$V_Z(r) = 2\left(1 - \frac{2M}{r}\right)\frac{\lambda^2 r^2\left[(\lambda+1)r + 3M\right] + 9M^2(\lambda r + M)}{r^3(\lambda r + 3M)^2}. \tag{3.34}$$

Figure 3.2 shows the value of $V_Z$ plotted for varying $\ell$ for a black hole with $M = 1/2$ (such that the horizon is at $r = 1$).

For both odd and even parity perturbations, we recover the Regge-Wheeler and Zerilli equations as in GR. These equations are in the form of Schroedinger-style wave equations, with the spectrum of frequencies $\omega$ dependent on the form of the potentials $V_{RW}$ and $V_Z$. Clearly for a given $\ell$, these spectra are entirely dependent on the mass of the black hole $M$, and in fact it can be shown that the two equations are *isospectral* [44] (i.e. both odd and even parity modes oscillate with the same frequencies). Furthermore, note the remarkable similarity between the plots of the potentials $V_{RW}$ and $V_Z$ in figures 3.1 and 3.2. In Chapter

5 we will examine black hole perturbations in GR in more detail, and calculate the QNM spectra analytically.

The recovery of GR is of course the expected result for a theory containing a single tensor perturbation about a Schwarzschild background. Having found that $C_1$ vanishes from the final gauge invariant action, and setting $C_{41} = -\frac{1}{4}M_{Pl}^2$, as explained above, there is no further parameter freedom in our theory. This result may seem to be in contrast to a similar calculation performed on a cosmological background in Chapter 2, where it was found that a time-dependent Planck mass was allowed, and the running of this generalised Planck mass induced modifications in the equations for linear cosmological perturbations. However, in such a case the background evolution of the metric was left free, but if the background evolution was fixed to be that of GR (as in this paper, by setting $f = 1-2M/r$), then the generalised Planck mass would have to be constant and thus no modified evolution for perturbations would be found.

## 3.3 Scalar-Tensor theories on a Schwarzschild background

Having studied the case of a single-tensor perturbation on a Schwarzschild background, we now construct the most general gravitational action for perturbations of a tensor and a scalar field, that leads to second order equations of motion and is linearly diffeomorphism invariant. The stability of stationary black holes under perturbations in scalar-tensor theories has been studied in [154, 155, 156]. We follow the covariant procedure as in the previous section, but with the addition of a gravitational scalar field $\chi$:

$$\chi = \bar{\chi}(r) + \delta\chi; \quad |\delta\chi| \ll |\bar{\chi}|, \tag{3.35}$$

where $\bar{\chi}$ is the background value of the scalar field and $\delta\chi$ is a linear perturbation non-minimally coupled to the metric $g_{\mu\nu}$ and its perturbation, $h_{\mu\nu}$. We will assume that we are considering scalar-tensor theories of gravity where a no-hair theorem exists, such that the background spacetime is still described by the Schwarzschild solution given by eq. (3.1) [140, 141, 157].

In the case that the background is given by eq. (3.1), the background value of the scalar field, $\bar{\chi}$ must correspond to the trivial solution of a constant [140, 141]:

$$\bar{\nabla}_\mu \bar{\chi} = 0. \tag{3.36}$$

Note that the perturbation to the scalar, $\delta\chi$, is non-trivial and still depends on the spacetime coordinates.

Since we have the same background as in the previous section, we continue to use the 1+1+2 split of spacetime with the projectors $u^\mu$, $r^\mu$, and $\gamma_{\mu\nu}$. We proceed to step 2 and write down the most general scalar-tensor gravitational action as:

$$\begin{aligned} S_G^{(2)} = \int d^4x r^2 \sin\theta \, \Big[ & \mathscr{A}^{\mu\nu\alpha\beta} h_{\mu\nu} h_{\alpha\beta} + \mathscr{B}^{\mu\nu\alpha\beta\delta} \bar{\nabla}_\delta h_{\mu\nu} h_{\alpha\beta} + \mathscr{C}^{\mu\nu\alpha\beta\kappa\delta} \bar{\nabla}_\kappa h_{\mu\nu} \bar{\nabla}_\delta h_{\alpha\beta} \\ & + A_\chi (\delta\chi)^2 + \mathscr{A}_\chi^{\mu\nu} \delta\chi h_{\mu\nu} + \mathscr{B}_\chi^{\mu\nu\delta} h_{\mu\nu} \bar{\nabla}_\delta \delta\chi + \mathscr{C}_\chi^{\mu\nu} \bar{\nabla}_\mu \delta\chi \bar{\nabla}_\nu \delta\chi \\ & + \mathscr{D}_\chi^{\mu\nu\delta\kappa} \bar{\nabla}_\kappa \delta\chi \bar{\nabla}_\delta h_{\mu\nu} \Big], \end{aligned} \tag{3.37}$$

where the $\mathscr{A}$, $\mathscr{B}$, and $\mathscr{C}$ are the same as those given by (3.9)-(3.11). We see that we also have two new tensors describing the self-interactions of the scalar field and three for the interactions between the scalar and tensor fields, analogously to eq. (2.43). These new tensors are arbitrary functions of the background, and hence must follow the background symmetry and can be constructed solely from the projectors $u^\mu$, $r^\mu$, and $\gamma_{\mu\nu}$. Similarly as in the previous section, we proceed to write down the most general forms these five new tensors can take:

$$\mathscr{A}_\chi^{\mu\nu} = A_{\chi1} u^\mu u^\nu + A_{\chi2} \gamma^{\mu\nu} + A_{\chi3} r^\mu r^\nu + A_{\chi4} r^\mu u^\nu, \tag{3.38}$$

$$\begin{aligned} \mathscr{B}_\chi^{\mu\nu\delta} = & B_{\chi1} u^\mu u^\nu u^\delta + B_{\chi2} u^\delta \gamma^{\mu\nu} + B_{\chi3} u^\mu \gamma^{\delta\nu} + B_{\chi4} r^\mu r^\nu r^\delta + B_{\chi5} r^\delta \gamma^{\mu\nu} + B_{\chi6} r^\mu \gamma^{\nu\delta} \\ & + B_{\chi7} r^\delta u^\mu u^\nu + B_{\chi8} u^\delta r^\mu r^\nu + B_{\chi9} u^\delta u^\mu r^\nu + B_{\chi10} r^\delta r^\mu u^\nu, \end{aligned} \tag{3.39}$$

$$\mathscr{C}_\chi^{\mu\nu} = C_{\chi1} u^\mu u^\nu + C_{\chi2} \gamma^{\mu\nu} + C_{\chi3} r^\mu r^\nu + C_{\chi4} u^\mu r^\nu, \tag{3.40}$$

$$\begin{aligned} \mathscr{D}_\chi^{\mu\nu\delta\kappa} = & D_{\chi1} u^\mu u^\nu u^\delta u^\kappa + D_{\chi2} u^\mu u^\nu \gamma^{\kappa\delta} + D_{\chi3} u^\kappa u^\delta \gamma^{\mu\nu} + D_{\chi4} u^\mu u^\kappa \gamma^{\delta\nu} + D_{\chi5} \gamma^{\mu\nu} \gamma^{\kappa\delta} \\ & + D_{\chi6} \gamma^{\mu\kappa} \gamma^{\nu\delta} + D_{\chi7} r^\mu r^\nu r^\delta r^\kappa + D_{\chi8} r^\mu r^\nu \gamma^{\kappa\delta} + D_{\chi9} r^\kappa r^\delta \gamma^{\mu\nu} + D_{\chi10} r^\mu r^\kappa \gamma^{\delta\nu} \\ & + D_{\chi11} \gamma^{\mu\nu} r^\kappa u^\delta + D_{\chi12} \gamma^{\mu\delta} u^\mu r^\kappa + D_{\chi13} \gamma^{\mu\delta} r^\mu u^\kappa + D_{\chi14} u^\mu r^\nu \gamma^{\kappa\delta} \\ & + D_{\chi15} r^\mu r^\nu u^\kappa u^\delta + D_{\chi16} r^\mu u^\nu r^\delta u^\kappa + D_{\chi17} u^\mu u^\nu r^\kappa r^\delta + D_{\chi18} r^\mu r^\nu r^\delta u^\kappa \\ & + D_{\chi19} u^\mu r^\nu r^\kappa r^\delta + D_{\chi20} u^\mu u^\nu u^\delta r^\kappa + D_{\chi21} r^\mu u^\nu u^\kappa u^\delta, \end{aligned} \tag{3.41}$$

while $A_\chi$ is a scalar and hence simply considered to be free function of $r$. Here, each of the coefficients $A_{\chi n}$, $B_{\chi n}$, $C_{\chi n}$, and $D_{\chi n}$ are free functions of $r$ also. We see that we have 30 additional free functions due to the inclusion of the scalar field $\chi$.

We now proceed to step 3. As before, we impose linear diffeomorphism invariance of the total action given by eq. (3.37). While the metric transforms as in eq. (3.12) under an infinitesimal coordinate transformation, the new scalar field transforms as:

$$\delta\chi \to \delta\chi + \varepsilon^\mu \bar{\nabla}_\mu \bar{\chi}. \tag{3.42}$$

Note that as we are assuming that our background is Schwarzschild, and as such has no scalar 'hair', $\bar{\nabla}_\mu \bar{\chi}$ vanishes leaving $\delta\chi$ gauge invariant.

The total action given by eq. (3.37) can now be varied under the gauge transformation. As in the previous sections, we obtain a number of Noether constraints by enforcing independent terms in the Noether identities to vanish. Due to $\delta\chi$ being gauge invariant, the Noether constraints that are obtained in Section 3.2 are also valid for the analysis of the action given by eq. (3.37). The additional Noether constraints found for the $A_{\chi n}$, $B_{\chi n}$, $C_{\chi n}$, and $D_{\chi n}$ are given in Appendix B.3. We find that the final action depends on 10 free parameters from the original action given by eq. (3.37):

$$C_{41},\, A_{\chi 0},\, C_{\chi 1-4},\, D_{\chi 5},\, D_{\chi 8},\, D_{\chi 11},\, D_{\chi 15}, \tag{3.43}$$

where once again $C_{41}$ is a constant whilst the other 9 parameters are free to be functions of $r$. Note that $A_{\chi 0}$ and $C_{\chi 1-4}$ are unconstrained due to $\delta\chi$ being gauge invariant on a Schwarzschild background. The final quadratic gauge-invariant action for scalar-tensor theories on a Schwarzschild background can be written as

$$S_G^{(2)} = \int d^4x\, r^2 \sin\theta\, M_{Pl}^2 \left[\mathscr{L}_{EH} + \mathscr{L}_\chi\right], \tag{3.44}$$

where $\mathscr{L}_{EH}$ is given by eq. (2.35), and again we have chosen $M_{Pl}^2 = -4C_{41}$ in order to describe modifications from GR. Thus, the entire action depends on 9 free parameters. The additional Lagrangian due to the inclusion of the scalar field $\chi$ is given by

$$\begin{aligned}
M_{Pl}^2\mathscr{L}_\chi = {} & A_{\chi 0}(\delta\chi)^2 + C_{\chi 1}u^\mu u^\nu \bar{\nabla}_\mu\delta\chi\bar{\nabla}_\nu\delta\chi + C_{\chi 2}\gamma^{\mu\nu}\bar{\nabla}_\mu\delta\chi\bar{\nabla}_\nu\delta\chi + C_{\chi 3}r^\mu\bar{\nabla}_\mu\delta\chi\bar{\nabla}_\nu\delta\chi r^\nu \\
& + C_{\chi 4}u^\mu r^\nu\bar{\nabla}_\mu\delta\chi\bar{\nabla}_\nu\delta\chi - \frac{1}{4m^2}\left(2D_{\chi 5}(f-1)^2 - 2D_{\chi 8}(f-1)^2\right. \\
& + m\left(4f\left(\frac{dD_{\chi 5}}{dr} + \frac{d^2D_{\chi 15}}{dr^2}m + \frac{dD_{\chi 8}}{dr}(f-1) - \frac{dD_{\chi 5}}{dr}f\right)\right. \\
& \left.\left. + \frac{dD_{\chi 15}}{dr}\left(1+2f-3f^2\right)\right)\right)u^\mu u^\nu h_{\mu\nu}\delta\chi + \frac{\sqrt{f}}{2m}D_{\chi 5}(f-1)r^\mu\gamma^{\nu\delta}h_{\mu\nu}\bar{\nabla}_\delta\delta\chi \\
& - \frac{1}{4m}\left(\frac{dD_{\chi 15}}{dr}(f-1)^2 + 4\left(\frac{dD_{\chi 8}}{dr}(1-f) + \frac{d^2D_{\chi 8}}{dr^2}mf\right)\right. \\
& \left. + \frac{dD_{\chi 5}}{dr}\left(f^2-1\right)\right)\gamma^{\mu\nu}h_{\mu\nu}\delta\chi + \frac{1}{4m^2}(f-1)\left(2D_{\chi 5}(f-1) - 2D_{\chi 8}(f-1)\right. \\
& \left. + m\left(\frac{dD_{\chi 15}}{dr}(f-1) + 4\frac{dD_{\chi 8}}{dr}f\right)\right)r^\mu r^\nu \\
& + \frac{1}{4m\sqrt{f}}\left(D_{\chi 11}\left(-1-2f+3f^2\right) - 4\frac{dD_{\chi 11}}{dr}mf\right)u^\delta\gamma^{\mu\nu}h_{\mu\nu}\bar{\nabla}_\delta\delta\chi \\
& + \frac{1}{2m\sqrt{f}}\left(D_{\chi 11}(1-f) + 2\frac{dD_{\chi 11}}{dr}mf\right)u^\mu\gamma^{\delta\nu}h_{\mu\nu}\bar{\nabla}_\delta\delta\chi \\
& + \frac{1}{4m\sqrt{f}}\left(D_{\chi 15}(f-1)^2 + 4D_{\chi 8}f(f-1)\right)r^\mu r^\nu r^\delta h_{\mu\nu}\bar{\nabla}_\delta\delta\chi
\end{aligned}$$

$$
\begin{aligned}
&+\frac{1}{4m\sqrt{f}}\left(-D_{\chi 15}-2D_{\chi 8}(f-1)^2-4\frac{dD_{\chi 8}}{dr}mf+D_{\chi 15}f(2-f)-D_{\chi 5}\left(f^2-1\right)\right)\\
&\times r^{\delta}\gamma^{\mu\nu}h_{\mu\nu}\bar{\nabla}_{\delta}\delta\chi\\
&+\frac{1}{4m\sqrt{f}}\left(D_{\chi 15}(f-1)^2-4f\left(\frac{dD_{\chi 15}}{dr}m-D_{\chi 5}(f-1)+D_{\chi 8}(f-1)\right)\right)\\
&\times r^{\delta}u^{\mu}u^{\nu}h_{\mu\nu}\bar{\nabla}_{\delta}\delta\chi\\
&-\frac{2\sqrt{f}(f-1)}{m}\left(D_{\chi 5}-D_{\chi 8}-D_{\chi 15}\right)u^{\delta}u^{\mu}r^{\nu}h_{\mu\nu}\bar{\nabla}_{\delta}\delta\chi\\
&-\frac{\sqrt{f}(f-1)}{m}D_{\chi 11}r^{\delta}r^{\mu}r^{\nu}h_{\mu\nu}h_{\mu\nu}\bar{\nabla}_{\delta}\delta\chi\\
&+\left(-D_{\chi 5}+D_{\chi 8}+D_{\chi 15}\right)u^{\mu}u^{\nu}\gamma^{\kappa\delta}\bar{\nabla}_{\kappa}\delta\chi\bar{\nabla}_{\delta}h_{\mu\nu}\\
&+\left(-D_{\chi 5}+D_{\chi 8}+D_{\chi 15}\right)u^{\kappa}u^{\delta}\gamma^{\mu\nu}\bar{\nabla}_{\kappa}\delta\chi\bar{\nabla}_{\delta}h_{\mu\nu}\\
&-2\left(-D_{\chi 5}+D_{\chi 8}+D_{\chi 15}\right)u^{\mu}u^{\kappa}\gamma^{\delta\nu}\bar{\nabla}_{\kappa}\delta\chi\bar{\nabla}_{\delta}h_{\mu\nu}+D_{\chi 5}\gamma^{\mu\nu}\gamma^{\kappa\delta}\bar{\nabla}_{\kappa}\delta\chi\bar{\nabla}_{\delta}h_{\mu\nu}\\
&-D_{\chi 5}\gamma^{\mu\kappa}\gamma^{\nu\delta}\bar{\nabla}_{\kappa}\delta\chi\bar{\nabla}_{\delta}h_{\mu\nu}+D_{\chi 8}r^{\mu}r^{\nu}\gamma^{\kappa\delta}\bar{\nabla}_{\kappa}\delta\chi\bar{\nabla}_{\delta}h_{\mu\nu}\\
&+D_{\chi 8}r^{\kappa}r^{\delta}\gamma^{\mu\nu}\bar{\nabla}_{\kappa}\delta\chi\bar{\nabla}_{\delta}h_{\mu\nu}-2D_{\chi 8}r^{\mu}r^{\kappa}\gamma^{\delta\nu}\bar{\nabla}_{\kappa}\delta\chi\bar{\nabla}_{\delta}h_{\mu\nu}\\
&+D_{\chi 11}\gamma^{\mu\nu}r^{\kappa}u^{\delta}\bar{\nabla}_{\kappa}\delta\chi\bar{\nabla}_{\delta}h_{\mu\nu}-D_{\chi 11}\gamma^{\mu\delta}u^{\mu}r^{\kappa}\bar{\nabla}_{\kappa}\delta\chi\bar{\nabla}_{\delta}h_{\mu\nu}\\
&-D_{\chi 11}\gamma^{\mu\delta}r^{\mu}u^{\kappa}\bar{\nabla}_{\kappa}\delta\chi\bar{\nabla}_{\delta}h_{\mu\nu}+D_{\chi 11}u^{\mu}r^{\nu}\gamma^{\kappa\delta}\bar{\nabla}_{\kappa}\delta\chi\bar{\nabla}_{\delta}h_{\mu\nu}\\
&+D_{\chi 15}r^{\mu}r^{\nu}u^{\kappa}u^{\delta}\bar{\nabla}_{\kappa}\delta\chi\bar{\nabla}_{\delta}h_{\mu\nu}-2D_{\chi 15}r^{\mu}u^{\nu}r^{\delta}u^{\kappa}\bar{\nabla}_{\kappa}\delta\chi\bar{\nabla}_{\delta}h_{\mu\nu}\\
&+D_{\chi 15}u^{\mu}u^{\nu}r^{\kappa}r^{\delta}\bar{\nabla}_{\kappa}\delta\chi\bar{\nabla}_{\delta}h_{\mu\nu}. \qquad (3.45)
\end{aligned}
$$

As in Section 3.2, having obtained a form for the fully covariant diffeomorphism invariant action, we can study the odd and even parity perturbations separately.

### 3.3.1 Odd parity perturbations

We will first consider odd parity perturbations, where $h_{\mu\nu}$ is given by eq. (3.17). Since $\delta\chi$ has no contribution to the odd parity sector due to being a scalar, and is also gauge invariant (hence the gravitational self-interactions are the same as in those in the previous section), the odd parity gravitational perturbations are again governed by the Regge-Wheeler equation given by eq. (3.23).

### 3.3.2 Even parity perturbations

For even parity perturbations $h_{\mu\nu}$ is given by eq. (3.18), whilst we decompose $\delta\chi$ into spherical harmonics like so (following the convention of [135])

$$
\delta\chi^{\ell m}=\frac{2\varphi(r)}{r}Y^{\ell m}e^{-i\omega t}, \qquad (3.46)
$$

where $Y^{\ell m}$ is again the standard scalar spherical harmonic [147, 148].

We again vary the gauge invariant scalar tensor action with respect to $H_0$, $H_1$, $H_2$, $K$, and $\varphi$. We find the following algebraic constraints:

$$a_1(r)\varphi = \left[\frac{6M}{r} + (\ell+2)(\ell-1)\right] H_0 - \left[(\ell+2)(\ell-1) - \frac{2\omega^2 r^3}{r-2M} + \frac{2M(r-3M)}{r(r-2M)}\right] K - \left[2i\omega r + \frac{\ell(\ell+1)M}{i\omega r^2}\right] H_1 \tag{3.47}$$

$$H_2 = H_0 + a_2(r)\varphi + b_2(r)\frac{d\varphi}{dr}. \tag{3.48}$$

The following evolution equations for the metric variables are found:

$$\frac{dK}{dr} + \frac{r-3M}{r(r-2M)}K - \frac{1}{r}H_0 + \frac{1}{2}\frac{\ell(\ell+1)}{i\omega r^2}H_1 = a_3(r)\varphi + b_3(r)\frac{d\varphi}{dr} \tag{3.49}$$

$$\frac{dH_1}{dr} + \frac{i\omega r}{r-2M}K + \frac{i\omega r}{r-2M}H_0 + \frac{2M}{r(r-2M)}H_1 = a_4(r)\varphi + b_4(r)\frac{d\varphi}{dr}, \tag{3.50}$$

whilst $\varphi$ obeys:

$$f(r)^2\frac{d^2\varphi}{dr^2} + b_5(r)\frac{d\varphi}{dr} + \left(\omega^2 - f(r)\left(\frac{\ell(\ell+1)}{r^2} + \frac{2M}{r^3}\right) + a_5(r)\right)\varphi = s_1(r)H_1 + s_2(r)K. \tag{3.51}$$

We see that the above equations are modified from those we found for the even sector in GR in section 3.2 through the functions $a_i, b_i, s_i$, which are themselves dependent on the unknown free functions given in eq. (3.43). These coefficient functions are extremely lengthy and unenlightening, so we do not present them explicitly here.

The two first order evolution equations for $H_1$ and $K$ could of course be combined into a single second order equation for a 'master' metric variable. We have then found that, as expected, these scalar-tensor theories propagate one additional degree of freedom, in addition to the two metric perturbations.

Furthermore, we can see that, in general, even though the background black hole has no hair and it is identical to GR, at the level of perturbations the QNM spectrum may be affected, and the evolution of metric perturbations will be generically modified. Hence the detection of ringdown in gravitational wave experiments would allow us to test and distinguish scalar-tensor models from GR.

Next, we proceed to work a specific example of a scalar-tensor theory and show explicitly how the equations of motion can be modified.

### 3.3.3 Jordan-Brans-Dicke

As explained in Section 3.3.1, the equation of motion for odd parity metric perturbations, i.e. the Regge-Wheeler equation, is unaffected by the presence of scalar field perturbations. This is due to the trivial background profile of the scalar field, and the fact that $\delta\chi$ is purely of even parity. Thus, in the following example only the equations for even parity perturbations will be shown in detail.

Let us take our test action to take the form of a simple JBD model with a massless scalar field [135]:

$$S = \int d^4x \sqrt{-g}\, \frac{M_{Pl}^2}{2} \left[\chi R - \frac{\Omega}{\chi}\nabla_\mu\chi\nabla^\mu\chi\right], \tag{3.52}$$

where $R$ is the Ricci scalar and $\Omega$ is a constant. Perturbing eq. (3.52) to quadratic order in linear perturbations we find the following values for the free parameters listed in eq. (A.10):

$$C_{\chi 1} = -C_{\chi 2} = -C_{\chi 3} = -\frac{\Omega}{2},\ D_{\chi 15} = -D_{\chi 5} = -D_{\chi 8} = \frac{1}{4}, \tag{3.53}$$

with $A_{\chi 0}$, $C_{\chi 4}$, and $D_{\chi 11}$ vanishing. Here we have ignored the overall scaling of $M_{Pl}^2$. With this parameter choice, we can in fact reconcile $H_1$, $K$ and $\varphi$ into a single master variable $\tilde{\psi}$ which obeys the Zerilli equation through the following transformations:

$$\begin{aligned} K =& g_1(r)\tilde{\psi} + \left(1 - \frac{2m}{r}\right)\frac{\partial\tilde{\psi}}{\partial r} + \frac{\varphi}{r}, \\ H_1 =& -i\omega\left(g_2(r)\tilde{\psi} + r\frac{\partial\tilde{\psi}}{\partial r}\right), \end{aligned} \tag{3.54}$$

leading to the following system of equations:

$$\frac{d^2\tilde{\psi}}{dr_*^2} + \left(\omega^2 - V_Z\right)\tilde{\psi} = 0, \tag{3.55}$$

$$\frac{d^2\varphi}{dr_*^2} + \left[\omega^2 - \left(1 - \frac{2M}{r}\right)\left(\frac{1}{r^2}\ell(\ell+1) + \frac{2M}{r^3}\right)\right]\varphi = 0, \tag{3.56}$$

Note that we have mixed the even parity metric and scalar perturbations in order to recover the homogenous Zerilli equation for the master variable $\tilde{\psi}$. The field $\tilde{\psi}$ obeying this Zerilli equation is now, however, a mixture of the even parity metric and scalar perturbations, rather than a pure metric perturbation as in the GR case. Furthermore, with the Brans-Dicke parameter choice given by eq. (3.53), the algebraic relationships between the metric perturbations $H_2$, $H_0$ and the other perturbations are also not as in GR, but rather involve the scalar perturbation $\varphi$ as well. Another way of interpreting the above set of equations is that of two oscillators, $\varphi$ which oscillates freely, and $\tilde{\psi}$ which is being driven by

$\varphi$, and thus will oscillate with both a 'transient' and 'forced' response. This phenomenon will be explored in more detail in Chapter 6 in the context of the full family of Horndeski scalar-tensor theories [103].

We can define a generalised Regge-Wheeler potential

$$\hat{V}_{RW} = \left(1 - \frac{2M}{r}\right)\left(\frac{1}{r^2}\ell(\ell+1) + \frac{2\sigma M}{r^3}\right), \tag{3.57}$$

where $\sigma = 1 - s^2$, and with $s$ being the spin of the field being perturbed. We see that in this case of a massless scalar field, the scalar perturbation $\varphi$ obeys an equation of motion of the form

$$\frac{d^2P}{dr_*^2} + \left(\omega^2 - \hat{V}_{RW}\right)P = 0, \tag{3.58}$$

where $P$ is some perturbed field of spin $s$. $\hat{V}_{RW}$ would, for example, be evaluated with $s = \pm 2$ for metric perturbations, and with $s = 0$ for scalar perturbations. Thus for a massless scalar field, both the odd parity metric perturbation and the scalar perturbation obey the generalised Regge-Wheeler equation given by eq. (3.58).

## 3.4 Vector-Tensor theories on a Schwarzschild background

We now study the case of vector-tensor theories of gravity, and construct the most general gravitational action for linear perturbations of a tensor and a vector field that leads to second order equations of motion and is linearly diffeomorphism invariant. We follow the covariant procedure as in the previous sections, but with the addition of a gravitational vector field $\zeta^\mu$:

$$\zeta^\mu = \bar{\zeta}_r(r)r^\mu + \bar{\zeta}_t(r)u^\mu + \delta\zeta^\mu; \quad |\delta\zeta^\mu| \ll |\bar{\zeta}^\mu|, \tag{3.59}$$

where $\bar{\zeta}_r$ and $\bar{\zeta}_t$ are the background values of the field in the $r^\mu$ and $u^\mu$ directions, respectively. We assume the background value of the vector field to be radius-dependent, and to only have components parallel to $u^\mu$ and $r^\mu$, in order to comply with the global symmetries of the background. The vector perturbation $\delta\zeta^\mu$ is a linear perturbation non-minimally coupled to the metric $g_{\mu\nu}$ and its perturbation, $h_{\mu\nu}$.

We again choose to use the 'hair-less' Schwarzschild solution as our background spacetime, as in previous sections. For consistency, in this case, we must impose that the background vector field vanishes:

$$\bar{\zeta}_r = \bar{\zeta}_t = 0. \tag{3.60}$$

The perturbed vector field $\delta\zeta^\mu$ is, however, non-zero. Note that this is slightly different to the case of the scalar-tensor theories discussed in Section 3.3, where the requirement of having no scalar hair simply imposed that the background value of the scalar field be constant (rather than vanishing). This is because in scalar-tensor theories, a constant non-zero background scalar field would only alter the action through the addition of an overall constant that has no physical effect, and hence the background metric solution is the same as the one in GR. However, in vector-tensor theories, a constant background vector field would generically couple to the metric through covariant derivatives (i.e. to the Christoffel symbols), forcing the background metric away from a Schwarzschild solution.

As we are using the same background spacetime as in previous sections, we continue to use a 1+1+2 split of the background with the projectors $u^\mu$, $r^\mu$, and $\gamma_{\mu\nu}$. We now proceed to step 2 and write down the most general vector-tensor gravitational action as:

$$\begin{aligned} S_G^{(2)} = \int d^4x r^2 \sin\theta \, \Big[ & \mathscr{A}^{\mu\nu\alpha\beta} h_{\mu\nu} h_{\alpha\beta} + \mathscr{B}^{\mu\nu\alpha\beta\delta} \bar{\nabla}_\delta h_{\mu\nu} h_{\alpha\beta} + \mathscr{C}^{\mu\nu\alpha\beta\kappa\delta} \bar{\nabla}_\kappa h_{\mu\nu} \bar{\nabla}_\delta h_{\alpha\beta} \\ & + \mathscr{A}^{\mu\nu}_{\zeta^2} \delta\zeta_\mu \delta\zeta_\nu + \mathscr{A}^{\mu\nu\lambda}_{\zeta h} \delta\zeta_\lambda h_{\mu\nu} + \mathscr{B}^{\mu\nu\lambda\kappa}_{\zeta h} h_{\mu\nu} \bar{\nabla}_\kappa \delta\zeta_\lambda + \mathscr{B}^{\mu\nu\kappa}_{\zeta^2} \delta\zeta_\mu \bar{\nabla}_\kappa \delta\zeta_\nu \\ & + \mathscr{C}^{\mu\nu\kappa\delta}_{\zeta} \bar{\nabla}_\kappa \delta\zeta_\mu \bar{\nabla}_\delta \delta\zeta_\nu + \mathscr{D}^{\mu\nu\lambda\delta\kappa}_{\zeta} \bar{\nabla}_\kappa \delta\zeta_\lambda \bar{\nabla}_\delta h_{\mu\nu} \Big], \end{aligned} \tag{3.61}$$

where the $\mathscr{A}$, $\mathscr{B}$, and $\mathscr{C}$ are the same as those given by (3.9)-(3.11). We see that we also have three new tensors describing the self-interactions of the vector field and three for the interactions between the vector and tensor fields, analogously to eq. (2.55). These new tensors are arbitrary functions of the background, and hence must follow the background symmetry and can be constructed solely from the projectors $u^\mu$, $r^\mu$, and $\gamma_{\mu\nu}$. Similarly as in the previous section, we proceed to write down the most general forms these six new tensors can take:

$$\mathscr{A}^{\mu\nu}_{\zeta^2} = A_{\zeta 1} u^\mu u^\nu + A_{\zeta 2} \gamma^{\mu\nu} + A_{\zeta 3} r^\mu r^\nu + A_{\zeta 4} u^\mu r^\nu, \tag{3.62}$$

$$\begin{aligned} \mathscr{A}^{\mu\nu\lambda}_{\zeta h} = & A_{\zeta 5} u^\mu u^\nu u^\lambda + A_{\zeta 6} \gamma^{\mu\nu} u^\lambda + A_{\zeta 7} u^\mu \gamma^{\nu\lambda} + A_{\zeta 8} r^\mu r^\nu r^\lambda + A_{\zeta 9} \gamma^{\mu\nu} r^\lambda + A_{\zeta 10} r^\mu \gamma^{\nu\lambda} \\ & + A_{\zeta 11} r^\mu r^\nu u^\lambda + A_{\zeta 12} u^\mu u^\nu r^\lambda + A_{\zeta 13} r^\mu u^\nu u^\lambda + A_{\zeta 14} u^\mu r^\nu r^\lambda, \end{aligned} \tag{3.63}$$

$$\begin{aligned} \mathscr{B}^{\mu\nu\lambda\kappa}_{\zeta h} = & B_{\zeta 1} u^\mu u^\nu u^\lambda u^\kappa + B_{\zeta 2} u^\mu u^\nu \gamma^{\lambda\kappa} + B_{\zeta 3} u^\kappa u^\lambda \gamma^{\mu\nu} + B_{\zeta 4} u^\mu u^\lambda \gamma^{\kappa\nu} + B_{\zeta 5} u^\mu u^\kappa \gamma^{\nu\lambda} \\ & + B_{\zeta 6} \gamma^{\mu\nu} \gamma^{\lambda\kappa} + B_{\zeta 7} \gamma^{\mu\kappa} \gamma^{\nu\lambda} + B_{\zeta 8} r^\mu r^\nu r^\lambda r^\kappa + B_{\zeta 9} r^\mu r^\nu \gamma^{\lambda\kappa} + B_{\zeta 10} r^\kappa r^\lambda \gamma^{\mu\nu} \\ & + B_{\zeta 11} r^\mu r^\lambda \gamma^{\kappa\nu} + B_{\zeta 12} r^\mu r^\kappa \gamma^{\nu\lambda} + B_{\zeta 13} u^\mu u^\nu r^\kappa r^\lambda + B_{\zeta 14} r^\mu r^\nu u^\kappa u^\lambda \\ & + B_{\zeta 15} u^\mu u^\nu u^\kappa r^\lambda + B_{\zeta 16} u^\mu u^\nu r^\kappa u^\lambda + B_{\zeta 17} r^\mu r^\nu r^\kappa u^\lambda + B_{\zeta 18} r^\mu r^\nu u^\kappa r^\lambda \\ & + B_{\zeta 19} r^\mu u^\nu r^\kappa u^\lambda + B_{\zeta 20} r^\mu u^\nu r^\kappa r^\lambda + B_{\zeta 21} r^\mu u^\nu u^\kappa r^\lambda + B_{\zeta 22} r^\mu u^\nu u^\kappa u^\lambda \\ & + B_{\zeta 23} \gamma^{\mu\nu} u^\kappa r^\lambda + B_{\zeta 24} \gamma^{\mu\nu} r^\kappa u^\lambda + B_{\zeta 25} \gamma^{\kappa\lambda} u^\mu r^\nu + B_{\zeta 26} \gamma^{\mu\kappa} u^\nu r^\lambda \\ & + B_{\zeta 27} \gamma^{\mu\kappa} r^\nu u^\lambda + B_{\zeta 28} \gamma^{\nu\lambda} u^\mu r^\kappa + B_{\zeta 29} \gamma^{\nu\lambda} r^\mu u^\kappa, \end{aligned} \tag{3.64}$$

$$\mathscr{B}^{\mu\nu\kappa}_{\zeta^2} = B_{\zeta 30}u^\mu\gamma^{\kappa\nu} + B_{\zeta 31}r^\mu\gamma^{\kappa\nu} + B_{\zeta 32}u^\mu u^\kappa r^\nu + B_{\zeta 33}u^\mu r^\kappa r^\nu, \tag{3.65}$$

$$\begin{aligned}\mathscr{C}^{\mu\nu\kappa\delta}_{\zeta} = {} & C_{\zeta 1}u^\mu u^\nu u^\kappa u^\delta + C_{\zeta 2}u^\mu u^\nu\gamma^{\kappa\delta} + C_{\zeta 3}u^\kappa u^\delta\gamma^{\mu\nu} + C_{\zeta 4}u^\mu u^\delta\gamma^{\nu\kappa} + C_{\zeta 5}\gamma^{\mu\nu}\gamma^{\kappa\delta} \\ & + C_{\zeta 6}\gamma^{\mu\delta}\gamma^{\nu\kappa} + C_{\zeta 7}r^\mu r^\nu r^\kappa r^\delta + C_{\zeta 8}r^\mu r^\nu\gamma^{\kappa\delta} + C_{\zeta 9}r^\kappa r^\delta\gamma^{\mu\nu} + C_{\zeta 10}r^\mu r^\delta\gamma^{\nu\kappa} \\ & + C_{\zeta 11}r^\mu u^\nu\gamma^{\kappa\delta} + C_{\zeta 12}r^\mu u^\kappa\gamma^{\delta\nu} + C_{\zeta 13}r^\kappa u^\delta\gamma^{\mu\nu} + C_{\zeta 14}r^\mu r^\nu u^\kappa u^\delta \\ & + C_{\zeta 15}r^\mu r^\nu u^\kappa r^\delta + C_{\zeta 16}u^\mu u^\nu r^\kappa r^\delta + C_{\zeta 17}u^\mu u^\nu u^\kappa r^\delta + C_{\zeta 18}r^\mu u^\nu u^\kappa u^\delta \\ & + C_{\zeta 19}r^\mu u^\nu r^\kappa r^\delta + C_{\zeta 20}r^\mu u^\nu u^\kappa r^\delta,\end{aligned} \tag{3.66}$$

$$\begin{aligned}\mathscr{D}^{\mu\nu\lambda\kappa\delta}_{\zeta} = {} & D_{\zeta 1}u^\mu u^\nu u^\lambda u^\kappa u^\delta + D_{\zeta 2}u^\lambda u^\kappa u^\delta\gamma^{\mu\nu} + D_{\zeta 3}u^\lambda u^\mu u^\nu\gamma^{\kappa\delta} + D_{\zeta 4}u^\lambda u^\mu u^\kappa\gamma^{\delta\nu} \\ & + D_{\zeta 5}u^\mu u^\nu u^\delta\gamma^{\kappa\lambda} + D_{\zeta 6}u^\mu u^\kappa u^\delta\gamma^{\nu\lambda} + D_{\zeta 7}u^\lambda\gamma^{\mu\nu}\gamma^{\kappa\delta} + D_{\zeta 8}u^\lambda\gamma^{\mu\kappa}\gamma^{\delta\nu} \\ & + D_{\zeta 9}u^\mu\gamma^{\nu\kappa}\gamma^{\delta\lambda} + D_{\zeta 10}u^\kappa\gamma^{\mu\nu}\gamma^{\delta\lambda} + D_{\zeta 11}u^\kappa\gamma^{\mu\delta}\gamma^{\nu\lambda} + D_{\zeta 12}u^\mu\gamma^{\nu\lambda}\gamma^{\kappa\delta} \\ & + D_{\zeta 13}r^\mu r^\nu r^\lambda r^\kappa r^\delta + D_{\zeta 14}r^\lambda r^\kappa r^\delta\gamma^{\mu\nu} + D_{\zeta 15}r^\lambda r^\mu r^\nu\gamma^{\kappa\delta} + D_{\zeta 16}r^\lambda r^\mu r^\kappa\gamma^{\delta\nu} \\ & + D_{\zeta 17}r^\mu r^\nu r^\delta\gamma^{\kappa\lambda} + D_{\zeta 18}r^\mu r^\kappa r^\delta\gamma^{\nu\lambda} + D_{\zeta 19}r^\lambda\gamma^{\mu\nu}\gamma^{\kappa\delta} + D_{\zeta 20}r^\lambda\gamma^{\mu\kappa}\gamma^{\delta\nu} \\ & + D_{\zeta 21}r^\mu\gamma^{\nu\kappa}\gamma^{\delta\lambda} + D_{\zeta 22}r^\kappa\gamma^{\mu\nu}\gamma^{\delta\lambda} + D_{\zeta 23}r^\kappa\gamma^{\mu\delta}\gamma^{\nu\lambda} + D_{\zeta 24}r^\mu\gamma^{\nu\lambda}\gamma^{\kappa\delta} \\ & + D_{\zeta 25}\gamma^{\mu\nu}r^\kappa r^\delta u^\lambda + D_{\zeta 26}\gamma^{\mu\nu}u^\kappa u^\delta r^\lambda + D_{\zeta 27}\gamma^{\mu\nu}u^\kappa r^\delta u^\lambda + D_{\zeta 28}\gamma^{\mu\nu}u^\kappa r^\delta r^\lambda \\ & + D_{\zeta 29}\gamma^{\lambda\kappa}r^\mu r^\nu u^\delta + D_{\zeta 30}\gamma^{\lambda\kappa}u^\mu u^\nu r^\delta + D_{\zeta 31}\gamma^{\lambda\kappa}r^\mu u^\nu u^\delta + D_{\zeta 32}\gamma^{\lambda\kappa}r^\mu u^\nu r^\delta \\ & + D_{\zeta 33}\gamma^{\mu\lambda}u^\nu r^\kappa r^\delta + D_{\zeta 34}\gamma^{\mu\lambda}u^\nu u^\kappa r^\delta + D_{\zeta 35}\gamma^{\mu\lambda}r^\nu u^\kappa u^\delta + D_{\zeta 36}\gamma^{\mu\lambda}r^\nu u^\kappa r^\delta \\ & + D_{\zeta 37}\gamma^{\kappa\delta}u^\mu u^\nu r^\lambda + D_{\zeta 38}\gamma^{\kappa\delta}r^\mu r^\nu u^\lambda + D_{\zeta 39}\gamma^{\kappa\delta}u^\mu r^\nu u^\lambda + D_{\zeta 40}\gamma^{\kappa\delta}u^\mu r^\nu r^\lambda \\ & + D_{\zeta 41}r^\mu r^\nu r^\lambda u^\kappa u^\delta + D_{\zeta 42}r^\mu r^\nu u^\lambda r^\kappa u^\delta + D_{\zeta 43}r^\mu r^\nu u^\lambda r^\kappa r^\delta + D_{\zeta 44}r^\mu r^\nu r^\lambda u^\kappa r^\delta \\ & + D_{\zeta 45}u^\mu u^\nu r^\lambda u^\kappa u^\delta + D_{\zeta 46}u^\mu u^\nu u^\lambda r^\kappa u^\delta + D_{\zeta 47}u^\mu u^\nu u^\lambda r^\kappa r^\delta + D_{\zeta 48}u^\mu u^\nu r^\lambda u^\kappa r^\delta \\ & + D_{\zeta 49}u^\mu r^\nu u^\lambda u^\kappa u^\delta + D_{\zeta 50}u^\mu r^\nu r^\lambda r^\kappa r^\delta + D_{\zeta 51}u^\mu r^\nu u^\lambda r^\kappa u^\delta + D_{\zeta 52}u^\mu r^\nu r^\lambda u^\kappa u^\delta \\ & + D_{\zeta 53}u^\mu r^\nu u^\lambda r^\kappa r^\delta + D_{\zeta 54}u^\mu r^\nu r^\lambda u^\kappa r^\delta + D_{\zeta 55}\gamma^{\mu\delta}r^\nu u^\lambda r^\kappa + D_{\zeta 56}\gamma^{\mu\delta}r^\nu r^\lambda u^\kappa \\ & + D_{\zeta 57}\gamma^{\mu\delta}r^\nu u^\lambda u^\kappa + D_{\zeta 58}\gamma^{\mu\delta}u^\nu u^\lambda r^\kappa + D_{\zeta 59}\gamma^{\mu\delta}u^\nu r^\lambda u^\kappa + D_{\zeta 60}\gamma^{\mu\delta}u^\nu r^\lambda r^\kappa \\ & + D_{\zeta 61}r^\mu r^\nu u^\lambda u^\kappa u^\delta + D_{\zeta 62}u^\mu u^\nu r^\lambda r^\kappa r^\delta.\end{aligned} \tag{3.67}$$

Each of the coefficients $A_{\zeta n}$, $B_{\zeta n}$, $C_{\zeta n}$, and $D_{\zeta n}$ are free functions of $r$, giving an additional 130 free functions in the most general action (given by eq. (3.61)) due to the inclusion of the vector field $\zeta^\mu$.

We now proceed to step 3. As before, we impose linear diffeomorphism invariance of the total action given by eq. (3.61). While the metric transforms as in eq. (3.12) under an infinitesimal coordinate transformation, a vector field perturbations generically transforms as

$$\delta\zeta^\mu \to \delta\zeta^\mu + \varepsilon^\nu\bar{\nabla}_\nu\left(\bar{\xi}_r(r)r^\mu + \bar{\xi}_t(r)u^\mu\right) - \left(\bar{\xi}_r(r)r^\nu + \bar{\xi}_t(r)u^\nu\right)\bar{\nabla}_\nu\varepsilon^\mu, \tag{3.68}$$

which means that the vector perturbation $\delta\zeta^\mu$ is diffeomorphism invariant in the background given by eq. (3.60).

The total action given by eq. (3.61) can now be varied under the gauge transformation. As in the previous sections, we obtain a number of Noether constraints by enforcing independent terms in the Noether identities to vanish. As in Section 3.3, due to $\delta\zeta^\mu$ being gauge invariant, the Noether constraints that are obtained in Section 3.2 are also valid for the analysis of the action given by eq. (3.61). The additional Noether constraints for the coefficients $A_{\zeta n}$, $B_{\zeta n}$, $C_{\zeta n}$, and $D_{\zeta n}$ are given in Appendix B.4.

We find that the final action depends on the following 39 free parameters from the original action given by eq. (3.61):

$$\begin{aligned} &C_{41},\, A_{\zeta 1-4},\, B_{\zeta 30-33},\, C_{\zeta 1-20},\, D_{\zeta 2},\, D_{\zeta 7},\, D_{\zeta 11},\\ &D_{\zeta 15},\, D_{\zeta 19},\, D_{\zeta 21},\, D_{\zeta 26},\, D_{\zeta 27},\, D_{\zeta 38},\, D_{\zeta 60}, \end{aligned} \tag{3.69}$$

where again $C_{41}$ is a constant, whereas all the other parameters are free functions of radius. We note that 28 of these free parameters, namely $A_{\zeta 1-4}$, $B_{\zeta 30-33}$, $C_{\zeta 1-20}$, describe vector self-interaction terms, and as such are left unconstrained due to the gauge invariant nature of $\delta\zeta^\mu$ in the background we are considering. The remaining 11 free parameters are those that are left after solving the Noether constraints generated by imposing diffeomorphism invariance. The final quadratic gauge-invariant action for vector-tensor theories on a pure Schwarzschild background can thus be written as

$$S_G^{(2)} = \int d^4x\, r^2 \sin\theta\, M_{Pl}^2 \left[\mathscr{L}_{EH} + \mathscr{L}_\zeta\right], \tag{3.70}$$

where $\mathscr{L}_{EH}$ is given by eq. (2.35), and we have chosen $M_{Pl}^2 = -4C_{41}$. Thus we find that the whole action depends on 38 free parameters. The additional Lagrangian $\mathscr{L}_\zeta$ due to the addition of the vector field $\zeta^\mu$ is not presented here for brevity's sake, however the Noether constraints presented in Appendix B.4 can simply be substituted into eq. (3.61) to find the full covariant action.

As in the previous sections, having obtained a form for the fully covariant diffeomorphism invariant action, we proceed to study the odd and even parity perturbations separately. In general, vector-tensor theories can propagate a massive or massless spin-1 particle and hence at most three different polarisations (or degrees of freedom). As we will see next, one of these polarisations couples to the odd parity metric perturbations, and thus modifies the evolution of odd perturbations, contrary to scalar-tensor theories. This suggests that the odd parity sector might be used to test and distinguish vector-tensor and scalar-tensor modified gravity theories.

### 3.4.1 Odd parity perturbations

We will first consider odd parity perturbations, where $h_{\mu\nu}$ is given by eq. (3.17), whilst $\delta\zeta^{\mu}$ is given by

$$\delta\zeta_{\mu}^{\ell m} = z_0(r)e^{-i\omega t}B_{\mu}^{\ell m}, \tag{3.71}$$

with $B_{\mu}^{\ell m}$ being the odd parity vector spherical harmonic as described in [147, 148]. After varying the action given by eq. (3.70) with respect to $h_0$, $h_1$, and $z_0$, we find the following system of second order ODEs:

$$\frac{d^2Q}{dr_*^2} + \left(\omega^2 - V_{RW}\right)Q + c_1\frac{d^2z_0}{dr_*^2} + c_2\frac{dz_0}{dr_*} + c_3 z_0 = 0, \tag{3.72}$$

$$d_4\frac{dQ}{dr_*} + d_5 Q + d_1\frac{d^2z_0}{dr_*^2} + d_2\frac{dz_0}{dr_*} + d_3 z_0 = 0, \tag{3.73}$$

where $Q$ is the Regge-Wheeler function given by eq. (3.24), $r_*$ is the tortoise coordinate given by eq. (3.25), and $V_{RW}$ is the Regge-Wheeler potential as given by eq. (3.26). The $c_n$ and $d_n$ are functions of $r$, $l$, $\omega$, and 10 of the 38 free functions of the theory. Again, these expressions are extremely lengthy and involved so we do not present them explicitly here. The relation linking the metric perturbation $h_0$ to $h_1$ (and thus to $Q$ through eq. (3.24)) and $z_0$ is given in Appendix B.4.

### 3.4.2 Even parity perturbations

For even parity perturbations $h_{\mu\nu}$ is given by eq. (3.18), whilst we decompose $\delta\zeta^{\mu}$ as:

$$\delta\zeta_{\mu}^{\ell m} = \left(-\frac{z_1(r)}{\sqrt{f}}Y^{\ell m}u_{\mu} + z_2(r)\sqrt{f}Y^{\ell m}r_{\mu} + z_3(r)E_{\mu}^{\ell m}\right)e^{-i\omega t}, \tag{3.74}$$

where $E_{\mu}^{\ell m}$ is the even parity vector spherical harmonic [147, 148].

Next, we vary the gauge-invariant vector-tensor action given by eq. (3.70) with respect to $H_0$, $H_1$, $H_2$, $K$, $z_1$, $z_2$, and $z_3$ in order to obtain the relevant set of equations of motion. We find the following constraint equations:

$$\begin{aligned}\mathscr{L}_1(z_1,z_2,z_3) = &\left[\frac{6M}{r} + (\ell+2)(\ell-1)\right]H_0 - \left[(\ell+2)(\ell-1) - \frac{2\omega^2r^3}{r-2M} + \frac{2M(r-3M)}{r(r-2M)}\right]K \\ &- \left[2i\omega r + \frac{\ell(\ell+1)M}{i\omega r^2}\right]H_1 \end{aligned} \tag{3.75}$$

$$H_2 = H_0 + \mathscr{L}_2(z_1,z_2,z_3). \tag{3.76}$$

The following evolution equations for the metric variables are found:

$$\frac{dK}{dr}+\frac{r-3M}{r(r-2M)}K-\frac{1}{r}H_0+\frac{1}{2}\frac{\ell(\ell+1)}{i\omega r^2}H_1=\mathscr{L}_3(z_1,z_2,z_3) \tag{3.77}$$

$$\frac{dH_1}{dr}+\frac{i\omega r}{r-2M}K+\frac{i\omega r}{r-2M}H_0+\frac{2M}{r(r-2M)}H_1=\mathscr{L}_4(z_1,z_2,z_3), \tag{3.78}$$

whilst we find the following evolution equations for the vector variables:

$$\frac{d^2z_1}{dr^2}+\mathscr{L}_5(Z_1,Z_2,Z_3)=\mathscr{S}_5(H_1,K) \tag{3.79}$$

$$\frac{d^2z_2}{dr^2}+\mathscr{L}_6(Z_1,Z_2,Z_3)=\mathscr{S}_6(H_1,K) \tag{3.80}$$

$$\frac{d^2z_3}{dr^2}+\mathscr{L}_7(Z_1,Z_2,Z_3)=\mathscr{S}_7(H_1,K) \tag{3.81}$$

In the above equations we are using the notation $\mathscr{L}_i(p_1,...,p_n)$ to denote a linear combination of the $p_i$ fields and their derivatives (up to second order), with each term having a coefficient which is a function of $r$ and of the free functions given in eq. (3.69). We also use $\mathscr{S}_i(H_1,K)$ to denote a linear combination of $H_1$ and $K$, similarly with radially dependent coefficients. As with the scalar tensor case, the linear combinations of variables representing the 'non-GR' behaviour of the system of equations is incredibly lengthy and unenlightening, so we do not present them explicitly.

Here we can see that there can be three dynamical vector degrees of freedom contributing to the even parity sector – namely $z_1$, $z_2$ and $z_3$ – which gives a total of four when counting the odd parity perturbation $z_0$ as well. As previously mentioned, we might have naively expected at most three vector degrees of freedom, corresponding to the three polarisations of a massive spin-1 particle. However, general vector-tensor theories can be unhealthy and propagate an additional ghostly mode. Indeed, in [89, 86] the same result was found for linear perturbations around a cosmological background in vector-tensor theories. This ghostly mode can be recast as a scalar field with negative kinetic energy that makes the physical system unstable. Usually, specific conditions must be imposed in vector-tensor theories (and modified gravity theories, more generally) in order to avoid such an unstable mode. In the case presented in this paper, we can fix some of the free parameters appropriately and reduce the number of vector dynamical degrees of freedom from four to three and hopefully, therefore, describe healthy vector-tensor theories only. For instance, we can choose the free parameters such that $z_3$ becomes an auxiliary variable that can simply be worked out from the above equations in terms of the other dynamical fields in order to reduce the whole even-parity system to a set of three second-order coupled ODEs (for two dynamical vector and one dynamical tensor degrees of freedom)[4].

[4]A more careful analysis may be required to *guarantee* the removal of the ghostly degree of freedom.

Next, similarly to the previous section, we proceed to work out a specific example of vector-tensor theories and show explicitly the equations of motion for odd and even parity sectors. Unfortunately, we have been unable to find non-linear vector-tensor models that lead to non-trivial metric perturbations. In particular, we looked at the currently most general fully diffeomorphism-invariant vector-tensor theory, known as Generalised Proca [143], which seems to be lacking second-order derivative couplings between the metric and vector perturbations for our chosen black hole background. Our results on the general parametrised vector-tensor action show that modified metric perturbations are allowed though, and therefore it will be interesting to explore in the future what non-linear interactions can be constructed to obtain such modifications.

### 3.4.3 Massless Vector field

For the case of a massless vector field the action is given by [143]:

$$S = \int d^4x \sqrt{-g} \left[ \frac{M_{Pl}^2}{2} R - \frac{1}{4} F_{\alpha\beta} F^{\alpha\beta} \right], \tag{3.82}$$

where $F_{\alpha\beta} = \nabla_\alpha \zeta_\beta - \nabla_\beta \zeta_\alpha$ is the field strength. Perturbing the fields, about a vanishing background for the case of the vector field $\zeta^\alpha$, and expanding to quadratic order, we find the following values of the parameters given in eq. (3.69)

$$\begin{aligned} C_{\zeta 2} =& C_{\zeta 3} = C_{\zeta 6} = C_{\zeta 14} = C_{\zeta 16} = -C_{\zeta 5} = -C_{\zeta 8} = \frac{1}{2}, \\ C_{\zeta 4} =& C_{\zeta 20} = -C_{\zeta 10} = 2C_{\zeta 9} = -1, \end{aligned} \tag{3.83}$$

with all other parameters vanishing. With this set of parameters, we find that for odd parity perturbations $Q$ and $z_0$ obey the following set of equations:

$$\begin{aligned} &\frac{d^2 Q}{dr_*^2} + \left(\omega^2 - \hat{V}_{RW}\right) Q = 0, \\ &\frac{d^2 z_0}{dr_*^2} + \left(\omega^2 - \hat{V}_{RW}\right) z_0 = 0, \end{aligned} \tag{3.84}$$

where $\hat{V}_{RW}$ is given by eq. (3.57) and is evaluated with $s = 1, 2$ for the vector and metric perturbations respectively.

For even parity perturbations, we find the following set of equations:

$$\begin{aligned} &\frac{d^2 \psi}{dr_*^2} + \left(\omega^2 - V_Z\right) \psi = 0 \\ &\frac{d^2 Z}{dr_*^2} + \left(\omega^2 - \hat{V}_{RW}\right) Z = 0 \end{aligned} \tag{3.85}$$

where $Z$ is given by (following the convention of [158]):

$$Z = r^2 \left( z_2 + \frac{1}{i\omega} \frac{dz_1}{dr} \right), \tag{3.86}$$

$z_3$ is related to the other fields through

$$z_3 = \frac{1}{\ell(\ell+1)} \left[ \left( 1 - \frac{2M}{r} \right) \frac{dZ}{dr} - \frac{1}{i\omega} \left( \ell(\ell+1) \right) z_1 \right], \tag{3.87}$$

and $\psi$ is the regular Zerilli function as in GR (given by eq. (3.31), $V_Z$ is given by eq. (3.34) while $\hat{V}_{RW}$, given by eq. (3.57), is again evaluated with $s = 1$ for the vector perturbations.

From these equations, we can make a number of remarks. We can see that, as expected, the massless vector perturbations propagate only two degrees of freedom in total ($z_0$ and $Z$), instead of four, because $z_2$ and $z_3$ have become auxiliary variables. This is because the Proca action is constructed in such a way that it is healthy and does not propagate any additional ghostly modes, and thus the two degrees of freedom for odd and even parity vector perturbations, respectively, correspond to the two polarisations of a massless spin-1 particle. Both of these fields now obey the standard Regge-Wheeler equation (with the potential $\hat{V}_{RW}$ evaluated for $s = 1$) [158, 159, 160].

We also note that the metric perturbations $Q$ and $\psi$ obey the usual Regge-Wheeler and Zerilli equations respectively, as in GR. Furthermore, we find that the metric perturbations $h_0$ and $H_2$ (of odd and even parity, respectively) are related to the other perturbed fields through their usual GR relations. Thus the metric perturbations evolve exactly as in GR, as expected for a minimally coupled Maxwell field.

## 3.5 Conclusion

In this chapter we have analysed the structure of linear perturbations around black holes in modified gravity theories. In particular, we applied the covariant approach developed in Chapter 2 to construct the most general diffeomorphism-invariant quadratic actions for linear perturbations around a Schwarzschild black hole for three families of gravity theories: single-tensor, scalar-tensor, and vector-tensor theories. These actions contain a number of free parameters – functions of the background – that describe all the possible modifications to GR that are compatible with the given field content and symmetries. Therefore, these actions allow us to study, in a unified manner, a number of scalar-tensor models such as JBD gravity, as well as vector-tensor models such as Maxwell and Proca.

Our focus has been on perturbations of Schwarzschild spacetimes but the method used here is general and systematic and can thus be straightforwardly applied to other spherically

symmetric backgrounds with non-trivial solutions for the additional gravity field. Such an extension would allow us to study the dynamics of linear perturbations in modified gravity with hairy solutions such as Einstein-Aether [161, 162] or scalar Gauss-Bonnet gravity . Furthermore, the method presented here is readily generalisable to non-spherically symmetric backgrounds, for example rotating black holes. For slowly rotating black holes, various no-hair theorems for scalar and vector fields (with non-minimal coupling or otherwise) are presented in [141, 54], however perturbations to hairy rotating black holes could also be analysed in the manner presented in this paper.

For each of the three families of modified gravity theories, we have found the equations of motion governing odd and even parity perturbations, in terms of the free parameters. In general, we found that even though at the level of the background all models considered have no hair (a Schwarzschild metric) and behave as GR, at the level of perturbations additional degrees of freedom are indeed excited and thus there is a dynamical hair that gives a modified evolution for linear perturbations [130]. Nevertheless, we also find specific examples in which the additional degrees of freedom are not excited and thus perturbations evolve as in GR. In particular, we find that general single-tensor models behave exactly as GR at the level of linear perturbations. For scalar-tensor theories, we find the most general action to have 9 free parameters (functions of radius). All of these parameters affect the evolution of even perturbations, while odd perturbations evolve as in GR. For vector-tensor theories, the most general action depends on 38 free parameters (all functions of radius) and generically they will modify the evolution of odd and even perturbations. More specifically, we find that 10 free parameters modify the evolution of odd perturbations, whilst all 38 affect even perturbations.

As a comparison, we mention that in the corresponding calculations of diffeomorphism-invariant quadratic actions about a cosmological FLRW background presented in Chapter 2, fewer free parameters were found. For instance, there are four free parameters for scalar-tensor theories about an FLRW background compared to 9 free parameters about a Schwarzschild background. As discussed in Chapter 2, the global symmetries of the background play a crucial role in determining the number of free parameters. In general, the less symmetric the background, the more free parameters are needed to describe general linear perturbations. Therefore, the larger number of free parameters found in this paper is not surprising. Furthermore, in the case of the pure Schwarzschild background studied here, the scalar self interactions are unconstrained because the scalar field perturbation is gauge invariant, contrary to the FLRW case. Similarly, a large number of free parameters in the vector-tensor action are left unconstrained due to the vector field perturbation being gauge invariant.

The equations of motion derived in this paper are the most general ones for each family theory, and they provide a valuable tool for exploring modified theories of gravity with gravitational waves, and also for exotic test fields. This provides a new tool to the usual approach to quasi-normal mode analysis of black holes. Given an equation of motion, one can calculate the quasi-normal modes of the system, for example through the methods of [138, 163]. With future improved observations of quasi-normal modes from binary black hole events one could constrain the free parameters presented in this paper by constraining the effect these terms would have on the waveform. Whereas in practice it may not be possible to constrain 9 or 38 arbitrary functions of radius, these free parameters can be reduced by adding theoretical stability constraints, or they can be chosen to, for example, correspond to a particular non-linear theory, or they can be fitted with some specific functional forms.

A particularly interesting case is that of JBD scalar-tensor gravity, where we found that it was possible to find a combination of metric and scalar variables that obeyed the Zerilli equation, leading to the same QNM spectrum as in GR. The field obeying this equation is now, however, a combination of the metric and scalar variables, and thus we can interpret this system as being analogous to that of a free and driven oscillator coupled together. We will see in Chapter 6 that this phenomenon is not restricted to JBD gravity, but rather to a large family of scalar-tensor theories with conformal coupling between the scalar field and curvature.

An interesting recent development is the detection of the binary neutron star merger with gravitational wave signal GW170817 [164] and an electromagnetic counterpart GRB 170817A [165, 166, 167, 168]. The fact that the gravitational and electromagnetic waves are effectively coincident was subsequently used to place tight constraints on the difference in their velocities and, as a result, to place strong constraints on the range of possible extensions to General Relativity. In particular it was found that, in some sense, the simplest forms of non-minimal coupling were allowed in scalar-tensor and vector-tensor theories [157, 169, 170, 171], severely limiting the allowed range of cosmological models. Given how restrictive the constraints are, it would make sense to focus on how it restricts the allowed families of black hole solutions to the classes of theories being considered in this paper. For a start, and more generally, it would be interesting to identify how many theories still allow for hairy black holes. Indeed, this will be the focus of Chapter 4.

# Chapter 4

# The speed of gravitational waves and black hole hair

# Abstract

The recent detection of GRB 170817A and GW170817 constrains the speed of gravity waves $c_T$ to be that of light, which severely restricts the landscape of modified gravity theories that impact the cosmological evolution of the universe. In this chapter, I investigate the presence of black hole hair in the remaining viable cosmological theories of modified gravity that respect the constraint $c_T = 1$. The focus will mainly be on scalar-tensor theories of gravity, analysing static, asymptotically flat black holes in Horndeski, Beyond Horndeski, Einstein-Scalar-Gauss-Bonnet, and Chern-Simons theories. We find that in all of the cases considered here, theories that are cosmologically relevant and respect $c_T = 1$ do not allow for hair, or have negligible hair. We further comment on vector-tensor theories including Einstein Yang-Mills, Einstein-Aether, and Generalised Proca theories, as well as bimetric theories. This chapter is based on [87].

## 4.1 Introduction

At high energies, unavoidable singularities arise during gravitational collapses and the so-called renormalization problem limits the analysis of quantum states using GR. At low energies, in particular, on cosmological scales, GR relies on the presence of an unknown component (such as dark energy or a cosmological constant) in order to explain the observed accelerated expansion of the Universe. Indeed the unexplained small value of the observed cosmological constant $\Lambda$, being defiantly 120 orders of magnitude smaller than one might predict from Quantum Field Theory, is a particularly troubling conundrum for modern physics [172]. These limitations suggest that GR may need modifications for both extreme energy regimes. Furthermore, modifications in the two regimes may be related as high energy corrections to GR might leak down to cosmological scales, showing up as low energy corrections. In this chapter we explore possible connections between these two regimes. In particular, we will show how recent local constraints on the speed of gravity waves limit solutions for compact objects.

In the past decades a large variety of gravity theories have been proposed [173]. They have been extensively studied and constrained with cosmological data from CMB and large scale structure. However, recently strong constraints have been imposed with the detection of gravitational waves emission GW170817 from a neutron star binary merger by LIGO and VIRGO [164], and its optical counterpart (the gamma ray burst GRB 170817A) [165, 166, 167, 168, 174]. The delay of the optical signal was of 1.7 seconds, which places a stringent constraint on the propagation speed of gravity waves $c_T$[1]. Indeed, it was found that $|c_T^2 - 1| < 1 \times 10^{-15}$ (with unity speed of light). As a result, a large class of modified gravity theories was highly disfavoured as argued in [175, 176, 169, 157, 170, 171].

On the other hand, there have also been efforts to test gravity theories from observations of black holes [59, 127, 177]. GR predicts that black holes are solely characterized by a few "charges" – their mass $m$, angular momentum $a$ and electric charge $Q$ – through what is known as the no-hair theorem. In extensions to GR additional degrees of freedom are usually introduced, which may add a new kind of charge to the spacetime solution. In this case, the metric carries additional information besides the mass, angular momentum and electric charge, and we say we are in the presence of a hairy black hole. These extra degrees of freedom will be carriers of fifth forces which may be detected from star orbits around the black holes [178, 179, 180] or from the overall structure of accreting gas near the event horizon [181, 182, 183]. These two examples correspond to non-dynamical tests

[1] Whilst the propagation of electromagnetic waves may in principle be affected by plasma (for example), the intergalactic medium dispersion is expected to have a "negligible impact on gamma-ray photon speed" [166].

which probe the stationary spacetime of a black hole. We note however, that even in the case where theories can avoid hair and have the same stationary black hole solutions as GR, new signatures may arise in dynamical situations; for example, when black holes are formed in a binary merger, the ringdown signal may carry modifications that can be traced back to the new degrees of freedom [130, 83, 37]. In general, dynamical tests allow us to distinguish models that have the same stationary spacetime. We saw this in Chapter 3 and will explore in more detail in Chapter 6.

In this chapter we consider gravity models that have $c_T = 1$ on a cosmological background – where the extra degrees of freedom can play a significant role on cosmological scales – and, as a first approach, expose the relation between the presence of hairy static black hole solutions and the speed of gravity waves. Before we proceed, it is important to clarify what type of "hair" we will be considering here. We will consider hair to be any modification to GR that can be measured with non-dynamical tests (such as analyses on orbits of stars or electromagnetic imaging of the accretion flow around the black hole). In particular, hair will be a permanent charge in a static, spherically symmetric, and asymptotically flat spacetime. When the metric profile is characterised by a new global charge (different to mass, spin or electric charge) we will say we have "primary" hair, and if the profile has modifications that depend on the same charges as in GR, we say we have "secondary" hair [184, 185]. This distinction is important to understand the number of independent parameters that fully determine the black hole solution, but both have physical consequences as they induce a geometry different to GR.

We mention that in some cases it may be possible to construct "stealth" black holes, where the geometry of spacetime is unchanged from the corresponding GR solution (i.e. no new charge), but the black hole is dressed with a non-trivial additional field profile. For example, some stealth black hole solutions in scalar-tensor and vector-tensor theories can be found in [186, 187]. In this situation, non-dynamical tests will not be able to distinguish these models from GR and, therefore, for the purpose of this chapter, these examples will not be considered as hairy solutions.

With a clear definition of hair, we explore static, asymptotically flat black hole solutions on different modified gravity theories that are cosmologically relevant. We find that all scalar-tensor theories considered here have no hair at all or hair with negligible effects (although exceptions can be found in theories with no cosmological effects). Other models such as vector-tensor or bimetric theories more easily lead to hairy black holes regardless of their cosmological solution. We find examples with primary and secondary hair. This study allows us to identify the theories which may lead to observable signatures on *both*

cosmological and astrophysical scales, and can be used to build a roadmap for a coordinated study with future large scale structure surveys and gravitational wave observations.

No-hair theorems for GR and modified gravity (e.g. [188]) have been constructed under quite strict conditions, e.g. the spacetime must be asymptotically flat and hair must be permanent. It is straightforward to break these conditions in a reasonable way [127] and thus obtain hairy solutions, even in GR. For instance, changing the boundary conditions may lead to the Schwarzschild-de Sitter solution which has a metric such that $g_{00} = 1 - 2M/r + \Lambda r^2/3$, i.e. an extra term proportional to $\Lambda$ which might be considered hair. Alternatively, in scalar-tensor theories, a time-dependent boundary condition for the scalar field can anchor hair on the surface of the black hole [189]. In the same way, more complex extra fields can be arranged to form hair. A notable example arises with a complex scalar field [184] or with coupled dilaton-Maxwell systems [190]. More recently, it has been shown that it is possible to construct solutions in which massive scalar fields hover around black holes for an extended period of time [191] leading to long-lived but not permanent hair. Given that we live in a cosmological spacetime with an abundance of fields, all of these examples show that hair can be easily present in black holes under reasonable assumptions.

Nevertheless, all the mechanisms that have been proposed so far lead to very mild hair which, arguably, may be unobservable. For example, "de Sitter" hair is remarkably weak compared to the usual Newtonian potential and any cosmological boundary condition that might lead to scalar hair will be highly suppressed. So if one can show that a theory must satisfy the no-hair theorem, it is extremely likely that any attempts at breaking it solely through changing the boundary condition will lead to effects which are too weak to be detected as a fifth force (although they might emerge in a stronger gravitational regime, like a black hole merger). This means that no-hair theorems are a useful guide to undertake a rough census of where to look in the panorama of gravitational theories.

This chapter is organized as follows. In Section 4.2 we discuss the speed of gravitational waves in the context of modified gravity. In Section 4.3 we focus on scalar-tensor theories with $c_T = 1$ and discuss the presence of hairy static black hole solutions. In Sections 4.4 we discuss mainly vector-tensor theories as well as other gravitational models with $c_T = 1$ that do evidence hair, such as bimetric theories. Finally, in Section 4.5 we summarise our results and discuss their consequences.

## 4.2 The speed of gravitational waves.

GR is a single metric theory for a massless spin-2 particle, and hence it propagates two physical degrees of freedom corresponding to two polarizations. On any given background spacetime, GR predicts that both polarizations propagate locally along null geodesics, and thus gravitational waves travel at the same speed as that of electromagnetic waves. This feature is particular of GR where Lorentz invariance is locally recovered, and hence all massless waves are expected to propagate at the same speed. However, such a feature can easily change in a theory of gravity where additional degrees of freedom are coupled to the metric in a non-trivial way. These additional fields can take special configurations in different backgrounds, and define a preferred direction that will spontaneously break local Lorentz invariance. In this case, there will be an effective medium for propagation of gravity waves, and their speed will change. Furthermore, depending on the configurations of the additional degrees of freedom, the speed of gravity waves could be anisotropic and even polarization dependent [192].

The speed of gravity waves can be used to discriminate and test various modified gravity theories. This has been a topic of special interest in cosmology where a number of models have been proposed. In this case, the metric background is given by:

$$\bar{g}_{\mu\nu} = -dt^2 + a(t)^2 d\vec{x}^2, \tag{4.1}$$

where $a(t)$ is the scale factor describing the expansion of the universe. Gravitational waves are described by small perturbations of the metric and thus we can write the total metric as:

$$g_{\mu\nu} = \bar{g}_{\mu\nu} + h_{\mu\nu}, \tag{4.2}$$

where $h_{\mu\nu}$ describes the amplitude of the waves and carries the information of all the metric polarizations. In this background, additional gravitational fields such as scalars or vectors will generically have a time-dependent solution which, even in a local frame, will define a preferred direction of time. It has been shown that for single-metric gravity models propagating a massless spin-2 particle, the action for gravity waves can generically be written as (see, for example, eq. (2.41) or [193]):

$$S_{GW} = \frac{1}{2}\int d^4x\, a^3\, M_*^2(t)\left[\dot{h}_A^2 - c_T^2(t)(\vec{\nabla} h_A)^2\right], \tag{4.3}$$

where we have expanded $h_{\mu\nu}$ in two polarization components $h_A$ with $A = +, \times$[2]. Here, $M_*$ is an effective Planck mass and $c_T$ is the propagation speed of gravity waves. Both of

[2]Bimetric gravity theories will propagate additional tensor modes that will generically be coupled to $h$, and hence the action for gravity waves will be different to that in eq. (4.3). Nevertheless, a similar analysis can be done to find $c_T$ (or some dispersion relation) in FRW.

these quantities may in general depend on time, and thus in this case the speed will always be isotropic and polarization independent. It is usual that $c_T$ depends on the background solution of the additional gravitational degrees of freedom.

Let us consider one particular example of a shift-symmetric quartic Horndeski gravity theory [103, 104] given by:

$$S = \frac{1}{2}\int d^4x\sqrt{-g}\left[G(X)R + G_{,X}(X)\left((\Box\phi)^2 - \nabla_\mu\nabla_\nu\phi\nabla^\mu\nabla^\nu\phi\right)\right], \tag{4.4}$$

where $\phi$ is an additional gravitational scalar field, and $G$ is an arbitrary function of the kinetic term $X = -\frac{1}{2}\nabla_\mu\phi\nabla^\mu\phi$ and $G_{,X}$ its derivative with respect to $X$. On a cosmological background, following [193], we obtain the following action for tensor perturbations:

$$S_{GW} = \frac{1}{2}\int d^4x a^3\left(G(X) - 2XG_{,X}(X)\right)\left[\dot{h}_A^2 - \frac{1}{1-2XG_{,X}(X)/G(X)}(\vec{\nabla}h_A)^2\right]. \tag{4.5}$$

In the above example we thus find a time dependent effective Planck mass $M_*^2 = (G - 2XG_{,X})$ and a tensor propagation speed of $c_T^2 = 1/(1 - \frac{2XG_{,X}}{G})$. One can see that, Taylor expanding, $G \simeq G_0 + XG_{,X}$, if $XG_{,X} \ll G_0$ then, $c_T \simeq 1$. This can occur if $XG_X$ is small but also if $G_0$ is large, i.e if the contribution of the scalar field to the overall cosmological dynamics is negligible. In this chapter we will consider the case when the contribution to the background dynamics is *not* negligible, i.e. the extra degree of freedom has a relevant impact on cosmological scales.

There are, of course, cases in which the additional degrees of freedom do not affect the propagation speed of gravity waves. A particular, well-studied, example is Jordan-Brans-Dicke theory [194, 195] given by:

$$S = \frac{1}{2}\int d^4x\sqrt{-g}\left[\phi R - \frac{\omega}{\phi}(\nabla_\mu\phi\nabla^\mu\phi)\right], \tag{4.6}$$

where $\omega$ is an arbitrary constant. In this case $c_T = 1$.

## 4.3 Scalar-Tensor Theories

Scalar-tensor theories have been extensively studied in both the strong gravity and cosmological regime. Much effort in recent years has been put into researching general theories of a scalar field non-minimally coupled with a metric; from Horndeski gravity [196], to Beyond Horndeski [197, 198], and Degenerate Higher Order Scalar Tensor (DHOST) theories [199]. Furthermore scalar-tensor theories are ubiquitous in that they appear as some limit of other theories of gravity, such as the decoupling limit of massive gravity [200]. The well-posedness and hyperbolicity of scalar-tensor theories has been studied in [201, 202].

We will focus on Horndeski and Beyond Horndeski theories in this section (as well as Chern-Simons [144] and Einstein-Scalar-Gauss-Bonnet gravity [203]) and show the solutions of static black holes when $c_T = 1$. In this chapter, we will ignore DHOST theories due to the relative infancy of research into their black hole solutions. Cosmological consequences of the detection of GW/GRB170817 to DHOST theories has, however, been investigated in [204, 205].

### 4.3.1 Horndeski

The most general action for scalar-tensor gravity with $2^{nd}$ order-derivative equations of motion is given by the Horndeski action [103]:

$$S = \int d^4x\sqrt{-g}\sum_{n=2}^{5} L_n, \tag{4.7}$$

where the Horndeski Lagrangians are given by:

$$L_2 = G_2(\phi,X) \tag{4.8}$$

$$L_3 = -G_3(\phi,X)\Box\phi \tag{4.9}$$

$$L_4 = G_4(\phi,X)R + G_{4,X}(\phi,X)((\Box\phi)^2 - \phi^{\mu\nu}\phi_{\mu\nu}) \tag{4.10}$$

$$L_5 = G_5(\phi,X)G_{\mu\nu}\phi^{\mu\nu} - \frac{1}{6}G_{5,X}(\phi,X)((\Box\phi)^3 - 3\phi^{\mu\nu}\phi_{\mu\nu} + 2\phi_{\mu\nu}\phi^{\mu\sigma}\phi^{\nu}_{\sigma}), \tag{4.11}$$

where $\phi$ is the scalar field with kinetic term $X = -\phi_\mu\phi^\mu/2$, $\phi_\mu = \nabla_\mu\phi$, $\phi_{\mu\nu} = \nabla_\nu\nabla_\mu\phi$, and $G_{\mu\nu} = R_{\mu\nu} - \frac{1}{2}Rg_{\mu\nu}$ is the Einstein tensor. The $G_i$ denote arbitrary functions of $\phi$ and $X$, with derivatives $G_{i,X}$ with respect to $X$.

For theories where the scalar field plays some role on the cosmological scales, the constraint $c_T = 1$ imposes $G_{4,X} = 0$ and $G_5$ has to be constant (in which case $L_5$ vanishes through Bianchi identity). Therefore, the resulting constrained Horndeski action is given by:

$$S = \int d^4x\sqrt{-g}\left[G_4(\phi)R + G_2(\phi,X) - G_3(\phi,X)\Box\phi\right]. \tag{4.12}$$

If we construct a modified Friedmann equation for Horndeski gravity such that $H^2 = H_0^2(\Omega_m + \Omega_\phi)$, where $H_0$ is the value of the Hubble parameter today and $\Omega_m$ includes the background energy densities of all other forms of matter, the energy density for the Horndeski scalar $\Omega_\phi$ is given for the above action by [105]:

$$\Omega_\phi = \frac{-G_2 + 2X\left(G_{2,X} - G_{3,\phi}\right) + 6\dot{\phi}H_0\left(XG_{3,X} - G_{4,\phi}\right)}{6G_4H_0^2}, \tag{4.13}$$

where $G_{i,\phi}$ denote derivatives of the functions $G_i$ with respect to $\phi$, and overdots denote derivatives with respect to time. In this case, we expect the cosmological energy density fraction of the scalar field $\Omega_\phi \sim O(1)$ due to our considering only *cosmologically relevant* theories.

We now proceed to analyse the black hole solutions arising from the action in equation (4.12). Even though there is no no-hair theorem for generic $G_i$ functions, there are a number of theorems for restricted cases. We mention three distinct families of models.

First, through a conformal transformation, the action in equation (4.12) can be re-expressed in the form of GR plus a minimally coupled scalar field (with modified $G_2$ and $G_3$ [206]). The Lagrangian would then resemble a Kinetic Gravity Braiding model [207]. For $G_2 = \omega(\phi)X$, $G_3 = 0$, the reduced Horndeski action can be seen to be in the form of generalised Brans-Dicke theories [33], for which a no hair theorem exists [188]. Second, a no-hair theorem for K-essence (i.e. $G_3 = 0$, $G_4 = 1$) is given in [208], provided that $G_{2,X}$ and $\phi G_{2,\phi}$ are of opposite and definite signs. Third, we mention that for shift-symmetric theories, which are invariant under $\phi \to \phi+$constant and hence $G_{i,\phi} = 0$ in eq. (4.12), the action takes the form of a minimally coupled scalar field with potentially unusual kinetic terms arising from $G_2(X)$ and $G_3(X)$. For such shift-symmetric theories, no-hair theorems exist for static black holes [209, 188]. The outline of these no-hair theorems for shift-symmetric theories is given by: (i) spacetime is spherically symmetric and static, and the scalar field shares the same symmetries; (ii) spacetime is asymptotically flat, $\frac{d\phi}{dr} \to 0$ when $r \to \infty$, and the norm of the Noether current associated to the shift symmetry is regular on the horizon; (iii) there is a canonical kinetic term $X$ in the action and the $G_{i,X}$ functions contain only positive or zero powers of $X$.

We note that this no-hair theorem is valid for all shift-symmetric Horndeski actions that satisfy the above conditions, even those that do not satisfy the constraint $c_T = 1$. Focusing on a spherically symmetric and static spacetime, we can still have hairy black hole solutions by breaking assumptions (ii) or (iii) of this no-hair theorem. It is indeed expected that realistic situations of dark-energy models will break assumption (ii) as the scalar field is responsible for the late-time accelerated expansion of the universe or, more generally, the scalar field can lead to large-scale effects and thus $\frac{d\phi}{dr}$ does not necessarily vanish when $r \to \infty$. Examples like this can easily be realized by adding a time-dependent boundary condition to the scalar field [189] associated to the cosmological expansion. However, such a scalar hair would be highly suppressed and negligible in the vicinity of a black hole.

We explore further cases that violate assumption (iii). A number of Lagrangians that break this assumption are discussed in [186] but we will focus on the only two examples which still obey the constraint $c_T = 1$ for Horndeski gravity. In addition, we will discuss a

class of theories that even though they explicitly depend on $\phi$, are related to shift-symmetric theories via conformal transformations and therefore they also satisfy the no-hair theorem previously mentioned.

#### 4.3.1.1 Quadratic term

The first potentially hair-inducing term posited in [186] is the addition of a square-root quadratic term to the canonical kinetic term, $G_2(X) = X + 2\beta\sqrt{-X}$, $G_4 = \frac{1}{2}M_P^2$, where $\beta$ is an arbitrary constant. As we can see, in this case $G_{2,X}$ does contain negative powers of $X$ and thus hairy black holes may appear.

First, we require the scalar field to be cosmologically relevant, and thus

$$\Omega_\phi = \frac{-X}{3M_P^2H_0^2} \sim O(1). \tag{4.14}$$

Now, assuming a spherically symmetric and static ansatz for the metric and scalar field:

$$ds^2 = -h(r)dt^2 + \frac{1}{f(r)}dr^2 + r^2d\Omega^2,\ \phi = \phi(r) \tag{4.15}$$

and requiring that the radial component of the Noether current $J^r = \frac{1}{\sqrt{-g}}\frac{\delta S}{\delta(\partial_r\phi)} = 0$ (to ensure a regular current on the horizon, as required in assumption 2 above) we find:

$$-X = \frac{1}{2}f(r)\left(\frac{d\phi}{dr}\right)^2 = \beta^2. \tag{4.16}$$

We can then solve the field equations (provided in [186]) for the metric function $f(r)$ to find:

$$f(r) = h(r) = 1 - \frac{2M}{r} + \frac{\beta^2}{3M_P^2}r^2. \tag{4.17}$$

Thus, we find a stealth Schwarzschild-AdS black hole of mass $M$ with an effective negative cosmological constant $\Lambda_{\text{eff}} = -\beta^2/M_P^2$ (assuming real $\beta$ and hence $\beta^2 > 0$.). If we required asymptotic flatness then this model would have the same solution as GR, and there would be no hair. Relaxing that assumption, we note that cosmologically relevant scalar fields satisfy eq. (4.14) and we then expect $\Lambda_{\text{eff}} \sim H_0^2$. Therefore, hair would be negligible near the black hole.

#### 4.3.1.2 Cubic term

A second possibility analysed in [186] is the introduction of a logarithmic cubic term with $G_2 = X$, $G_3 = \alpha M_P \log(-X)$, $G_4 = M_P^2/2$, where $\alpha$ is an arbitrary dimensionless constant.

Again, we see that in this example, $G_{3,X}$ has negative powers of $X$. If the scalar field is to have cosmological relevance, we need:

$$\Omega_\phi = \frac{X + 6\dot{\phi}H_0\alpha M_P}{3M_P^2 H_0^2} \sim O(1). \tag{4.18}$$

Again, using the ansatz given by eq. (4.15) we find the following expression for $d\phi/dr$ by requiring $J^r = 0$:

$$\frac{d\phi}{dr} = -\alpha M_P \left( \frac{1}{h(r)} \frac{dh(r)}{dr} + \frac{4}{r} \right), \tag{4.19}$$

To proceed we assume that $h(r) = f(r)$. Making use of the field equations calculated in [187] (translating from a vector-tensor theory to a shift-symmetric scalar-tensor theory such that $A_\mu \to \partial_\mu \phi$, i.e. $A_0 = X_0 = 0, A_1 = d\phi/dr$), we find the following hairy solution:

$$\begin{aligned} ds^2 = &- \left( 1 - \frac{2M}{r} + \frac{c}{r^{4+\frac{1}{\alpha^2}}} \right) dt^2 + \left( 1 - \frac{2M}{r} + \frac{c}{r^{4+\frac{1}{\alpha^2}}} \right)^{-1} dr^2 \\ &+ \frac{r^2}{1+4\alpha^2} d\Omega^2, \end{aligned} \tag{4.20}$$

where we have rescaled $r$ and $t$ by constant pre-factors to obtain a Schwarzschild-like solution. If we imposed asymptotic flatness, we would find that the solution cannot have hair as the metric line element does not approach Minkowski when $r \to \infty$ due to the factor of $1/(1+4\alpha^2)$ in the angular part. Thus, we cannot construct a static, spherically symmetric, asymptotically flat solution with scalar hair in this theory (under the assumption that $h(r) = f(r)$). Furthermore, the fact that $G_3$ generically diverges for $X = 0$ is suggestive that Minkowski space is not a solution for this theory, and therefore this model does not seem to be viable.

#### 4.3.1.3 Conformally shift-symmetric theories

We now proceed to discuss models that depend explicitly on $\phi$, and hence break the assumptions of the shift-symmetric no-hair theorem. While such models could generically lead to hairy black holes, here we analyse a special class that is conformally related to shift-symmetric theories, and thus avoids scalar hair.

In the prototypical scalar-tensor theory of gravity, Brans-Dicke theory, it is well known that the theory can be recast from the 'Jordan frame' (in which a non-minimal coupling between the scalar and curvature exists) into that of GR with a minimally coupled scalar field through the use of a conformal transformation [206, 188]. The trade off is that, in this so-called 'Einstein frame' where the non-minimal coupling between the scalar field

and curvature has been eliminated, any additional matter fields no longer couple solely to the metric but also to the gravitational scalar field. However, if we work in a vacuum then both Jordan and Einstein frames are entirely physically equivalent. We can use this same analysis to show that theories in the Jordan frame of the type:

$$S_J = \frac{M_P^2}{2}\int d^4x\,\sqrt{-g}\,\left[\phi R + \phi^2 F_2(X/\phi) - \phi F_3(X/\phi)\Box\phi - V(\phi)\right] \tag{4.21}$$

can be transformed from the Jordan frame into the Einstein frame through the conformal transformation $\tilde{g}_{\mu\nu} = \phi g_{\mu\nu}$. Here, $F_i$ are arbitrary functions of $X/\phi$ and $V$ is a potential for the scalar field. Eq. (4.21) leads to the following action in the Einstein frame:

$$S_E = \frac{M_P^2}{2}\int d^4x\,\sqrt{-\tilde{g}}\,\left[\tilde{R} + F_2(\tilde{X}) + 2\tilde{X}F_3(\tilde{X}) - F_3(\tilde{X})\tilde{\Box}\phi - \phi^{-2}V(\phi)\right], \tag{4.22}$$

where tildes refer to quantities evaluated using the metric $\tilde{g}_{\mu\nu}$.

In the case of vanishing potential $V = 0$, the Einstein frame action $S_E$ is clearly shift symmetric in the scalar field $\phi$. Thus, via the no-hair theorem in [209], static black hole solutions for $\tilde{g}_{\mu\nu}$ should be the same as in GR with no scalar hair. As a consequence, solutions for $g_{\mu\nu}$ from $S_J$ will not have hair either.

For cosmologically relevant models, $\phi$ will have a fractional energy density given by:

$$\Omega_\phi = \frac{V - \phi^2 F_2 + 2X\left(\phi^2 F_{2,X} - F_3 - \phi F_{2,\phi}\right) + 3\dot{\phi}H_0\left(2\phi X F_{3,X} - M_P^2\right)}{3M_P^2 H_0^2 \phi} \sim O(1). \tag{4.23}$$

Generalizing to the case with $V \neq 0$, it is known that if $F_3 = 0$ we then have a K-essence model and static black hole solutions will not have hair provided that $V_{,\phi\phi} > 0$ and $F_{2,X} > 0$ (these conditions can be interpreted as constraining the scalar field to be stable and to satisfy the null energy condition [208, 188]).

For non-zero $V$ and $F_3$, the no-hair condition can be shown to be (through integrating $(\phi^{-2}V)_\phi \mathscr{E}_\phi$ from the horizon to spatial infinity, with $\mathscr{E}_\phi$ being the equation of motion for the scalar field *in the Einstein frame* [210]):

$$\begin{aligned}
&(F_2 + 2\tilde{X}F_3)_{,\tilde{X}} + f(r)\frac{d\phi}{dr}F_{3\tilde{X}}\left(\frac{1}{2h(r)}\frac{dh(r)}{dr} - \frac{2}{r}\right) \geq 0 \text{ and } (\phi^{-2}V)_{\phi\phi} \geq 0 \\
\text{or } &(F_2 + 2\tilde{X}F_3)_{,\tilde{X}} + f(r)\frac{d\phi}{dr}F_{3\tilde{X}}\left(\frac{1}{2h(r)}\frac{dh(r)}{dr} - \frac{2}{r}\right) \leq 0 \text{ and } (\phi^{-2}V)_{\phi\phi} \leq 0,
\end{aligned} \tag{4.24}$$

where $h(r), f(r)$ are the metric functions in the spherically symmetric ansatz given by eq. (4.15).

### 4.3.2 Beyond Horndeski

Horndeski gravity can be extended by the addition of terms which lead to higher order derivative equations of motion, but without an extra propagating degree of freedom [197, 198]. The beyond Horndeski terms are given by

$$L_4^{BH} = F_4(\phi, X)\varepsilon^{\mu\nu\rho}_{\sigma}\varepsilon^{\mu'\nu'\rho'\sigma}\phi_\mu\phi_{\mu'}\phi_{\nu\nu'}\phi_{\rho\rho'} \tag{4.25}$$

$$L_5^{BH} = F_5(\phi, X)\varepsilon^{\mu\nu\rho\sigma}\varepsilon^{\mu'\nu'\rho'\sigma'}\phi_\mu\phi_{\mu'}\phi_{\nu\nu'}\phi_{\rho\rho'}\phi_{\sigma\sigma'} \tag{4.26}$$

The condition $c_T = 1$ generalizes to:

$$F_5 = 0, \quad G_{5,X} = 0, \quad G_{4,X} - G_{5,\phi} = 2XF_4. \tag{4.27}$$

Note that by setting $F_4 = 0$ in the above equation (i.e. recovering Horndeski theory), the condition for $c_T = 1$ appears to be $G_{4,X} = G_{5,\phi}$ rather than $G_{4,X} = G_{5,\phi} = 0$ as stated in section 4.3.1. This is not inconsistent, as Horndeski theories with $G_{4,X} = G_{5,\phi}$ will indeed result in $c_T = 1$ [169, 157, 170, 171]. As discussed in [169], however, in the Horndeski case we require both $G_{4,X}$ and $G_{5,\phi}$ to vanish *independently* rather than relying on any finely tuned or coincidental cancellation between the two terms. On the other hand, for Beyond Horndeski theories we can make use of the presence of the additional free function $F_4$ to cancel the contributions of $G_{4,X}$ and $G_{5,\phi}$ in $c_T$, thus preserving a richer landscape of viable theories with $c_T = 1$.

Similarly to the Horndeski case, we first require the scalar energy density parameter to be cosmologically relevant, i.e. $\Omega_\phi \sim O(1)$, with $\Omega_\phi$ given by:

$$\begin{aligned}\Omega_\phi = &\left(-G_2 + 2X\left(G_{2,X} - G_{3,\phi}\right) + 6H_0\dot{\phi}\left(XG_{3,X} - G_{4\phi} - 2XG_{4,\phi X}\right)\right.\\ &\left.+24H_0^2X^2\left(F_4 + G_{4,XX}\right) - 48H_0^2X^2\left(2F_4 + XF_{4,X}\right)\right)\\ &\times\left(6H_0^2\left(G_4 - 2XG_{4,X} + XG_{5\phi}\right)\right)^{-1}.\end{aligned} \tag{4.28}$$

In [211], it is shown that shift-symmetric Horndeski *and* Beyond Horndeski have no hair for a regular, asymptotically flat spacetime, with canonical kinetic term $X$ in action and positive powers of $G_{i,X}$ and $F_{i,X}$. In what follows, we focus again on models that break the last assumption. We investigate two terms given in [186] that respect the constraint $c_T = 1$.

#### 4.3.2.1 Square root Quartic models

We first consider including a $\sqrt{-X}$ term in $G_4$ (with the choice of $F_4$ corresponding to the above conditions that lead to $c_T = 1$):

$$G_2 = X,\ G_4 = \frac{1}{2}M_P^2 + \gamma\sqrt{-X},\ F_4 = \frac{\gamma}{4(-X)^{\frac{3}{2}}}, \tag{4.29}$$

where $\gamma$ is an arbitrary constant.

For this choice of $G_i, F_i$, the condition for the scalar field to be cosmologically relevant is given by:

$$\Omega_\phi = \frac{X - 6H_0^2\gamma\sqrt{-X}}{3H_0^2M_P^2} \sim O(1). \tag{4.30}$$

Assuming a spherically symmetric ansatz for the metric as in eq. (4.15), we find two branches of solutions for $X$:

$$X(r) = 0 \Rightarrow \frac{d\phi}{dr} = 0, \tag{4.31}$$

or

$$X(r) = -\left(\frac{4\gamma^2 + M_P^2r^2}{3\gamma r^2}\right)^2 \Rightarrow \frac{d\phi}{dr} = \sqrt{\frac{2}{f(r)}}\frac{4\gamma^2 + M_P^2r^2}{3\gamma r^2}, \tag{4.32}$$

respectively. We see that the first branch results in a solution with a constant scalar field, i.e. no-scalar hair, resulting in regular GR black holes. We thus try to find solutions for the metric functions $f(r)$ and $h(r)$ for the second branch of solutions for $X(r)$. We find the following for $f(r)$:

$$f(r) = \frac{64\gamma^6 + 9\gamma^2c_1r^3 - M_P^6r^6 + 45\gamma^2M_P^4r^4 + 144\gamma^4M_P^2r^2}{9\left(\gamma M_P^2r^2 - 8\gamma^3\right)^2}. \tag{4.33}$$

For large $r$, $f(r) \sim r^2$, this solution is clearly not asymptotically flat. Thus we have not been able to construct an asymptotically flat spherically symmetric black hole solution with scalar hair for this model.

#### 4.3.2.2 Purely Quartic models

Purely quartic models are proposed in [186] (i.e. only $G_4$ and $F_4$ non-zero and with no canonical kinetic term for the scalar field). One such model that obeys the $c_T = 1$ constraint is given by:

$$G_4 = \frac{1}{2}M_P^2 + \sum_{n\geq 2} 2a_n \frac{(X - X_0)^{n+1}}{(n+1)(n+2)}\left[(n+1)X + X_0\right] \tag{4.34}$$

$$F_4 = \sum_{n\geq 2} a_n(X - X_0)^n, \tag{4.35}$$

where $X = X_0$ is the constant value of the background scalar field kinetic term around the black hole:

$$\frac{d\phi}{dr} = \pm\sqrt{-\frac{2X_0}{f(r)}}, \tag{4.36}$$

thus leading to non-trivial scalar field profile for $X_0 \neq 0$.

The cosmological density parameter for the scalar field in this case is:

$$\Omega_\phi = \frac{-8X^2 \sum_{n\geq 2} a_n (X - X_0)^n}{M_P^2 + 4\sum_{n\geq 2} \frac{a_n (X-X_0)^n}{n+2} \left[(3-2n)X^2 - \frac{1}{n+1} X_0 (nX + X_0)\right]} \tag{4.37}$$

and we expect it to be of order 1.

The black hole solution of this model is a stealth black hole, where the spacetime geometry is given by the appropriate GR solution, but the scalar field takes a non-trivial profile (as shown above). For a stealth Schwarzschild black hole with mass $M$, the scalar field is thus given by [186]:

$$\phi(r) = \sqrt{-2X_0} \left[\sqrt{r^2 - 2Mr} + M \log\left(r - M + \sqrt{r^2 - 2Mr}\right)\right]. \tag{4.38}$$

The above profile for the scalar field is regular everywhere outside the horizon of the black hole, with $\phi \sim r$ as $r \to \infty$.

Since the spacetime geometry is the same as that of GR, we do not expect to be able to distinguish this model through non-dynamical tests. Nevertheless, we may expect to see a difference in dynamical situations. In particular, it has been suggested that while scalar-tensor theories with $\phi$ =constant may not lead to any new signature during the inspiral of two black holes, the no-hair theorem can be pierced if the scalar field has some dynamics [212]. In the case of stealth black holes, the scalar field will have a non-trivial initial profile as in eq. (4.38) which may trigger a subsequent dynamical evolution which may lead to dipole gravitational wave radiation which in turn will change the evolution of the emitted GW waveform phasing compared to that of GR.

### 4.3.3 Einstein-Scalar-Gauss-Bonnet

In four dimensions, the Gauss-Bonnet (GB) term is a topological invariant, and as such the addition of the GB term to the usual Einstein-Hilbert action of GR does not affect the equations of motion. If, however, the GB term is non-minimally coupled to a dynamical scalar field in the action, the dynamics are significantly altered. Consider the action of Einstein-Scalar-Gauss-Bonnet (ESGB) gravity [203]:

$$S_{GB} = \int d^4x \sqrt{-g} \left[\frac{M_P^2}{2} R - \frac{1}{2} g^{\mu\nu} \phi_\mu \phi_\nu - V(\phi) - \frac{1}{2} \xi(\phi) R^2_{GB}\right], \tag{4.39}$$

where we have introduced a scalar field $\phi$ with potential $V(\phi)$, which for simplicity we will neglect from now on, and a coupling function $\xi(\phi)$. In addition, we have defined $R^2_{GB} = R_{\mu\nu\alpha\beta} R^{\mu\nu\alpha\beta} - 4R_{\mu\nu} R^{\mu\nu} + R^2$ as the Gauss-Bonnet term.

It is well known that models given by eq. (4.39) can produce scalar hair on black hole backgrounds in both the static [203, 213, 68] and slowly rotating [162, 214, 215, 216, 217] regimes. However, on a cosmological background they lead to a modified speed of gravity waves. Indeed, we find that

$$c_T = 1 + 4\frac{\left(H\dot{\phi} - \ddot{\phi}\right)\xi' - \dot{\phi}^2\xi''}{M_P^2 - 4H\dot{\phi}\xi'}, \tag{4.40}$$

where a prime denotes a derivative with respect to $\phi$ (see also [218]). Equivalently, eq. (4.39) can be recast into the form of Horndeski gravity with the following choice of functions $G_i$:

$$\begin{aligned} G_2 =& X - V + 4\xi''''X^2\left(\log X - 3\right) \\ G_3 =& 2\xi'''X\left(3\log X - 7\right) \\ G_4 =& \frac{M_P^2}{2} + 2\xi''X\left(\log X - 2\right) \\ G_5 =& 2\xi'\log X. \end{aligned} \tag{4.41}$$

In this form, it is clear the ESGB gravity does not conform to the constraints of [169, 157, 170, 171] that $G_{4,X} = 0 = G_5$ to ensure that $c_T = 1$. Furthermore, it is well known that the case of coupling to the GB term is a loophole in the no-hair theorems for shift-symmetric Horndeski theories [188, 203, 210].

Assuming that the scalar field is cosmologically relevant, we find that $\Omega_\phi \sim O(1)$ where

$$\Omega_\phi = \frac{V + X + 4\left(\xi'''' - \xi'''\right)X^2\left(3 - \log X\right) + 24H_0X\left(H_0\xi'' + 3\dot{\phi}\xi'''\right)}{3H_0^2\left(M_P^2 + 4\xi''X\log X - 4\xi'H_0\dot{\phi}\right)}. \tag{4.42}$$

We then impose $c_T = 1$ for a generic background evolution. Therefore, from eq. (4.40) we get $\xi' = \xi'' = 0$, in which case the GB term decouples from the scalar field $\phi$ and we obtain GR with a minimally coupled scalar field plus a GB term. In this case, as mentioned above, the addition of the GB term to the usual Einstein-Hilbert term represents nothing more than the addition of a total divergence that leaves the equations of motion unaffected. Thus the constraint on $c_T$ rules out the possibility of ESGB gravity having any cosmological relevance. As discussed above, the scalar field $\phi$ could avoid modifying $c_T$ at an observable level only if it is assumed to be incredibly sub-dominant on cosmological scales, i.e. if $\Omega_\phi \ll 1$.

As a counter-example to the above discussion of the cosmological impact of ESGB gravity, the following theory is studied in [219]:

$$S = \int d^4x\sqrt{-g}\left[\frac{M_P^2}{2}R - \frac{1}{2}g^{\mu\nu}\phi_\mu\phi_\nu - V(\phi) + F_1(\phi)G^{\mu\nu}\phi_\mu\phi_\nu - \frac{1}{2}F_2(\phi)R_{GB}^2\right], \tag{4.43}$$

with string-inspired exponential forms for $F_1, F_2$, and $V$. It is shown in [219] that this theory, including *both* scalar coupling to the GB term and scalar derivative coupling to the Einstein tensor, can admit de-Sitter like and power-law cosmological solutions whilst maintaining $c_T = 1$. This theory is clearly not shift-symmetric and so the no-hair theorem of [209] is not applicable, whilst a coupling to the GB term is known to produce black holes with scalar hair [203, 213, 68], or at least that are unstable to spontaneous scalarization [220, 66]. Thus we expect that, in general, black holes in this string-inspired theory can possess scalar hair and satisfy current constraints on the speed of gravity waves, although with no cosmological effects.

### 4.3.4 Chern-Simons

Chern-Simons (CS) gravity [144] is characterised by the addition of the Pontryagin invariant, ${}^*RR = \frac{1}{2}\varepsilon^{\mu\nu\alpha\beta}R^{\lambda}_{\sigma\alpha\beta}R^{\sigma}_{\lambda\mu\nu}$ to the standard Einstein-Hilbert term of the action. The Pontryagin invariant can be coupled to either a dynamical or non-dynamical scalar field, leading to two different formulations of the theory. For concreteness, consider the dynamical formulation of CS gravity

$$S_{CS} = \int d^4x\sqrt{-g}\left[\frac{M_P^2}{2}R - \frac{1}{2}g^{\mu\nu}\phi_\mu\phi_\nu + \alpha f(\phi){}^*RR\right], \tag{4.44}$$

where $\alpha$ is a constant coupling parameter and $f(\phi)$ is an arbitrary function of the scalar field.

In [221, 222, 223] it is shown that in CS gravity, gravitational waves propagate at the speed of light on conformally flat background spacetimes such as FRW. As such, [221] postulates that it is not possible to constrain CS gravity purely through the propagation speed of gravitational waves. Regardless, static and spherically symmetric black holes in CS gravity do not have hair and admit the same solutions as in GR [138].

## 4.4 Other theories

We now consider other theories which go beyond the broad span of scalar-tensor theories. As one expects, the moment one considers fields with more "structure" (i.e. more indices), there is a greater possibility of non-trivial coupling with the metric which, in turn, can lead to black hole hair.

### 4.4.1 Einstein gravity with Maxwell, Yang-Mills and Skyrme fields

The simplest theory with a vector field corresponds to an Einstein-Maxwell system. In this case, the black hole solution is Kerr-Newman which, besides mass and spin, is characterized by an electric charge. While this black hole solution is not considered hairy, we will start by mentioning this case (and its non-abelian extensions) to get a flavor of what to expect in the case of fields with more structure.

The Einstein-Maxwell theory is given by

$$S = \int d^4x\sqrt{-g}\left[\frac{M_P^2}{2}R - \frac{1}{4}F_{\alpha\beta}F^{\alpha\beta}\right], \tag{4.45}$$

where $F_{\mu\nu} = \partial_\mu A_\nu - \partial_\nu A_\mu$ is the Maxwell tensor associated with a vector field $A^\alpha$. In this model, we have that the FRW cosmological fractional energy density of the vector field is:

$$\Omega_A = \frac{F_{0\alpha}F^{\alpha}_{\ 0} + \frac{1}{4}F_{\alpha\beta}F^{\alpha\beta}}{3M_{\rm Pl}^2H_0^2} \sim \frac{|\vec{B}|^2}{H_0^2M_{\rm Pl}^2}, \tag{4.46}$$

where $\vec{B}$ is the associated magnetic field. In this isotropic background, one has that $A^\mu = (A_0(t), \vec{0})$ and gravity wave propagation will be direction independent with exactly $c_T = 1$. Furthermore, in this case, the cosmological evolution is exactly the same as that of GR as the magnetic field vanishes ($\vec{B} = 0$) in this homogeneous background, and hence $\Omega_A = 0$ from eq. (4.46).

If the vector field is cosmologically relevant, taking into account the fact that the electrical conductivity of the universe is large, we expect the presence of magnetic fields which will lead to anisotropies. On the one hand, in the case of stochastic magnetic fields, the metric may be locally anisotropic but too weak to affect local gravitational wave propagation.

On the other hand, in the case of a global magnetic component, the vector field will have a spatial dependence $\vec{A} \neq 0$ and the universe will be anisotropic. Therefore, the propagation of gravitational waves will be direction dependent [224]. Current constraints on global anisotropy (and homogeneous magnetic fields) from the cosmic microwave background are remarkably tight [225, 226, 227] and we will enforce strict isotropy in what follows (although it is conceivable that multiple measurements of $c_T$ in different directions might improve these constraint).

The black hole solutions for the Einstein-Maxwell system are Kerr-Newman, which are fully characterized by three charges – mass $M$, spin $a$ and electric charge $Q$ – and with a non-trivial profile for the vector potential $A^\alpha$. In the spherically symmetric case (where

$a = 0$), one has the Reissner-Nordstrom solution given by:

$$h(r) = 1 - \frac{2M}{r} + \frac{Q^2}{4\pi\varepsilon_0 r^2} \text{ and } A_0(r) = \frac{Q}{r}, \tag{4.47}$$

where $\varepsilon_0$ is the vacuum permittivity constant. Here, we have again used a metric of the form of eq. (4.15) and $A^\mu = (A_0(r), A_1(r), 0, 0)$, with $A_1$ being an unphysical gauge mode.

The above description can be extended to the case where the gauge field is non-abelian – the Einstein-Yang-Mills system – or the vector field has a stronger non-linear self coupling – the Einstein-Skyrme system; in this case we are considering genuine hair. In both of these cases, new phenomena can come into play. While, on the whole, the energy density of the fields can remain sub-dominant at cosmological scales, non-perturbative structures (topological and non-topological defects) can in principle make a non-trivial contribution to the overall energy density and to the global isotropy of space (although, generally, these effects are expected to be weak). Again, we can enforce $c_T = 1$ yet still allow for non-abelian hair. Notable examples can be found in the Einstein-Yang-Mills case [228, 229] which combine solitonic cores with long range forces; in the Einstein-Skyrme cases there is a range of solutions combined with solitonic states [230, 231, 232].

### 4.4.2 Einstein-Aether

Generalized Einstein-Aether is a gravity theory where the metric is coupled to a unit time-like vector field, dubbed the aether. This model provides a simple scenario for studying effects of local Lorentz symmetry violation. In particular, the vector field defines a preferred frame where boosts symmetry is broken but rotational symmetry is still preserved. The action describing this model is given by:

$$S = \int d^4x\sqrt{-g}\left[\frac{M_P^2}{2}R + \mathscr{F}(K) + \lambda\left(A^\mu A_\mu + 1\right)\right], \tag{4.48}$$

where $\lambda$ is a Lagrange multiplier that forces the vector field to be unit time-like. Also, $\mathscr{F}(K)$ is an arbitrary function of the kinetic term $K$ given by

$$K = c_1\nabla_\mu A_\nu \nabla^\mu A^\nu + c_2(\nabla_\mu A^\mu)^2 + c_3\nabla_\mu A_\nu \nabla^\nu A^\mu, \tag{4.49}$$

with $c_i$ constants (an additional quartic term in $A^\mu$ contributing to $K$ is sometimes considered).

The cosmological consequences of Einstein-Aether have been extensively explored in [110, 233, 234]. The case where the aether field can play the role of either dark matter or dark energy were explored in [233] where the existing cosmological constraints ruled it

out as an alternative to a cosmological constant. In the case of the standard Einstein-Aether case (with $\mathscr{F}(K) \sim K$), current Solar System constraints [235] combined with binary pulsar constraints [236, 237] place $|c_1|, |c_3| \leq 10^{-2}$ and $c_2 \leq 1$. Cosmological constraints allow $\Omega_A \sim 0.3$ so the aether field can still have a non-negligible contribution to the cosmological evolution [238].

The propagation speed of gravitational waves on a cosmological background is such that $c_T^2 = 1/[1+(c_1+c_3)\mathscr{F}_{,K}]$, and thus the constraint on $c_T$ implies $c_1 = -c_3$. This means that $K$ is reduced to a canonical kinetic term (an "$F^2$" term) supplemented by a $(\nabla_\mu A^\mu)^2$ term.

For models which respect $c_T = 1$, the condition that the aether field $A^\mu$ has cosmological relevance is thus given by:

$$\Omega_A = \frac{-\mathscr{F}}{3M_P^2 H_0^2 (1 - 3c_2 \mathscr{F}_{,K})} \sim O(1), \tag{4.50}$$

where $\mathscr{F}_{,K}$ denotes the derivative $\mathscr{F}$ with respect to $K$.

Little has been done on black hole solutions for general $\mathscr{F}(K)$ and thus we will restrict ourselves to the standard Einstein-Aether case. Black hole solutions with hair have been found in such a case, that are regular, asymptotically flat and depend on only one free parameter [161, 239, 240, 241, 242]. For instance, in the case where $c_3 = 0$, $c_2$ must satisfy the condition:

$$c_2 = -\frac{c_1^3}{2 - 4c_1 + 3c_1^2}, \tag{4.51}$$

where $c_1$ is the only free parameter of the black hole solution. We can use a spherically symmetric ansatz for the line element as in eq. (4.15). The full solution must be found numerically, but an analytical perturbative solution can be given when $x = 2M/r \ll 1$:

$$h(r) = 1 + x + (1 + c_1/8)x^2 + \ldots, \tag{4.52}$$

$$f(r)^{-1} = 1 - x - c_1/48x^2 + \ldots \tag{4.53}$$

We note that this is an example of primary hair, where the spacetime geometry is different to that of GR and, furthermore, the solution depends on an additional independent free parameter $c_1$.

More general solutions satisfying $c_3 = -c_1$ (and hence $c_T = 1$) are expected to have the same behaviour [161]. This shows that BH solutions always have hair, regardless of additional cosmological constraints. While in static black holes deviations from GR are typically of a few percent [242], generalizations to spinning black holes may offer better prospects for observing hair in these models.

### 4.4.3 Generalised Proca

The generalised Proca theory [111, 243, 244, 245, 246] is given by

$$S = \int d^4x \sqrt{-g} \left\{ F + \sum_{i=2}^{6} \mathscr{L}_i[A_\alpha, g_{\mu\nu}] \right\}, \tag{4.54}$$

where $\mathscr{L}_i$ are gravitational vector-tensor Lagrangians given by:

$$\begin{aligned}
\mathscr{L}_2 &= G_2(X,F,Y), \\
\mathscr{L}_3 &= G_3(X)\nabla_\mu A^\mu, \\
\mathscr{L}_4 &= G_4(X)R + G_{4X}\left[(\nabla_\mu A^\mu)^2 - \nabla_\mu A^\nu \nabla_\nu A^\mu\right], \\
\mathscr{L}_5 &= G_5(X)G_{\mu\nu}\nabla^\mu A^\mu - \frac{1}{6}G_{5X}\left[(\nabla_\mu A^\mu)^3 - 3(\nabla_\alpha A^\alpha)(\nabla_\mu A^\nu \nabla_\nu A^\mu)\right. \\
&\left. +2\nabla_\mu A^\alpha \nabla_\nu A^\mu \nabla_\alpha A^\nu\right] - g_5(X)\tilde{F}^{\alpha\mu}\tilde{F}_{\beta\mu}\nabla_\alpha A^\beta, \\
\mathscr{L}_6 &= G_6(X)L^{\mu\nu\alpha\beta}\nabla_\mu A_\alpha \nabla_\alpha A_\beta + \frac{1}{2}G_{6X}\tilde{F}^{\alpha\beta}\tilde{F}^{\mu\nu}\nabla_\alpha A_\mu \nabla_\beta A_\nu,
\end{aligned} \tag{4.55}$$

which are written in terms of 6 free functions $G_2$, $G_3$, $G_4$, $G_5$, $g_5$, and $G_6$. We can define the following tensors:

$$F_{\mu\nu} = \nabla_\mu A_\nu - \nabla_\nu A_\mu, \tag{4.56}$$

$$\tilde{F}^{\mu\nu} = \frac{1}{2}\varepsilon^{\mu\nu\alpha\beta}F_{\alpha\beta}, \tag{4.57}$$

$$L^{\mu\nu\alpha\beta} = \frac{1}{4}\varepsilon^{\mu\nu\rho\sigma}\varepsilon^{\alpha\beta\gamma\delta}R_{\rho\sigma\gamma\delta}, \tag{4.58}$$

where $R_{\rho\sigma\gamma\delta}$ is the Riemann tensor and $\varepsilon^{\mu\nu\alpha\beta}$ is the Levi-Civita antisymmetric tensor. The 5 free parameters $G_i$ are free functions of the following scalar quantities of the previously defined tensors:

$$X = -\frac{1}{2}A_\mu A^\mu, \tag{4.59}$$

$$F = -\frac{1}{4}F^{\mu\nu}F_{\mu\nu}, \tag{4.60}$$

$$Y = A^\mu A^\nu F_\mu{}^\alpha F_{\nu\alpha}. \tag{4.61}$$

The conditions to have $c_T = 1$ are $G_{4,X} = G_{5,X} = 0$ (with the term proportional to $G_{\mu\nu}\nabla^\mu A^\nu$ vanishing due to the Bianchi identity). In this case, the condition for cosmological relevance of the vector field $A^\mu$ is given by [115]:

$$\Omega_A = \frac{-G_2 + G_{2,X}A_0^2 + 3G_{3,X}H_0A_0^3}{6G_4H_0^2} \sim O(1), \tag{4.62}$$

where $A^\mu = \left(A_0(t), \vec{0}\right)$.

Most of the theories that satisfy $c_T = 1$ are of the form of GR with a minimally coupled vector field possessing 'exotic' kinetic terms, in which case hairy black holes are to be expected. It can be easily shown that spherically symmetric BHs can indeed have hair. For instance, [187] shows the solution when $G_3 \neq 0$, $G_4 = M_P^2/2$, in which case:

$$f(r) = \left(1 - \frac{M}{r}\right)^2, \; A_0 = \sqrt{2} M_{Pl} \left(1 - \frac{M}{r}\right), \; A_1 = 0, \tag{4.63}$$

where we have again assumed a metric ansatz given by eq. (4.15) (with $h(r) = f(r)$), and that $A^\mu = (A_0(r), A_1(r), 0, 0)$. This resembles an extremal Reissner-Nordstrom black hole with a 'charge' that depends on mass. This is an example of secondary hair, where the spacetime metric is different to that of GR, but both theories depend on the same number of independent free parameters.

In contrast, since the Lagrangian $\mathscr{L}_6$ couples the vector field non-minimally to curvature through $L^{\mu\nu\alpha\beta}$ this Lagrangian corresponds to an intrinsic vector mode, and as such does not contribute to the background equations of motion for a homogenous and isotropic cosmological background (where $A^\mu = \left(A_0(t), \vec{0}\right)$) [117]. In this case, with non-minimal coupling to curvature, one solution is that of a stealth Schwarzschild black hole with a non-trivial profile for the background vector field [187]:

$$f(r) = 1 - \frac{2M}{r}, \; A_0 = const, \; A_1 = \frac{\sqrt{A_0^2 - 2X_0 f(r)}}{f(r)}, \tag{4.64}$$

where $X = X_0 = const$.

### 4.4.4 Scalar-Vector-Tensor

We now consider theories in which there are two additional fields to the metric: a scalar and a vector. A specific model was analysed in [247], where a shift-symmetric scalar field $\phi$ *and* a $U(1)$ gauge invariant vector field $A^\mu$ are coupled [248]. Specifically, the action of interest is given by:

$$\begin{aligned} S = \int d^4x \sqrt{-g} \Bigg[ & \frac{M_P^2}{2} R + X + F + \beta_3 \tilde{F}^\mu_{\;\rho} \tilde{F}^{\nu\rho} \phi_\mu \phi_\nu \\ & + \beta_4 X^{n-1} \left( X L^{\mu\nu\alpha\beta} F_{\mu\nu} F_{\alpha\beta} + \frac{n}{2} \tilde{F}^{\mu\nu} \tilde{F}^{\alpha\beta} \phi_{\mu\alpha} \phi_{\nu\beta} \right) \Bigg], \end{aligned} \tag{4.65}$$

where $\beta_3$ and $\beta_4$ are arbitrary constants, $X = -\phi_\mu \phi^\mu/2$ is the scalar kinetic term as in scalar-tensor theories, and with all other terms being defined as in Section 4.4.3.

Given that the vector field strength $F_{\mu\nu}$ vanishes on isotropic cosmological backgrounds (with $A^{\mu} = (A_0(t), \vec{0})$), the action given by eq. (4.65) reduces to that of GR with a minimally coupled, massless scalar field in cosmological settings. The speed of gravitational waves $c_T$ will, therefore, be equal to unity in these theories, thus satisfying the constraint determined by GRB 170817A and GW170817.

Black hole solutions in this model were studied in [247], where asymptotically flat, static and spherically symmetric black holes with hair are found for $\beta_4 = 0$ and for $\beta_4 \neq 0$ in the cases of $n = 0$ or 1. In all of the cases studied, modified Reissner-Nordstrom-like solutions with global charges $M$ and $Q$ are found, with the black hole further endowed with a secondary scalar hair sourced by the vector charge $Q$.

### 4.4.5 Bigravity

We now consider bimetric theories. The only non-linear Lorentz invariant ghost-free model is given by the deRham-Gabadadze-Tolley (dRGT) [249, 113, 250] massive (bi-)gravity action:

$$S = \frac{M_g^2}{2}\int d^4x\,\sqrt{-g}R_g + \frac{M_f^2}{2}\int d^4x\,\sqrt{-f}R_f - m^2M_g^2\int d^4x\,\sqrt{-g}\sum_{n=0}^{4}\beta_n e_n\left(\sqrt{g^{-1}f}\right), \tag{4.66}$$

where we have two dynamical metrics $g_{\mu\nu}$ and $f_{\mu\nu}$ with their associated Ricci scalars $R_g$ and $R_f$, and constant mass scales $M_g$ and $M_f$, respectively. Here, $\beta_n$ are free dimensionless coefficients, while $m$ is an arbitrary constant mass scale. The interactions between the two metrics are defined in terms of the functions $e_n(\mathbb{X})$, which correspond to the elementary symmetric polynomials of the matrix $\mathbb{X} = \sqrt{g^{-1}f}$.

This bigravity action generally propagates one massive and one massless graviton, with the field $g_{\mu\nu}$ being a combination of *both* modes. There is one special case where $M_f/M_g \to \infty$, and only the massive graviton propagates (while the metric $f_{\mu\nu}$ becomes a frozen reference metric). As discussed in [169], constraints on the speed of gravity waves lead to bounds on the graviton mass of the order $m \lesssim 10^{-22}$eV, which are weak compared Solar System fifth force constraints of order $m \lesssim 10^{-30}$eV. As long as $m \sim H_0$ we expect the massive graviton to have some cosmological relevance.

Regarding black hole solutions, massive gravity (with one dynamical metric) has some static solutions, although they have been found to be problematic as they can describe infinitely strongly coupled regimes or have singular horizons. One well-behaved solution was proposed recently in [251], for a time-dependent black hole.

On the other hand, massive bigravity has a much more rich phenomenology with a number of possible stationary solutions (static, rotating, and with or without charge) (see a review in [252]). Focusing on asymptotically flat solutions, it is possible to have Schwarzschild or Kerr solutions for both metrics [253]. However, these solutions are generically unstable, although they can still fit data as long as $m \lesssim 5 \times 10^{-23}$eV [254]. Hairy static solutions can also be found for some parameter space [255]. Using the ansatz in eq. (4.15) for the metric $g_{\mu\nu}$ and the following ansatz for $f_{\mu\nu}$ :

$$ds_f^2 = -P(r)dt^2 + \frac{1}{B(r)}dr^2 + U(r)^2 d\Omega^2. \tag{4.67}$$

Here, there are five independent functions $\{h, f, P, B, U\}$ to be determined by the equations of motion. However, due to the presence of a Bianchi constraint, there are only three independent functions $\{f, B, U\}$ satisfying first-order differential equations. The complete solution must be found numerically, but an expansion can be made for $r \to \infty$ [255]:

$$\begin{aligned} f(r)^{1/2} &= 1 - \frac{c_1}{2r} + \frac{c_2(1+r\mu)}{2r}e^{-r\mu}, \\ Y(r) &= 1 - \frac{c_1}{2r} - \frac{c_2(1+r\mu)}{2r}e^{-r\mu}, \\ U(r) &= r + \frac{c_2(1+r\mu+r^2\mu^2)}{r^2\mu^2}e^{-r\mu} \end{aligned} \tag{4.68}$$

where $c_i$ are integration constants, $\mu = m\sqrt{1 + M_g^2/M_f^2}$, and $Y$ is a proxy function for $B$ given by $Y = U'/B^{1/2}$. While the constant $c_1$ may be identified with the mass of the black hole, $c_2$ is a new charge that adds a Yukawa-type suppression to the metric due to the massive graviton.

Here we have mentioned some possible black hole solutions for bimetric theories, but we note that since these solutions are not unique, it is not clear what the physical spacetime and the outcome of gravitation collapse will be. Future simulations on non-linear gravitational collapse should allow us to find the physical solution.

## 4.5 Conclusion

Modifications to general relativity may affect the evolution of the universe and lead to cosmologically observable effects. The range of possible modifications has been drastically reduced with the discovery of GW170817 and the resulting constraint on the speed of gravitational waves. We have looked at the reduced space of theories to see which of them will lead to distinctive signatures around black holes, specifically black hole hair. By

looking for observable signatures of that hair and combining them with constraints from current and future cosmological surveys, it should be possible to further narrow down the span of allowed modifications to general relativity and, if the data points that way, single out new physics.

We have focused on scalar-tensor theories. Of all theories, these are the most thoroughly understood and, furthermore, emerge as low energy limits of other, more intricate theories. Not only is there a reasonably general classification of scalar-tensor theories, but there is also a comprehensive body of work on black holes and black hole hair arising in them. As was shown in [169, 157, 170, 171], the discovery of GW170817 places severe constraints on these models. We have found that, generally, and in the cases where they have been studied more carefully, these theories do not have hair for static, spherically symmetric, and asymptotically flat black holes. Specific examples that were constructed to have hair (as suggested in [186]), in the case where they contribute cosmologically and satisfy $c_T = 1$, do not have hair. We found that the case where Einstein-Scalar-Gauss-Bonnet gravity is cosmologically relevant, it is ruled out by the GW170817 constraint, while Chern-Simons gravity is left unconstrained (and furthermore, known to have hair in the rotating regime [256, 257, 258, 259, 260, 261]). We also looked at other theories, primarily involving vectors, and found that in that case it is possible for them to satisfy the various cosmological conditions and still have black holes with hair for spherically symmetric and rotating black holes. We also discussed bimetric theories, which allow for hairy and non-hairy asymptotically flat black holes, and understanding which solution describes physical setups require further work on gravitational collapse.

Our analysis is limited in scope in the sense that we have not considered the most general actions allowed. For example we have not considered combinations of the Beyond Horndeski models studied in [186]. We have done this for two reasons. The first reason is that these models were constructed as proofs of concept without any strong underlying physical motivation – questions of analyticity arise in the limit where $X \to 0$. The second reason is that the equations of motion become vastly more complicated with multiple non-analytic leading terms which means it is difficult to obtain solutions which can be easily interpreted and classified. Lacking more general results (such as the Galileon no-hair theorem of [209]) it is always plausible that theories, which satisfy the constraints we impose and lead to hair, exist.

Nevertheless, our analysis is useful for determining how to move forward with the theories we looked at. Given their cosmological relevance, we take for granted that they will be thoroughly tested when the next generation of cosmological data is made available.

What we can now do is determine how to combine these cosmological tests with non-dynamical tests in the strong-field regime. In the cases where the black holes do have hair, one would look for evidence of a fifth force for example in the accreting material or nearby objects.

For theories where black holes have no hair the situation is more complex. In that case, the only observations that might lead to data which allow us to constrain the extra fields are dynamical tests which include inspirals of binary black holes, extreme mass-ratio inspirals (EMRI) or ringdown of single black holes. In GR, due to the strong equivalence principle, the orbital motion and the gravitational wave signal of binary inspirals or EMRI only depend on the masses and spins of the objects involved. On the contrary, in modified gravity theories this principle is violated, and the additional degrees of freedom will determine the effective gravitational coupling constant which will depend on the new field or its derivatives at the location of the relevant object (e.g. see [262, 263, 264, 212] for binary inspirals in scalar-tensor theories and a general analysis in [265, 266], as well as [267, 268] for EMRI in scalar-tensor theories). In the case of ringdown, one would expect that the violent event would have excited any putative extra degree of freedom (such as a scalar or a vector). And while the end state might be a Kerr-Newman solution, the perturbations around this background (i.e. the quasi-normal modes) should contain information about the extra degrees of freedom [83]. It would be interesting further work to study the specific quasi-normal-mode signatures of the theories investigated here that do not exhibit hairy black hole solutions (yet still abide by the $c_T$ constraint).

Finally, given that we have found that most scalar-tensor theories abide to the no-hair theorem and present trivial constant profiles around black holes, it would be interesting to explore black hole solutions in the presence of screening. It has been argued that models satisfying Solar System constraints (i.e. which hide the presence of fifth forces in the weak-field limit) do so through screening. The main screening mechanisms which have been advocated are the Vainshtein [269], chameleon [270] and symmetron [271] mechanisms, all of which suppress the fifth force compared to the Newtonian force, depending on the local environment. The current approach is to assume that the self gravity of compact objects is sufficiently substantial that it decouples the scalar charge from the mass – in the limit of a black hole, the scalar charge is set to zero [272]. However, little has been done to construct screened black hole solutions by, for example, violating the condition of asymptotic flatness. Such an analysis might give us insight on the presence of hair in more realistic setups. A particularly interesting scenario might arise in the case of a binary neutron star merger, such as GW170817. There, screened compact objects (neutron stars) end up forming a black hole; if indeed the black hole has no hair (and no screening)

one might expect that the process of shedding the scalar field could lead to an observable effect. Alternatively, if the black hole adopts the screening mechanism, it would be useful to understand what is the final, stable, solution and how it jibes with the no-hair theorem.

We have entered a new era in gravitational physics in which multiple regimes can be tested with high precision. While multi-messenger gravitational wave physics has grown to prominence, we believe it should now also include other, significantly different, arenas; from the cosmological, through the galactic all the way down to astrophysical and compact objects, a wide range of observations can be brought together to construct a highly precise understanding of gravity.

# Chapter 5

# Kerr-(Anti-)de Sitter Black Holes: Perturbations and quasi-normal modes in the slow rotation limit

# Abstract

In this chapter we study the perturbations of scalar, vector, and tensor fields in a slowly rotating Kerr-(Anti-)de Sitter black hole spacetime, presenting new and existing Schrödinger style master equations for each type of perturbation up to linear order in black hole spin $a$. For each type of field we calculate analytical expressions for the fundamental quasi-normal mode frequencies. These frequencies are compared to existing results for Schwarzschild-de Sitter, slowly rotating Kerr, and slowly rotating Kerr-de Sitter black holes. In all cases good agreement is found between the analytic expressions and those frequencies calculated numerically. In addition, the axial and polar gravitational frequencies are shown to be isospectral to linear order in $a$ for all cases other than for *both* non-zero $a$ and $\Lambda$. This chapter is based on research presented in [88].

## 5.1 Introduction

Black holes are among the most captivating aspects GR, and their properties have been studied extensively since the dawn of GR in the early 20th century. Of great interest to physicists and mathematicians alike is the response of black holes to perturbations. Notably, perturbed black holes 'ring', emitting gravitational waves at a characteristic set of frequencies known as the quasi-normal mode (QNM) frequencies [44, 45, 46, 47, 48].

As has been discussed previously in this thesis, these QNM frequencies are dependent on the background properties of the black hole (e.g. mass or angular momentum), acting like a 'fingerprint' for a given black hole. Furthermore, the presence of a cosmological constant, or a modification to the theory of gravity itself, can and will affect the spectrum of frequencies that a black hole will emit gravitational waves at. Thus studying the QNM frequencies of black holes (and other fields propagating on the black hole spacetime) provides a window from which to observe not only the properties of the black hole itself, but also of the wider universe and indeed of the fundamental laws governing gravity [55, 56, 59, 37, 273, 274].

From an observational point of view, given the dawn of the gravitational wave era of astronomy (with multiple direct observations of gravitational waves from mergers of highly compact objects, i.e. black holes or neutron stars, having now been made by advanced LIGO and VIRGO [16]), determining and detecting the QNM frequencies of the remnant black holes left perturbed after the merger of compact objects is an interesting and important area of study.

In this chapter, we will study the responses a variety of fields to linear perturbations on a black hole spacetime, and present analytical expressions for the QNM frequencies that each type of field characteristically 'rings' at. The black holes we will consider will possess angular momentum and be embedded in a universe with a cosmological constant that can be positive or negative (i.e. the spacetime will be either asymptotically de Sitter or Anti-de Sitter). For the case of a positive cosmological constant, the black holes studied here will represent the kind of astrophysical black holes that we expect to observe in our universe (assuming the $\Lambda$CDM paradigm of cosmology [275], and that astrophysical black holes have negligible electric charge [276]). For a negative cosmological constant, on the other hand, the AdS/CFT correspondence provides an interesting motivation to study the QNMs of asymptotically Anti-de Sitter black holes as a method of gaining insight into certain conformal quantum field theories [277, 278, 279, 280, 281].

*Summary*: In section 5.2, we will present the background spacetime of the black holes that are to be studied in this work. In section 5.3, we will review aspects of black hole

perturbation theory before presenting second order Schrödinger-style master equations for perturbations of massive scalar (spin $s = 0$), massive vector ($s = \pm 1$), and massless tensor ($s = \pm 2$) fields. Some of the master equations presented are known from the literature, with others (to the author's best knowledge) being new results. In section 5.4 we will then present analytic expressions for the QNM frequencies that satisfy each of the master equations present in section 5.3, and compare these analytic expressions to previously obtained numerical results. Finally, in section 5.5, we will discuss the results presented and make some concluding remarks.

## 5.2 Background

The background spacetime that we will be concerned with in this work is that of a *slowly* rotating black hole in a universe with a cosmological constant $\Lambda$. The black hole spacetime is described by the Kerr-(Anti)-de Sitter (henceforth referred to as Kerr-(A)dS) solution which, to linear order in dimensionless black hole spin $a$, is given in Boyer-Lindquist coordinates by [14]:

$$ds^2 = \bar{g}_{\mu\nu}dx^\mu dx^\nu = -F(r)dt^2 + F^{-1}(r)dr^2 + r^2 d\Omega^2 - 2aM\left(\frac{2M}{r} + \frac{\Lambda}{3}r^2\right)\sin^2\theta dt d\phi \tag{5.1}$$

with $d\Omega^2$ being the metric on the surface of the unit 2-sphere, $M$ the black hole mass, and we assume $|a| \ll 1$. The metric function $F(r)$ is given by:

$$F(r) = 1 - \frac{2M}{r} - \frac{\Lambda}{3}r^2. \tag{5.2}$$

The spacetime is asymptotically de Sitter (thus describing a Kerr-dS black hole) for $\Lambda > 0$ ; for $\Lambda < 0$, we have a Kerr-AdS black hole with an asymptotically Anti-de Sitter spacetime.

## 5.3 Perturbation Master Equations

As discussed in Chapter 3, when considering perturbations on a spherically symmetric background spacetime, it is standard to decompose the perturbed fields into spherical harmonics to factor out the angular dependence of the perturbation [44, 45, 46, 47, 147, 148]. Using $Y^{\ell m}_{\mu_1\ldots\mu_n}(\theta,\phi)$ to schematically represent the appropriate choice of scalar, vector, or tensor spherical harmonics depending on the perturbed field $f$ in question:

$$f_{\mu_1\ldots\mu_n}(t,r,\theta,\phi) = \sum_{\ell,m} f^{\ell m}(r,t)Y^{\ell m}_{\mu_1\ldots\mu_n}(\theta,\phi). \tag{5.3}$$

About a spherically symmetric background, perturbations of different polarity (either axial/odd or polar/even) decouple from each other, greatly simplifying the analysis of the equations of motion for the perturbed fields. In addition perturbations of different $\ell$ decouple. The result is that, if we further assume a harmonic time dependence of the form $e^{-i\omega t}$, the equations of motion can often be cast into homogeneous Schrödinger style second order differential equations for some unknown function of $\mathscr{F}(r)$ representing the wavefunction fo the perturbation:

$$\left[\frac{d^2}{dr^2} + \omega_{\ell m}^2 - V_{\ell m}(r)\right] \mathscr{F}^{\ell m}(r) = 0. \tag{5.4}$$

By requiring that we have purely outgoing waves at each boundary of our spacetime, i.e. no waves originate from within the black hole horizon or from spatial infinity (or the cosmological horizon)[1], we can solve eq. (5.4) to find the $\omega_{\ell m}$ as the characteristic QNM frequencies associated with the perturbation (as discussed previously in this thesis) with $V_{\ell m}(r)$ acting as a potential [44, 45, 46, 47]. The fact that the equations of motion governing the perturbations can often be cast into a single Schrödinger style second order differential equation is useful, with the techniques of quantum mechanics and time-independent scattering theory being available to the modern physicist to analyse such an equation (see, for example, the Appendix of [46]).

Unfortunately the decoupling of perturbations of different polarity and $\ell$ no longer occurs when the background is not spherically symmetric (e.g. in axisymmetric spacetimes such as the Kerr family of black holes [282]), and thus the task of simplifying the equations of motion governing the perturbations is greatly complicated. For example, for a Kerr black hole one has to solve the more complex Teukolsky equation [283] to find the QNM frequencies, rather than the simpler Regge-Wheeler [145] or Zerilli [153] equations that one calculates for Schwarzschild black holes.

In [284], however, it was shown that in slowly rotating backgrounds, where the 'breaking' of spherical symmetry is controlled by the dimensionless black hole spin $a$ (and terms $O(a^2)$ are neglected), it is sufficient to continue to use spherical harmonics and to treat perturbations of different polarity and $\ell$ as completely decoupled. This technique yields equations of motion that are sufficient to determine the QNM frequency spectrum of the system accurately to linear order in $a$ (and has been utilised in, for example, [285, 286, 254]). The benefit of this approach is that one can continue to exploit the useful properties of spherical harmonics and often still arrive at simple second order equations of motion for the perturbed fields, whilst now including the effects of (slow) rotation.

[1]Note that for asymptotically Anti-de Sitter spacetimes, we actually require a reflective boundary condition at the cosmological horizon. This point will be addressed later in the chapter.

In the following sections we will make use of the above technique for perturbations in slowly rotating backgrounds to derive Schrödinger style master equations for various type of perturbations on a slowly rotating Kerr-(A)dS background, keeping terms linear in black hole spin and neglecting terms $O(a^2)$ and higher. This will allow us in Section 5.4 to determine the QNM frequency spectra for each type of perturbation to linear order in $a$. From now on we will also suppress spherical harmonic indices so as not to clutter notation, with each equation assumed to hold for a given $(\ell, m)$.

### 5.3.1 Massive Scalar field

First we consider a massive test scalar field $\Phi$ (such that $\Phi$ does not contribute to the background energy momentum and thus does not affect the background spacetime) with field mass $\mu$ propagating on the slowly rotating Kerr-(A)dS background given by eq. (5.1). Such a field obeys the massive Klein-Gordon equation:

$$\Box\Phi = \mu^2\Phi. \tag{5.5}$$

In [284, 285] it was shown that for scalar perturbations such that:

$$\Phi = \sum_{\ell m} \frac{\varphi_{\ell m}(r)}{r} e^{-i\omega t} Y^{\ell m}(\theta, \phi), \tag{5.6}$$

the massive Klein-Gordon equation (linearised to first order in black hole spin $a$) takes the form:

$$\left[\frac{d^2}{dr_*^2} + \omega^2 - \frac{2amM\omega}{r^2}\left(\frac{2M}{r} + \frac{\Lambda}{3}r^2\right) - F(r)\left(\frac{\ell(\ell+1)}{r^2} + \frac{2M}{r^3} - \frac{2\Lambda}{3} + \mu^2\right)\right]\varphi = 0. \tag{5.7}$$

We see that the effective potential of eq. (5.7) is modified from the usual spin zero Regge Wheeler equation [44, 45, 46, 47] through $\Lambda$ and $a$. Eq. (5.7) is, nonetheless, still in the generic form of a Schrödinger style wave equation.

### 5.3.2 Massive Vector field

We now consider a massive vector field propagating on the black hole background. We again assume that the test field does not contribute to the background energy momentum and thus does not affect the background spacetime.

Whilst vector fields can have both axial and polar parity components of their perturbations, it was shown in [284] that the polar perturbations for a *massive* vector field on a slowly rotating background cannot be reconciled into a single Schrödinger style wave

equation. Thus in this chapter we will only consider axial parity perturbations for simplicity. It is worth noting that, in the case of a massless vector field (i.e. electromagnetic perturbations), the equations for axial and polar perturbations coincide.

In [284] the master equation governing the axial component of a massive vector perturbation is given for a generic slowly rotating background. For the slowly rotating Kerr-(A)dS background that we are concerned with, the radial wavefunction of the vector perturbation $A(r)$ (i.e. playing the role of $z_0(r)$ in eq. (3.71)) satisfies:

$$\left[\frac{d^2}{dr_*^2}+\omega^2-\frac{2amM\omega}{r^2}\left(\frac{2M}{r}+\frac{\Lambda}{3}r^2\right)-F(r)\left(\frac{\ell(\ell+1)}{r^2}+\mu^2\right)\right]A=0, \tag{5.8}$$

where $\mu$ is now the vector field mass. In the case that $a=0$, eq. (5.8) agrees with the master equations derived in [287].

### 5.3.3 Gravitational field

Finally, we consider perturbations to the black hole spacetime itself, such that the metric $g_{\mu\nu}$ can be decomposed into a background part $\bar{g}$ and a perturbation $h$:

$$g_{\mu\nu}=\bar{g}_{\mu\nu}+h_{\mu\nu}, \tag{5.9}$$

where $\bar{g}_{\mu\nu}$ is given by eq. (5.1). The perturbed Einstein equations then read

$$\delta R_{\mu\nu}+\Lambda h_{\mu\nu}=0 \tag{5.10}$$

with $\delta R_{\mu\nu}$ representing the Ricci tensor expanded to linear order in the metric perturbation $h_{\mu\nu}$.

As in Chapter 3, for the gravitational perturbations we adopt the Regge-Wheeler gauge and decompose the metric perturbation into tensor spherical harmonics, with the tensor perturbation $h_{\mu\nu}$ having both axial and polar parity perturbations [145, 146]:

$$h^{ax}_{\mu\nu,\ell m}=\begin{pmatrix}0 & 0 & h_0(r)B^{\ell m}_\theta & h_0(r)B^{\ell m}_\phi\\ 0 & 0 & h_1(r)B^{\ell m}_\theta & h_1(r)B^{\ell m}_\phi\\ sym & sym & 0 & 0\\ sym & sym & 0 & 0\end{pmatrix}e^{-i\omega_{\ell m}t}, \tag{5.11}$$

$$h^{p}_{\mu\nu,\ell m}=\begin{pmatrix}H_0(r)F(r) & H_1(r) & 0 & 0\\ sym & H_2(r)F(r)^{-1} & 0 & 0\\ 0 & 0 & K(r)r^2 & 0\\ 0 & 0 & 0 & K(r)r^2\sin\theta\end{pmatrix}Y^{\ell m}e^{-i\omega_{\ell m}t}, \tag{5.12}$$

where *sym* indicates a symmetric entry, $B^{\ell m}_\mu$ is the axial parity vector spherical harmonic and $Y^{\ell m}$ is the standard scalar spherical harmonic, as described in [147, 148].

Once again we can treat perturbations of different parity separately in order to study the QNM spectrum to linear order in $a$ [284].

#### 5.3.3.1 Axial sector

For the axial sector, we can find that the gravitational degree of freedom can be described by the function $Q$:

$$Q(r) = h_1(r)\frac{F(r)}{r}\left(1+\frac{2maM^2}{r^3\omega}\right) \tag{5.13}$$

which satisfies the following Schrödinger style master equation (with $h_0(r)$ as an auxiliary field):

$$\left[\frac{d^2}{dr_*^2}+\omega^2-\frac{2amM\omega}{r^2}\left(\frac{2M}{r}+\frac{\Lambda}{3}r^2\right)-F(r)V_{RW}\right]Q=0 \tag{5.14}$$

where $V_{RW}$ is a generalised Regge-Wheeler potential[2], taking into account nonzero $a$ and $\Lambda$:

$$V_{RW}=\frac{\ell(\ell+1)}{r^2}-\frac{6M}{r^3}+am\frac{24M^2(3r-7M-2r^3\Lambda/3)}{\ell(\ell+1)r^6\omega}. \tag{5.15}$$

For $\Lambda=0$, eq. (5.14) agrees with the Schrödinger style equation for axial gravitational perturbations of a slowly rotating Kerr black hole given in [285]. With $a=0$, eq. (5.14) agrees with the result of [287] for the axial perturbations of a Schwarzschild-(A)dS black hole. With $a=\Lambda=0$, we recover the familiar Regge-Wheeler equation [145].

#### 5.3.3.2 Polar sector

For the polar sector, we can define a function $\Psi(r)$ in terms of the perturbation fields $H_1$, and $K$ (with $H_0, H_2$ as auxiliary fields):

$$\begin{aligned}\Psi=\frac{1}{3M+\lambda r}\left(r^2K+\frac{rF}{i\omega}H_1\right)\Big[1-\frac{2amM^2}{r^4\omega(3M+\lambda r)^2}\times\big(12M^3-6M^2r+3Mr^4\omega^2\\ -2\lambda^2Mr^2+\lambda r^3(r^2\omega+\lambda)\big)\Big]\end{aligned} \tag{5.16}$$

which obeys the following Schrödinger style master equation:

$$\left[\frac{d^2}{dr_*^2}+\omega^2-\frac{2amM\omega}{r^2}\left(\frac{2M}{r}+\frac{\Lambda}{3}r^2\right)-F(r)\left(V_Z^{(0)}+amV_Z^{(1)}\right)\right]\Psi=0 \tag{5.17}$$

where $V_Z^{(0)}$ is the familiar Zerilli-like potential[3] for Schwarzschild-(A)dS perturbations given by:

$$V_Z^{(0)}=\frac{2}{r^3}\frac{9M^3+3\lambda^2Mr^2+\lambda^2(1+\lambda)r^3+3M^2(3\lambda r-r^3\Lambda)}{(3M+\lambda r)^2} \tag{5.18}$$

[2]Note that here we have factored out the metric function $F(r)$ in the definition of $V_{RW}$, unlike in eq. (3.26) when we were concerned with exclusively Schwarzschild black holes.

[3]Again, similarly to our definition of $V_{RW}$ in this chapter, we have not included the factor of $F(r)$ in the definition of $V_Z^{(0)}$ here, in contrast to Chapter 3.

and with $2\lambda = (\ell+2)(\ell-1)$ [287]. $V_Z^{(1)}(r)$ is the $O(a)$ correction to the potential given in Appendix C.1. For $\Lambda = 0$, i.e. when considering a slowly rotating Kerr black hole, $V_Z^{(1)}(r)$ agrees with the linear in spin correction to the polar potential given in [285]. With $a = \Lambda = 0$, we recover the familiar Zerilli equation [153].

## 5.4 Quasinormal modes

### 5.4.1 Analytical Expressions

As a complement to other methods of calculating the QNM frequencies $\omega$ that satisfy the equations presented in section 5.3 [46, 45, 47, 288, 289], we will present analytic expressions for the QNM frequencies calculated via the method developed in [290]. By making an appropriate ansatz for the radial wavefunctions of the perturbed fields, the $\omega$ for each perturbation master equation can be expressed as a sum over inverse powers of $L = \ell + 1/2$, with $\ell$ being the multi-polar spherical harmonic index:

$$\omega = \sum_{k=-1}^{k=\infty} \omega_k L^{-k}. \tag{5.19}$$

The form of this expansion is inspired by the analytic formula for Schwarzschild QNMs in the *eikonal* (high $\ell$) limit [47, 291, 292]:

$$\omega = \frac{1}{3\sqrt{3}M}\left(\left(\ell+\frac{1}{2}\right) - i\left(n+\frac{1}{2}\right)\right) + \mathscr{O}(\ell^{-1}), \tag{5.20}$$

where $n$ is the overtone index, an integer labelling the discrete QNMs of the same $\ell$ by how quickly they decay (with $n = 0$ being the most long lived, 'fundamental' mode).

For a spacetime described by eq. (5.1), the appropriate ansatz for a generic wavefunction $\mathscr{F}^{\ell m}(r)$ satisfying eq. (5.4) is:

$$\mathscr{F}^{\ell m}(r) = exp\left(i\omega \int^{r_*} \left(1+\frac{6M}{r}\right)^{1/2} \left(1-\frac{3M}{r}\right) \left(1-9M^2\Lambda\right)^{-1/2} dr_*\right) v^{\ell m}(r) \tag{5.21}$$

with $dr_* = F(r)^{-1}dr$. The function $v^{\ell m}$ is expanded in a similar way to eq. (5.19):

$$v^{\ell m}(r) = exp\left(\sum_{k=0}^{k=\infty} S_k(r)\, L^{-k}\right). \tag{5.22}$$

The ansatz above is appropriate for the wavefunction $\mathscr{F}$ because as $r_* \to \pm\infty$ (i.e. to the black hole horizon or to the cosmological horizon/asymptotically flat space), $\mathscr{F} \sim e^{\pm i\omega r_*}$, which is what we require to have purely 'outgoing' waves at each boundary of our

spacetime, as discussed earlier in this chapter. As explained in [290], however, this ansatz is *not* applicable to asymptotically AdS spacetimes (i.e. for $\Lambda < 0$) due to the reflective boundary condition required as $r_* \to \infty$. Thus in the following examples we will limit ourselves solely to $\Lambda \geq 0$ cases. Nonetheless, the equations presented in section 5.3 remain valid for both positive and negative $\Lambda$.

By inserting the series expansions given by eq. (5.19) and (5.22) into a QNM equation such as eq. (5.4), one can solve for the $\omega_k$ and $S_k$ at each order in $L$. In appendix C.2 we present the $\omega_k$ that satisfy eqs. (5.7), (5.8), (5.14), and (5.17) for the fundamental $n = 0$ mode. In principle one can calculate the $\omega_k$ for arbitrary $n$, but for simplicity's sake we focus on the fundamental modes in this work. In each case we have calculated the first eight terms in the expansion, i.e. to $O(L^{-6})$. One can straightforwardly calculate terms to higher order in inverse powers of $L$ through the use of a computer algebra package. We will see in the following section that the QNM frequencies calculated via this analytic expansion method give results in very strong agreement with those calculated via, for example, 6th order WKB methods.

In the limit that $\ell \to \infty$ (the previously mentioned 'eikonal' limit) we find that the QNM frequencies, irrespective of field spin or mass, are given by:

$$M\omega_{\ell m} = \frac{\sqrt{1-9\Lambda M^2}}{6\sqrt{3}}(2\ell+1-i) + am\left(\frac{2}{27}+\frac{\Lambda M^2}{3}\right) + O(\ell^{-1}). \tag{5.23}$$

One result of interest garnered from calculating the $\omega_k$ that satisfy eq. (5.14) and (5.17) analytically is that the axial and polar gravitational frequencies appear to be isospectral to $O(L^{-3})$, with any differences between the $\omega_k$ at higher orders in $1/L$ being proportional to both $a$ and $\Lambda$ (see appendix C.2). Thus, to linear order in $a$, it is only in the case of non-zero black hole spin *and* non-zero cosmological constant that the spectra of the axial and polar perturbations split. The isospectrality of the gravitational modes for a Schwarzschild-de Sitter black hole is well known [44, 45, 46, 293, 294], with the isospectrality of slowly rotating Kerr-Newman black holes having been observed numerically in [286].

It is worth noting that the expansion technique of [290] is designed for use in spherically symmetric background spacetimes; indeed we will see in the following section that the results for Schwarzschild-de-Sitter black holes are highly accurate. We will see, however, relatively good agreement between those frequencies calculated numerically and those using the analytic expansion method for small values of the black hole spin $a$ despite the background spacetime no longer being spherically symmetric. Thus the expressions presented here can be regarded as a useful analytic tool for calculating QNMs of slowly rotating black holes.

We note that for *massive* fields, such as the scalar and vector fields discussed in this chapter, there exists a second branch of solutions for the $\omega$ other than the regular QNMs. These are long lived (i.e. with very small imaginary component of $\omega$) field configurations around the black hole known as 'quasi-bound states' [295, 296, 297, 298, 191, 299, 300, 301]. We will not consider the bound states in this work and only focus on the QNM family of solutions. Furthermore, in the case of asymptotically de Sitter spacetimes, a family of QNMs associated with the cosmological horizon is present which we do not capture here [302, 303, 294]. These modes are present even in pure de Sitter space (i.e. with $M = 0$) and are purely imaginary in such a scenario. The family of QNMs studied in this section is that associated with the photon sphere of the black hole, and as such the results obtained here can be seen as a deformation from the QNMs one would calculate if $\Lambda = 0$.

In the following section we will calculate the QNM frequencies satisfying each of eqs. (5.7), (5.8), (5.14), and (5.17) for varying $a$ and $\Lambda$, and investigate how well an approximation the $\omega_k$ presented in appendix C.2 provide for the QNM frequencies at linear order in black hole spin. In fact, we will see that for $a \ll 1$, the frequencies calculated in this chapter provide a very good approximation to those calculated in the literature.

## 5.4.2 Comparison to Other Results

### 5.4.2.1 Schwarzschild-de-Sitter

We first consider the case of a unit mass Schwarzschild-de-Sitter black hole ($a = 0$, $M = 1$, $0 \leq 9\Lambda \leq 1$) [304]. The QNM frequencies for electromagnetic, gravitational, and massless scalar perturbations in a Schwarzschild-de-Sitter background have been calculated, for example, using the 6th order WKB method in [293]. We find that in general the frequencies calculated using the analytic expansion method of [290] (utilising the expansion coefficients given in Appendices C.2-C.2) are in good agreement with those presented in [293].

Tables C.1 – C.3 in Appendix C.3 give the QNM frequencies for massless scalar perturbations, massless vector (i.e. electromagnetic) perturbations, and gravitational perturbations for a selection of $\Lambda$ values. We do not distinguish between axial and polar gravitational frequencies in this case as, further to the discussion above, the coefficients presented in appendix C.2 show that for $a = 0$ the axial and polar QNM frequencies are isospectral (this was also shown in [293]). In all cases the frequencies are presented as calculated via the WKB method as in [293] and via the analytical expansion method of [290] used in this work, with the errors between the two methods also given. Figures 5.1-5.3 show QNM frequencies in the complex plane as calculated via both methods.

Figure 5.1: Complex massless scalar frequencies for the $n = 0$ mode for varying values of $\Lambda$

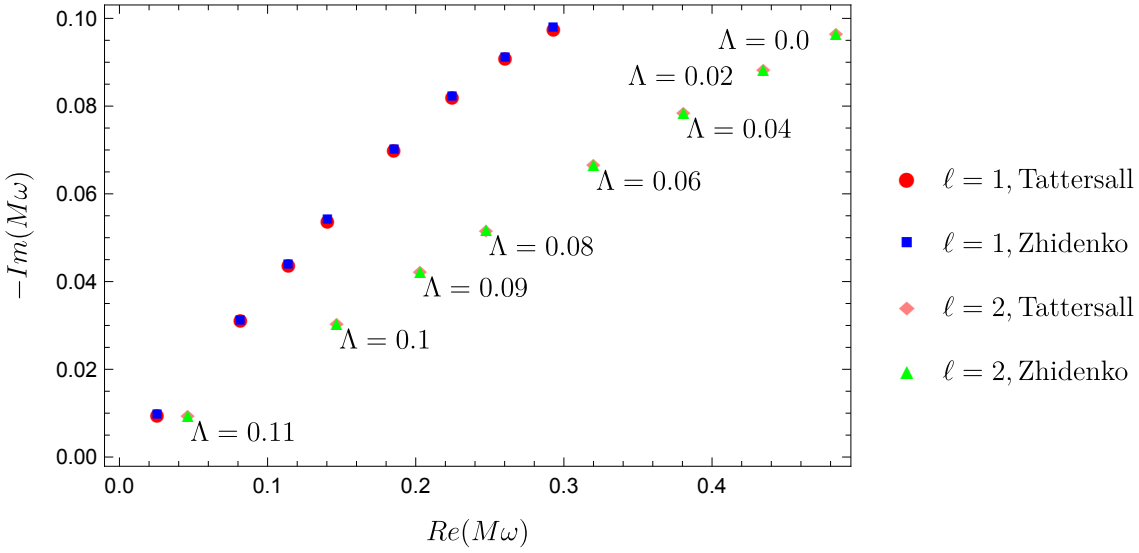


Tables C.1 – C.3 show that in all cases the relative errors between methods stays comfortably below 1%, with figures 5.1-5.3 showing almost complete alignment of frequencies in the complex plane. The expressions for the QNM frequencies given in appendix C.2 thus appear to compare very well with other methods of calculating QNM frequencies in the case that $a = 0$.

#### 5.4.2.2 Slowly rotating Kerr

We will now consider the case of a unit mass slowly rotating Kerr black hole ($a > 0$, $M = 1$, $\Lambda = 0$) [12]. The QNM frequencies for electromagnetic, gravitational, and massless scalar perturbations in a Kerr background have been calculated, for example, in [47] using Leaver's continued fraction method [288]. We will compare the results of using the expansion coefficients given in appendix C.2 to the QNM frequency data provided at `http://www.phy.olemiss.edu/~berti/ringdown/`.

Tables C.4 – C.6 in appendix C.3 give QNM frequencies for massless scalar perturbations, massless vector (i.e. electromagnetic) perturbations, and gravitational perturbations for a selection of $a$ values. As discussed above, we do not distinguish between axial and polar gravitational frequencies as to linear order in $a$ the axial and polar spectra are isospectral for $\Lambda = 0$ (see appendix C.2). In all cases the frequencies are presented as calculated via continued fractions in [47] and via the analytical expansion method of [290] used in this work, with the errors between the two methods also given.

Figure 5.2: Complex electromagnetic frequencies for the $n = 0$ mode for varying values of $\Lambda$

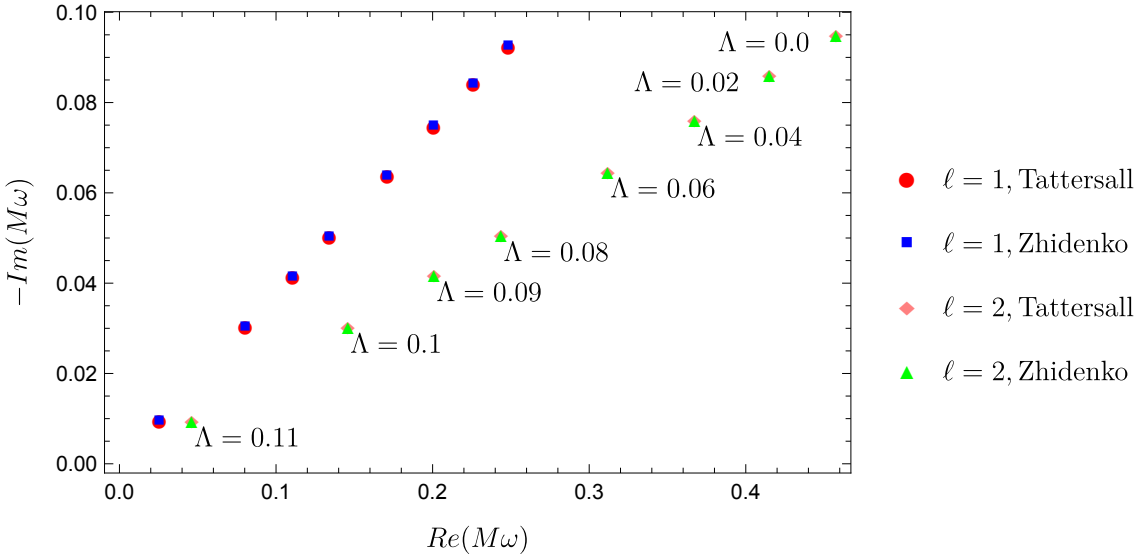


Figure 5.3: Complex gravitational frequencies for the $n = 0$ mode for varying values of $\Lambda$

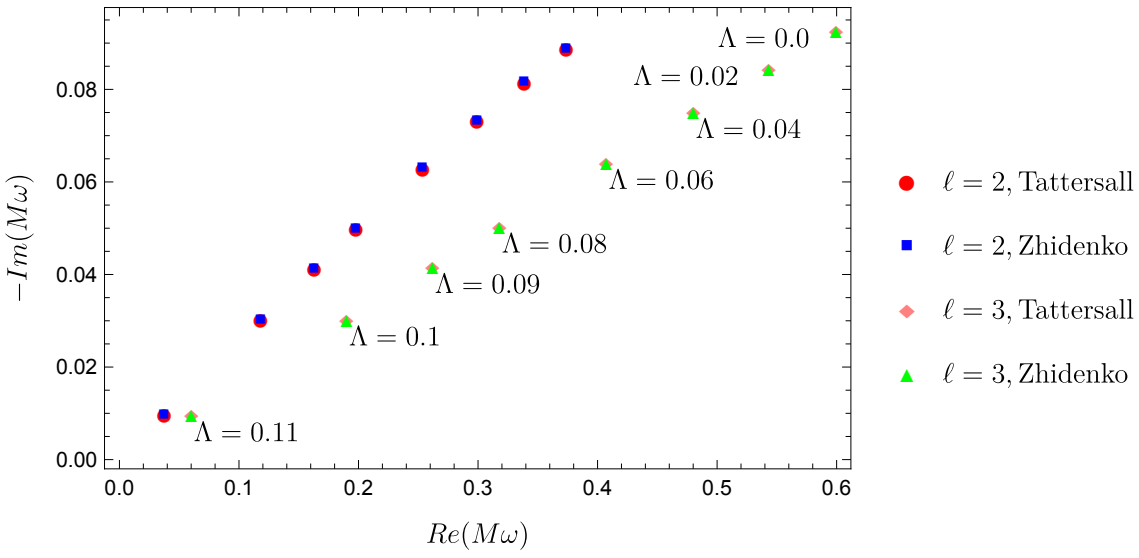

For $a \ll 1$, figures 5.4-5.6 show that the linear in $a$ approximation to the QNM frequencies calculated from the expressions in appendix C.2 match well with the numerical data, with tables C.4 – C.6 show the relative errors between methods staying below 1% for spins of up to $a \sim 0.2$. From figures 5.4-5.6, however, we see that the linear in $a$ approximation for the QNM frequencies clearly starts to fail at smaller values of $a$. This is particularly noticeable for the imaginary frequency components, where the departure from the linear approximation is clearly seen by $a \sim 0.1$. Predictably, in all cases, as $a$ increases the difference between linear in spin approximation used in this work and the frequencies calculated numerically increases.

The higher accuracy of the real frequency components compared to the imaginary components can be understood by considering that $O(a)$ contributions to the imaginary component only appear in two terms in the QNM expansion up to $O(L^{-6})$, $\omega_3$ and $\omega_5$ (see appendix C.2). This is contrast to the real frequency component which receives contributions linear in $a$ in $\omega_0$, $\omega_2$, $\omega_4$, and $\omega_6$. Thus one should compute higher order terms in the expansion to calculate further $O(a)$ corrections to the imaginary component of the QNM frequencies, and thus improve agreement.

Nonetheless, for small $a$ the analytic expressions for the QNM frequencies appear to be a good approximation to those calculated numerically.

We also consider the case of a *massive* scalar field propagating on a slowly rotating Kerr background, comparing to the continued fractions results of [305, 298]. QNM frequencies as calculated by each method, with relative error between the methods, are presented in tables C.7 and C.8 in appendix C.3. We see that across the mass range $0 \leq \mu M \leq 0.2$ and black hole spin range $0 \leq a \leq 0.2$, the analytic expressions presented here compare well to other methods, with relative errors staying below 1%.

Finally, note that the ansatz for the radial wavefunction given in eq. (5.22) is not, in fact, strictly accurate for *massive* fields. Instead, as $r_* \to \infty$, the asymptotic behaviour of $\mathscr{F}(r)$ should be $e^{qr}$ where $q = \pm\sqrt{\mu^2 - \omega^2}$ [298]. Nevertheless, we see from the results of tables C.7 and C.8 show that the analytic expressions presented in this chapter represent a good approximation to the massive QNMs.

#### 5.4.2.3 Slowly rotating Kerr-de Sitter

We now turn to the most general case of a slowly rotating Kerr-dS black hole, where both $a$ and $\Lambda$ are non-zero and positive. The gravitational QNM frequencies for a Kerr-dS black hole of varying mass were calculated in [306] by continued fractions, whilst their asymptotics were studied in [307]. Kerr-de Sitter black holes have further been studied in [308].

Figure 5.4: Real and imaginary components of the $\ell = m = 2$, $n = 0$ massless scalar mode for varying values of $a$

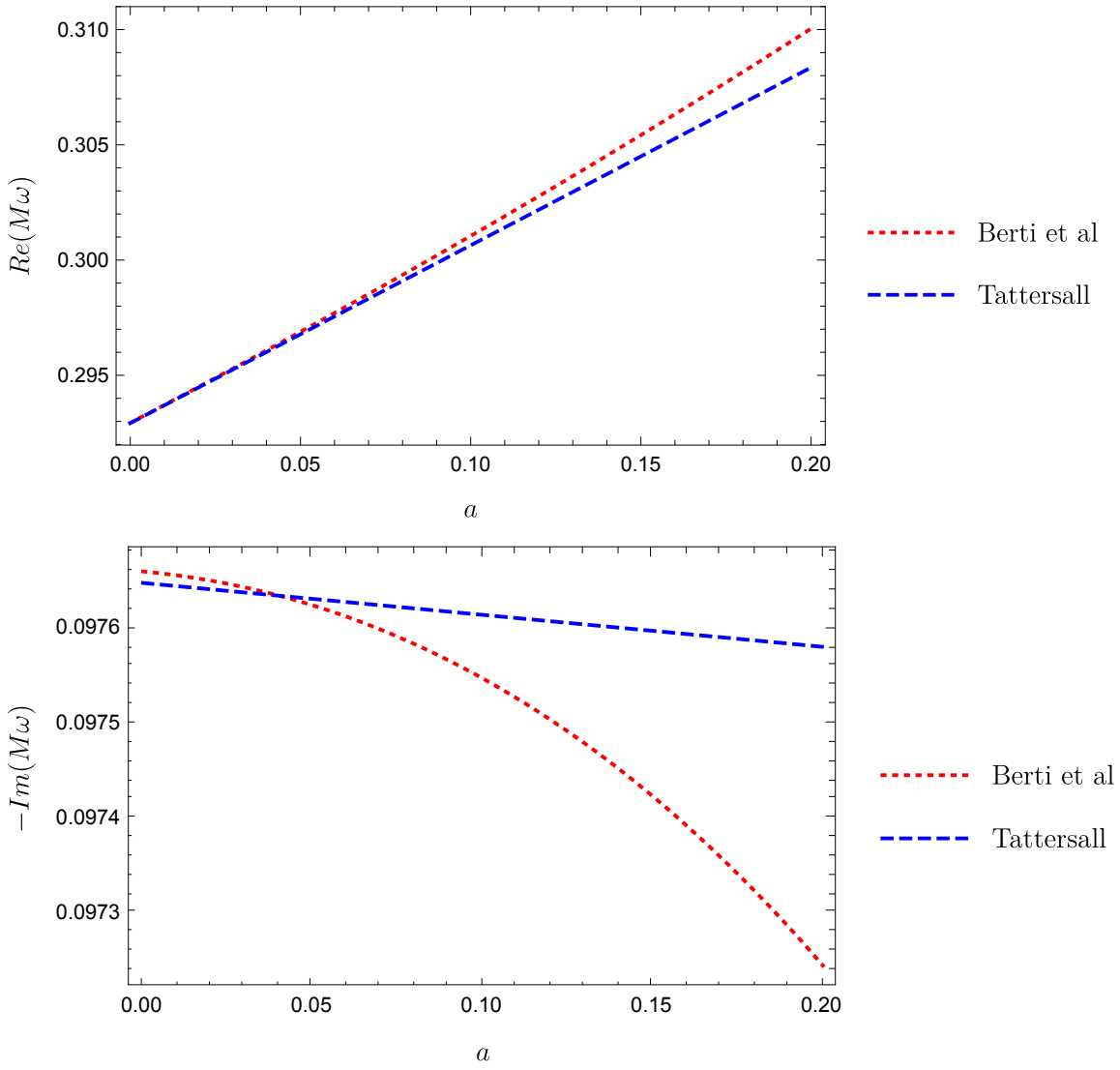

Figure 5.5: Real and imaginary components of the $\ell = m = 2$, $n = 0$ electromagnetic mode for varying values of $a$

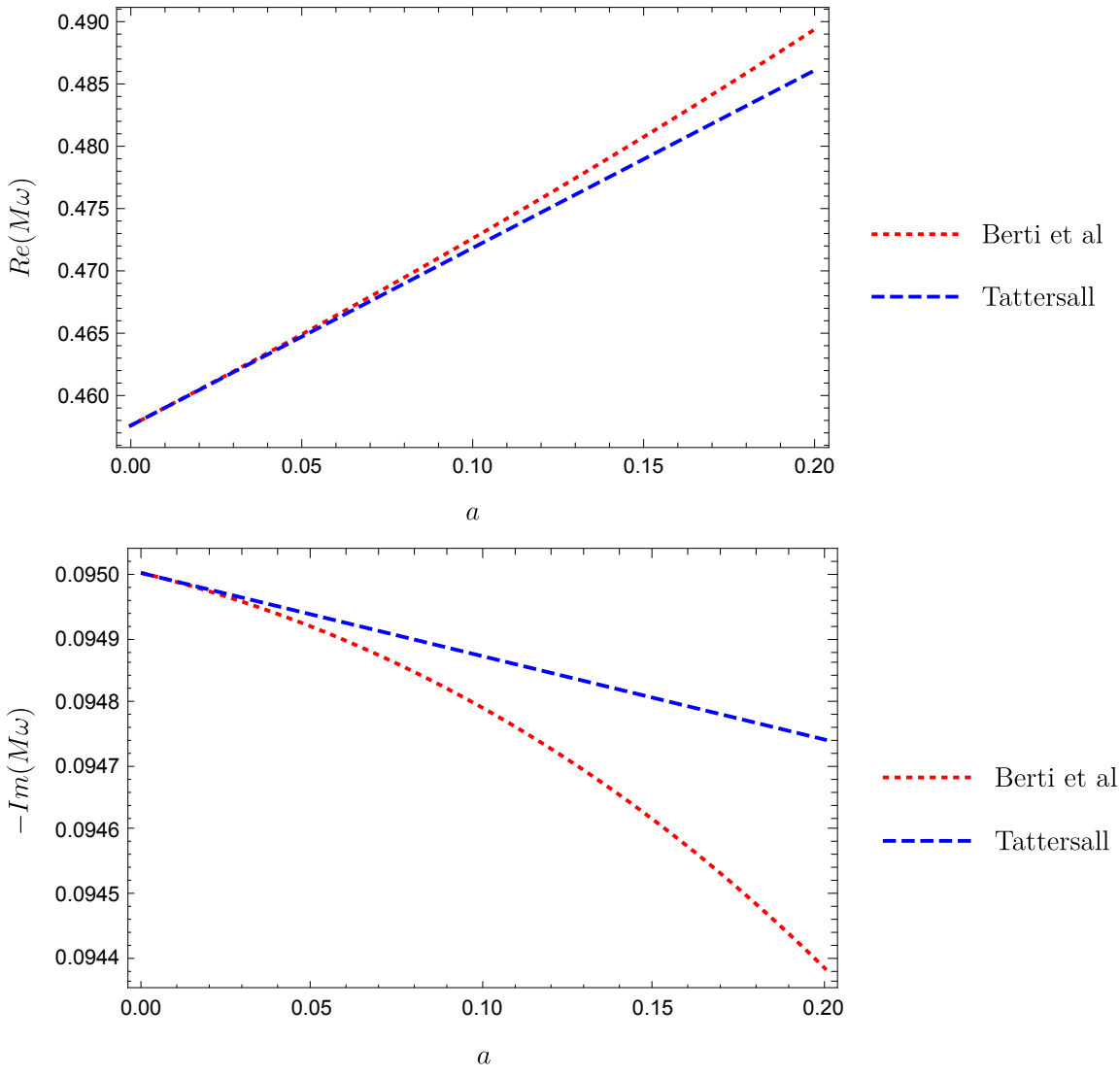

Figure 5.6: Real and imaginary components of the $\ell = m = 3$, $n = 0$ gravitational mode for varying values of $a$

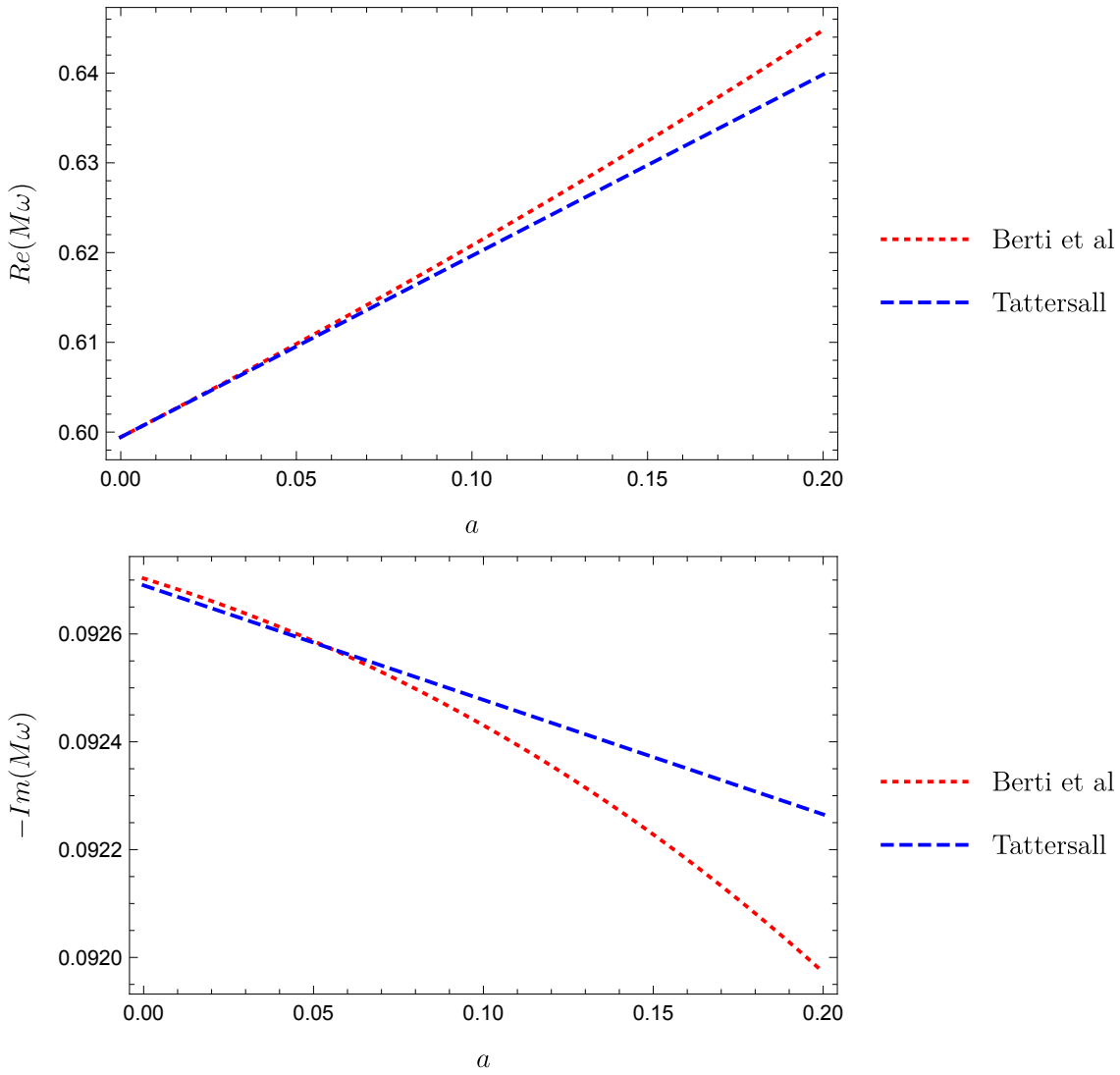

The expressions for $\omega_{-1}$ and $\omega_0$ in appendix C.2 (i.e. the first two terms in the $L$ expansion, as explained in section 5.4.1) agree exactly with the expressions given by eq. (0.3) and (0.4) in [307], thus verifying the dominant $O(a)$ correction to $Re(\omega)$ calculated in this chapter.

Turning to comparisons with [306], a table of fitting parameters $(\bar{\omega}, \omega_a)$ (referred to as $(\omega_0, \omega_1)$ in [306]) is provided to approximate the QNM frequencies of slowly rotating Kerr-dS black holes in the form:

$$\omega = \bar{\omega} + am\omega_a + O(a^2), \tag{5.24}$$

where $\bar{\omega}$ is the QNM frequency evaluated for $a = 0$, i.e. the corresponding Schwarzschild-dS frequency for a black hole of the same $M$ and $\Lambda$; $\omega_a$ represents the linear in $a$ correction term.

Table 5.1 compares data for $\bar{\omega}$ and $\omega_a$ from [306] and as calculated in this chapter for two black holes of differing mass, with the relative errors between both methods given in parentheses. Note that the fitting parameters $(\bar{\omega}, \omega_a)$ are rescaled by $M$ from their values in [306] to coincide with the dimensionless black hole spin $a$ that we are using in this chapter. Also note that, as previously mentioned, in the case that both $a$ and $\Lambda$ are non-zero, the axial and polar gravitational frequencies are no longer isospectral (see appendix C.2). Thus in table 5.1 we compare the results of [306] to both axial and polar frequencies as calculated in this chapter.

As demonstrated in section 5.4.2.1 for the case of a Schwarzschild-dS black hole, we find good agreement between the $\bar{\omega}$ calculated in [306] and those calculated in this work. We also find good agreement in the real part of $\omega_a$, with errors staying comfortably below 1% when considering either the polar or axial frequencies. The imaginary part of $\omega_a$ does not agree as well, with relative errors of order $\sim 10 - 20\%$. This can be understood similarly to the case of the imaginary Kerr frequencies as discussed above. For the imaginary frequency component, $O(a)$ contributions only appear in two terms in the QNM expansion up to $O(L^{-6})$ ($\omega_3$ and $\omega_5$). This is in contrast to the real frequency component which receives contributions linear in $a$ in all $\omega_n$ for even $n$. One should compute higher order terms in the expansion to calculate further $O(a)$ corrections to the imaginary component of the QNM frequencies. Indeed if one calculates, for example, $\omega_7$ for axial gravitational modes, the error in the imaginary component of $\omega_a$ for $M = 0.1789$ drops from 9.1% to 5.1%, whilst for $M = 0.1205$ the error drops from 27% to 11%. See appendix C.2 for the explicit expressions of the QNM frequencies calculated in this chapter to $O(L^{-6})$.

Table 5.1: Comparison of the $n = 0$ gravitational QNM frequency fitting parameters as calculated by Leaver's continued fraction method in [306] and analytical expansion techniques for varying $M$ with $\Lambda = 3, \ell = 2$.

| | Leaver | | L-expansion (axial) | | L-expansion (polar) | |
|---|---|---|---|---|---|---|
| $M$ | $\bar{\omega}$ | $\omega_a$ | $\bar{\omega}$ | $\omega_a$ | $\bar{\omega}$ | $\omega_a$ |
| 0.1205 | $2.418 - 0.5944i$ | $0.67564 + 0.0092i$ | $2.419 - 0.5931i$ | $0.67391 + 0.0117i$ | $2.419 - 0.5931i$ | $0.67720 + 0.0112i$ |
| (% error) | | | $(+0.04, -0.22)$ | $(-0.26, +27)$ | $(+0.04, -0.22)$ | $(+0.23, +22)$ |
| 0.1789 | $0.769 - 0.1964i$ | $0.58375 + 0.0022i$ | $0.770 - 0.1962i$ | $0.58324 + 0.0024i$ | $0.770 - 0.1962i$ | $0.58380 + 0.0022i$ |
| (% error) | | | $(+0.13, -0.10)$ | $(-0.09, +9.1)$ | $(+0.13, -0.10)$ | $(+0.01, +0.00)$ |

## 5.5 Conclusion

In this chapter we have presented Schrödinger style master equations for the perturbations of massive scalar, massive vector, and gravitational fields on a slowly rotating Kerr-(A)dS black hole. These represent generalisations of the Regge-Wheeler and Zerilli equations (for fields of spin $0, -1$, or $-2$) to include the effects of both a non-zero cosmological constant $\Lambda$ *and* of slow rotation (i.e. to linear order in dimensionless black hole spin $a$). Some of these equations have been presented before in their entirety (e.g. eq. (5.7) and (5.8) in [284]), whilst versions of the equations with either $a = 0$ or $\Lambda = 0$ have been presented in, for example, [285, 287]. The generalisation of the gravitational perturbation equations to include both the effects of rotation and of a cosmological constant presented here should, however, prove useful given the wealth of knowledge accumulated to address such Schrödinger style equations.

We have also presented, following the method of [290], analytical expressions for the QNM frequencies that satisfy each of the perturbation master equations present in section 5.3 (eq. (5.7), (5.8), (5.14), and (5.17)). The expressions given in appendix C.2 are intended as a complement to existing methods of QNM calculation, with the equations presented in section 5.3 of course being amenable to being solved via one's preferred method. Given that there are relatively few numerical results for QNM frequencies in the literature for some categories of black holes (e.g. Kerr-de Sitter), numerically investigating the perturbation master equations presented in this chapter and elsewhere is worthy of further attention. In addition, a natural extension of this work would be to consider black holes possessing non-zero electric charge [309, 13].

In section 5.4 we find that the analytic expressions calculated in this chapter agree well with the QNM frequencies calculated via other methods for a Schwarzschild-dS black hole [293], for a slowly rotating Kerr black hole [47], and for a slowly rotating Kerr-de Sitter black hole [306, 307]. They are not, however, valid for asymptotically AdS spacetimes (as explained in [290]). The frequencies calculated in this chapter support the numerically observed isospectrality of gravitational modes to linear order in spin for Kerr black holes [286], whilst the axial and polar gravitational spectra are shown to split for $a \neq 0$ *and* $\Lambda \neq 0$. Given the good agreement with numerical results, the analytic expressions for QNM frequencies presented here provide a useful addition to those techniques already in the modern physicist's toolbox, allowing one to see the explicit dependence of the QNM frequencies on the parameters of the black hole and/or field, and to quickly calculate frequencies without needing access to (or to develop new) numerical routines.

The study of gravitational QNM frequencies is, of course, of great interest in the context of gravitational wave observations. Properties of black hole merger remnants can be inferred from the observation of the QNM ringing, as well as tests of GR and of the 'no-hair hypothesis' [55, 56, 59, 310, 37, 273, 274]. Meanwhile, the study of the QNM frequencies of massive bosons (e.g. the scalar and vector cases considered here) propagating on rotating black hole backgrounds finds great relevance in the study of black hole superradiance [311]. Furthermore, the AdS/CFT correspondence continues to provide motivation for studying QNMs in asymptotically AdS spacetimes [277, 278, 279, 280, 281].

The technique of recasting the complicated, multidimensional, equations of motion governing black hole perturbations in GR into decoupled one-dimensional Schrödinger style equations is an incredibly useful one that has allowed great advances in the understanding and numerical calculation of QNM frequencies. The ability to execute such a simplification of the equations of motion, and in particular to include the effects of rotation, in theories of gravity *beyond* GR is in many cases still a work in progress [84, 75, 137, 138, 136, 254, 312, 313, 64, 65, 76, 314]. Given that the strong gravity regime of black hole mergers is likely to be one of the best 'laboratories' available to us to probe any potential deviations from Einstein's theory, continuing the analysis of black hole perturbations for a variety of fields in alternative theories of gravity will remain an important avenue of research as gravitational wave astronomy matures in the coming years.

# Chapter 6

# Ringdown and Black Hole Spectroscopy in Horndeski Gravity

# Abstract

In this chapter I will study black hole perturbations in Horndeski gravity and investigate the prospect of using black hole spectroscopy to constrain the parameters of the theory through gravitational wave observations. We study the gravitational waves emitted during ringdown from black holes without hair in Horndeski gravity, demonstrating the qualitative differences between such emission in General Relativity and Horndeski theory. In particular, Quasi-Normal Mode frequencies associated with the scalar field spectrum can appear in the emitted gravitational radiation. Analytic expressions for error estimates for both the black hole and Horndeski parameters are calculated using a Fisher Matrix approach, with constraints on the 'effective mass' of the Horndeski scalar field of order $\sim 10^{-17}\mathrm{eV}c^{-2}$ or tighter being shown to be achievable in some scenarios. Estimates for the minimum signal-noise-ratio required to observe such a signal are also presented. The material in this chapter is based on [84, 85].

## 6.1 Introduction

The advent of gravitational wave (GW) astronomy, with numerous observations of mergers of compact objects now made by advanced LIGO and VIRGO [16], has opened new avenues for testing Einstein's theory of General Relativity (GR) [4, 273]. With these tests have come constraints on the landscape of modified gravity theories, most significantly those constraints garnered from the propagation of gravitational waves over cosmological distances [175, 176, 315, 157, 170, 171], as explored in Chapter 4. In the future, next generation ground and space based GW detectors bring the promise of black hole spectroscopy: observing the frequency spectrum of gravitational waves emitted by perturbed black holes – specifically the QNM spectrum – and using them as a fingerprint to both infer the properties of the emitting black holes, as well as to test the predictions of GR against competing theories of gravity [55, 56, 57, 58, 59, 60, 37, 61].

When considering testing the predictions of GW emission between various theories of gravity, one can look for discrepancies induced either by: (a) a background black hole solution in a modified theory of gravity that differs from the standard GR description of black holes (i.e. the Kerr metric for realistic astrophysical sources) and/or by (b) a different dynamical evolution of gravitational waves with respect to GR from the perturbed system, regardless of the properties of the background black hole. The emphasis of this chapter will be on (b): we will focus on the case, where the background black hole solution is given by the same solution as in GR, but the emitted GW signal is governed by modified equations of motion leading to *extra* QNMs.

Partial motivation for pursuing this line of research comes from Chapter 4, where it was argued that scalar-tensor theories in which the scalar field had cosmological relevance would, in many cases, have black holes with no-hair. But more generally, case (b) can be considered a more generic prediction of extensions to GR: while black holes might or might not have hair, the field equations will, for sure, be modified leading to extra or new QNMs [130, 138, 83, 316]. This possibility was explored in a theory agnostic manner in Chapter 3.

In this chapter we will consider the Horndeski family of scalar-tensor theories of gravity [103]. We will first demonstrate the qualitative differences in GW emission in GR and Horndeski gravity – the sourcing of gravitational perturbations by the Horndeski scalar field leading to the presence of extra QNMs – before quantifying what one could learn about the parameters of a GW emitting system given an observation of sufficient 'loudness'. We will show that, in certain circumstances, the observation of (at least) two distinct frequencies of

the damped gravitational waves emitted during 'ringdown' from a black hole in Horndeski gravity can provide strong constraints on fundamental parameters of the theory.

*Summary*: In section 6.2 we will introduce the action for Horndeski gravity and look at black hole perturbations in this family of theories. We will then move on to parameter estimation in section 6.3; we introduce a simple analytical model for the gravitational waves emitted from a perturbed black hole in Horndeski gravity and, building on [56], we employ a Fisher matrix analysis to predict quantitatively what one could learn about the fundamental theory from a GW observation. This will include both analytic and numerical results, as well as considerations on the properties of the observed GW signal required to perform such an analysis. In section 6.4 we will discuss the results and limitations of our analysis before making some concluding remarks.

## 6.2 Horndeski Gravity

Extensions to General Relativity normally involve additional fields (other than the metric and standard matter fields) that interact non-trivially with gravity. In this chapter we will focus on the family of Horndeski theories which introduces an additional scalar field.

### 6.2.1 Action

A general action for scalar-tensor gravity with $2^{nd}$ order-derivative equations of motion is given by the Horndeski action [103, 317], which we first discussed in Chapter 4, but which we present again here for clarity:

$$S = \int d^4x\sqrt{-g}\sum_{n=2}^{5} L_n, \tag{6.1}$$

where the Horndeski Lagrangians are given by:

$$\begin{aligned}
L_2 &= G_2(\phi,X)\\
L_3 &= -G_3(\phi,X)\Box\phi\\
L_4 &= G_4(\phi,X)R + G_{4,X}(\phi,X)((\Box\phi)^2 - \phi^{\alpha\beta}\phi_{\alpha\beta})\\
L_5 &= G_5(\phi,X)G_{\alpha\beta}\phi^{\alpha\beta} - \frac{1}{6}G_{5,X}(\phi,X)((\Box\phi)^3 - 3\phi^{\alpha\beta}\phi_{\alpha\beta}\Box\phi + 2\phi_{\alpha\beta}\phi^{\alpha\sigma}\phi^{\beta}_{\sigma}),
\end{aligned} \tag{6.2}$$

where $\phi$ is the scalar field with kinetic term $X = -\phi_\alpha\phi^\alpha/2$, $\phi_\alpha = \nabla_\alpha\phi$, $\phi_{\alpha\beta} = \nabla_\alpha\nabla_\beta\phi$, and $G_{\alpha\beta} = R_{\alpha\beta} - \frac{1}{2}R\,g_{\alpha\beta}$ is the Einstein tensor. The $G_i$ denote arbitrary functions of $\phi$ and $X$, with derivatives $G_{i,X}$ with respect to $X$ and derivatives $G_{i,\phi}$ with respect to $\phi$. GR is given by the choice $G_4 = M_P^2/2$ with all other $G_i$ vanishing and $M_P$ being the reduced

Planck mass. Eq. (6.1) is not the most general scalar-tensor action and it has been shown that it can be extended to an arbitrary number of terms [198, 318, 197, 319].

### 6.2.2 Background Solutions and Perturbations

Let us assume that Horndeski gravity admits a background solution such that the spacetime is Ricci flat, $R_{\alpha\beta} = 0 = R$ (e.g. Minkowski or Schwarzschild), and the scalar field $\phi$ has a trivial constant profile, $\phi = \phi_0 = const$. Several no-hair theorems for various manifestations of Horndeski gravity, leading to such solutions, exist in the literature [188, 209, 210] (see also Chapter 4).

Now consider perturbations to this background solution such that:

$$g_{\alpha\beta} = \bar{g}_{\alpha\beta} + h_{\alpha\beta} \tag{6.3}$$

$$\phi = \phi_0 + \delta\phi, \tag{6.4}$$

where $\delta\phi$ and $h_{\alpha\beta}$ are considered to be small and of the same perturbative order, and the metric $\bar{g}_{\alpha\beta}$ describes the background Ricci-flat spacetime. Varying the action given by eq. (6.1) with respect to $g_{\alpha\beta}$ and $\phi$, we find from the background equations of motion that $G_2 = G_{2\phi} = 0$ (with the $G_i$ functions being evaluated at the level of the background, i.e. for $\phi = \phi_0$). The following system of equations is found for the *perturbed* fields:

$$G^{(1)}_{\alpha\beta} = \frac{G_{4,\phi}}{G_4}\left(\nabla_\alpha\nabla_\beta\delta\phi - g_{\alpha\beta}\Box\delta\phi\right) \tag{6.5a}$$

$$\Box\delta\phi = \mu^2\delta\phi \tag{6.5b}$$

where $G^{(1)}_{\alpha\beta}$ is the Einstein tensor perturbed to linear order in $h_{\mu\nu}$, $\Box = \bar{g}^{\mu\nu}\nabla_\mu\nabla_\nu$ and $\mu^2$ is given by:

$$\mu^2 = \frac{-G_{2,\phi\phi}}{G_{2,X} - 2G_{3,\phi} + 3G^2_{4,\phi}/G_4}. \tag{6.6}$$

Once again, all of the Horndeski $G_i$ functions are evaluated at the background i.e. they are functions of the constant $\phi_0$ only. Thus $\mu^2$ is a constant and acts like an effective mass term squared for the scalar field. Eq. (6.6) clearly shows that for some combination of the Horndeski parameters, $\mu^2$ could be negative. We will assume that $\mu^2 > 0$ for the rest of this work, but considering a negative effective mass squared could be an interesting area of future research. Furthermore, we will assume that $G_{2,X} - 2G_{3,\phi} + 3G^2_{4,\phi}/G_4 \neq 0$. The right hand side of eq. (6.5a) shows the new gravitational scalar field sourcing the gravitational perturbations.

### 6.2.3 Black Holes and Ringdown

From eq. (6.5a)-(6.5b), we can see that *any* Ricci flat black hole solution with a constant scalar field profile will have gravitational perturbations sourced by the Horndeski scalar perturbations.

For the rest of this chapter we will be concerned with the effect of Horndeski gravity on the GW signal emitted from a black hole as it 'rings down' following a merger event or some other process which leaves the black hole perturbed. To do so, we can consider the background spacetime to be Schwarzschild and decompose the metric and scalar perturbations into tensor spherical harmonics, as is standard when studying the response of spherically symmetric black holes to perturbations [44, 45, 46, 47, 147, 148] (and has been discussed in Chapters 3 and 5). We will further assume a harmonic time dependence of $e^{-i\omega t}$ for the metric and scalar perturbations, leading to the following system of equations:

$$\frac{d^2Q}{dr_*^2} + \left[\omega^2 - f(r)V_{RW}(r)\right]Q = 0 \tag{6.7a}$$

$$\frac{d^2\Psi}{dr_*^2} + \left[\omega^2 - f(r)V_Z(r)\right]\Psi = \frac{G_{4\phi}}{G_4}S_\varphi\left(\varphi,\varphi'\right) \tag{6.7b}$$

$$\frac{d^2\varphi}{dr_*^2} + \left[\omega^2 - f(r)V_S(r,\mu^2)\right]\varphi = 0, \tag{6.7c}$$

where $\varphi(r)$ is the radial wave function of $\delta\phi$, $Q(r)$ and $\Psi(r)$ represent the odd and even parity degrees of freedom in the metric perturbations (see section 5.3 with $a = \Lambda = 0$ for their definitions), and $r$ is the usual Schwarzschild radial coordinate. The tortoise coordinate $r_*$ is defined by $dr_* = f(r)^{-1}dr$, with $f(r) = 1 - 2M/r$ and $M$ being the black hole mass.

The various potentials appearing in the above equations are given by:

$$V_{RW}(r) = \left(\frac{\ell(\ell+1)}{r^2} - \frac{6M}{r^3}\right) \tag{6.8a}$$

$$V_Z(r) = 2\frac{\lambda^2 r^2\left[(\lambda+1)r+3M\right] + 9M^2(\lambda r+M)}{r^3(\lambda r+3M)^2} \tag{6.8b}$$

$$V_S(r) = \left(\frac{\ell(\ell+1)}{r^2} + \frac{2M}{r^3} + \mu^2\right) \tag{6.8c}$$

with $2\lambda = (\ell+2)(\ell-1)$, whilst the 'source term' $S_\varphi\left(\varphi,\varphi'\right)$ is given by:

$$\begin{aligned} S_\varphi\left(\varphi,\varphi'\right) &= \frac{-(1-2M/r)U_\varphi\left(\varphi,\varphi'\right)}{2r^2\left(\lambda r+3M\right)^2} \\ U_\varphi\left(\varphi,\varphi'\right) &= \left(4M\left(3M+\left(2\ell(\ell+1)-1\right)r\right)+2r^3\left(3M+\lambda r\right)\mu^2\right)\varphi + 12Mr(r-2M)\varphi'. \end{aligned} \tag{6.9}$$

Note that we have suppressed spherical harmonic indices, but each equation is assumed to hold for a given $\ell$.

These equations can be solved to find the complex solutions of the $\omega$, the QNM frequencies, subject to boundary conditions such that the emitted waves are are purely ingoing at the black hole horizon and purely outgoing at spatial infinity [44, 45, 46, 47, 45]. As discussed previously in this thesis, but is worth repeating, the fact that the $\omega$ are complex means that the gravitational waves emitted from this system are not only oscillatory in nature, but also decay in time: the gravitational waves emitted are essentially a superposition of exponentially damped sinusoids. The $\omega$ describe the oscillation frequency $f$ and damping time $\tau$ of the gravitational (and, in this case, scalar) waves via

$$\omega_{\ell m} = 2\pi f_{\ell m} + i/\tau_{\ell m}, \tag{6.10}$$

where we have reinserted spherical harmonic indices $\ell$ and $m$ to emphasise that these relations are general for any $\omega_{\ell m}$.

The system of equations given by eq. (6.7a)-(6.7c) shows that the odd parity gravitational degree of freedom $Q$ is decoupled from $\varphi$ and evolves exactly as in GR according to the Regge-Wheeler equation [145]. On the other hand, whilst the even parity gravitational field $\Psi$ obeys the well known Zerilli equation as in GR [153] on the 'left hand side' of eq. (6.7b), $\Psi$ is now also sourced by the freely evolving scalar wave function $\varphi$.

We can interpret eq. (6.7b) and eq. (6.7c) as leading to the gravitational field oscillating with both the 'transient' GR solution and the 'driving' scalar field solution. An analogous mode-mixing situation arises in a certain parameter limit of Chern-Simons gravity [138], where it is the odd parity gravitational degree of freedom that is driven by a free massless scalar field. In this case a two-mode fit of each of the fundamental $\ell = 2$ modes from the gravitational and scalar spectra fits the numerical evolution of the QNM equations well. In [316] the 'reverse' effect was observed numerically in scalar Gauss-Bonnet gravity. In this case, again due to a system of coupled QNM equations, the emitted *scalar* waves appear to be 'contaminated' with modes arising from the gravitational spectrum.

A similar perturbation analysis can be done for a slowly rotating Kerr black hole (leading to more complex, but qualitatively similar equations of motion to eq. (6.7a)-(6.7c)). For perturbations of Kerr black holes of arbitrary spin, however, one requires the Teukolsky equation [283]. Eq. (6.5a) shows that any modified gravity effects on the 'right hand side' of the equation can be packaged as the 'source' of the Teukolsky equation. This opens up the possibility of analytically studying perturbations to black holes of arbitrary spin in modified gravity, assuming that the background scalar field takes a trivial constant profile. We will leave such an analysis to future work.

As was mentioned in Chapter 5, it is worth noting that for *massive* scalar fields there exists a second family of solutions other than the QNMs, the 'quasi-bound states', that represent long lived field configurations around the black hole [295, 296, 297, 298, 191, 299, 300, 301]. We will not consider the bound states in this work and instead focus on the QNM family of solutions driving the emitted gravitational waves. A full analysis of the black hole-scalar system for arbitrary spin black holes would, of course, warrant consideration of such bound states. It is an intriguing question as to how the quasi-bound states around black holes might drive gravitational radiation during ringdown.

Figure 6.1 shows the qualitative effect of the scalar perturbations 'driving' the gravitational waves. The gravitational waves are modulated from their usual GR frequencies by the frequency of the scalar mode. The scalar amplitude in the centre and right hand panels of figure 6.1 is exaggerated to make the effect noticeable to the eye, but the qualitative picture of the mode mixing effect is valid.

As has been discussed before, but bears repeating, the system described by eq. (6.7a)-(6.7c) exhibits clear non-GR behaviour due to the presence of the scalar field perturbation, despite the background solution being identical to GR (i.e. a Schwarzschild black hole with no scalar hair). Thus the detection of modified gravity effects in the ringdown part of a GW signal is *not necessarily* indicative of violations of the no-hair theorem. Stated another way, even black holes in theories that obey no-hair theorems could exhibit non-GR behaviour in their perturbations [130].

## 6.3 Parameter Estimation

Throughout this section we will follow the formalism laid out by Berti, Cardoso, and Will in [56] (henceforth referred to as BCW), the main elements of which are recapped below.

### 6.3.1 Fisher Matrix formalism

We wish to study the response of a gravitational wave detector to the exponentially damped sinusoidal gravitational waves emitted by a perturbed black hole in Horndeski gravity, as described in section 6.2. Firstly, we assume that each of the gravitational waveforms received at our detector is such that the strain $h$ is given by:

$$h = h_+ F_+ + h_\times F_\times \tag{6.11}$$

Figure 6.1: Waveform 'cartoon' of a superposition of $\ell = 2$ gravitational and massless scalar modes for a unit mass Schwarzschild black hole. The amplitude of the gravitational waveform is fixed to $A_g = 1$ with $A_s$ varying from 0.1 to 1.

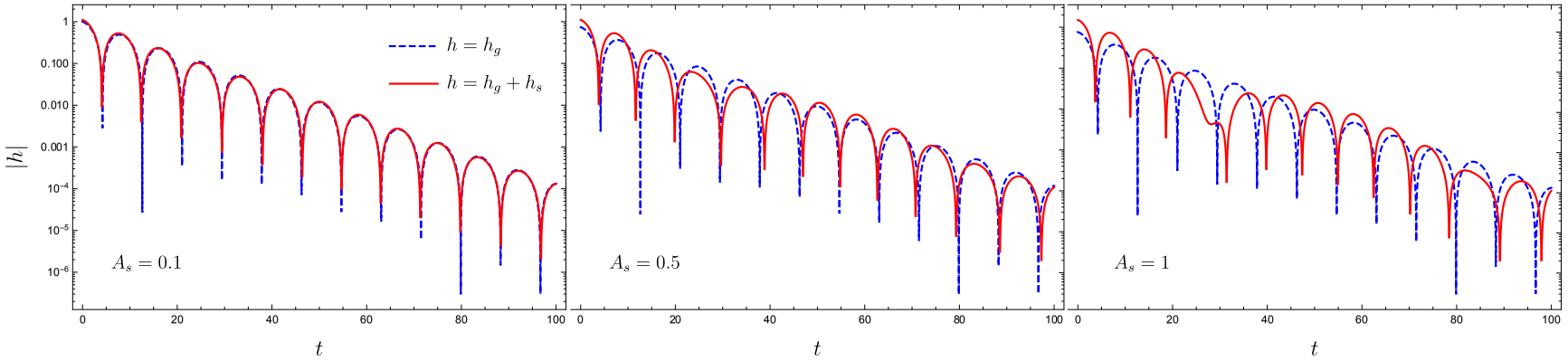

where $h_+$ and $h_\times$ are the two polarisations of the GW given by (in the frequency domain):

$$\tilde{h}_+ = A_+ \left[ S_{\ell m} e^{i\phi^+} b_+(f) + S_{\ell m} e^{-i\phi^+} b_-(f) \right] \tag{6.12}$$

$$\tilde{h}_\times = -iN_\times A_+ \left[ S_{\ell m} e^{i\phi^\times} b_+(f) - S_{\ell m} e^{-i\phi^\times} b_-(f) \right], \tag{6.13}$$

with

$$b_\pm(f) = \frac{1/\tau_{\ell m}}{(1/\tau_{\ell m})^2 + 4\pi^2 (f \pm f_{\ell m})^2}. \tag{6.14}$$

and $\phi^\times = \phi^+ + \phi^0$.

The $F_{+,\times}$ pattern functions represent detector orientation and source direction dependence, and are given by [56]:

$$F_+ = \frac{1}{2}\left(1 + \cos^2\theta_S\right)\cos 2\phi_S \cos 2\psi_S - \cos\phi_S \sin 2\phi_S \sin 2\psi_S \tag{6.15a}$$

$$F_\times = \frac{1}{2}\left(1 + \cos^2\theta_S\right)\cos 2\phi_S \sin 2\psi_S + \cos\phi_S \sin 2\phi_S \cos 2\psi_S. \tag{6.15b}$$

The angles $\theta_S$ and $\phi_S$ give the angular position of the GW source in usual spherical coordinates, whilst $\psi_S$ describes the rotation of the GW polarisation axes relative to the detector arm axes [320]. The $S_{\ell m}$ are spin-2 spheroidal functions that are in principle complex. As explained in BCW (and explored quantitatively in [321]), however, it is sufficient to assume that $S_{\ell m} \approx \Re(S_{\ell m})$ due to $\Re(S_{\ell m}) \gg \Im(S_{\ell m})$. This will allow us in the following to make use of the angle averages $< S^2_{\ell m} >= 1/4\pi$, $< F^2_+ >=< F^2_\times >= 1/5$, and $< F_+ F_\times >= 0$.

Finally, we assume that the gravitational waves emitted from a system governed by eqs. (6.7b)-(6.7c) are given as a superposition of two modes, the most dominant mode of each of the gravitational and scalar spectra, such that the total strain is given by:

$$h = h_g + h_s, \tag{6.16}$$

where $h_g$ and $h_s$ have the same functional form as outlined above, however with different amplitudes, phases, and appropriate frequencies and damping times. In reality, of course, the signal will be more accurately represented as having contributions from multiple $(\ell, m)$ modes from both gravitational and scalar spectra, as well as overtones. But for ease of calculation, and for the sake of illustrating the core 'mode mixing' effect, we consider this two mode model as sufficient.

We can define an inner product in frequency space between two generic waveforms $h_1$ and $h_2$ using the noise spectral density of the detector $S_h(f)$:

$$(h_1|h_2) \equiv 2\int_0^\infty \frac{\tilde{h}_1^* \tilde{h}_2 + \tilde{h}_2^* \tilde{h}_1}{S_h(f)} df. \tag{6.17}$$

The signal to noise ratio (SNR) $\rho$ of the signal given by eq. (6.16) is thus:

$$\rho^2 = (h|h) = 4\int_0^\infty \frac{\tilde{h}^*(f)\tilde{h}(f)}{S_h(f)}df, \tag{6.18}$$

and the components of the Fisher matrix $\Gamma_{ab}$ associated with the signal are given by:

$$\Gamma_{ab} \equiv \left(\frac{\partial h}{\partial \theta^a}\middle|\frac{\partial h}{\partial \theta^b}\right), \tag{6.19}$$

where the $\theta^a$ are the parameters upon which the waveform depends. Note that in each of the above integrals in the frequency domain, we are also implicitly angle-averaging over the sky.

Clearly from eq. (6.19) we will need to evaluate derivatives of the waveform with respect to the various parameters $\theta^a$. For example, in BCW, analytic fits to numerical results for Kerr gravitational QNM frequencies are presented as functions of black hole mass $M$ and dimensionless angular momentum $j$[1] so that derivatives can be performed analytically. In the case of Horndeski gravity, as studied here, of particular interest is the dependence of the waveform on the effective scalar mass (squared) $\mu^2$.

For simplicity's sake, when evaluating our analytical results numerically in section 6.3.2, we will restrict ourselves to considering (at most) slowly rotating Kerr black holes. Clearly we would ideally like to consider black holes with dimensionless spin $\sim 0.7$ to best replicate the events observed by aLIGO/Virgo so far, but we use the case of a slowly rotating black hole as a starting point. Thus, when evaluating parameter derivatives for the rest of this chapter, we will use the analytic expressions for massive scalar and gravitational QNM frequencies of slowly rotating black holes calculated in Chapter 5. For example, for $j = 0, \ell = 2$, we can make use of the following:

$$\begin{aligned}
\omega_g^{\ell=2} &= 2\pi f_g^{\ell=2} + i/\tau_g^{\ell=2} \approx \frac{1}{M}(0.374 - 0.0887i) \\
\omega_s^{\ell=2} &= 2\pi f_s^{\ell=2} + i/\tau_s^{\ell=2} \approx \frac{1}{M}\Big(0.484 + 0.316\,(\mu M)^2 + 0.0372\,(\mu M)^4 + 0.0232\,(\mu M)^6 \\
&\qquad - \Big[0.0968 - 0.108\,(\mu M)^2 - 0.0272\,(\mu M)^4 - 0.0246\,(\mu M)^6\Big]\,i\Big)
\end{aligned} \tag{6.20}$$

We do, however, emphasise that the analytic expressions presented in section 6.3.2 are applicable to *any black hole* emitting a mixed mode waveform - it is only in the numerical evaluations of these expressions that we have chosen to limit ourselves to at most slowly rotating Kerr black holes.

[1] Note that previously in this thesis, we have used the symbol $a$ for the dimensionless angular momentum, or 'spin', of a black hole. In this chapter we will use $j$ so as not to confuse with amplitudes $A$

We are now in a position to analytically calculate the SNR and Fisher Matrix components for our mixed mode GW signal, from which we can calculate error estimates from the covariance matrix $\Sigma_{ab} = (\Gamma_{ab})^{-1}$. To do so we will use the '$\delta$-function approximation' introduced in BCW to evaluate frequency integrals, replacing products of the $b_{\pm}(f)$ that arise in constructing the various inner products with appropriately normalised $\delta$-functions. In making this approximation we assume that $S_h(f_{g,\ell m}) \approx S_h(f_{s,\ell m}) = S$, which is appropriate given that $f_{g,\ell m}$ and $f_{s,\ell m}$ will be very close to each other in practice.

From now on we will suppress the $(\ell, m)$ index on, for example, $f$ and $\tau$, with each expression assumed to hold for a specific choice of harmonic indices. We will retain 'g' and 's' subscripts to differentiate between those parameters belonging to the gravitational mode and those belonging to the scalar mode in the mixed mode waveform.

### 6.3.2 Results

To find error estimates for each of the parameters of the mixed mode waveform we invert the Fisher matrix and take the diagonal components of $\Sigma_{ab} = (\Gamma_{ab})^{-1}$. In practice, the components of $\Gamma_{ab}$ were first calculated in the parameter basis of $(A_g, \phi_g^+, f_g, Q_g, A_s, \phi_s^+, f_s, Q_s)$, where the quality factor $Q$ of a mode is given by $Q_{\ell m} = \pi f_{\ell m} \tau_{\ell m}$. We then changed basis from $(f_g, Q_g, f_s, Q_s)$ to $(M, j, \mu^2)$ before inverting and extracting the error estimates.

In the $(f, Q)$ parameter basis, those components of the Fisher Matrix $\Gamma_{ab}$ that do not involve mixing of gravitational and scalar parameters are given in Section IV A of BCW. For those components that do mix gravitational and scalar parameters, analytic expressions are presented in a Mathematica notebook [322], as is an expression for the total SNR $\rho^2$. We do not reproduce the expressions in this thesis as in most cases they are exceedingly lengthy and unenlightening. The most important results are the error estimates in the $(M, j, \mu^2)$ basis, which are presented below.

From now on we will work in a simplified regime were we assume that $N_{\times}$, $\phi_+$, and $\phi_0$ are known for both gravitational and scalar modes. In particular, we follow the conventions of BCW for a mixed mode waveform, assuming that for each mode $N_{\times} = 1$ with the phases given by $\phi_g^+ = -\pi/2$, $\phi_g^0 = \phi_s^0 = \pi/2$, $\phi_s^+ = -\pi/2 + \phi$. With this choice of parameters for the waveform we will be able to work with more digestible analytic expressions.

We will further split our analysis in two separate cases: firstly, fixing $j = 0$ leaving us with 4 unknown parameters $(A_g, M, A_s, \mu^2)$ to find error estimates for, and secondly, allowing $j$ to be free (but still constrained to be small, $j \ll 1$).

#### 6.3.2.1 $j = 0$

In the case of a Schwarzschild black hole, for a mixed mode waveform with the above choice of parameters for $N_\times$ and phases, we find the following for the total SNR of the signal $\rho^2$

$$\rho^2 = \rho_g^2 + \rho_s^2 + \frac{A_g A_s}{5\pi^2 S}\left[\frac{16 f_g f_s Q_g^3 Q_s^3 \left(f_g Q_s + f_s Q_g\right)\cos\phi}{\Lambda_+ \Lambda_-}\right] \tag{6.21}$$

with the individual SNRs for each mode being

$$\rho_g^2 = \frac{A_g^2 Q_g^3}{5\pi^2 f_g \left(1+4Q_g^2\right) S} \tag{6.22}$$

$$\rho_s^2 = \frac{A_s^2 Q_s \left(\sin^2\phi + 2Q_s^2\right)}{10\pi^2 f_s \left(1+4Q_s^2\right) S} \tag{6.23}$$

and where $\Lambda_\pm$ are given by

$$\Lambda_\pm = f_s^2 Q_g^2 + 2 f_g f_s Q_g Q_s + Q_s^2\left[f_g^2 + 4\left(f_g \pm f_s\right)^2 Q_g^2\right]. \tag{6.24}$$

This is the same result found in BCW for the total SNR of a two-mode waveform. BCW also showed that the phase $\phi$ only weakly affected their results, so for simplicity we chose to fix $\phi = \pi/2$ in the following so that the total SNR is simply given by the sum in quadrature of the individual SNRs.

We now present analytic expressions for the error estimates for $A_g, M, A_s$ and $\mu^2$ (where $\sigma_a^2 = \Sigma_{aa}$) to the *leading order term* in the relative scalar amplitude $A_s/A_g$, as we assume that the amplitude of the scalar mode will be subdominant compared to the gravitational mode amplitude:

$$\rho\frac{\sigma_{A_g}}{A_g} = \sqrt{1 + \frac{1}{Q_g^2}\frac{1+3Q_g^2}{3+8Q_g^2}}\left[1 + \left(\frac{A_s}{A_g}\right)^2 \frac{\eta^2}{2}\left(1 - \frac{\Lambda_2}{\Lambda_1}\frac{1+4Q_g^2}{1+2Q_g^2}\right)\right] \tag{6.25a}$$

$$\rho\frac{\sigma_M}{M} = \frac{1}{Q_g}\sqrt{\frac{1+4Q_g^2}{3+8Q_g^2}}\left[1 + \left(\frac{A_s}{A_g}\right)^2 \frac{\eta^2}{2}\left(1 - 4\frac{\Lambda_2}{\Lambda_1}\left(1+4Q_g^2\right)\right)\right] \tag{6.25b}$$

$$\rho\frac{\sigma_{A_s}}{A_s} = \left(\frac{A_s}{A_g}\right)^{-1}\sqrt{\frac{\left(1+4Q_s^2\right)\Lambda_3}{\eta^2\Lambda_1}} \tag{6.25c}$$

$$\rho\,\sigma_{\mu^2} = f_s Q_s \left(\frac{A_s}{A_g}\right)^{-1}\sqrt{\frac{2\left(1+4Q_s^2\right)^3\left(1+2Q_s^2\right)}{\eta^2\Lambda_1}}. \tag{6.25d}$$

We've introduced $\eta^2$, $\Lambda_i$ to compactify the expressions; their explicit forms are given by:

$$\eta^2 = \frac{1}{2}\frac{f_g Q_s}{f_s Q_g}\frac{1+4Q_g^2}{Q_g^2}\frac{1+2Q_s^2}{1+4Q_s^2} \tag{6.26a}$$

$$\begin{aligned}\Lambda_1 = {} & f_s^2\left(4\left(16\left(Q_s^2+2\right)Q_s^2+7\right)Q_s^4+1\right)Q_{s,\mu^2}^2 \\ & -2f_sQ_sf_{s,\mu^2}Q_{s,\mu^2}\left(64Q_s^8+64Q_s^6+28Q_s^4+8Q_s^2+1\right) \\ & +f_{s,\mu^2}^2Q_s^2\left(32Q_s^6+28Q_s^4+8Q_s^2+1\right)\left(1+4Q_s^2\right)^2\end{aligned} \tag{6.26b}$$

$$\Lambda_2 = \frac{2M^2Q_s^4\left(16Q_s^6+32Q_s^4+10Q_s^2+1\right)\left(f_{s,\mu^2}Q_{s,M}-f_{s,M}Q_{s,\mu^2}\right)^2}{Q^2\left(8Q^2+3\right)} \tag{6.26c}$$

$$\begin{aligned}\Lambda_3 = {} & f_s^2\left(32Q_s^6+24Q_s^4+1\right)Q_{s,\mu^2}^2-2f_sf_{s,\mu^2}\left(32Q_s^7+16Q_s^5+6Q_s^3+Q_s\right)Q_{s,\mu^2} \\ & +f_{s,\mu^2}^2Q_s^2\left(8Q_s^4+4Q_s^2+1\right)\left(1+4Q_s^2\right)^2,\end{aligned} \tag{6.26d}$$

where we are using the notation $\mathscr{F}_{,\theta} = \frac{\partial \mathscr{F}}{\partial \theta}$. Note that the ratio of single waveform SNRs is given by:

$$\frac{\rho_s}{\rho_g} = \eta\frac{A_s}{A_g}. \tag{6.27}$$

As expected, the error estimates of the non-scalar parameters become independent of any of the scalar waveform parameters as $A_s \to 0$, with the leading order corrections entering at quadratic order in the scalar amplitude. For the scalar parameters, we see that the leading term of $\sigma_{\mu^2}$ scales as $(A_s/A_g)^{-1}$, thus diverging as the scalar amplitude $A_s \to 0$ (as is reasonable).

Having calculated the error estimates analytically, we can consider the effect that introducing the scalar waveform has on $\sigma_{A_g}$ and $\sigma_M$. For $\ell = 2$, $\mu^2 = 0$, the leading order corrections to the error estimates of $A_g$ and $M$ are given by:

$$\frac{\rho\Delta\sigma_{A_g}}{A_g} \approx 0.52\left(\frac{A_s}{A_g}\right)^2, \quad \frac{\rho\Delta\sigma_M}{M} \approx 0.13\left(\frac{A_s}{A_g}\right)^2 \tag{6.28}$$

where again we are assuming that $A_s \ll A_g$. Clearly, with small $A_s$, the error estimates on $A_g$ and $M$ are only weakly degraded by the introduction of the scalar mode. We have also checked that the value of $(\mu M)^2$ only weakly affects $\sigma_M$ and $\sigma_A$. For $\sigma_{A_s}$ and $\sigma_{\mu^2}$, on the other hand, to leading order in both $A_s/A_g$ and $(\mu M)^2$ (again with $\ell = 2$):

$$\rho\sigma_{\mu^2} = \frac{1}{M^2}\left(\frac{A_s}{A_g}\right)^{-1}\left(0.42-0.76\left(\mu M\right)^2\right) \tag{6.29}$$

$$\frac{\rho\sigma_{A_s}}{A_s} = \left(\frac{A_s}{A_g}\right)^{-1}\left(1.00-0.40\left(\mu M\right)^2\right). \tag{6.30}$$

If we return to assuming that the effective scalar mass $\mu^2 = 0$, we can calculate $\sigma_{\mu^2}$ to estimate a 'detectability' limit on the scalar 'particle' effective mass $m_s$. Reinserting $G$ and $c$ to restore units, we find that

$$\rho\sigma_{\mu^2} \sim 2\times 10^{-7}\left(\frac{A_s}{A_g}\right)^{-1}\left(\frac{M_\odot}{M}\right)^2 \mathrm{m}^{-2}, \tag{6.31}$$

where we now interpret $\mu^2$ as the square of the inverse Compton wavelength $\lambda_c$ of the scalar (thus the combination $\mu M$ is really a ratio of the black hole to scalar length scales). Converting to a mass using $m_s = h/\lambda_c c$, we find

$$\sqrt{\rho} m_s \sim 5\times 10^{-10}\left(\frac{A_s}{A_g}\right)^{-1/2}\left(\frac{M_\odot}{M}\right)\mathrm{eV}c^{-2}. \tag{6.32}$$

Figure 6.2 shows a contour plot of $\sqrt{\rho}m_s$ as a function of relative scalar amplitude $A_s/A_g$ and black hole mass $M$ for a mass range of likely events observed by aLIGO/VIRGO, while figure 6.3 shows a similar contour plot but for more massive black holes of the type LISA might observe. In figure 6.2 a mass range of $0 < \log_{10}(M/M_\odot) < 3$ is covered, whilst for figure 6.3 we consider a range of $5 < \log_{10}(M/M_\odot) < 9$, over which LISA is expected to be sensitive to BH ringdowns out to large redshifts [61]. Note that in figures 6.2 and 6.3 we have used the full expressions for the covariance matrix as calculated using the Fisher matrix formalism, rather than the $A_s \ll A_g$ approximation used to arrive at eq. (6.32).

In figures 6.2 and 6.3 we see that with increasing black hole mass the constraint on $m_s$ tightens considerably, even for small $A_s/A_g$. For example, constraints on $\sqrt{\rho}m_s \sim 10^{-17}\mathrm{eV}c^{-2}$ are possible with $A_s/A \sim 0.01$ for a $10^9 M_\odot$ black hole.

#### 6.3.2.2 $j \neq 0$

We now consider the case of a slowly rotating black hole with $j \ll 1$. In this case the total SNR is still given by eq. (6.21), and again we choose $\phi = \pi/2$. The introduction of $j$ into the Fisher matrix analysis makes the analytic expressions for the error estimates extremely unwieldy, so we will not present the leading order corrections due to $A_s$ to $\sigma_{A_g}$, $\sigma_j$ or $\sigma_M$. Section VI B of BCW addresses the effect of increasing black hole spin on the error estimates of $j$ and $M$ in a two-mode waveform where the modes have the same $(\ell, m)$ (in their case, the motivation was to consider overtones). They showed that with increasing $j$, $\sigma_M$ and $\sigma_j$ increase (decrease) for the $\ell = m = 2$ ($\ell = -m = 2$) modes. In this section we will focus on the effect of $j$ on $\sigma_{A_s}$ and $\sigma^2_\mu$.

In fact, we find that to leading order in $(A_s/A_g)$, that the error estimates of $A_s$ and $\mu^2$ are given once again by eq. (6.25c)-(6.25d). We can now evaluate these numerically for

Figure 6.2: Contour plot for $m_s$ as a function of relative scalar amplitude $A_s/A_g$ and black hole mass $M$ (in solar units) for values representative of LIGO events. The $[-8,...,-12] \times \log_{10}\left(\sqrt{\rho} m_s/\mathrm{eV}c^{-2}\right)$ contours are shown.

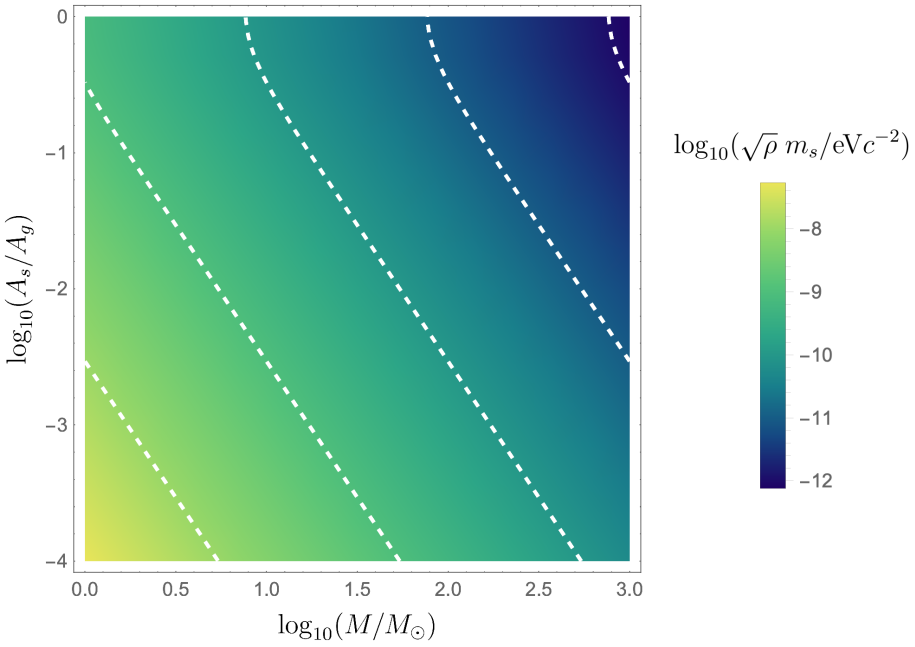


Figure 6.3: Contour plot for $m_s$ as a function of relative scalar amplitude $A_s/A_g$ and black hole mass $M$ (in solar units) for values representative of LISA events. The $[-13,...,-17] \times \log_{10}\left(\sqrt{\rho} m_s/\mathrm{eV}c^{-2}\right)$ contours are shown.

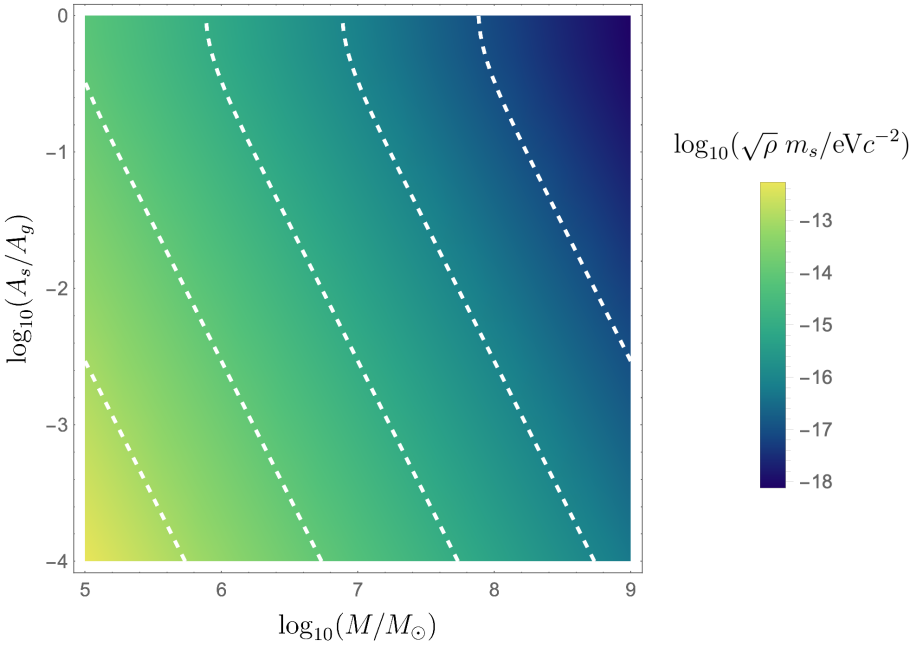

non-zero (small) $j$. For $\ell = 2$, $\mu^2 = 0$, we find the following error estimates to linear order in $j$ and to leading order in $A_s/A_g$:

$$\rho \frac{\sigma_{A_s}}{A_s} = (1.00 + 0.03jm) \left(\frac{A_s}{A_g}\right)^{-1} \tag{6.33}$$

$$\rho \sigma_{\mu^2} = \frac{0.42}{M^2} \left(1 + \frac{jm}{3}\right) \left(\frac{A_s}{A_g}\right)^{-1}, \tag{6.34}$$

where $m$ is the azimuthal spherical harmonic index ranging from $(-\ell, ..., \ell)$. This corresponds to a scalar mass detectability limit of

$$\sqrt{\rho} m_s \sim 5 \times 10^{-10} \left(1 + \frac{jm}{3}\right) \left(\frac{A_s}{A_g}\right)^{-1/2} \left(\frac{M_\odot}{M}\right) \mathrm{eV}c^{-2}, \tag{6.35}$$

again valid for $j \ll 1$, $A_s \ll A_g$. We see that, in this slow rotation regime, the introduction of spin very weakly increases (decreases) the error estimates for the scalar parameters for positive (negative) $m$.

It would of course be interesting to repeat this analysis for larger values of $j$, however there are currently no accurate fitting formulae for massive scalar QNMs as a function of both scalar mass *and* black hole spin[2]. This is a potential avenue for future research.

The phenomenon of black hole superradiance [311] provides a method of constraining ultralight boson masses through observations of rotating black holes [323, 324, 325, 326, 327]. In [326] masses of minimally coupled axion like particles are excluded in the range $[6 \times 10^{-13}\mathrm{eV}, 10^{-11}\mathrm{eV}]$, and it is argued that current and future observations can probe a mass range of such particles from $10^{-19}$eV to $10^{-11}$eV. In fact, if we posit that a modified gravity theory admits Kerr black hole solutions (and that these are indeed the astrophysical black holes we observe), then the same bounds calculated from superradiant instabilities in [326] apply equally to such modified gravity theories.

Whilst it would take a very large black hole mass $M$ or SNR $\rho$ to compete with the lowest end of the mass range probed by back hole superradiance, the constraints that could be garnered from ringdown observations can be complementary to those obtained from other methods. Furthermore, in this case we are considering a phenomenon arising specifically from the non-minimal coupling between gravity and the scalar field.

### 6.3.3 Resolvability

To use a mixed-mode GW signal to test GR one must, of course, first be able to discriminate between the two frequencies buried in the noisy signal. As explored in BCW as well as in

[2]To the best of the author's knowledge.

[131, 138], such considerations lead to postulating a minimum SNR required to resolve the individual frequencies and damping times of the gravitational and scalar modes. It is commonly given that a natural criterion for resolving frequencies and damping times is given by

$$|f_g - f_s| > \max\left(\sigma_{f_g}, \sigma_{f_s}\right), \; |\tau_g - \tau_s| > \max\left(\sigma_{\tau_g}, \sigma_{\tau_s}\right). \tag{6.36}$$

As explained in BCW, the above criteria state that the frequencies are barely resolvable if "the maximum of the diffraction pattern of object 1 is located at the minimum of the diffraction pattern of object 2". Using the above, critical SNRs required to resolve the individual frequencies and damping times can be introduced

$$\rho > \rho^{f}_{\text{crit}} = \frac{\max\left(\rho\sigma_{f_g}, \rho\sigma_{f_s}\right)}{|f_g - f_s|} \tag{6.37}$$

$$\rho > \rho^{\tau}_{\text{crit}} = \frac{\max\left(\rho\sigma_{\tau_g}, \rho\sigma_{\tau_s}\right)}{|\tau_g - \tau_s|}. \tag{6.38}$$

We can use the Fisher matrix formalism to calculate these error estimates analytically, now in the $(f, \tau)$ parameter basis. Again to leading order in $A_s/A_g$, we find the following expressions for the errors in $f$ and $\tau$ for each waveform:

$$\rho\sigma_{f_g} = \frac{f_g}{8Q_g^3}\sqrt{6+32Q_g^4}\left(1+\left(\frac{A_s}{A_g}\right)^2\frac{\eta^2}{2}\right) \tag{6.39a}$$

$$\rho\sigma_{\tau_g} = \frac{1}{\pi f_g}\sqrt{3+4Q_g^2}\left(1+\left(\frac{A_s}{A_g}\right)^2\frac{\eta^2}{2}\right) \tag{6.39b}$$

$$\rho\sigma_{f_s} = \frac{f_s}{2\sqrt{2}Q_s^2\eta}\left(\frac{A_s}{A_g}\right)^{-1}\sqrt{\frac{1+4Q_s^4\left(7+16Q_s^2\left(2+Q_s^2\right)\right)}{1+2Q_s^4\left(5+8Q_s^2\left(2+Q_s^2\right)\right)}} \tag{6.39c}$$

$$\rho\sigma_{\tau_s} = \frac{\sqrt{2}Q_s}{\pi f_s\eta}\left(\frac{A_s}{A_g}\right)^{-1}\sqrt{1+\frac{3+4Q_s^2-24Q_s^4}{1+2Q_s^4\left(5+8Q_s^2\left(2+Q_s^2\right)\right)}} \tag{6.39d}$$

with $\eta^2$ given by eq. (6.26a).

Figure 6.4 shows the two critical SNRs $\rho^{f}_{\text{crit}}$ and $\rho^{\tau}_{\text{crit}}$ required to resolve individual frequencies and damping times respectively as a function of the relative scalar mode amplitude. We've again chosen a superposition of $\ell = 2$ modes for a Schwarzschild black hole and a massless scalar field. As with figures 6.2 and 6.3, here we have used the full analytic expressions for the critical SNRs in figure 6.4, rather than the $A_s \ll A_g$ approximation used in eqs. (6.39b)-(6.39d).

We see that the SNR required to resolve damping times is consistently about an order of magnitude greater than that required to resolve frequency times. Thus $\rho^{\tau}_{\text{crit}}$ sets the lower bound on SNR to resolve *both* frequencies and damping times. The minimum of $\rho^{\tau}_{\text{crit}}$ is found numerically, in this case, to be at $A_s/A_g \approx 0.81$, giving a critical SNR of $\approx 34$.

Assuming that we wish to resolve both frequencies and damping times, and noting that for small $A_s$ the critical SNR is given by $\rho\sigma_{\tau_s}$, we can use eq. (6.38) and (6.39d) to find a minimum requirement on $A_s/A_g$ for a given SNR. For a superposition of $\ell = 2$ modes with $\mu^2 = 0$, we find

$$\frac{A_s}{A_g} > \frac{21}{\rho}. \tag{6.40}$$

If we only wish to distinguish frequencies and not damping times, the requirement on $A_s$ drops to

$$\frac{A_s}{A_g} > \frac{1.2}{\rho}. \tag{6.41}$$

For example, with an SNR of $\rho \sim 10^2$ (achievable in single detections through LISA, third generation ground based detectors, or through stacking several signals together [60, 132, 328, 329, 330, 63]), we would require $A_s \approx 0.2$ to ensure $\rho > \rho^{\tau}_{\text{crit}}$. If, on the other hand, we considered single, loud, aLIGO/Virgo detections such as GW150914, an SNR of $\rho \sim 5 - 10$ is more realistic [25]. In which case $A_s \approx 0.2$ would be required just to discern distinct oscillation frequencies in the signal, whilst an observation of distinct damping times would be impossible given that the approximate minimum of $\rho^{\tau}_{\text{crit}}$ is 34 as discussed above (and as shown in figure 6.4).

## 6.4 Conclusion

In this chapter we have studied the mixing of gravitational and scalar modes in the GW emission during ringdown of static and slowly rotating black holes in Horndeski gravity. The generic perturbation equations to a Ricci flat background with a constant scalar field profile are presented in section 6.2.2; these are specialised to apply to a Schwarzschild black hole in section 6.2.3, where coupled QNM equations in the even parity sector are presented.

The qualitative nature of the mode mixing effect on the GW emission is shown in figure 6.1, with a related phenomenon in scalar Gauss-Bonnet gravity having been observed numerically in [316]. Additionally, we demonstrated its occurence in any Ricci flat black hole background (see eq. (6.5a)). Indeed, a natural progression of this work is to study in

Figure 6.4: Critical SNRs $\rho^f_{\rm crit}$ and $\rho^\tau_{\rm crit}$ required to resolve frequencies and damping times as a function of relative scalar amplitude $A_s/A$ for $\ell = 2$, $\mu^2 = j = 0$.

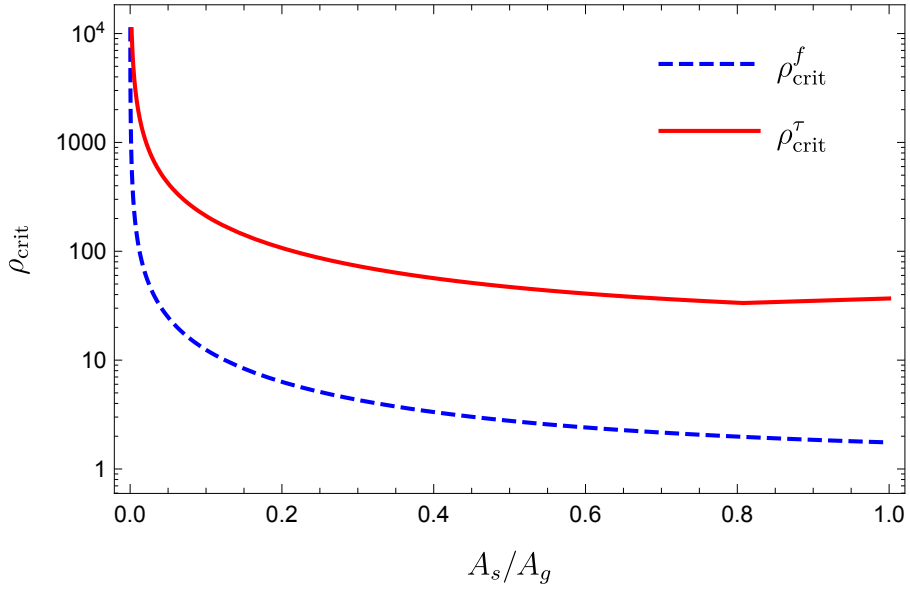


detail the perturbations of Kerr black holes of arbitrary spin in Horndeski gravity, through both analytical and numerical methods.

We then proceeded to apply the Fisher matrix formalism for black hole ringdown as developed in BCW [56] to a mixed mode waveform containing both gravitational and scalar frequencies, and in section 6.3.2 derived analytic expressions for the estimated errors on the parameters of such a waveform assuming a static or slowly rotating black hole background. Of particular interest is the estimated error in the determination of the effective mass of the Horndeski scalar field (see eq. (6.25d), and figures 6.2 and 6.3). For certain parameter ranges of the black hole mass and relative scalar mode amplitude, we've shown that constraints on the effective mass of the Horndeski scalar field can be very tight, for example $m_s \sim \rho^{-1/2} 10^{-17} \mathrm{eV} c^{-2}$ for a $10^9 M_\odot$ black hole observed with LISA; competitive with the kind of constraints on ultralight axion masses obtained via black hole superradiance.

We further found that, assuming an SNR of $\rho \sim 10^2$ (achievable through next generation space and ground based detectors or through the stacking of multiple signals [60, 132, 328, 329, 330, 63]) a scalar perturbation with an amplitude of roughly 20% that of the dominant gravitational mode would be required so that the presence of multiple, distinct oscillations frequencies and damping times in the signal could be detected. With the SNRs typical of single LIGO events [25], on the other hand, detecting the presence of distinct oscillation frequencies in the ringdown signal is the best one can hope for, with a scalar

mode amplitude again of the order $10-20\%$ that of the gravitational mode amplitude required.

A key assumption in this chapter is that the scalar perturbations will be present in the ringdown: specifically, if mode mixing is to occur in the ringdown, the scalar field perturbation needs to be excited, which is by no means guaranteed given that $\varphi = 0$ is a solution to eq. (6.7a)-(6.7c) (leading to perturbations identical to those in GR). Furthermore, in the case of two black holes without hair merging, it is difficult to envisage generating any scalar field perturbations (though perhaps non-linear interactions during the merger could source excitations). However, if $\phi$ interacts non-trivially with matter, then events involving one or more compact stars may provide an initial non-trivial scalar field profile from which perturbations can be sourced [331, 332, 333, 334, 335]. In addition, one could imagine merger events whereby surrounding matter 'contaminates' the 'clean' merger of two compact objects without hair, thus sourcing scalar perturbations in situations where one might not initially expect them. An important avenue of research is then to study the possibility of how hair can be dynamically generated in no-hair theories.

An obvious limitation of this work is the inclusion of only two modes in the mixed-mode waveform - one from each of the gravitational and scalar spectra. In [336] it is shown that including higher overtones[3] as well as fundamental modes is highly important for accurately extracting parameters from a GW signal. In addition, the study of mode amplitudes in black hole ringdown [125, 337, 338, 339] shows that in some cases the second most dominant gravitational mode may have a significant relative amplitude of $\mathcal{O}(1)$. In which case modelling our signal as a two-mode waveform with $A_2 \ll A_1$ may be a simplification too far (of course if a scenario heavily excited the scalar mode then the two mode approach would be more valid). Including additional gravitational modes in addition to the scalar mode(s) would be a more accurate approach, and an intriguing area of future research.

Finally, the numerical results shown in this chapter are limited to Schwarzschild and slowly rotating Kerr black holes, but of course it is our aim to apply such an analysis to Kerr black holes of arbitrary spin (especially given the so far observed spins of black holes by aLIGO/VIRGO). Analytic fits of massive scalar QNM frequencies on a Kerr background, or a more in depth numerical analysis of sourced gravitational radiation for rapidly rotating black holes, will be required to make such a step to higher spins; these are interesting areas of future work.

[3]Modes with the same $\ell$ and $m$ but with different overtone index $n$, as described in section 5.4.1.

With the maturation of GW astronomy, and the prospect of black hole spectroscopy with next generation detectors in the near future, the exploration of what we can learn about the nature of gravity from ringdown observations is an exciting and timely endeavour.

# Conclusion

*"Gravity has taken better men than me"*

— John Mayer, *Gravity*

I will now conclude by summarising the key results of the research presented in this thesis, as well as looking forward to potential future areas of research.

## 7.1 Summary of Results

In Chapter 2, cosmological perturbations in different families of modified gravity theories are considered. In a theory agnostic manner, i.e. without assuming any knowledge of a full non-linear gravity theory, I presented a formalism for constructing general gauge invariant quadratic actions for describing the evolution of perturbations on a cosmological FLRW background. Theories involving a single tensor field, a tensor and a scalar, and a tensor and a vector are considered. In each case we find that the resulting action is dependent on a finite (small) number of parameters, irregardless of whatever non-linear theory the action for the perturbations may originate from. In this way, cosmological observations can constrain large classes of modified gravity theories all at once, rather than focussing on individual theory specific tests.

In Chapter 3, the formalism of Chapter 2 is applied to a black hole background, where perturbations to a Schwarzschild black hole were considered. Repeating the analysis of Chapter 2 again for single tensor, scalar-tensor, and vector-tensor theories, gauge invariant actions depending on a finite number of parameters are constructed. In this case, the equations of motion for the perturbations are analysed in the context of ringdown and QNMs. I show that, despite the background black hole being identical to the corresponding GR solution, the QNM spectrum and ringdown signal of the perturbed black hole may be affected due to the presence of additional degrees of freedom (in the scalar-tensor and vector-tensor

case). This opens the possibility of testing gravity, and discerning between GR and modified gravity gravitational wave signals, through black hole ringdown even if the background black hole solutions are indistinguishable from GR.

Chapter 4 concerns background black hole solutions in modified theories of gravity, specifically in theories where one constrains the propagation speed of gravitational waves to be equal to that of light, i.e. $c_T = 1$. I show that in the context of scalar-tensor theories of gravity, the restriction on $c_T$ greatly hinders one's ability to find 'hairy' black hole solutions; theories with other additional degrees of freedom with more structure (e.g. gravitationally coupled vector fields) still provide avenues to find hairy solutions.

In Chapter 5, black hole perturbations in GR are studied. I present QNM master equations for scalar, vector, and tensor perturbations on a slowly rotating Kerr-(Anti-)de Sitter background. In each case I calculate analytic expressions for the QNM frequency spectra, and compare to known results in the literature. Good agreement is found between numerical results and those analytic results presented in this thesis. Additionally, I show that the isospectrality between odd and even parity gravitational spectra is broken in the case of non-zero black hole spin *and* cosmological constant.

Finally, in Chapter 6, I consider black hole ringdown in Horndeski theory in detail. I show that for any Ricci flat background solution (i.e. a Schwarzschlid or Kerr black hole), gravitational perturbations will be sourced by scalar perturbations, leading to a qualitatively different gravitational wave signal than in GR. I specifically present the QNM equations for the case of a perturbed Schwarzschild black hole, and show that the Horndeski scalar field obeys an effective massive Klein Gordon equation. The sourcing of the even parity metric degree of freedom by the Horndeski scalar field leads to gravitational waves being emitted as a superposition between those QNM frequencies associated with the gravitational and scalar spectra. Assuming such a superposition, I forecast how the experimental errors on the black hole parameters as determined through ringdown observations will be affected by the scalar perturbations. Furthermore, I show that one could constrain the effective mass of the Horndeski scalar 'particle' to $\sim 10^{-17}\text{eV}c^{-2}$ through LISA observations, in particularly favourable circumstances.

## 7.2 Future Research

In this thesis I have explored the ways in which we might test gravity through consideration of modified theories of gravity, particularly in the context of black holes. I have shown that, even in the case where black holes look identical to GR solutions at the level of the background (i.e. identical spacetime geometry, no non-trivial profiles of additional fields),

their emission of gravitational waves when perturbed can be markedly different. Clearly this has great importance with observations of binary black hole mergers (and other events involving compact objects) now becoming commonplace.

One clear avenue of future research is to consider perturbations to rapidly rotating black holes in modified theories of gravity. This thesis has been concerned with, at most, slowly rotating black holes, and whilst this is a good starting point to analyse the ways in which modified gravity might make itself known in a gravitational wave signal, most astrophysical black holes are expected to have non-negligible angular momentum. Thus to truly take advantage the tests of gravity possible with current and future gravitational wave observations, perturbations of black holes of arbitrary spin must be analysed.

In Chapter 6 I presented the fully covariant equations of motion that perturbations to a Kerr black hole would obey, in a way such that the 'right hand side' of eq. (6.5a) can be interpreted as the source of the Teukolsky equation describing Kerr black hole perturbations in GR [283]. Analysing the perturbations in this way would allow us to study rapidly rotating Horndeski black hole using the same numerical and analytic tools already developed for GR (including consideration of the phenomenon of black hole superradiance [311]). This is, of course, assuming that the scalar field possesses no hair at the level of the background, but this is certainly a potential step forward in the study of ringdown in modified gravity theories. Additionally, the calculation of analytic expressions (or fits to numerical values) of massive scalar QNMs as a function of both black hole spin *and* scalar field mass would enable the forecasting analysis of Chapter 6 to be extended to include rapidly rotating Kerr black holes.

Whilst the modified gravity theories studied here have mostly involved introducing an additional gravitational degree of freedom, theories with more than one additional gravitational fields (for example Scale Invariant gravity with $N$ scalar fields [340]) will potentially lead to even richer modified gravity effects during ringdown. The analysis of black hole solutions and perturbations in such theories is thus an interesting area of future research.

The black holes considered in this thesis have, for the most part, have been assumed to have no hair, and are thus at the level of the background indistinguishable from GR black holes. Whilst finding specific hairy solutions, or introducing arbitrary black hole hair, greatly increases the complexity of the problem of analysing black hole perturbations in modified gravity theories, one could consider 'stepping stones' on the way to a general description of QNMs and ringdown in modified gravity. For example, in [341] it was shown that by enforcing oscillatory boundary conditions on the scalar field, one could grow scalar hair on a Schwarzschild black hole whilst only negligibly affecting the geometry of the black hole itself (indeed it would be interesting to explore in more scenarios ways in which

scalar hair might be dynamically generated in systems that 'traditionally' one might not expect). Perhaps such 'stealth' black holes, where additional gravitational fields acquire non-trivial profiles without affecting the spacetime geometry, present a way forward in considering more general black hole solutions. Perturbations to a 'stealth Kerr' black hole in degenerate higher order scalar-tensor (DHOST) theories are considered in [342].

Another possible avenue is to consider 'almost Schwarzschild/Kerr' black holes, where any hair is treated perturbatively. The QNM spectrum of such black holes could then be determined with respect to the original GR spectrum, for example via the parameterised methods introduced in [81, 82]. Of course hairy black hole solutions in specific realisations of modified gravity are known, and their perturbations analysed [64, 65, 75, 76, 79, 136, 137, 138, 254, 312, 313, 314], but I am considering ways of analysing hairy black holes in a more general and arbitrary sense. Such an approach might allow a general parameterisation of black hole hair, and with it a way of analysing modifications to the QNM spectrum of black holes due to such perturbative hair.

The LIGO/Virgo collaboration is now finding gravitational wave sources with stunning regularity, and with the arrival of next generation gravitational wave detectors on the horizon, the era of gravitational wave astronomy is clearly upon us. The opportunity to test GR in the most violent, strongly gravitating laboratories nature has to offer has never been greater, and our ability to test gravity with black holes will only grow in the future.

# Appendix A

## A.1 Scalar Tensor Theories

### A.1.1 Covariant quantities

With the introduction of a matter sector, the background space-time will no longer be flat. Thus we need expressions for the Christoffel symbols and curvature tensors of the background *in terms of the background quantities* to properly evaluate the Noether constraints arising from the variation of (2.20). The relevant expressions can be shown to be:

$$\Gamma^{\rho}_{\mu\nu} = H(\gamma_{\mu\nu}u^{\rho} - \gamma^{\rho}_{\mu}u_{\nu} - \gamma^{\rho}_{\nu}u_{\mu}) \tag{A.1}$$

$$\bar{\nabla}_{\mu}u_{\nu} = H\gamma_{\mu\nu} \tag{A.2}$$

$$\bar{\nabla}_{\mu}\gamma_{\alpha\beta} = u_{\alpha}\bar{\nabla}_{\mu}u_{\beta} + u_{\beta}\bar{\nabla}_{\mu}u_{\alpha} \tag{A.3}$$

$$\begin{aligned}\bar{R}^{\rho}_{\sigma\mu\nu} = {} & \dot{H}(-u_{\mu}u^{\rho}\gamma_{\nu\sigma} + u_{\nu}u^{\rho}\gamma_{\mu\sigma} + \gamma^{\rho}_{\nu}u_{\mu}u_{\sigma} - \gamma^{\rho}_{\mu}u_{\nu}u_{\sigma}) \\ & + H^{2}(u_{\nu}u^{\rho}\gamma_{\mu\sigma} - u_{\mu}u^{\rho}\gamma_{\nu\sigma} - \gamma^{\rho}_{\mu}u_{\nu}u_{\sigma} + \gamma^{\rho}_{\nu}u_{\mu}u_{\sigma} \\ & + \gamma^{\rho}_{\mu}\gamma_{\sigma\nu} - \gamma^{\rho}_{\nu}\gamma_{\sigma\mu})\end{aligned} \tag{A.4}$$

$$\bar{R}_{\mu\nu} = -3\left(\dot{H} + H^{2}\right)u_{\mu}u_{\nu} + \left(3H^{2} + \dot{H}\right)\gamma_{\mu\nu} \tag{A.5}$$

$$\bar{R} = 12H^{2} + 6\dot{H}. \tag{A.6}$$

$H = \frac{d\log a}{dt}$ is the Hubble parameter, $\bar{R}^{\rho}_{\sigma\mu\nu}$ is the Riemann curvature tensor, $\bar{R}_{\mu\nu} = \bar{R}^{\rho}_{\mu\rho\nu}$ is the Ricci tensor, and $\bar{R} = \bar{g}^{\mu\nu}\bar{R}_{\mu\nu}$ is the Ricci scalar. Note that, unlike in the 1+3 covariant formalism introduced in [102], we have not introduced 'shear' or 'velocity' tensors, nor a 'volume expansion' scalar or 'acceleration' vector. Every background tensor can be expressed in terms of functions of time and the projectors $u^{\mu}$ and $\gamma_{\mu\nu}$. These expressions are, however, only valid in the chosen coordinate basis.

### A.1.2 Noether constraints

The following Noether constraints are obtained in Section 2.4 for the $A_n$, $B_n$, and $C_n$:

$$
\begin{aligned}
A_1 &= -\frac{\dot{\bar{\varphi}}^2}{16} - H\dot{\bar{\chi}}D_{\chi 5} \\
A_2 &= \frac{1}{8}\left(\dot{\bar{\varphi}}^2 + 8H\dot{\bar{\chi}}D_{\chi 5} - 32H^2C_1\right) \\
A_3 &= \frac{1}{8}\left(-\dot{\bar{\varphi}}^2 - 32H^2C_1 - 32H^2C_5 - 8H\dot{\bar{\chi}}D_{\chi 2} - 16H\dot{\bar{\chi}}D_{\chi 5}\right) \\
A_4 &= \frac{1}{4}\left(\dot{\bar{\varphi}}^2 - 32H^2C_1 - 16\dot{H}C_5 + 4H\dot{\bar{\chi}}D_{\chi 5}\right) \\
A_5 &= \frac{1}{16}\left(-\dot{\bar{\varphi}}^2 - 96H^2C_5 + 4C_{\chi 1}\dot{\bar{\chi}}^2 - 24H\dot{\bar{\chi}}D_{\chi 2}\right) \\
B_1 &= \dot{\bar{\chi}}D_{\chi 5} - 4HC_1 \\
B_3 &= -\dot{\bar{\chi}}D_{\chi 5} \\
B_3 &= 4HC_5 + \frac{1}{2}\dot{\bar{\chi}}D_{\chi 2} \\
B_4 &= -4HC_5 - \dot{\bar{\chi}}D_{\chi 2} \\
C_1 &= -H^{-1}\left(HC_5 + \dot{C}_6 + \frac{1}{4}\dot{\bar{\chi}}D_{\chi 5}\right) \\
C_2 &= -C_1 \\
C_3 &= -C_4 = -2C_1 \\
C_6 &= -C_5 \\
C_8 &= -C_8 = 2C_5 \\
C_9 &= C_{10} = 0 \\
C_{11} &= -C_{12} = -2C_5 \\
C_{13} &= -C_{14} = -4C_5 \\
C_{15} &= C_{16} = C_{17} = 0.
\end{aligned}
\tag{A.7}
$$

For the $A_{\chi n}$, $B_{\chi n}$, $C_{\chi n}$, and $D_{\chi n}$:

$$
\begin{aligned}
A_{\chi 0} = \frac{1}{\dot{\bar{\chi}}}&\left(C_{\chi 1}\dddot{\bar{\chi}} - 3\dot{H}\dot{\bar{\chi}}C_{\chi 2} + \dot{C}_{\chi 1}\ddot{\bar{\chi}} + 3HC_{\chi 1}\ddot{\bar{\chi}}\right. \\
&\left. + 6H\dot{H}D_{\chi 2} + 3\ddot{H}D_{\chi 2} - 6H\dot{H}D_{\chi 5}\right) \\
A_{\chi 1} = 3H\dot{D}_{\chi 2} &+ 3H\dot{\bar{\chi}}C_{\chi 2} - \ddot{\bar{\chi}}C_{\chi 1} + 3H^2D_{\chi 2} \\
&- 3\dot{H}D_{\chi 2} + 6H^2D_{\chi 5} \\
A_{\chi 2} = -\ddot{D}_{\chi 2} &- 4H\dot{D}_{\chi 2} - 2H\dot{D}_{\chi 5} - \dot{\bar{\chi}}\dot{C}_{\chi 2} \\
&- 3H\dot{\bar{\chi}}C_{\chi 2} - \ddot{\bar{\chi}}C_{\chi 2} - 3H^2D_{\chi}2 - \dot{H}D_{\chi 2} - 6H^2D_{\chi 5}
\end{aligned}
$$

$$
\begin{aligned}
&\quad -2\dot{H}D_{\chi 5} \\
B_{\chi 1} &= C_{\chi 1}\dot{\bar{\chi}} + 3HD_{\chi 2} \\
B_{\chi 2} &= -\dot{D}_{\chi 2} - C_{\chi 2}\dot{\bar{\chi}} - HD_{\chi 2} - 2HD_{\chi 5} \\
B_{\chi 3} &= 2C_{\chi 2}\dot{\bar{\chi}} \\
D_{\chi 1} &= 0 \\
D_{\chi 3} &= D_{\chi 2} \\
D_{\chi 4} &= -2D_{\chi 2} \\
D_{\chi 6} &= -D_{\chi 5}.
\end{aligned} \tag{A.8}
$$

In addition, a Friedmann-like equation analogous to (2.33) is found:

$$
\begin{aligned}
-\dot{\bar{\chi}}^2 C_{\chi 2} = &-\frac{1}{2}\dot{\bar{\varphi}}^2 + 8\dot{H}C_5 + HD_{\chi 2}\dot{\bar{\chi}} + \dot{D_{\chi 2}}\dot{\bar{\chi}} \\
&+ D_{\chi 2}\ddot{\bar{\chi}} + 2H\dot{\bar{\chi}}D_{\chi 5}.
\end{aligned} \tag{A.9}
$$

Before imposing diffeomorphism invariance, our action contained 42 unknown free functions of time: the 26 $A_n$, $B_n$, and $C_n$; the 14 $A_{\chi n}$, $B_{\chi n}$, $C_{\chi n}$, and $D_{\chi n}$; the scale factor $a$, and the background value of the scalar field $\chi_0$ ($\bar{\varphi}$ is related to $a$ through (2.26)). 36 Noether constraints are obtained, thus leaving us with 6 unknown free functions of time in the final gauge invariant action: $C_5$, $C_{\chi 1}$, $D_{\chi 2}$, $D_{\chi 5}$, the scale factor $a$, and the background value of the scalar field $\bar{\chi}$. We can make the following re-definitions of some of our remaining free functions to match the $\alpha_i$ described in [99] and [105]:

$$
M^2 = -8C_5,\ \alpha_M = \frac{d\log M^2}{d\log a},\ \alpha_B = -\frac{D_{\chi 2}\dot{\bar{\chi}}}{HM^2},\ \alpha_K = \frac{2C_{\chi 1}\dot{\bar{\chi}}^2}{H^2M^2}\ \alpha_T = -\frac{2\dot{\bar{\chi}}D_{\chi 5}}{HM^2} + \alpha_M. \tag{A.10}
$$

The $\alpha_i$ can be understood through the physical effects they parameterize [105].

### A.1.3 Lagrangian

The Lagrangian $\mathscr{L}_{\chi^+}$ calculated in Chapter 2 is given by:

$$
\begin{aligned}
\mathscr{L}_{\chi^+} = &\frac{1}{2}H^2(\alpha_M - 2\alpha_T)h_{\mu\nu}h^{\mu\nu} - \frac{1}{8}H^2(5\alpha_M - 4\alpha_T)h^2 \\
&+ \frac{1}{2}H^2(3\alpha_M - 7\alpha_T)h^{\sigma}_{\mu}h_{\nu\sigma}u^{\mu}u^{\nu} + \frac{1}{4}H^2(4\alpha_B - 9\alpha_M + 6\alpha_T)hh_{\mu\nu}u^{\mu}u^{\nu} \\
&+ \frac{1}{8}H(\alpha_K + 2H(10\alpha_B - \alpha_M - 6\alpha_T))h_{\mu\nu}h_{\sigma\lambda}u^{\mu}u^{\nu}u^{\sigma}u^{\lambda} \\
&- \frac{1}{8}\alpha_T\bar{\nabla}_{\mu}h^{\sigma\lambda}\bar{\nabla}_{\nu}h_{\sigma\lambda}u^{\mu}u^{\nu} - \frac{1}{4}H\alpha_M h^{\nu}_{\mu}u^{\mu}\bar{\nabla}_{\nu}h + \frac{1}{8}\alpha_T\bar{\nabla}_{\mu}h\bar{\nabla}_{\nu}hu^{\mu}u^{\nu}
\end{aligned}
$$

$$
\begin{aligned}
&+\frac{1}{8}\alpha_T\bar{\nabla}_\mu h\bar{\nabla}^\mu h+\frac{1}{2}H\left(\alpha_T-\alpha_M\right)hu^\mu\bar{\nabla}_\nu h^\nu_\mu\\
&-\frac{1}{2}H\left(2\alpha_T-\alpha_M\right)h^{\nu\sigma}u^\mu\bar{\nabla}_\sigma h_{\mu\nu}+\frac{1}{2}H\left(\alpha_T-\alpha_M\right)hu^\mu u^\nu u^\lambda\bar{\nabla}_\lambda h_{\mu\nu}\\
&-\frac{1}{4}\alpha_T\bar{\nabla}_\mu h\bar{\nabla}^\sigma h_{\nu\sigma}u^\mu u^\nu+\frac{1}{4}\alpha_T\bar{\nabla}_\mu h^{\mu\nu}\bar{\nabla}^\sigma h_{\nu\sigma}-\frac{1}{4}\alpha_T\bar{\nabla}_\mu h\bar{\nabla}_\nu h^{\mu\nu}\\
&-\frac{1}{2}H\left(2\alpha_T-\alpha_M\right)h_{\mu\rho}u^\mu u_\nu u^\sigma\bar{\nabla}_\sigma h^{\nu\rho}\\
&-\frac{1}{4}H\left(2\alpha_B+\alpha_M\right)h_{\mu\nu}u^\mu u^\nu u^\sigma\bar{\nabla}_\sigma h-\frac{1}{4}\alpha_T u^\mu u^\nu\bar{\nabla}_\nu h_{\mu\sigma}\bar{\nabla}^\sigma h\\
&+\frac{1}{4}\alpha_T u^\mu u^\nu\bar{\nabla}_\sigma h\bar{\nabla}^\sigma h_{\mu\nu}-\frac{1}{8}\alpha_T\bar{\nabla}_\sigma h_{\mu\nu}\bar{\nabla}^\sigma h^{\mu\nu}\\
&-\frac{1}{4}H\left(4\alpha_T-\alpha_M\right)h_{\mu\rho}u^\mu u^\nu u^\sigma\bar{\nabla}^\rho h_{\nu\sigma}+\frac{1}{4}\alpha_T u^\mu u^\nu\bar{\nabla}^\sigma h_{\mu\sigma}\bar{\nabla}^\rho h_{\nu\rho}\\
&+\frac{1}{4}H\left(4\alpha_B-\alpha_M+2\alpha_T\right)h_{\mu\nu}u^\mu u^\nu u^\sigma\bar{\nabla}^\rho h_{\sigma\rho}\\
&+\frac{1}{2}\alpha_T u^\mu u^\nu\bar{\nabla}_\nu h_{\mu\sigma}\bar{\nabla}_\rho h^{\sigma\rho}-\frac{1}{4}\alpha_T u^\mu u^\nu\bar{\nabla}_\sigma h_{\mu\nu}\bar{\nabla}_\rho h^{\sigma\rho}-\frac{1}{4}\alpha_T u_\mu u^\nu\bar{\nabla}_\rho h_{\nu\sigma}\bar{\nabla}^\rho h^{\mu\sigma}\\
&-\frac{1}{2}H\left(\alpha_T-\alpha_B\right)h_{\mu\nu}u^\mu u^\nu u^\sigma u^\rho u^\lambda\bar{\nabla}_\lambda h_{\sigma\rho}+\frac{1}{4}\alpha_T u^\mu u^\nu u^\sigma u^\rho\bar{\nabla}_\sigma h_{\mu\nu}\bar{\nabla}^\lambda h_{\rho\lambda}\\
&-\frac{1}{4}\alpha_T u^\mu u^\nu u^\sigma u^\rho\bar{\nabla}_\rho h_{\sigma\lambda}\bar{\nabla}^\lambda h_{\mu\nu}\\
&-\frac{1}{2\dot{\bar{\chi}}^4}\left(6\alpha_B\dot{H}^2\dot{\bar{\chi}}^2+\dot{H}\dot{\bar{\chi}}\left(6H\left(H\alpha_B\left(3+\alpha_M\right)+\dot{\alpha}_B\right)\dot{\bar{\chi}}-\alpha_K\ddot{\bar{\chi}}\right)\right.\\
&\left.-H\left(-6\alpha_B\dot{\bar{\chi}}^2\ddot{H}-2\alpha_K\ddot{\bar{\chi}}^2+\dot{\bar{\chi}}\left(\left(H\alpha_K\left(3+\alpha_M\right)+\dot{\alpha}_K\right)\ddot{\bar{\chi}}+\alpha_K\dddot{\bar{\chi}}\right)\right)\right)\left(\delta\chi\right)^2\\
&+\frac{1}{2\dot{\bar{\chi}}^2}\left(\alpha_B\dot{H}+H\left(H\left(\alpha_B-\alpha_M+\alpha_B\alpha_M+\alpha_T\right)+\dot{\alpha}_B\right)\right)\bar{\nabla}_\mu\delta\chi\bar{\nabla}^\mu\delta\chi\\
&+\frac{1}{2\dot{\bar{\chi}}^2}\left(2\alpha_B\dot{H}+H\left(\alpha_K+2H\left(\alpha_B-\alpha_M+\alpha_B\alpha_M+\alpha_T\right)+2\dot{\alpha}_B\right)\right)u^\mu u^\nu\bar{\nabla}_\mu\delta\chi\bar{\nabla}_\nu\delta\chi\\
&+\frac{1}{2\dot{\bar{\chi}}^2}u^\mu u^\nu u^\rho h_{\nu\rho}\bar{\nabla}_\mu\delta\chi\left(\dot{\bar{\chi}}\left(H\left(4\dot{\alpha}_B+\alpha_K+2H(2\alpha_B\alpha_M-\alpha_B-\alpha_M+\alpha_T)\right)\right.\right.\\
&\left.\left.+4\alpha_B\dot{H}\right)-2\alpha_B H\ddot{\bar{\chi}}\right)-\frac{1}{2\dot{\bar{\chi}}}Hu^\mu u^\nu(2\alpha_B-\alpha_M+\alpha_T)\bar{\nabla}_\mu\delta\chi\bar{\nabla}_\nu h\\
&+\frac{1}{2\dot{\bar{\chi}}}Hu^\mu u^\nu(4\alpha_B-\alpha_M+\alpha_T)\bar{\nabla}^\rho\delta\chi\bar{\nabla}_\nu h_{\mu\rho}+\frac{1}{2\dot{\bar{\chi}}}H(\alpha_M-\alpha_T)\bar{\nabla}^\mu\delta\chi\bar{\nabla}_\mu h\\
&-\frac{1}{2\dot{\bar{\chi}}}Hu^\mu u^\nu(2\alpha_B-\alpha_M+\alpha_T)\bar{\nabla}^\rho\delta\chi\bar{\nabla}_\rho h_{\mu\nu}+\frac{1}{2\dot{\bar{\chi}}}Hu^\mu u^\nu(\alpha_T-\alpha_M)\bar{\nabla}_\mu\delta\chi\bar{\nabla}_\rho h^\rho_\nu\\
&+\frac{1}{2\dot{\bar{\chi}}}H(\alpha_T-\alpha_M)\bar{\nabla}^\mu\delta\chi\bar{\nabla}_\nu h^\nu_\mu-\frac{\alpha_B H\ddot{\bar{\chi}}u^\mu h\bar{\nabla}_\mu\delta\chi}{\dot{\bar{\chi}}^2}\\
&+\frac{1}{\dot{\bar{\chi}}}u^\mu h_{\mu\nu}\bar{\nabla}^\nu\delta\chi\left(H\left(2\dot{\alpha}_B+H(2\alpha_B(\alpha_M+1)-\alpha_M+\alpha_T)\right)+2\alpha_B\dot{H}\right)\\
&-\frac{1}{2\dot{\bar{\chi}}^2}\delta\chi u^\mu u^\nu h_{\mu\nu}\left(2\dot{C}_{\chi 2}\dot{\bar{\chi}}^3+2\dot{\bar{\chi}}^2(\ddot{D}_{\chi 2}+2\dot{D}_{\chi 5}H)\right.
\end{aligned}
$$

$$
\begin{aligned}
&+\ddot{\bar{\chi}}\left(H\left(2\dot{\alpha}_B+\alpha_K+2H(\alpha_B(\alpha_M+2)-\alpha_M+\alpha_T)\right)+2\alpha_B\dot{H}\right)\\
&-2H\dot{\bar{\chi}}\left(\dot{H}(5\alpha_B-\alpha_M+\alpha_T)+H\left(\dot{\alpha}_B+\alpha_B\alpha_M H\right)\right)\\
&-\frac{1}{\dot{\bar{\chi}}^2}\delta\chi h\left(\dot{C}_{\chi 2}\dot{\bar{\chi}}^3+\dot{\bar{\chi}}^2(\ddot{D}_{\chi 2}+2\dot{D}_{\chi 5}H)-H\dot{\bar{\chi}}\left(\dot{H}(2\alpha_B-\alpha_M+\alpha_T)\right.\right.\\
&\left.\left.+H\left(\dot{\alpha}_B+\alpha_B\alpha_M H\right)\right)+\ddot{\bar{\chi}}\left(H\left(\dot{\alpha}_B+H(\alpha_B(\alpha_M+5)-\alpha_M+\alpha_T)\right)+\alpha_B\dot{H}\right)\right)
\end{aligned}
\tag{A.11}
$$

## A.2 Vector-tensor gravity

### A.2.1 Noether constraints

The following Noether constraints are obtained in Section 4.4.3 for the $A_n$, $B_n$, and $C_n$:

$$
\begin{aligned}
A_1 &= \frac{1}{16}\left(-\dot{\bar{\varphi}}^2-16HD_{\zeta 7}(\dot{\bar{\zeta}}-H\bar{\zeta})\right)\\
A_2 &= \frac{1}{8}\left(\dot{\bar{\varphi}}^2-8HD_{\zeta 7}(\dot{\bar{\zeta}}-H\bar{\zeta})-32H^2C_1\right)\\
A_3 &= \frac{1}{8}\left(-\dot{\bar{\varphi}}^2-32H^2C_1-32H^2C_5-4\dot{H}D_{\zeta 4}\bar{\zeta}-24H^2D_{\zeta 7}\bar{\zeta}-8H^2D_{\zeta 9}\bar{\zeta}-8H^2C_{\zeta 2}\bar{\zeta}^2\right.\\
&\quad +8H^2C_{\zeta 3}\bar{\zeta}^2+8\dot{H}C_{\zeta 3}\bar{\zeta}^2-8H^2C_{\zeta 5}\bar{\zeta}^2+8H^2C_{\zeta 6}\bar{\zeta}^2-4HD_{\zeta 4}\dot{\bar{\zeta}}+16HD_{\zeta 7}\dot{\bar{\zeta}}\\
&\quad \left.+8HC_{\zeta 2}\bar{\zeta}\dot{\bar{\zeta}}\right)\\
A_4 &= \frac{1}{4}\left(-\dot{\bar{\varphi}}^2+4C_{\zeta 2}\dot{\bar{\zeta}}^2-4C_{\zeta 2}\bar{\zeta}^2H^2-12C_{\zeta 3}\bar{\zeta}^2H^2-4\dot{C_{\zeta 3}}\bar{\zeta}^2H-4C_{\zeta 3}\bar{\zeta}^2\dot{H}-8C_{\zeta 3}\bar{\zeta}\dot{\bar{\zeta}}H\right.\\
&\quad +4C_{\zeta 5}\bar{\zeta}^2\dot{H}-4C_{\zeta 6}\bar{\zeta}^2\dot{H}+2\dot{D_{\zeta 4}}\dot{\bar{\zeta}}+2D_{\zeta 4}\ddot{\bar{\zeta}}+4D_{\zeta 4}\bar{\zeta}H^2+2D_{\zeta 4}\dot{\bar{\zeta}}H+8D_{\zeta 7}\bar{\zeta}H^2\\
&\quad \left.-12D_{\zeta 7}\dot{\bar{\zeta}}H+4D_{\zeta 9}\bar{\zeta}\dot{H}-32H^2C_1+16\dot{H}C_5\right)\\
A_5 &= \frac{1}{16\dot{\bar{\zeta}}}\left(6B_\zeta\dot{H}\bar{\zeta}^3+12B_\zeta H\dot{\bar{\zeta}}\bar{\zeta}^2+12C_{\zeta 1}H\ddot{\bar{\zeta}}\bar{\zeta}^2+4\dot{C}_{\zeta 1}\ddot{\bar{\zeta}}\bar{\zeta}^2+4C_{\zeta 1}\dddot{\bar{\zeta}}\bar{\zeta}^2+8C_{\zeta 1}\dot{\bar{\zeta}}\ddot{\bar{\zeta}}\bar{\zeta}\right.\\
&\quad -24C_{\zeta 2}H^2\dot{\bar{\zeta}}\bar{\zeta}^2+12C_{\zeta 2}H\dot{H}\bar{\zeta}^3-12C_{\zeta 2}\dot{H}\dot{\bar{\zeta}}\bar{\zeta}^2+24C_{\zeta 2}H\dot{\bar{\zeta}}^2\bar{\zeta}-24C_{\zeta 3}H^2\dot{\bar{\zeta}}\bar{\zeta}^2\\
&\quad +24C_{\zeta 3}\dot{H}\dot{\bar{\zeta}}\bar{\zeta}^2-48C_{\zeta 3}H\dot{\bar{\zeta}}^2\bar{\zeta}-18C_{\zeta 4}H^2\dot{\bar{\zeta}}\bar{\zeta}^2-18C_{\zeta 4}H\dot{H}\bar{\zeta}^3-6\dot{C}_{\zeta 4}\dot{H}\bar{\zeta}^3\\
&\quad -6\dot{C}_{\zeta 4}H\dot{\bar{\zeta}}\bar{\zeta}^2-24C_{\zeta 4}\dot{H}\dot{\bar{\zeta}}\bar{\zeta}^2-12C_{\zeta 4}H\dot{\bar{\zeta}}^2\bar{\zeta}-60C_{\zeta 5}H^2\dot{\bar{\zeta}}\bar{\zeta}^2-12C_{\zeta 5}H\dot{H}\bar{\zeta}^3\\
&\quad -36C_{\zeta 6}H\dot{H}\bar{\zeta}^3+42D_{\zeta 4}H^2\dot{\bar{\zeta}}\bar{\zeta}+12D_{\zeta 4}H\dot{H}\bar{\zeta}^2+6D_{\zeta 4}\ddot{H}\bar{\zeta}^2+6\dot{D}_{\zeta 4}H\dot{\bar{\zeta}}\bar{\zeta}\\
&\quad -6D_{\zeta 4}H\dot{\bar{\zeta}}^2+24D_{\zeta 7}H\dot{H}\bar{\zeta}^2-48D_{\zeta 9}H^2\dot{\bar{\zeta}}\bar{\zeta}-96H^2\dot{\bar{\zeta}}C_5-24\dot{C}_{\zeta 3}H\dot{\bar{\zeta}}\bar{\zeta}^2\\
&\quad \left.+6D_{\zeta 4}\dot{H}\dot{\bar{\zeta}}\bar{\zeta}-12C_{\zeta 6}H^2\dot{\bar{\zeta}}\bar{\zeta}^2-6C_{\zeta 4}\ddot{H}\bar{\zeta}^3-\dot{\bar{\zeta}}\dot{\bar{\varphi}}^2\right)\\
B_1 &= D_{\zeta 7}(H\bar{\zeta}-\dot{\bar{\zeta}})-4HC_1\\
B_2 &= \frac{1}{4}\left(-\dot{C_{\zeta 5}}\bar{\zeta}^2-2C_{\zeta 5}\dot{\bar{\zeta}}\bar{\zeta}-C_{\zeta 5}\bar{\zeta}^2H+\dot{C_{\zeta 6}}\bar{\zeta}^2+2C_{\zeta 6}\dot{\bar{\zeta}}\bar{\zeta}+C_{\zeta 6}\zeta^2H+D_{\zeta 7}\dot{\bar{\zeta}}-\dot{D}_{\zeta 9}\bar{\zeta}\right.\\
&\quad \left.-D_{\zeta 9}\dot{\bar{\zeta}}D_{\zeta 9}\bar{\zeta}H-4HC_1-4HC_5\right)
\end{aligned}
$$

$$
\begin{aligned}
B_3 &= \frac{1}{4}\Big(B_\zeta\bar{\xi}^2 - 2C_{\zeta 2}\dot{\bar{\xi}}\bar{\xi} + 2C_{\zeta 2}\bar{\xi}^2 H + 4C_{\zeta 3}\bar{\xi}^2 H - 4C_{\zeta 6}\bar{\xi}^2 H - \dot{D_{\zeta 4}}\bar{\xi} - 3D_{\zeta 4}\bar{\xi}H \\
&\quad + 4D_{\zeta 7}\bar{\xi}H + 16C_5 H\Big) \\
B_4 &= -4HC_5 - \frac{1}{2}\bar{\xi}\Big(-2C_{\zeta 2}\dot{\bar{\xi}} + 2C_{\zeta 2}\bar{\xi}H + 2\dot{C}_{\zeta 3}\bar{\xi} + 4C_{\zeta 3}\dot{\bar{\xi}} + 4C_{\zeta 3}\bar{\xi}H + 2C_{\zeta 5}\bar{\xi}H \\
&\quad - 2C_{\zeta 6}\bar{\xi}H - 3D_{\zeta 4}H - \dot{D}_{\zeta 4} + 2D_{\zeta 7}H + 2D_{\zeta 9}H\Big) \\
C_1 &= \frac{1}{4H}\Big(-\dot{C}_{\zeta 5}\bar{\xi}^2 - 2C_{\zeta 5}\dot{\bar{\xi}}\bar{\xi} - C_{\zeta 5}\bar{\xi}^2 H + \dot{C_{\zeta 6}}\bar{\xi}^2 + 2C_{\zeta 6}\dot{\bar{\xi}}\bar{\xi} + C_{\zeta 6}\bar{\xi}^2 H + D_{\zeta 7}\dot{\bar{\xi}} \\
&\quad - \dot{D}_{\zeta 9}\bar{\xi} - D_{\zeta 9}\dot{\bar{\xi}} - D_{\zeta 9}\bar{\xi}H - 4\dot{C}_6 - 4C_5 H\Big) \\
C_2 &= -C_1 \\
C_3 &= -2C_1 \\
C_4 &= 2C_1 \\
C_7 &= \frac{1}{4}\left(-4C_5 + C_{\zeta 5}\bar{\xi}^2 + C_{\zeta 6}\bar{\xi}^2\right) \\
C_7 &= \frac{1}{2}\left(4C_5 + D_{\zeta 7}\bar{\xi} + D_{\zeta 9}\bar{\xi} + C_{\zeta 5}\bar{\xi}^2 - C_{\zeta 6}\bar{\xi}^2\right) \\
C_8 &= -\frac{1}{2}\left(4C_5 + D_{\zeta 7}\bar{\xi} + D_{\zeta 9}\bar{\xi} + C_{\zeta 5}\bar{\xi}^2 - C_{\zeta 6}\bar{\xi}^2\right) \\
C_9 &= \frac{1}{4}\bar{\xi}\left(C_{\zeta 4}\bar{\xi} - D_{\zeta 4}\right) \\
C_{10} &= \frac{1}{4}\bar{\xi}\left(C_{\zeta 2}\bar{\xi} + C_{\zeta 3}\bar{\xi} - D_{\zeta 4}\right) \\
C_{11} &= -\frac{1}{2}\left(4C_5 + 2D_{\zeta 9}\bar{\xi} + C_{\zeta 5}\bar{\xi}^2 + C_{\zeta 6}\bar{\xi}^2\right) \\
C_{12} &= \frac{1}{2}\left(4C_5 + 2D_{\zeta 9}\bar{\xi} + C_{\zeta 5}\bar{\xi}^2 + C_{\zeta 6}\bar{\xi}^2\right) \\
C_{13} &= -\left(4C_5 + D_{\zeta 9}\bar{\xi} + C_{\zeta 5}\bar{\xi}^2 - C_{\zeta 6}\bar{\xi}^2\right) \\
C_{14} &= 4C_5 + D_{\zeta 9}\bar{\xi} + C_{\zeta 5}\bar{\xi}^2 - C_{\zeta 6}\bar{\xi}^2 \\
C_{15} &= C_{\zeta 3}\bar{\xi}^2 \\
C_{16} &= \frac{1}{2}\left(D_{\zeta 4}\bar{\xi} - 2C_{\zeta 3}\bar{\xi}^2\right) \\
C_{17} &= \frac{1}{4}C_{\zeta 1}\bar{\xi}^2.
\end{aligned}
\tag{A.12}
$$

For the $A_{\zeta n}$, $B_{\zeta n}$, $C_{\zeta n}$, and $D_{\zeta n}$:

$$
\begin{aligned}
A_{\zeta 1} &= -\frac{1}{2\bar{\xi}}\Big(-2A_{\zeta 3} + 2C_{\zeta 2}\ddot{\bar{\xi}} + 6C_{\zeta 2}\bar{\xi}H^2 - 6C_{\zeta 2}\dot{\bar{\xi}}H + 12C_{\zeta 3}\bar{\xi}H^2 - 6C_{\zeta 3}\dot{\bar{\xi}}H + 6C_{\zeta 3}\bar{\xi}\dot{H} \\
&\quad - 3C_{\zeta 4}\dot{\bar{\xi}}H - 3C_{\zeta 4}\bar{\xi}\dot{H} - 12C_{\zeta 5}\bar{\xi}H^2 - 3\dot{D}_{\zeta 4}H + 3D_{\zeta 4}\dot{H} + 12D_{\zeta 7}H^2 - 12D_{\zeta 9}H^2\Big) \\
A_{\zeta 2} &= -\frac{1}{2\bar{\xi}}\Big(-B_\zeta\dot{\bar{\xi}} + 2C_{\zeta 2}\bar{\xi}H^2 - 2C_{\zeta 2}\dot{\bar{\xi}}H - 2\dot{C_{\zeta 3}}\dot{\bar{\xi}} - 2C_{\zeta 3}\ddot{\bar{\xi}} + 4C_{\zeta 3}\bar{\xi}H^2 + 2\dot{C_{\zeta 3}}\bar{\xi}H -
\end{aligned}
$$

$$
\begin{aligned}
&2C_{\zeta 3}\dot{\bar{\xi}}H + 2C_{\zeta 3}\bar{\xi}\dot{H} - C_{\zeta 4}\ddot{\bar{\xi}} + 2C_{\zeta 5}\dot{\bar{\xi}}H - 2C_{\zeta 5}\bar{\xi}\dot{H} + 6C_{\zeta 6}\dot{\bar{\xi}}H + 6C_{\zeta 6}\bar{\xi}\dot{H} \\
&-4D_{\zeta 9}\dot{H}\Big) \\
A_{\zeta 3} = &\frac{1}{2\dot{\bar{\xi}}}\Big(3B_{\zeta}\bar{\xi}^2\dot{H} + 6B_{\zeta}\bar{\xi}\dot{\bar{\xi}}H + 2\dot{C_{\zeta 1}}\zeta\ddot{\bar{\xi}} + 2C_{\zeta 1}\dot{\bar{\xi}}\ddot{\bar{\xi}} + 2C_{\zeta 1}\bar{\xi}\dddot{\bar{\xi}} + 6C_{\zeta 1}\bar{\xi}\ddot{\bar{\xi}}H \\
&+6C_{\zeta 2}\bar{\xi}\dot{\bar{\xi}}H^2 + 6C_{\zeta 2}\bar{\xi}^2\dot{H}H - 6C_{\zeta 2}\dot{\bar{\xi}}^2H - 6C_{\zeta 2}\bar{\xi}\dot{\bar{\xi}}\dot{H} + 12C_{\zeta 3}\bar{\xi}\dot{\bar{\xi}}H^2 - 6C_{\zeta 3}\dot{\bar{\xi}}^2H \\
&+6C_{\zeta 3}\bar{\xi}\dot{\bar{\xi}}\dot{H} - 9C_{\zeta 4}\bar{\xi}\dot{\bar{\xi}}H^2 - 9C_{\zeta 4}\bar{\xi}^2\dot{H}H - 3\dot{C_{\zeta 4}}\bar{\xi}^2\dot{H} - 3C_{\zeta 4}\bar{\xi}^2\ddot{H} - 3C_{\zeta 4}\dot{\bar{\xi}}^2H \\
&-3\dot{C_{\zeta 4}}\bar{\xi}\dot{\bar{\xi}}H - 9C_{\zeta 4}\bar{\xi}\dot{\bar{\xi}}\dot{H} - 18C_{\zeta 5}\bar{\xi}\dot{\bar{\xi}}H^2 - 6C_{\zeta 5}\bar{\xi}^2\dot{H}H - 18C_{\zeta 6}\zeta\dot{\bar{\xi}}H^2 \\
&+6D_{\zeta 4}\bar{\xi}\dot{H}H - 3\dot{D}_{\zeta 4}\dot{\bar{\xi}}H + 3D_{\zeta 4}\dot{\bar{\xi}}\dot{H} + 3D_{\zeta 4}\bar{\xi}\ddot{H} + 12D_{\zeta 7}\dot{\bar{\xi}}H^2 + 12D_{\zeta 7}\bar{\xi}\dot{H}H \\
&-12D_{\zeta 9}\dot{\bar{\xi}}H^2 - 18C_{\zeta 6}\bar{\xi}^2\dot{H}H\Big) \\
A_{\zeta 4} = &\frac{1}{2}\Big(-\dot{B_{\zeta}}\bar{\xi} - B_{\zeta}\dot{\bar{\xi}} - 3B_{\zeta}\bar{\xi}H + 2\dot{C}_{\zeta 2}\dot{\bar{\xi}} + 2C_{\zeta 2}\ddot{\bar{\xi}} - 6C_{\zeta 2}\bar{\xi}H^2 - 2\dot{C}_{\zeta 2}\bar{\xi}H + 4C_{\zeta 2}\dot{\bar{\xi}}H \\
&-2C_{\zeta 2}\bar{\xi}\dot{H} + 10C_{\zeta 5}\bar{\xi}H^2 + 4\dot{C_{\zeta 5}}\bar{\xi}H + 4C_{\zeta 5}\dot{\bar{\xi}}H + 2C_{\zeta 5}\bar{\xi}\dot{H} + 6C_{\zeta 6}\bar{\xi}H^2 + 6C_{\zeta 6}\bar{\xi}\dot{H} \\
&+3D_{\zeta 4}H^2 + 4\dot{D}_{\zeta 4}H + D_{\zeta 4}\dot{H} + \ddot{D_{\zeta 4}} - 16D_{\zeta 7}H^2 - 4\dot{D}_{\zeta 7}H - 4D_{\zeta 7}\dot{H} + 8D_{\zeta 9}H^2 \\
&+4\dot{D}_{\zeta 9}H\Big) \\
A_{\zeta 5} = &B_{\zeta}\dot{\bar{\xi}} + 2\dot{C}_{\zeta 3}\dot{\bar{\xi}} + 2C_{\zeta 3}\ddot{\bar{\xi}} - 4C_{\zeta 3}\bar{\xi}H^2 - 2\dot{C}_{\zeta 3}\bar{\xi}H + 2C_{\zeta 3}\dot{\bar{\xi}}H - 2C_{\zeta 3}\bar{\xi}\dot{H} + C_{\zeta 4}\ddot{\bar{\xi}} \\
&-2C_{\zeta 5}\dot{\bar{\xi}}H + 2C_{\zeta 5}\bar{\xi}\dot{H} - 6C_{\zeta 6}\dot{\bar{\xi}}H - 6C_{\zeta 6}\bar{\xi}\dot{H} - D_{\zeta 4}H^2 - \dot{D}_{\zeta 4}H + 4D_{\zeta 7}H^2 \\
&+4D_{\zeta 9}\dot{H} \\
B_{\zeta 1} = &\frac{3}{2}H\left(D_{\zeta 4} + 2C_{\zeta 3}\bar{\xi}\right) \\
B_{\zeta 2} = &\frac{1}{2}\Big(HD_{\zeta 4} - 4HD_{\zeta 9} - 2\dot{C}_{\zeta 3}\bar{\xi} + B_{\zeta}\bar{\xi} - 2HC_{\zeta 3}\bar{\xi} - 4HC_{\zeta 5}\bar{\xi} - 4C_{\zeta 3}\dot{\bar{\xi}}\Big) \\
B_{\zeta 3} = &\frac{1}{2}\Big(\dot{D}_{\zeta 4} + 3HD_{\zeta 4} - 4HD_{\zeta 7} - B_{\zeta}\bar{\xi} - 2HC_{\zeta 2}\bar{\xi} + 2HC_{\zeta 5}\bar{\xi} + 6HC_{\zeta 6}\bar{\xi} + 2C_{\zeta 2}\dot{\bar{\xi}}\Big) \\
B_{\zeta 4} = &-\dot{D}_{\zeta 4} - 2HD_{\zeta 4} + 2HD_{\zeta 7} + 2HC_{\zeta 2}\bar{\xi} - 2C_{\zeta 2}\dot{\bar{\xi}} \\
B_{\zeta 5} = &2\Big(HD_{\zeta 9} + 3HC_{\zeta 5}\bar{\xi} + HC_{\zeta 6}\bar{\xi} + C_{\zeta 3}\dot{\bar{\xi}}\Big) \\
B_{\zeta 6} = &\dot{D}_{\zeta 9} - HD_{\zeta 7} + 2HD_{\zeta 9} + \dot{C}_{\zeta 5}\bar{\xi} - \dot{C}_{\zeta 6}\bar{\xi} + 2HC_{\zeta 5}\bar{\xi} - 2HC_{\zeta 6}\bar{\xi} + C_{\zeta 5}\dot{\bar{\xi}} - C_{\zeta 6}\dot{\bar{\xi}} \\
B_{\zeta 7} = &-\dot{D}_{\zeta 9} + HD_{\zeta 7} - 2HD_{\zeta 9} - 2\dot{C}_{\zeta 5}\bar{\xi} - 4HC_{\zeta 5}\bar{\xi} - 2C_{\zeta 5}\dot{\bar{\xi}} \\
D_{\zeta 1} = &C_{\zeta 1}\bar{\xi} \\
D_{\zeta 2} = &\frac{1}{2}\left(-D_{\zeta 4} + C_{\zeta 4}\bar{\xi}\right) \\
D_{\zeta 3} = &\frac{1}{2}\left(-D_{\zeta 4} + C_{\zeta 2}\bar{\xi}\right) \\
D_{\zeta 5} = &\frac{1}{2}\bar{\xi}\left(-2C_{\zeta 3} + C_{\zeta 4}\right) \\
D_{\zeta 6} = &2C_{\zeta 3}\bar{\xi}
\end{aligned}
$$

$$
\begin{aligned}
D_{\zeta 8} &= -D_{\zeta 7} \\
D_{\zeta 10} &= -D_{\zeta 9} - C_{\zeta 5}\bar{\zeta} + C_{\zeta 6}\bar{\zeta} \\
D_{\zeta 11} &= D_{\zeta 9} + 2C_{\zeta 5}\bar{\zeta} \\
D_{\zeta 12} &= -D_{\zeta 9}.
\end{aligned} \tag{A.13}
$$

In addition, a Friedmann-like equation analogous to (2.33) is found:

$$
\begin{aligned}
B_\zeta = -\frac{1}{\bar{\zeta}\dot{\bar{\zeta}}}\Big( & -2C_{\zeta 2}\dot{\bar{\zeta}}^2 + 2C_{\zeta 2}\dot{\bar{\zeta}}\bar{\zeta}H + C_{\zeta 4}\ddot{\bar{\zeta}}\bar{\zeta} - 2C_{\zeta 5}\bar{\zeta}^2\dot{H} \\
& -2C_{\zeta 5}\dot{\bar{\zeta}}\bar{\zeta}H - 2C_{\zeta 6}\bar{\zeta}^2\dot{H} - 6C_{\zeta 6}\dot{\bar{\zeta}}\bar{\zeta}H - \dot{D}_{\zeta 4}\dot{\bar{\zeta}} - D_{\zeta 4}\ddot{\bar{\zeta}} \\
& -D_{\zeta 4}\dot{\bar{\zeta}}H + 4D_{\zeta 7}\dot{\bar{\zeta}}H - 16C_6\dot{H} + \dot{\bar{\varphi}}^2\Big).
\end{aligned} \tag{A.14}
$$

### A.2.2 Dictionary for scalar perturbations

The following dictionary of parameters for the action for scalar perturbations for vector-tensor gravity models, given by eq. (2.65), is provided:

$$T_{\Phi^2} = 3H^2\left(3\left(C_{\zeta 5}+C_{\zeta 6}\right)\bar{\zeta}^2 - M^2\right) + 3H\left(D_{\zeta 4} - C_{\zeta 4}\bar{\zeta}\right)\dot{\bar{\zeta}} + C_{\zeta 1}\dot{\bar{\zeta}}^2 + \frac{1}{2}\dot{\bar{\varphi}}^2 \tag{A.15}$$

$$T_{\partial^2\Phi^2} = C_{\zeta 3}\bar{\zeta}^2 \tag{A.16}$$

$$T_{\dot{\Psi}^2} = 9\left(C_{\zeta 5}+C_{\zeta 6}\right)\bar{\zeta}^2 - 3M^2 \tag{A.17}$$

$$T_{\partial^2\Psi^2} = (1+\alpha_T)M^2 \tag{A.18}$$

$$T_{\Phi\Psi} = 36H\frac{\bar{\zeta}}{\dot{\bar{\zeta}}}\dot{\bar{\varphi}}^2 \tag{A.19}$$

$$T_{\dot{\Psi}\Phi} = 3\Big(2H\left(3\left(C_{\zeta 5}+C_{\zeta 6}\right)\bar{\zeta}^2 - M^2\right) + \left(D_{\zeta 4} - C_{\zeta 4}\bar{\zeta}\right)\dot{\bar{\zeta}}\Big) \tag{A.20}$$

$$T_{\partial\Phi\partial\Psi} = -2M^2 + 4\bar{\zeta}\left(D_{\zeta 9} + 2C_{\zeta 5}\bar{\zeta}\right) \tag{A.21}$$

$$
\begin{aligned}
T_{Z_0\Phi} = \frac{1}{\dot{\bar{\zeta}}}\Big( & \ddot{\bar{\zeta}}\left(2C_{\zeta 1}\dot{\bar{\zeta}} - 3C_{\zeta 4}H\bar{\zeta} + 3D_{\zeta 4}H\right) \\
& -3\dot{H}\left(\dot{\bar{\zeta}}(C_{\zeta 4}\bar{\zeta} - D_{\zeta 4}) + 2H\left(M^2 - 3\bar{\zeta}^2(C_{\zeta 5}+C_{\zeta 6})\right)\right) - 3H\dot{\bar{\varphi}}^2\Big)
\end{aligned} \tag{A.22}
$$

$$T_{\dot{Z}_0\Phi} = 3H\left(C_{\zeta 4}\bar{\zeta} - D_{\zeta 4}\right) - 2C_{\zeta 1}\dot{\bar{\zeta}} \tag{A.23}$$

$$T_{\partial Z_0\partial\Phi} = -D_{\zeta 4} \tag{A.24}$$

$$
\begin{aligned}
T_{Z_0\Psi} = \frac{3}{\dot{\bar{\zeta}}^2}\Big( & \dot{\bar{\zeta}}\Big(-3C_{\zeta 4}H\bar{\zeta}\ddot{\bar{\zeta}} - \dot{C_{\zeta 4}}\bar{\zeta}\ddot{\bar{\zeta}} - C_{\zeta 4}\bar{\zeta}\dddot{\bar{\zeta}} \\
& + \dot{H}\left(-2H\left((\alpha_M+3)M^2 - 9\bar{\zeta}^2(C_{\zeta 5}+C_{\zeta 6})\right) + 6\dot{C_{\zeta 5}}\bar{\zeta}^2 + 6\dot{C_{\zeta 6}}\bar{\zeta}^2\right) \\
& + 6C_{\zeta 5}\ddot{H}\bar{\zeta}^2 + 6C_{\zeta 6}\ddot{H}\bar{\zeta}^2 + 3D_{\zeta 4}H\ddot{\bar{\zeta}} + \dot{D}_{\zeta 4}\ddot{\bar{\zeta}} + D_{\zeta 4}\dddot{\bar{\zeta}} - 2\ddot{H}M^2 + 3H\dot{\bar{\varphi}}^2\Big)
\end{aligned}
$$

$$+\ddot{\bar{\xi}}\left(\ddot{\bar{\xi}}(C_{\zeta 4}\bar{\xi}-D_{\zeta 4})+2\dot{H}\left(M^2-3\bar{\xi}^2(C_{\zeta 5}+C_{\zeta 6})\right)+\dot{\bar{\varphi}}^2\right)$$
$$+\dot{\bar{\xi}}^2\left(12\dot{H}\bar{\xi}(C_{\zeta 5}+C_{\zeta 6})-C_{\zeta 4}\ddot{\bar{\xi}}\right)\Big) \tag{A.25}$$

$$T_{\dot{Z}_0\Psi}=\frac{3}{\dot{\bar{\xi}}}\left(\ddot{\bar{\xi}}(C_{\zeta 4}\bar{\xi}-D_{\zeta 4})+2\dot{H}\left(M^2-3\bar{\xi}^2(C_{\zeta 5}+C_{\zeta 6})\right)+\dot{\bar{\varphi}}^2\right) \tag{A.26}$$

$$T_{\dot{Z}_0\Psi}=3\left(C_{\zeta 4}\bar{\xi}-D_{\zeta 4}\right) \tag{A.27}$$

$$T_{\partial Z_0\partial\Psi}=\frac{2}{\dot{\bar{\xi}}}\left(4C_{\zeta 5}\bar{\xi}\left(H\bar{\xi}+2\dot{\bar{\xi}}\right)+4\dot{C}_{\zeta 5}\bar{\xi}^2+2D_{\zeta 9}\left(H\bar{\xi}+\dot{\bar{\xi}}\right)+2\dot{D}_{\zeta 9}\bar{\xi}-\alpha_M HM^2\right.$$
$$\left.+\alpha_T HM^2\right) \tag{A.28}$$

$$T_{Z_0^2}=\frac{1}{2\dot{\bar{\xi}}^2}\left(\dot{\bar{\xi}}\left(2\left(\ddot{\bar{\xi}}\left(3C_{\zeta 1}H+\dot{C}_{\zeta 1}\right)+C_{\zeta 1}\dddot{\bar{\xi}}\right)+3\ddot{H}(D_{\zeta 4}-C_{\zeta 4}\bar{\xi})\right)\right.$$
$$-3\dot{H}\left(\dot{\bar{\xi}}\left(3C_{\zeta 4}H\bar{\xi}+\dot{C}_{\zeta 4}\bar{\xi}-3D_{\zeta 4}H-\dot{D}_{\zeta 4}\right)+\ddot{\bar{\xi}}(C_{\zeta 4}\bar{\xi}-D_{\zeta 4})+C_{\zeta 4}\dot{\bar{\xi}}^2+\dot{\bar{\varphi}}^2\right)$$
$$\left.-6\dot{H}^2\left(M^2-3\bar{\xi}^2(C_{\zeta 5}+C_{\zeta 6})\right)\right) \tag{A.29}$$

$$T_{\dot{Z}_0^2}=C_{\zeta 1} \tag{A.30}$$

$$T_{\partial^2 Z_0^2}=C_{\zeta 2} \tag{A.31}$$

$$T_{\partial\dot{Z}_0\partial Z_1}=C_{\zeta 4} \tag{A.32}$$

$$T_{\partial Z_0\partial Z_1}=-\frac{1}{\bar{\xi}\dot{\bar{\xi}}}\left(-2C_{\zeta 2}\dot{\bar{\xi}}^2+C_{\zeta 4}\bar{\xi}\ddot{\bar{\xi}}+8C_{\zeta 5}H^2\bar{\xi}^2+8\dot{C}_{\zeta 5}H\bar{\xi}^2-6C_{\zeta 5}\dot{H}\bar{\xi}^2+16C_{\zeta 5}H\bar{\xi}\dot{\bar{\xi}}\right.$$
$$-6C_{\zeta 6}\dot{H}\bar{\xi}^2-D_{\zeta 4}H\dot{\bar{\xi}}-\dot{D}_{\zeta 4}\dot{\bar{\xi}}-D_{\zeta 4}\ddot{\bar{\xi}}+4D_{\zeta 9}H^2\bar{\xi}+4\dot{D}_{\zeta 9}H\bar{\xi}+4D_{\zeta 9}H\dot{\bar{\xi}}$$
$$\left.+2\left(\alpha_T-\alpha_M\right)H^2M^2+2\dot{H}M^2+\dot{\bar{\varphi}}^2\right) \tag{A.33}$$

$$T_{\partial\Phi\partial Z_1}=-2H\left(D_{\zeta 9}+\left(C_{\zeta 5}-3C_{\zeta 6}\right)\bar{\xi}\right)-\left(2C_{\zeta 3}+C_{\zeta 4}\right)\dot{\bar{\xi}} \tag{A.34}$$

$$T_{\partial\Phi\partial\dot{Z}_1}=2C_{\zeta 3}\bar{\xi} \tag{A.35}$$

$$T_{\Psi\dot{Z}_1}=\frac{2H}{\dot{\bar{\xi}}}\left(4C_{\zeta 5}\bar{\xi}\left(H\bar{\xi}+2\dot{\bar{\xi}}\right)+4\dot{C}_{\zeta 5}\bar{\xi}^2+2D_{\zeta 9}\left(H\bar{\xi}+\dot{\bar{\xi}}\right)+2\dot{D}_{\zeta 9}\bar{\xi}-\alpha_M HM^2\right.$$
$$\left.+\alpha_T HM^2\right) \tag{A.36}$$

$$T_{\partial\Psi\partial Z_1}=2\left(C_{\zeta 5}H\bar{\xi}+\dot{C}_{\zeta 5}\bar{\xi}+C_{\zeta 5}\dot{\bar{\xi}}-3C_{\zeta 6}H\bar{\xi}-3\dot{C}_{\zeta 6}\bar{\xi}-3C_{\zeta 6}\dot{\bar{\xi}}+2D_{\zeta 9}H+2\dot{D}_{\zeta 9}\right) \tag{A.37}$$

$$T_{\partial\Psi\partial Z_1}=4D_{\zeta 9}+(2C_{\zeta 5}-6C_{\zeta 6})\bar{\xi} \tag{A.38}$$

$$T_{\partial^2 Z_1^2}=\frac{1}{2\bar{\xi}^2}\left(2C_{\zeta 1}\dot{\bar{\xi}}^2+2C_{\zeta 3}H\bar{\xi}\dot{\bar{\xi}}+2\dot{C}_{\zeta 3}\bar{\xi}\dot{\bar{\xi}}+2C_{\zeta 3}\bar{\xi}\ddot{\bar{\xi}}-8C_{\zeta 5}H^2\bar{\xi}^2-8\dot{C}_{\zeta 5}H\bar{\xi}^2\right.$$
$$+8C_{\zeta 5}\dot{H}\bar{\xi}^2-16C_{\zeta 5}H\bar{\xi}\dot{\bar{\xi}}+D_{\zeta 4}H\dot{\bar{\xi}}+\dot{D}_{\zeta 4}\dot{\bar{\xi}}+D_{\zeta 4}\ddot{\bar{\xi}}-4D_{\zeta 9}H^2\bar{\xi}-4\dot{D}_{\zeta 9}H\bar{\xi}$$
$$\left.-4D_{\zeta 9}H\dot{\bar{\xi}}+4D_{\zeta 9}\dot{H}\bar{\xi}+2\left(\alpha_M-\alpha_T\right)H^2M^2-2\dot{H}M^2-\dot{\bar{\varphi}}^2\right) \tag{A.39}$$

$$T_{\partial^2\dot{Z}_1^2}=C_{\zeta 3} \tag{A.40}$$

$$T_{\partial^4 Z_1^2}=C_{\zeta 5}+C_{\zeta 6}. \tag{A.41}$$

We see that all these functions $T$ depend only on 9 combinations of the 10 free parameters:

$$M^2,\, C_{\zeta 1},\, C_{\zeta 2},\, C_{\zeta 3},\, C_{\zeta 4},\, C_{\zeta 5}+C_{\zeta 6},\, D_{\zeta 4},\, \alpha_T,$$
$$D_{\zeta 9}+2\bar{\zeta}C_{\zeta 5}, \tag{A.42}$$

and hence only these combinations can be constrained by observing the effect of scalar perturbations in the Universe.

### A.2.3 Dictionary for vector perturbations

The following dictionary of parameters for the action for scalar perturbations in vector-tensor gravity models, given by eq. (2.67), is provided:

$$T_{\partial^2 N^2} = \frac{1}{4}M^2 \tag{A.43}$$

$$T_{\partial N \partial \delta Z} = -D_{\zeta 9} - 2\bar{\zeta}C_{\zeta 5} \tag{A.44}$$

$$\begin{aligned} T_{\delta Z^2} = \frac{1}{2\bar{\zeta}^2}\Big(&2C_{\zeta 2}\dot{\bar{\zeta}}^2 - 2C_{\zeta 3}H^2\bar{\zeta}^2 - 2C_{\zeta 3}\dot{H}\bar{\zeta}^2 + 2C_{\zeta 3}H\bar{\zeta}\dot{\bar{\zeta}} + 2\dot{C}_{\zeta 3}\bar{\zeta}\left(\dot{\bar{\zeta}} - H\bar{\zeta}\right) \\ &+ 2C_{\zeta 3}\bar{\zeta}\ddot{\bar{\zeta}} - 8C_{\zeta 5}H^2\bar{\zeta}^2 - 8\dot{C}_{\zeta 5}H\bar{\zeta}^2 - 4D_{\zeta 9}H\dot{\bar{\zeta}} + 4D_{\zeta 9}\dot{H}\bar{\zeta} \\ &+ 8C_{\zeta 5}\dot{H}\bar{\zeta}^2 - 16C_{\zeta 5}H\bar{\zeta}\dot{\bar{\zeta}} + D_{\zeta 4}H\dot{\bar{\zeta}} + \dot{D}_{\zeta 4}\dot{\bar{\zeta}} + D_{\zeta 4}\ddot{\bar{\zeta}} - 4D_{\zeta 9}H^2\bar{\zeta} - 4\dot{D}_{\zeta 9}H\bar{\zeta} \\ &+ 2\left(\alpha_M - \alpha_T\right)H^2M^2 - 2\dot{H}M^2 - \dot{\bar{\varphi}}^2\Big) \end{aligned} \tag{A.45}$$

$$T_{\delta \dot{Z}^2} = C_{\zeta 3} \tag{A.46}$$

$$T_{\partial^2 \delta Z^2} = C_{\zeta 5}. \tag{A.47}$$

We see that this action depends only on 5 combinations of the free parameters:

$$M^2,\, C_{\zeta 3},\, C_{\zeta 5},\, D_{\zeta 9},$$
$$2C_{\zeta 2}\dot{\bar{\zeta}}^2 + D_{\zeta 4}H\dot{\bar{\zeta}} + \dot{D}_{\zeta 4}\dot{\bar{\zeta}} + D_{\zeta 4}\ddot{\bar{\zeta}} - 2\alpha_T H^2M^2, \tag{A.48}$$

and hence only these combinations can be constrained by searching observational signatures of vector perturbations in these models.

## A.3 Axisymmetric Bianchi-I

### A.3.1 Most general quadratic action

The tensors used in action (2.79), where we again only include tensor terms which will give independent terms in the action, are given by:

$$\begin{aligned}\mathscr{D}^{\mu\nu\alpha\beta} =& D_1\gamma^{\mu\nu}\gamma^{\alpha\beta} + \gamma^{\mu\nu}\left(D_4 u^\alpha x^\beta + D_2 u^\alpha u^\beta + D_3 x^\alpha x^\beta\right) \\ &+ \gamma^{\mu\alpha}\left(D_5\gamma^{\nu\beta} + D_8 u^\nu x^\beta + D_6 u^\nu u^\beta + D_7 x^\nu x^\beta\right) + u^\mu D_{14} x^\nu u^\alpha x^\beta \\ &+ u^\mu u^\nu\left(D_{11}u^\alpha x^\beta + D_9 u^\alpha u^\beta + D_{10}x^\alpha x^\beta\right) + x^\mu x^\nu\left(D_{13}x^\alpha u^\beta + D_{12}x^\alpha x^\beta\right)\end{aligned} \tag{A.49}$$

$$\begin{aligned}\mathscr{E}^{\mu\nu\alpha\beta\delta\delta} =& \gamma^{\mu\nu}\left(u^\alpha x^\beta u^\delta E_7 + x^\alpha x^\beta u^\delta E_9 + u^\alpha u^\beta x^\delta E_{10} + u^\alpha x^\beta x^\delta E_8 + u^\alpha u^\beta u^\delta E_5\right. \\ &\left.+ x^\alpha x^\beta x^\delta E_6\right) + \gamma^{\mu\alpha}\left(u^\nu x^\beta u^\delta E_{17} + u^\nu x^\beta x^\delta E_{18}\right) + x^\mu x^\nu u^\alpha u^\beta\left(u^\delta E_{20} + x^\delta E_{19}\right) \\ &+ \gamma^{\mu\delta}\left(x^\nu u^\alpha u^\beta E_{16} + u^\nu u^\alpha x^\beta E_{13} + x^\nu u^\alpha x^\beta E_{14} + u^\nu x^\alpha x^\beta E_{15} + u^\nu u^\alpha u^\beta E_{11}\right. \\ &\left.+ x^\nu x^\alpha x^\beta E_{12}\right) + \gamma^{\mu\delta}\gamma^{\nu\alpha}\left(u^\beta E_3 + x^\beta E_4\right) + \gamma^{\mu\nu}\gamma^{\alpha\delta}\left(u^\beta E_1 + x^\beta E_2\right) \\ &+ x^\mu x^\nu x^\alpha u^\beta u^\delta E_{23} + x^\mu x^\nu x^\alpha u^\beta x^\delta E_{21} + u^\mu u^\nu u^\alpha x^\beta u^\delta E_{22} + u^\mu u^\nu u^\alpha x^\beta x^\delta E_{24}\end{aligned} \tag{A.50}$$

$$\begin{aligned}\mathscr{F}^{\mu\nu\alpha\beta\kappa\delta} =& F_1\gamma^{\mu\nu}\gamma^{\alpha\beta}\gamma^{\kappa\delta} + F_2\gamma^{\mu\alpha}\gamma^{\nu\beta}\gamma^{\kappa\delta} + F_3\gamma^{\mu\nu}\gamma^{\alpha\kappa}\gamma^{\beta\delta} + F_4\gamma^{\mu\kappa}\gamma^{\alpha\beta}\gamma^{\nu\delta} \\ &+ \left(F_5\gamma^{\mu\nu}\gamma^{\alpha\beta} + F_6\gamma^{\mu\alpha}\gamma^{\nu\beta}\right)u^\kappa u^\delta + \left(F_7\gamma^{\mu\nu}\gamma^{\kappa\delta} + F_8\gamma^{\mu\kappa}\gamma^{\nu\delta}\right)u^\alpha u^\beta \\ &+ F_9\gamma^{\alpha\beta}u^\mu u^\nu u^\kappa u^\delta + F_{10}\gamma^{\kappa\delta}u^\alpha u^\beta u^\mu u^\nu + \left(F_{11}\gamma^{\kappa\delta}\gamma^{\beta\nu} + F_{12}\gamma^{\kappa\beta}\gamma^{\delta\nu}\right)u^\mu u^\alpha \\ &+ \left(F_{13}\gamma^{\alpha\beta}\gamma^{\nu\delta} + F_{14}\gamma^{\alpha\nu}\gamma^{\delta\beta}\right)u^\mu u^\kappa + F_{15}\gamma^{\mu\alpha}u^\nu u^\beta u^\kappa u^\delta + F_{16}\gamma^{\mu\kappa}u^\nu u^\beta u^\alpha u^\delta \\ &+ F_{17}u^\mu u^\alpha u^\nu u^\beta u^\kappa u^\delta + \left(F_{18}\gamma^{\mu\nu}\gamma^{\alpha\beta} + F_19\gamma^{\mu\alpha}\gamma^{\nu\beta}\right)x^\kappa x^\delta \\ &+ \left(F_{20}\gamma^{\mu\nu}\gamma^{\kappa\delta} + F_{21}\gamma^{\mu\kappa}\gamma^{\nu\delta}\right)x^\alpha x^\beta + F_{22}\gamma^{\alpha\beta}x^\mu x^\nu x^\kappa x^\delta + F_{23}\gamma^{\kappa\delta}x^\alpha x^\beta x^\mu x^\nu \\ &+ \left(F_{24}\gamma^{\kappa\delta}\gamma^{\beta\nu} + F_{25}\gamma^{\kappa\beta}\gamma^{\delta\nu}\right)x^\mu x^\alpha + \left(F_{26}\gamma^{\alpha\beta}\gamma^{\nu\delta} + F_{27}\gamma^{\alpha\nu}\gamma^{\delta\beta}\right)x^\mu x^\kappa \\ &+ F_{28}\gamma^{\mu\alpha}x^\nu x^\beta x^\kappa x^\delta + F_{29}\gamma^{\mu\kappa}x^\nu x^\beta x^\alpha x^\delta + F_{30}x^\mu x^\alpha x^\nu x^\beta x^\kappa x^\delta \\ &+ \gamma^{\mu\nu}\left(F_{31}\gamma^{\alpha\beta}x^\kappa u^\delta + F_{32}\gamma^{\alpha\kappa}u^\beta x^\delta + F_{33}\gamma^{\alpha\kappa}u^\delta x^\beta + F_{34}\gamma^{\kappa\delta}x^\alpha u^\beta\right) \\ &+ \gamma^{\mu\alpha}\left(F_{35}\gamma^{\nu\beta}u^\kappa x^\delta + F_{36}\gamma^{\kappa\delta}x^\nu u^\beta\right) + \gamma^{\mu\nu}\left(u^\alpha x^\beta u^\kappa u^\delta F_{55} + u^\alpha u^\beta u^\kappa x^\delta F_{54}\right) \\ &+ \gamma^{\mu\kappa}\left(F_{37}\gamma^{\alpha\delta}x^\nu u^\beta + F_{38}\gamma^{\nu\delta}x^\alpha u^\beta + F_{39}\gamma^{\nu\alpha}x^\beta u^\delta + F_{40}\gamma^{\nu\alpha}u^\beta x^\delta\right) \\ &+ \gamma^{\mu\nu}\left(x^\alpha x^\beta u^\kappa u^\delta F_{41} + x^\alpha u^\beta x^\kappa u^\delta F_{43} + u^\alpha u^\beta x^\kappa x^\delta F_{42}\right) \\ &+ \gamma^{\mu\nu}\left(x^\alpha x^\beta x^\kappa u^\delta F_{62} + x^\alpha u^\beta x^\kappa x^\delta F_{63}\right) + \gamma^{\mu\alpha}\left(u^\nu x^\beta u^\kappa u^\delta F_{60} + u^\nu u^\beta u^\kappa x^\delta F_{59}\right)\end{aligned}$$

$$
\begin{aligned}
&+\gamma^{\mu\alpha}\left(x^\nu x^\beta u^\kappa u^\delta F_{50}+u^\nu x^\beta u^\kappa x^\delta F_{52}+u^\nu u^\beta x^\kappa x^\delta F_{51}\right)\\
&+\gamma^{\mu\alpha}\left(x^\nu x^\beta x^\kappa u^\delta F_{67}+x^\nu u^\beta x^\kappa x^\delta F_{68}\right)+u^\mu u^\nu u^\alpha x^\beta x^\kappa x^\delta F_{84}\\
&+\gamma^{\mu\kappa}\left(x^\nu u^\alpha u^\beta u^\delta F_{58}+u^\nu u^\alpha x^\beta u^\delta F_{56}+u^\nu u^\alpha u^\beta x^\delta F_{57}\right)\\
&+\gamma^{\mu\kappa}\left(x^\nu u^\alpha x^\beta u^\delta F_{49}+u^\nu x^\alpha x^\beta u^\delta F_{46}+u^\nu u^\alpha x^\beta x^\delta F_{48}+x^\nu u^\alpha u^\beta x^\delta F_{47}\right)\\
&+\gamma^{\mu\kappa}\left(x^\nu x^\alpha x^\beta u^\delta F_{65}+u^\nu x^\alpha x^\beta x^\delta F_{66}+x^\nu x^\alpha u^\beta x^\delta F_{64}\right)+x^\mu x^\nu x^\alpha u^\beta F_{61}\gamma^{\kappa\delta}\\
&+u^\mu u^\nu u^\alpha x^\beta F_{53}\gamma^{\kappa\delta}+\gamma^{\kappa\delta}\left(x^\mu u^\nu x^\alpha u^\beta F_{45}+u^\mu u^\nu x^\alpha x^\beta F_{44}\right)\\
&+x^\mu u^\nu u^\alpha u^\beta u^\kappa u^\delta F_{70}+x^\mu x^\nu u^\alpha u^\beta u^\kappa u^\delta F_{75}+x^\mu u^\nu x^\alpha u^\beta u^\kappa u^\delta F_{76}\\
&+x^\mu x^\nu x^\alpha x^\beta u^\kappa u^\delta F_{77}+x^\mu u^\nu u^\alpha u^\beta x^\kappa u^\delta F_{74}+x^\mu x^\nu x^\alpha x^\beta x^\kappa u^\delta F_{71}\\
&+u^\mu x^\nu x^\alpha x^\beta u^\kappa u^\delta F_{81}+u^\mu u^\nu u^\alpha u^\beta x^\kappa u^\delta F_{69}+u^\mu u^\nu u^\alpha u^\beta x^\kappa x^\delta F_{73}\\
&+u^\mu x^\nu u^\alpha x^\beta u^\kappa x^\delta F_{83}+u^\mu u^\nu x^\alpha x^\beta u^\kappa x^\delta F_{82}+u^\mu x^\nu x^\alpha x^\beta u^\kappa x^\delta F_{78}\\
&+u^\mu x^\nu u^\alpha x^\beta x^\kappa x^\delta F_{80}+u^\mu u^\nu x^\alpha x^\beta x^\kappa x^\delta F_{79}+u^\mu x^\nu x^\alpha x^\beta x^\kappa x^\delta F_{72},
\end{aligned}
\tag{A.51}
$$

where each of the $D_n$, $E_n$, and $F_n$ are free functions of time.

### A.3.2 Covariant quantities

For an anisotropic background, the background space-time will no longer be flat. Thus we need expressions for the Christoffel symbols and curvature tensors of the background *in terms of the background quantities* to properly evaluate the Noether constraints arising from the variation of (2.79). The relevant expressions can be shown to be:

$$\bar{\nabla}_\mu u_\nu = H_1 x_\mu x_\nu + H_2 \gamma_{\mu\nu} \tag{A.52}$$

$$\bar{\nabla}_\mu x_\nu = H_1 x_\mu u_\nu \tag{A.53}$$

$$\bar{\nabla}_\mu \gamma_{\alpha\beta} = u_\alpha \bar{\nabla}_\mu u_\beta + u_\beta \bar{\nabla}_\mu u_\alpha - x_\alpha \bar{\nabla} x_\beta - x_\beta \bar{\nabla} x_\alpha \tag{A.54}$$

$$
\begin{aligned}
\bar{R}^\rho_{\sigma\mu\nu} = \dot{H}_1(&-u_\mu u^\rho x_\nu x_\sigma + u_\nu u^\rho x_\mu x_\sigma + x^\rho x_\nu u_\mu u_\sigma\\
&- x^\rho x_\mu u_\nu u_\sigma) + H_1^2(-u_\mu u^\rho x_\nu x_\sigma + u_\nu u^\rho x_\mu x_\sigma\\
&+ x^\rho x_\nu u_\mu u_\sigma - x^\rho x_\mu u_\nu u_\sigma) + \dot{H}_2(-\gamma^\rho_\mu u_\sigma u_\nu\\
&+ \gamma^\rho_\nu u_\sigma u_\mu + u^\rho u_\nu \gamma_{\mu\sigma} - u^\rho u_\mu \gamma_{\sigma\nu})\\
&+ H_2^2(-\gamma^\rho_\mu u_\sigma u_\nu + \gamma^\rho_\nu u_\sigma u_\mu + u^\rho u_\nu \gamma_{\mu\sigma}\\
&- u^\rho u_\mu \gamma_{\sigma\nu}) + H_1 H_2(\gamma^\rho_\mu x_\sigma x_\nu - \gamma^\rho_\nu x_\sigma x_\mu\\
&- x^\rho x_\nu \gamma_{\mu\sigma} + x^\rho x_\mu \gamma_{\sigma\nu})
\end{aligned}
$$

$$
\begin{aligned}
\bar{R}_{\mu\nu} = &-\left(\dot{H}_1 + H_1^2 + 2\dot{H}_2 + 2H_2^2\right) u_\mu u_\nu\\
&+\left(\dot{H}_1 + H_1^2 + 2H_1 H_2\right) x_\mu x_\nu
\end{aligned}
$$

$$+\left(2H_2^2+H_1H_2+\dot{H}_2\right)\gamma_{\mu\nu} \tag{A.55}$$

$$\bar{R}=2H_1^2+6H_2^2+4H_1H_2+2\dot{H}_1+4\dot{H}_2. \tag{A.56}$$

$H_1=\frac{d\log a}{dt}$ and $H_2=\frac{d\log b}{dt}$ are the two Hubble parameters, $\bar{R}^{\rho}_{\sigma\mu\nu}$ is the Riemann curvature tensor, $\bar{R}_{\mu\nu}=\bar{R}^{\rho}_{\mu\rho\nu}$ is the Ricci tensor, and $\bar{R}=\bar{g}^{\mu\nu}\bar{R}_{\mu\nu}$ is the Ricci scalar.

### A.3.3 Solutions

The following Noether constraints are obtained in Section 2.6 for the $D_n$, $E_n$, and $F_n$:

$$\begin{aligned}
-F_2 &= -\frac{1}{2}F_3=\frac{1}{2}F_4=F_1\\
2F_5 &= -2F_6=F_7=-F_8=-F_{11}=F_{12}=-\frac{1}{2}F_{13}=\frac{1}{2}F_{14}=F_{41}\\
F_9 &= F_{10}=F_{15}=F_{16}=F_{17}=0\\
-2F_{18} &= 2F_{19}=-F_{20}=F_{21}=F_{24}=-F_{25}=\frac{1}{2}F_{26}=-\frac{1}{2}F_{27}=F_{41}\\
F_{22} &= F_{23}=F_{28}=F_{29}=F_{30}=0\\
F_{31} &= ...=F_{40}=0\\
F_{42} &= -\frac{1}{2}F_{43}=F_{44}=-F_{45}=-\frac{1}{2}F_{46}=-\frac{1}{2}F_{47}=\frac{1}{2}F_{48}=\frac{1}{2}F_{49}=-F_{50}=-F_{51}\\
&= \frac{1}{2}F_{52}=F_{41}\\
F_{53} &= ...=F_{84}=0\\
\frac{1}{2}E_1 &= -\frac{1}{4}E_3=F_1H_2\\
E_2 &= E_4=E_6=E_7=E_{10}=E_{12}=E_{13}=E_{16}=E_{17}=E_{19}=E_{21}=E_{22}=E_{23}=0\\
E_5 &= E_9=-F_{41}\left(H_1+H_2\right)\\
\frac{1}{4}E_8 &= E_{11}=-\frac{1}{2}E_{14}=E_{15}=\frac{1}{4}E_{18}=\frac{1}{2}E_{20}=\frac{1}{4}E_{24}=F_{41}H_2\\
\frac{1}{2}D_1 &= -\frac{1}{4}D_5=F_1H_2^2\\
D_2 &= -2F_{41}H_2\left(H_1+H_2\right)\\
D_3 &= 2F_{41}H_1H_2\\
D_4 &= D_8=D_{11}=D_{12}=D_{13}=0\\
D_6 &= 2H_2\left(F_{41}H_1+F_{41}H_2-F_1H_2\right)\\
D_7 &= 2F_{41}H_2\left(H_1-H_2\right)\\
2D_9 &= D_{10}=4F_{41}H_2\left(H_1+\frac{1}{2}H_2\right)\\
D_{14} &= 4F_{41}H_2\left(H_1-\frac{1}{2}H_2\right).
\end{aligned} \tag{A.57}$$

The following evolution equations are also found:

$$\dot{F}_{41} = 0 \tag{A.58}$$

$$\dot{H}_1 = -(H_1 - H_2)(H_1 + H_2) \tag{A.59}$$

$$\dot{H}_2 = (H_1 - H_2) H_2. \tag{A.60}$$

eq. (A.58) requires that $F_{41}$ be a constant, which we relabel as $c_1$. We also relabel $F_1 = \frac{1}{8}M^2$. Eqs (A.59) and (A.60) can be combined to find:

$$H_1 = \frac{c_2}{H_2} - \frac{1}{2}H_2, \tag{A.61}$$

where $c_2$ is a constant of integration.

### A.3.4 Gauge Invariant Action

The final gauge invariant action for the anisotropic Bianchi-I background considered in Chapter 2 is given by:

$$S_G^{(2)} = \int d^4x\, a\, b^2\, M^2\, \mathscr{L}_B \tag{A.62}$$

with

$$\begin{aligned}
\mathscr{L}_B = & -\frac{1}{2}h_{\mu\nu}h^{\mu\nu}H_2^2 + \frac{1}{4}h^2H_2^2 - \frac{1}{2}h^{\nu\lambda}u^\mu\bar{\nabla}_\lambda h_{\mu\nu}H_2 + \frac{1}{4}hu^\mu\bar{\nabla}_\lambda h^\lambda_\mu H_2 \\
& + \left(\frac{4c_1}{M^2} - \frac{1}{4}\right)hu^\mu x^\nu x^\lambda\bar{\nabla}_\lambda h_{\mu\nu}H_2 + \frac{4c_1 h^\sigma_\mu u^\mu x^\nu x^\lambda\bar{\nabla}_\lambda h_{\nu\sigma}H_2}{M^2} \\
& + \frac{1}{2}h^\sigma_\nu u^\mu x^\nu x^\lambda\bar{\nabla}_\lambda h_{\mu\sigma}H_2 - \frac{1}{2}h^\sigma_\mu u^\mu u^\nu u^\lambda\bar{\nabla}_\lambda h_{\nu\sigma}H_2 \\
& + \left(\frac{1}{2} - \frac{2c_1}{M^2}\right)\left[h_{\mu\sigma}u^\mu u^\nu u^\lambda x^\sigma x^\alpha\bar{\nabla}_\lambda h_{\nu\alpha}H_2 h^\sigma_\nu u^\mu x^\nu x^\lambda\bar{\nabla}_\sigma h_{\mu\lambda}H_2\right] \\
& - \frac{1}{4}h_{\nu\lambda}u^\mu x^\nu x^\lambda\bar{\nabla}_\sigma h^\sigma_\mu H_2 + \left(\frac{c_1}{M^2} - \frac{1}{2}\right)h^\sigma_\mu u^\mu u^\nu u^\lambda\bar{\nabla}_\sigma h_{\nu\lambda}H_2 \\
& + \frac{c_1 h^\sigma_\mu u^\mu x^\nu x^\lambda\bar{\nabla}_\sigma h_{\nu\lambda}H_2}{M^2} + \left(\frac{1}{2} - \frac{c_1}{M^2}\right)h_{\mu\sigma}u^\mu u^\nu u^\lambda x^\sigma x^\alpha\bar{\nabla}_\alpha h_{\nu\lambda}H_2 \\
& + \left(-\frac{2c_1}{M^2} - \frac{1}{4}\right)h_{\nu\lambda}u^\mu x^\nu x^\lambda x^\sigma x^\alpha\bar{\nabla}_\alpha h_{\mu\sigma}H_2 + \frac{1}{4}h_{\mu\nu}u^\mu u^\nu u^\lambda\bar{\nabla}_\sigma h^\sigma_\lambda H_2 \\
& + \left(\frac{12c_1}{M^2} - \frac{1}{4}\right)h_{\mu\nu}u^\mu u^\nu u^\lambda x^\sigma x^\alpha\bar{\nabla}_\alpha h_{\lambda\sigma}H_2 - \frac{5c_1 h_{\mu\nu}u^\mu x^\nu x^\lambda x^\sigma x^\alpha\bar{\nabla}_\alpha h_{\lambda\sigma}H_2}{M^2} \\
& + \left(\left(\frac{c_1}{M^2} - \frac{3}{2}\right)H_2^2 + \frac{2c_2c_1}{M^2}\right)h^\lambda_\mu h_{\nu\lambda}u^\mu u^\nu + \frac{\left(H_2^2\left(M^2 - 2c_1\right) - 4c_2c_1\right)h_{\mu\nu}hu^\mu u^\nu}{2M^2}
\end{aligned}$$

$$
+\left(\frac{2c_2c_1}{M^2}-\frac{3H_2^2}{4}\right)h_{\mu\nu}h_{\lambda\sigma}u^\mu u^\nu u^\lambda u^\sigma+\frac{\left(\left(M^2-3c_1\right)H_2^2+2c_2c_1\right)h_\mu^\lambda h_{\nu\lambda}x^\mu x^\nu}{M^2}
$$

$$
+\frac{\left(4c_2c_1-H_2^2\left(M^2+2c_1\right)\right)h_{\mu\nu}hx^\mu x^\nu}{2M^2}+\left(\frac{8c_2c_1}{M^2}-\frac{H_2^2}{2}\right)h_{\mu\nu}h_{\lambda\sigma}u^\mu u^\nu x^\lambda x^\sigma
$$

$$
+\left(\left(\frac{3}{2}-\frac{8c_1}{M^2}\right)H_2^2+\frac{4c_2c_1}{M^2}\right)h_{\mu\lambda}h_{\nu\sigma}u^\mu u^\nu x^\lambda x^\sigma
$$

$$
+\left(H_2^2\left(\frac{4c_1}{M^2}-\frac{1}{4}\right)-\frac{4c_2c_1}{M^2}\right)h_{\mu\nu}h_{\lambda\sigma}x^\mu x^\nu x^\lambda x^\sigma+\frac{1}{8}\bar{\nabla}_\nu h\bar{\nabla}^\nu h
$$

$$
+\left(-\frac{c_1}{2M^2}-\frac{1}{8}\right)u^\mu u^\nu\bar{\nabla}_\mu h^{\lambda\sigma}\bar{\nabla}_\nu h_{\lambda\sigma}+\left(\frac{c_1}{2M^2}+\frac{1}{8}\right)x^\mu x^\nu\bar{\nabla}_\mu h^{\lambda\sigma}\bar{\nabla}_\nu h_{\lambda\sigma}
$$

$$
+\left(\frac{c_1}{M^2}+\frac{1}{4}\right)u^\mu u^\nu x^\lambda x^\sigma\bar{\nabla}_\mu h_\lambda^\alpha\bar{\nabla}_\nu h_{\sigma\alpha}+\left(\frac{c_1}{2M^2}+\frac{1}{8}\right)u^\mu u^\nu\bar{\nabla}_\mu h\bar{\nabla}_\nu h
$$

$$
+\left(-\frac{c_1}{2M^2}-\frac{1}{8}\right)x^\mu x^\nu\bar{\nabla}_\mu h\bar{\nabla}_\nu h+\left(-\frac{c_1}{M^2}-\frac{1}{4}\right)u^\mu u^\nu x^\lambda x^\sigma\bar{\nabla}_\mu h_{\lambda\sigma}\bar{\nabla}_\nu h
$$

$$
+\left(H_2\left(\frac{1}{4}-\frac{c_1}{2M^2}\right)-\frac{c_2c_1}{H_2M^2}\right)hu^\mu u^\nu u^\lambda\bar{\nabla}_\lambda h_{\mu\nu}
$$

$$
+\left(\frac{c_2c_1}{H_2M^2}+H_2\left(\frac{5c_1}{2M^2}-\frac{1}{4}\right)\right)h_{\sigma\alpha}u^\mu u^\nu u^\lambda x^\sigma x^\alpha\bar{\nabla}_\lambda h_{\mu\nu}
$$

$$
-\frac{1}{4}u^\mu u^\nu\bar{\nabla}_\nu h\bar{\nabla}_\lambda h_\mu^\lambda+\frac{1}{4}x^\mu x^\nu\bar{\nabla}_\nu h\bar{\nabla}_\lambda h_\mu^\lambda+\frac{1}{4}\bar{\nabla}_\mu h^{\mu\nu}\bar{\nabla}_\lambda h_\nu^\lambda-\frac{1}{4}\bar{\nabla}^\nu h\bar{\nabla}_\lambda h_\nu^\lambda
$$

$$
-\left(\frac{2c_1}{M^2}+\frac{1}{4}\right)\left[u^\mu u^\nu\bar{\nabla}_\nu h_\mu^\lambda\bar{\nabla}_\lambda h-x^\mu x^\nu\bar{\nabla}_\nu h_\mu^\lambda\bar{\nabla}_\lambda h\right]
$$

$$
+\left(\frac{c_1}{M^2}+\frac{1}{4}\right)\left[u^\mu u^\nu\bar{\nabla}_\lambda h\bar{\nabla}^\lambda h_{\mu\nu}-x^\mu x^\nu\bar{\nabla}_\lambda h\bar{\nabla}^\lambda h_{\mu\nu}\right]
$$

$$
-\frac{1}{8}\bar{\nabla}_\lambda h_{\mu\nu}\bar{\nabla}^\lambda h^{\mu\nu}+\left(\frac{c_1}{M^2}-\frac{1}{4}\right)u^\mu u^\nu x^\lambda x^\sigma x^\alpha x^\beta\bar{\nabla}_\nu h_{\alpha\beta}\bar{\nabla}_\sigma h_{\mu\lambda}
$$

$$
+\left(\frac{2c_1}{M^2}+\frac{1}{4}\right)u^\mu u^\nu x^\lambda x^\sigma\bar{\nabla}_\nu h\bar{\nabla}_\sigma h_{\mu\lambda}+\left(-\frac{c_1}{M^2}-\frac{1}{4}\right)u^\mu u^\nu\bar{\nabla}^\lambda h_{\mu\nu}\bar{\nabla}_\sigma h_\lambda^\sigma
$$

$$
+\frac{1}{4}u^\mu u^\nu\bar{\nabla}_\lambda h_\mu^\lambda\bar{\nabla}_\sigma h_\nu^\sigma-\frac{1}{4}x^\mu x^\nu\bar{\nabla}_\lambda h_\mu^\lambda\bar{\nabla}_\sigma h_\nu^\sigma+\left(\frac{c_1}{M^2}+\frac{1}{4}\right)u^\mu u^\nu x^\lambda x^\sigma\bar{\nabla}_\lambda h_\mu^\alpha\bar{\nabla}_\sigma h_{\nu\alpha}
$$

$$
+\left(\frac{2c_1}{M^2}+\frac{1}{2}\right)u^\mu u^\nu\bar{\nabla}_\nu h_\mu^\lambda\bar{\nabla}_\sigma h_\lambda^\sigma+\left(-\frac{2c_1}{M^2}-\frac{1}{2}\right)x^\mu x^\nu\bar{\nabla}_\nu h_\mu^\lambda\bar{\nabla}_\sigma h_\lambda^\sigma
$$

$$
+\left(\frac{c_1}{M^2}+\frac{1}{4}\right)x^\mu x^\nu\bar{\nabla}^\lambda h_{\mu\nu}\bar{\nabla}_\sigma h_\lambda^\sigma+\left(-\frac{2c_1}{M^2}-\frac{1}{2}\right)u^\mu u^\nu x^\lambda x^\sigma\bar{\nabla}_\nu h_\mu^\alpha\bar{\nabla}_\sigma h_{\lambda\alpha}
$$

$$
+\frac{1}{4}u^\mu u^\nu x^\lambda x^\sigma\bar{\nabla}_\nu h_{\mu\lambda}\bar{\nabla}_\sigma h-\frac{c_1x^\mu x^\nu\bar{\nabla}_\lambda h_{\nu\sigma}\bar{\nabla}^\sigma h_\mu^\lambda}{M^2}
$$

$$
-\left(\frac{c_1}{M^2}+\frac{1}{4}\right)u^\mu u^\nu x^\lambda x^\sigma\bar{\nabla}_\lambda h_{\mu\nu}\bar{\nabla}_\sigma h+\frac{c_1u^\mu u^\nu\bar{\nabla}_\lambda h_{\nu\sigma}\bar{\nabla}^\sigma h_\mu^\lambda}{M^2}
$$

$$
-\left(\frac{c_1}{M^2}+\frac{1}{4}\right)\left[u^\mu u^\nu\bar{\nabla}_\sigma h_{\nu\lambda}\bar{\nabla}^\sigma h_\mu^\lambda-x^\mu x^\nu\bar{\nabla}_\sigma h_{\nu\lambda}\bar{\nabla}^\sigma h_\mu^\lambda\right]
$$

$$
\begin{aligned}
&+\left(\frac{1}{4}-\frac{3c_1}{M^2}\right)u^\mu u^\nu u^\lambda u^\sigma x^\alpha x^\beta \bar{\nabla}_\sigma h_{\lambda\beta}\bar{\nabla}_\alpha h_{\mu\nu}+\left(\frac{1}{4}-\frac{c_1}{M^2}\right)u^\mu u^\nu x^\lambda x^\sigma \bar{\nabla}_\nu h_{\lambda\sigma}\bar{\nabla}_\alpha h^\alpha_\mu\\
&-\frac{1}{2}u^\mu u^\nu x^\lambda x^\sigma \bar{\nabla}_\sigma h_{\mu\lambda}\bar{\nabla}_\alpha h^\alpha_\nu+\left(H_2\left(\frac{c_1}{2M^2}-\frac{1}{4}\right)-\frac{c_1c_2}{H_2M^2}\right)h_{\mu\nu}u^\mu u^\nu u^\lambda u^\sigma u^\alpha \bar{\nabla}_\alpha h_{\lambda\sigma}\\
&+\left(\frac{3c_1}{M^2}+\frac{1}{4}\right)u^\mu u^\nu x^\lambda x^\sigma \bar{\nabla}_\nu h^\alpha_\mu \bar{\nabla}_\alpha h_{\lambda\sigma}-\frac{1}{2}u^\mu u^\nu x^\lambda x^\sigma \bar{\nabla}_\nu h_{\mu\lambda}\bar{\nabla}_\alpha h^\alpha_\sigma\\
&+\left(\frac{c_1}{M^2}+\frac{1}{4}\right)\left[u^\mu u^\nu u^\lambda u^\sigma \bar{\nabla}_\lambda h_{\mu\nu}\bar{\nabla}_\alpha h^\alpha_\sigma u^\mu u^\nu x^\lambda x^\sigma \bar{\nabla}_\alpha h_{\nu\sigma}\bar{\nabla}^\alpha h_{\mu\lambda}\right]\\
&+\left(\frac{1}{4}-\frac{c_1}{M^2}\right)u^\mu u^\nu x^\lambda x^\sigma \bar{\nabla}_\lambda h_{\mu\nu}\bar{\nabla}_\alpha h^\alpha_\sigma+\left(\frac{c_1}{M^2}+\frac{1}{4}\right)x^\mu x^\nu x^\lambda x^\sigma \bar{\nabla}_\lambda h_{\mu\nu}\bar{\nabla}_\alpha h^\alpha_\sigma\\
&+\left(-\frac{c_1}{M^2}-\frac{1}{4}\right)u^\mu u^\nu u^\lambda u^\sigma \bar{\nabla}_\sigma h_{\lambda\alpha}\bar{\nabla}h_{\mu\nu}+\left(\frac{3c_1}{M^2}+\frac{1}{4}\right)u^\mu u^\nu x^\lambda x^\sigma \bar{\nabla}_\sigma h_{\lambda\alpha}\bar{\nabla}^\alpha h_{\mu\nu}\\
&-\left(\frac{c_1}{M^2}+\frac{1}{4}\right)\left[x^\mu x^\nu x^\lambda x^\sigma \bar{\nabla}_\sigma h_{\lambda\alpha}\bar{\nabla}^\alpha h_{\mu\nu}+u^\mu u^\nu x^\lambda x^\sigma \bar{\nabla}_\alpha h_{\lambda\sigma}\bar{\nabla}^\alpha h_{\mu\nu}\right]\\
&-\frac{2c_1}{M^2}\left[u^\mu u^\nu x^\lambda x^\sigma \bar{\nabla}_\nu h_{\sigma\alpha}\bar{\nabla}^\alpha h_{\mu\lambda}+u^\mu u^\nu x^\lambda x^\sigma \bar{\nabla}_\sigma h_{\nu\alpha}\bar{\nabla}^\alpha h_{\mu\lambda}\right]\\
&+\left(\frac{1}{4}-\frac{c_1}{M^2}\right)u^\mu u^\nu x^\lambda x^\sigma x^\alpha x^\beta \bar{\nabla}_\nu h_{\mu\lambda}\bar{\nabla}_\beta h_{\sigma\alpha}\\
&+\left(\frac{3c_1}{M^2}-\frac{1}{4}\right)u^\mu u^\nu u^\lambda u^\sigma x^\alpha x^\beta \bar{\nabla}_\lambda h_{\mu\nu}\bar{\nabla}_\beta h_{\sigma\alpha}\\
&-\frac{c_1\left(H_2^2+2c_2\right)}{2M^2H_2}\left[h\,u^\mu x^\nu x^\lambda \bar{\nabla}_\mu h_{\nu\lambda}-h_{\nu\lambda}u^\mu x^\nu x^\lambda x^\sigma x^\alpha \bar{\nabla}_\mu h_{\sigma\alpha}\right]\\
&+\frac{c_1\left(H_2^2-2c_2\right)}{2M^2H_2}h_{\mu\nu}u^\mu u^\nu u^\lambda x^\sigma x^\alpha \bar{\nabla}_\lambda h_{\sigma\alpha}. \qquad \text{(A.63)}
\end{aligned}
$$

# Appendix B

## B.1 Covariant quantities for the Schwarzschild background

For the Schwarzschild background, the background spacetime is not flat. Thus we need expressions for the Christoffel symbols and curvature tensors of the background *in terms of the background quantities* to properly evaluate the Noether constraints arising from the variation of (3.8). The relevant expressions can be shown to be:

$$\bar{\nabla}_\mu u_\nu = -\frac{(1-f)^2}{4m\sqrt{f}} u_\mu r_\nu, \tag{B.1}$$

$$\bar{\nabla}_\mu r_\nu = -\frac{(1-f)^2}{4m\sqrt{f}} u_\mu u_\nu + \frac{(1-f)\sqrt{f}}{2m}\gamma_{\mu\nu}, \tag{B.2}$$

$$\bar{\nabla}_\mu \gamma_{\alpha\beta} = u_\alpha \bar{\nabla}_\mu u_\beta + u_\beta \bar{\nabla}_\mu u_\alpha - r_\alpha \bar{\nabla} r_\beta - r_\beta \bar{\nabla} r_\alpha, \tag{B.3}$$

$$\begin{aligned}\bar{R}^\rho_{\sigma\mu\nu} =& \frac{(1-f)^3}{8m^2}\left(-2\left(u^\rho x_\sigma u_\mu x_\nu - x^\rho u_\sigma u_\mu x_\nu - u^\rho x_\sigma x_\mu u_\nu\right.\right.\\ &\left. + x^\rho u_\sigma x_\mu u_\nu\right) + \left(u^\rho u_\mu \gamma_{\sigma\nu} - \gamma^\rho_\nu u_\sigma u_\mu - u^\rho u_\nu \gamma_{\sigma\mu}\right.\\ &\left. + \gamma^\rho_\mu u_\sigma u_\nu\right) - \left(r^\rho r_\mu \gamma_{\sigma\nu} - \gamma^\rho_\nu r_\sigma r_\mu - r^\rho r_\nu \gamma_{\sigma\mu}\right.\\ &\left.\left. + \gamma^\rho_\mu r_\sigma r_\nu\right) + 2\left(\gamma^\rho_\mu \gamma_{\sigma\nu} - \gamma^\rho_\nu \gamma_{\sigma\mu}\right)\right)\end{aligned} \tag{B.4}$$

$$\bar{R}_{\mu\nu} = 0, \tag{B.5}$$

$$\bar{R} = 0, \tag{B.6}$$

where $f = 1 - \frac{2M}{r}$, $\bar{R}^\rho_{\sigma\mu\nu}$ is the background Riemann curvature tensor, $\bar{R}_{\mu\nu} = \bar{R}^\rho_{\mu\rho\nu}$ is the background Ricci tensor, and $\bar{R} = \bar{g}^{\mu\nu}\bar{R}_{\mu\nu}$ is the background Ricci scalar.

## B.2 Single-Tensor theories

The Noether constraints for the coefficients $A_i$, $B_i$ and $C_i$ are the following:

$$-C_2 = -\frac{1}{2}C_3 = \frac{1}{2}C_4 = C_1$$

$$
\begin{aligned}
2C_5 =& -2C_6 = C_7 = -C_8 = -C_{11} = C_{12} = -\frac{1}{2}C_{13} = \frac{1}{2}C_{14} = -2C_{18} \\
&= 2C_{19} = -C_{20} = C_{41}, \\
C_{21} =& C_{24} = -C_{25} = \frac{1}{2}C_{26} = -\frac{1}{2}C_{27} = C_{42} = -\frac{1}{2}C_{43} = C_{44} = -C_{45} = -\frac{1}{2}C_{46} \\
&= -\frac{1}{2}C_{47} = \frac{1}{2}C_{48} = \frac{1}{2}C_{49} = -C_{50} = C_{41}, \\
-C_{51} =& \frac{1}{2}C_{52} = C_{41} \\
B_{19} =& -\frac{1}{2}B_{23} = 2B_{12} = -B_{13} = B_{16} = -\frac{1}{2}B_{17} = -\frac{C_{41}}{m}\sqrt{f}(f-1) \\
B_4 =& -\frac{1}{2}B_2 - \frac{-2C_1}{m}\sqrt{f}(f-1) \\
B_6 =& B_{10} = \frac{C_{41}}{4M\sqrt{f}}(f-1)(3f-1) \\
A_1 =& -A_5 = -\frac{C_1}{4M^2}(f-1)^2(2f-1) \\
A_2 =& A_3 = \frac{C_{41}}{4M^2}(f-1)^3 \\
A_6 =& -\frac{C_{41}}{4M^2}(f-1)^2 f, \\
A_7 =& \frac{(f-1)^2}{4M^2}(-4C_1 + C_{41}(3f-2)) \\
A_{12} =& -\frac{C_{41}}{4M^2}(f-1)^2 \\
A_{14} =& -\frac{C_{41}}{4M^2}(f-1)^2(2f-1),
\end{aligned}
\tag{B.7}
$$

with all other remaining coefficients vanishing. In addition, we find that $C_{41}$ must be a constant.

## B.3 Scalar-Tensor theories

### B.3.1 Noether Constraints

The Noether constraints for the $A_{\chi n}$, $B_{\chi n}$, $C_{\chi n}$, and $D_{\chi n}$ are given by:

$$
\begin{aligned}
A_{\chi 1} =& -\frac{1}{4M^2}\left(2D_{\chi 5}(f-1)^2 - 2D_{\chi 8}(f-1)^2 + M\left(4f\left(\frac{dD_{\chi 5}}{dr} + \frac{d^2D_{\chi 15}}{dr^2}M\right.\right.\right. \\
&\left.\left.\left. + \frac{dD_{\chi 8}}{dr}(f-1) - \frac{dD_{\chi 5}}{dr}f\right) + \frac{dD_{\chi 15}}{dr}\left(1+2f-3f^2\right)\right)\right) \\
A_{\chi 2} =& -\frac{1}{4M}\left(\frac{dD_{\chi 15}}{dr}(f-1)^2 + 4\left(\frac{dD_{\chi 8}}{dr}(1-f) + \frac{d^2D_{\chi 8}}{dr^2}Mf\right) + \frac{dD_{\chi 5}}{dr}\left(f^2-1\right)\right)
\end{aligned}
$$

$$
\begin{aligned}
A_{\chi 3} &= \frac{1}{4M^2}(f-1)\left(2D_{\chi 5}(f-1)-2D_{\chi 8}(f-1)+M\left(\frac{dD_{\chi 15}}{dr}(f-1)+4\frac{dD_{\chi 8}}{dr}f\right)\right)\\
B_{\chi 2} &= \frac{1}{4M\sqrt{f}}\left(D_{\chi 11}\left(-1-2f+3f^2\right)-4\frac{dD_{\chi 11}}{dr}Mf\right)\\
B_{\chi 3} &= \frac{1}{2M\sqrt{f}}\left(D_{\chi 11}(1-f)+2\frac{dD_{\chi 11}}{dr}Mf\right)\\
B_{\chi 4} &= \frac{1}{4M\sqrt{f}}\left(D_{\chi 15}(f-1)^2+4D_{\chi 8}f(f-1)\right)\\
B_{\chi 5} &= \frac{1}{4M\sqrt{f}}\left(-D_{\chi 15}-2D_{\chi 8}(f-1)^2-4\frac{dD_{\chi 8}}{dr}Mf+D_{\chi 15}f(2-f)-D_{\chi 5}\left(f^2-1\right)\right)\\
B_{\chi 6} &= \frac{\sqrt{f}}{2M}D_{\chi 5}(f-1)\\
B_{\chi 7} &= \frac{1}{4M\sqrt{f}}\left(D_{\chi 15}(f-1)^2-4f\left(\frac{dD_{\chi 15}}{dr}M-D_{\chi 5}(f-1)+D_{\chi 8}(f-1)\right)\right)\\
B_{\chi 9} &= -\frac{2\sqrt{f}(f-1)}{M}\left(D_{\chi 5}-D_{\chi 8}-D_{\chi 15}\right)\\
B_{\chi 10} &= -\frac{\sqrt{f}(f-1)}{M}D_{\chi 11}\\
D_{\chi 2} &= D_{\chi 3} = -\frac{1}{2}D_{\chi 4} = -D_{\chi 5}+D_{\chi 8}+D_{\chi 15}\\
D_{\chi 6} &= -D_{\chi 5}\\
D_{\chi 9} &= -\frac{1}{2}D_{\chi 10} = D_{\chi 8}\\
D_{\chi 12} &= D_{\chi 13} = -D_{\chi 14} = -D_{\chi 11}\\
-\frac{1}{2}D_{\chi 16} &= D_{\chi 17} = D_{\chi 15},
\end{aligned}
\tag{B.8}
$$

with all other remaining coefficients vanishing. We also mention that $C_1$ is left unconstrained but does not appear in the final action.

## B.4 Vector-Tensor theories

### B.4.1 Noether Constraints

The Noether constraints for the $A_{\zeta n}$, $B_{\zeta n}$, $C_{\zeta n}$, and $D_{\zeta n}$ are given by

$$
\begin{aligned}
A_{\zeta 5} = -\frac{1}{4M^2}\Bigg(M\Bigg(&4\left(\frac{d^2D_{\zeta 2}}{dr^2}\right)fM-4\left(\frac{d^2D_{\zeta 38}}{dr^2}\right)fM+4\left(\frac{d^2D_{\zeta 7}}{dr^2}\right)fM\\
&-3\left(\frac{dD_{\zeta 2}}{dr}\right)f^2+2\left(\frac{dD_{\zeta 2}}{dr}\right)f+\left(\frac{dD_{\zeta 2}}{dr}\right)+7\left(\frac{dD_{\zeta 38}}{dr}\right)f^2-6\left(\frac{dD_{\zeta 38}}{dr}\right)f\\
&-\left(\frac{dD_{\zeta 38}}{dr}\right)-7\left(\frac{dD_{\zeta 7}}{dr}\right)f^2+6\left(\frac{dD_{\zeta 7}}{dr}\right)f+\left(\frac{dD_{\zeta 7}}{dr}\right)\Bigg)
\end{aligned}
$$

$$
\begin{aligned}
&+2(f-1)^2 D_{\zeta 7} - 2(f-1)^2 D_{\zeta 38}\Big) \\
A_{\zeta 6} = &\frac{1}{16fM^2}\left(-4fM\left(4\left(\frac{d^2 D_{\zeta 38}}{dr^2}\right)fM + \left(\frac{dD_{\zeta 2}}{dr}\right)(f-1)^2\right.\right. \\
&-\left(\frac{dD_{\zeta 38}}{dr}\right)\left(f^2+2f-3\right) - \left(\frac{dD_{\zeta 60}}{dr}\right)f^2 + 2\left(\frac{dD_{\zeta 60}}{dr}\right)f \\
&\left.-\left(\frac{dD_{\zeta 60}}{dr}\right) + 2\left(\frac{dD_{\zeta 7}}{dr}\right)f^2 - 2\left(\frac{dD_{\zeta 7}}{dr}\right)f\right) + (f-1)^4(-D_{\zeta 2}) \\
&+(3f-1)(f-1)^3 D_{\zeta 60}\Big) \\
A_{\zeta 7} = &-\frac{1}{16fM^2}\left(-4f\left(2M\left(f\left(2\left(\frac{d^2 D_{\zeta 11}}{dr^2}\right)M + \left(\frac{dD_{\zeta 60}}{dr}\right)(f-1)\right)\right.\right.\right. \\
&\left.\left.-\left(\frac{dD_{\zeta 11}}{dr}\right)f^2 + \left(\frac{dD_{\zeta 11}}{dr}\right)\right) + (f-1)^3 D_{\zeta 60}\right) + 4f(f-1)^3 D_{\zeta 2} \\
&+(9f-1)(f-1)^3 D_{\zeta 11}\Big) \\
A_{\zeta 8} = &\frac{(f-1)}{16fM^2}\left(\left(12\left(\frac{dD_{\zeta 15}}{dr}\right)f^2 M + 4\left(\frac{dD_{\zeta 15}}{dr}\right)fM + 4\left(\frac{dD_{\zeta 19}}{dr}\right)f^2 M\right.\right. \\
&-4\left(\frac{dD_{\zeta 19}}{dr}\right)fM + 4\left(\frac{dD_{\zeta 26}}{dr}\right)f^2 M - 4\left(\frac{dD_{\zeta 26}}{dr}\right)fM + 4\left(\frac{dD_{\zeta 27}}{dr}\right)f^2 M \\
&-4\left(\frac{dD_{\zeta 27}}{dr}\right)fM - 4f^3 D_{\zeta 21} - f^3 D_{\zeta 26} - f^3 D_{\zeta 27} + 3f^2 D_{\zeta 26} \\
&+3f^2 D_{\zeta 27} + 4fD_{\zeta 21} - 3fD_{\zeta 26} - 3fD_{\zeta 27} \\
&-\left(f^3 - 11f^2 + 11f - 1\right)D_{\zeta 19} \\
&\left.+(f-1)^2(9f-1)D_{\zeta 15} + D_{\zeta 26} + D_{\zeta 27}\right)\Big) \\
A_{\zeta 9} = &-\frac{1}{16fM^2}\left(16\left(\frac{d^2 D_{\zeta 15}}{dr^2}\right)f^2 M^2 - 4\left(\frac{dD_{\zeta 15}}{dr}\right)f^3 M - 8\left(\frac{dD_{\zeta 15}}{dr}\right)f^2 M\right. \\
&+12\left(\frac{dD_{\zeta 15}}{dr}\right)fM + 8\left(\frac{dD_{\zeta 19}}{dr}\right)f^3 M - 8\left(\frac{dD_{\zeta 19}}{dr}\right)f^2 M - 8\left(\frac{dD_{\zeta 21}}{dr}\right)f^3 M \\
&+8\left(\frac{dD_{\zeta 21}}{dr}\right)f^2 M + 4\left(\frac{dD_{\zeta 26}}{dr}\right)f^3 M - 8\left(\frac{dD_{\zeta 26}}{dr}\right)f^2 M + 4\left(\frac{dD_{\zeta 26}}{dr}\right)fM \\
&+4\left(\frac{dD_{\zeta 27}}{dr}\right)f^3 M - 8\left(\frac{dD_{\zeta 27}}{dr}\right)f^2 M + 4\left(\frac{dD_{\zeta 27}}{dr}\right)fM + f^4 D_{\zeta 26} + f^4 D_{\zeta 27} \\
&-4f^3 D_{\zeta 26} - 4f^3 D_{\zeta 27} - 4(f-1)^2 f^2 D_{\zeta 19} + 6f^2 D_{\zeta 26} + 6f^2 D_{\zeta 27} \\
&\left.+2(f-1)^2(f+1)fD_{\zeta 21} - 4fD_{\zeta 26} - 4fD_{\zeta 27} + D_{\zeta 26} + D_{\zeta 27}\right) \\
A_{\zeta 10} = &-\frac{(f-1)}{4M^2}\left(4\left(\frac{dD_{\zeta 15}}{dr}\right)fM + f^2 D_{\zeta 26} + f^2 D_{\zeta 27} + (f-1)^2 D_{\zeta 15} + 2f(f-1)D_{\zeta 19}\right. \\
&\left.-2fD_{\zeta 21} - 2fD_{\zeta 26} - 2fD_{\zeta 27} + 2D_{\zeta 21} + D_{\zeta 26} + D_{\zeta 27}\right)
\end{aligned}
$$

$$
\begin{aligned}
A_{\zeta 11} = & -\frac{(f-1)}{16fM^2}\left(-4\left(\frac{dD_{\zeta 2}}{dr}\right)f^2M+4\left(\frac{dD_{\zeta 2}}{dr}\right)fM-12\left(\frac{dD_{\zeta 38}}{dr}\right)f^2M\right.\\
& -4\left(\frac{dD_{\zeta 38}}{dr}\right)fM-4\left(\frac{dD_{\zeta 7}}{dr}\right)f^2M+4\left(\frac{dD_{\zeta 7}}{dr}\right)fM-4f^3D_{\zeta 11}-f^3D_{\zeta 38}\\
& +4f^3D_{\zeta 60}+8f^2D_{\zeta 11}+11f^2D_{\zeta 38}-8f^2D_{\zeta 60}+\left(f^3-11f^2+11f-1\right)D_{\zeta 7}\\
& \left.+(f-1)^3D_{\zeta 2}-4fD_{\zeta 11}-11fD_{\zeta 38}+4fD_{\zeta 60}+D_{\zeta 38}\right)\\
A_{\zeta 12} = & \frac{1}{4M^2}\left(4\left(\frac{d^2D_{\zeta 15}}{dr^2}\right)fM^2-4\left(\frac{d^2D_{\zeta 19}}{dr^2}\right)fM^2-4\left(\frac{d^2D_{\zeta 26}}{dr^2}\right)fM^2\right.\\
& -4\left(\frac{d^2D_{\zeta 27}}{dr^2}\right)fM^2-7\left(\frac{dD_{\zeta 15}}{dr}\right)f^2M+6\left(\frac{dD_{\zeta 15}}{dr}\right)fM+\left(\frac{dD_{\zeta 15}}{dr}\right)M\\
& +7\left(\frac{dD_{\zeta 19}}{dr}\right)f^2M-6\left(\frac{dD_{\zeta 19}}{dr}\right)fM-\left(\frac{dD_{\zeta 19}}{dr}\right)M-4\left(\frac{dD_{\zeta 21}}{dr}\right)f^2M\\
& +4\left(\frac{dD_{\zeta 21}}{dr}\right)fM+3\left(\frac{dD_{\zeta 26}}{dr}\right)f^2M-2\left(\frac{dD_{\zeta 26}}{dr}\right)fM-\left(\frac{dD_{\zeta 26}}{dr}\right)M\\
& +3\left(\frac{dD_{\zeta 27}}{dr}\right)f^2M-2\left(\frac{dD_{\zeta 27}}{dr}\right)fM-\left(\frac{dD_{\zeta 27}}{dr}\right)M+3f^3D_{\zeta 21}+2f^3D_{\zeta 26}\\
& +2f^3D_{\zeta 27}-5f^2D_{\zeta 21}-4f^2D_{\zeta 26}-4f^2D_{\zeta 27}+fD_{\zeta 21}+2fD_{\zeta 26}+2fD_{\zeta 27}\\
& \left.+2(f-1)^2D_{\zeta 15}-2(f-1)^2D_{\zeta 19}+D_{\zeta 21}\right),\\
A_{\zeta 13} = & -\frac{(f-1)^2}{8fM^2}\left(4\left(\frac{dD_{\zeta 15}}{dr}\right)fM-4\left(\frac{dD_{\zeta 19}}{dr}\right)fM-4\left(\frac{dD_{\zeta 26}}{dr}\right)fM\right.\\
& -4\left(\frac{dD_{\zeta 27}}{dr}\right)fM-2f^2D_{\zeta 21}-3f^2D_{\zeta 26}-3f^2D_{\zeta 27}-(f-1)^2D_{\zeta 15}\\
& \left.+(f-1)^2D_{\zeta 19}+2fD_{\zeta 21}+2fD_{\zeta 26}+2fD_{\zeta 27}+D_{\zeta 26}+D_{\zeta 27}\right)\\
A_{\zeta 14} = & -\frac{(f-1)}{8fM^2}\left(8\left(\frac{dD_{\zeta 11}}{dr}\right)f^2M-4\left(\frac{dD_{\zeta 2}}{dr}\right)f^2M+4\left(\frac{dD_{\zeta 2}}{dr}\right)fM\right.\\
& +4\left(\frac{dD_{\zeta 38}}{dr}\right)f^2M-4\left(\frac{dD_{\zeta 38}}{dr}\right)fM-4\left(\frac{dD_{\zeta 7}}{dr}\right)f^2M+4\left(\frac{dD_{\zeta 7}}{dr}\right)fM\\
& -4f^3D_{\zeta 11}-5f^3D_{\zeta 38}+4f^3D_{\zeta 60}+4f^2D_{\zeta 11}+11f^2D_{\zeta 38}-4f^2D_{\zeta 60}\\
& \left.+(f-1)^3D_{\zeta 2}+(5f-1)(f-1)^2D_{\zeta 7}-7fD_{\zeta 38}+D_{\zeta 38}\right)\\
B_{\zeta 2} = & -\frac{(D_{\zeta 21}+D_{\zeta 26}+D_{\zeta 27})\sqrt{f}}{r}\\
B_{\zeta 3} = & -\frac{1}{2}B_{\zeta 4} = -\frac{M(D_{\zeta 26}+D_{\zeta 27})}{r^2\sqrt{f}}\\
B_{\zeta 5} = & \frac{D_{\zeta 21}\sqrt{f}}{r}\\
B_{\zeta 6} = & \frac{\left(\frac{dD_{\zeta 21}}{dr}\right)r^2f-D_{\zeta 19}rf+D_{\zeta 21}(r-M)}{r^2\sqrt{f}}
\end{aligned}
$$

$$B_{\zeta 7} = \frac{\left(-\frac{dD_{\zeta 21}}{dr}\right) r^2 f + D_{\zeta 19} r f + D_{\zeta 21}(M-r)}{r^2\sqrt{f}}$$

$$B_{\zeta 8} = \frac{D_{\zeta 15}(2r-5M) + m(D_{\zeta 19} + D_{\zeta 26} + D_{\zeta 27})}{r^2\sqrt{f}}$$

$$B_{\zeta 9} = \frac{(D_{\zeta 21} - D_{\zeta 15})\sqrt{f}}{r}$$

$$B_{\zeta 10} = \frac{2\left(\frac{dD_{\zeta 15}}{dr}\right) Mr - \left(\frac{dD_{\zeta 15}}{dr}\right) r^2 + D_{\zeta 15}(3M-2r) + D_{\zeta 19} f r - MD_{\zeta 26} - MD_{\zeta 27}}{r^2\sqrt{f}}$$

$$B_{\zeta 11} = \frac{2(\left(\frac{dD_{\zeta 15}}{dr}\right) r^2 f + MD_{\zeta 26} + MD_{\zeta 27}) - 2D_{\zeta 15}(M-r) - D_{\zeta 19} r f}{r^2\sqrt{f}}$$

$$B_{\zeta 12} = -\frac{D_{\zeta 21}\sqrt{f}}{r}$$

$$\begin{aligned} B_{\zeta 13} = & \frac{1}{r^2\sqrt{f}}\left(-2\left(\frac{dD_{\zeta 15}}{dr}\right) Mr + \left(\frac{dD_{\zeta 15}}{dr}\right) r^2 + 2\left(\frac{dD_{\zeta 19}}{dr}\right) Mr \right. \\ & - \left(\frac{dD_{\zeta 19}}{dr}\right) r^2 + 2\left(\frac{dD_{\zeta 26}}{dr}\right) Mr - \left(\frac{dD_{\zeta 26}}{dr}\right) r^2 + 2\left(\frac{dD_{\zeta 27}}{dr}\right) Mr \\ & - \left(\frac{dD_{\zeta 27}}{dr}\right) r^2 + D_{\zeta 15}(2r-5M) + D_{\zeta 19}(5M-2r) - 4MD_{\zeta 21} \\ & \left. + MD_{\zeta 26} + MD_{\zeta 27} + 2rD_{\zeta 21}\right) \end{aligned}$$

$$B_{\zeta 14} = -\frac{1}{2} B_{\zeta 19} = \frac{M(D_{\zeta 15} - D_{\zeta 19} - D_{\zeta 26} - D_{\zeta 27})}{r^2\sqrt{f}}$$

$$\begin{aligned} B_{\zeta 16} = & \frac{1}{r^2\sqrt{f}}\left(2\left(\frac{dD_{\zeta 2}}{dr}\right) Mr - \left(\frac{dD_{\zeta 2}}{dr}\right) r^2 - 2\left(\frac{dD_{\zeta 38}}{dr}\right) Mr + \left(\frac{dD_{\zeta 38}}{dr}\right) r^2 \right. \\ & \left. + 2\left(\frac{dD_{\zeta 7}}{dr}\right) Mr - \left(\frac{dD_{\zeta 7}}{dr}\right) r^2 + D_{\zeta 7}(3M-2r) - MD_{\zeta 2} - 3MD_{\zeta 38} + 2rD_{\zeta 38}\right) \end{aligned}$$

$$B_{\zeta 17} = \frac{D_{\zeta 38}(2r-3M) - MD_{\zeta 2} - MD_{\zeta 7}}{r^2\sqrt{f}}$$

$$B_{\zeta 18} = \frac{-MD_{\zeta 2} - MD_{\zeta 7} + 4MD_{\zeta 11} + mD_{\zeta 38} - 2rD_{\zeta 11}}{r^2\sqrt{f}},$$

$$B_{\zeta 20} = \frac{2(D_{\zeta 11} - D_{\zeta 60})\sqrt{f}}{r}$$

$$B_{\zeta 21} = -\frac{2D_{\zeta 21}\sqrt{f}}{r},$$

$$B_{\zeta 22} = \frac{2\sqrt{f}(\left(\frac{dD_{\zeta 2}}{dr}\right) r - \left(\frac{dD_{\zeta 38}}{dr}\right) r + \left(\frac{dD_{\zeta 7}}{dr}\right) r + 2D_{\zeta 2} + 2D_{\zeta 7} - 2D_{\zeta 38})}{r}$$

$$B_{\zeta 23} = \frac{M(D_{\zeta 60} - D_{\zeta 2})}{r^2\sqrt{f}},$$

$$
\begin{aligned}
B_{\zeta 25} &= \frac{D_{\zeta 60}\sqrt{f}}{r} \\
B_{\zeta 26} &= \frac{2MD_{\zeta 2} - r(\left(\frac{dD_{\zeta 60}}{dr}\right) fr + D_{\zeta 60})}{r^2\sqrt{f}}, \\
B_{\zeta 27} &= \frac{-4\left(\frac{dD_{\zeta 38}}{dr}\right) Mr + 2\left(\frac{dD_{\zeta 38}}{dr}\right) r^2 - D_{\zeta 7} fr + 2MD_{\zeta 2} - 2MD_{\zeta 38} - MD_{\zeta 60} + 2rD_{\zeta 38}}{r^2\sqrt{f}}, \\
B_{\zeta 28} &= \left(\frac{dD_{\zeta 11}}{dr}\right)\sqrt{f} \\
B_{\zeta 29} &= \frac{D_{\zeta 11}(2r-5M)}{r^2\sqrt{f}} \\
D_{\zeta 3} &= -\frac{1}{2}D_{\zeta 4} = D_{\zeta 2} \\
D_{\zeta 8} &= -D_{\zeta 7} \\
D_{\zeta 9} &= -D_{\zeta 10} = -D_{\zeta 12} = D_{\zeta 11} \\
D_{\zeta 14} &= -\frac{1}{2}D_{\zeta 16} = D_{\zeta 15} \\
D_{\zeta 20} &= -D_{\zeta 19} \\
D_{\zeta 22} &= D_{\zeta 23} = -D_{\zeta 24} = -D_{\zeta 21} \\
D_{\zeta 25} &= D_{\zeta 38} \\
D_{\zeta 28} &= -D_{\zeta 60} \\
D_{\zeta 29} &= -D_{\zeta 32} = D_{\zeta 33} = -D_{\zeta 36} = -D_{\zeta 11} \\
D_{\zeta 30} &= -D_{\zeta 31} = -D_{\zeta 34} = D_{\zeta 35} = D_{\zeta 21} \\
D_{\zeta 37} &= D_{\zeta 26} + D_{\zeta 27} \\
D_{\zeta 40} &= -D_{\zeta 56} = -D_{\zeta 60} \\
D_{\zeta 41} &= -\frac{1}{2}D_{\zeta 54} = -(D_{\zeta 15} - D_{\zeta 19} - D_{\zeta 26} - D_{\zeta 27}) \\
D_{\zeta 47} &= -\frac{1}{2}D_{\zeta 51} = D_{\zeta 2} + D_{\zeta 7} - D_{\zeta 38} \\
D_{\zeta 55} &= -2D_{\zeta 38} \\
D_{\zeta 59} &= -2(D_{\zeta 26} + D_{\zeta 27}) \\
D_{\zeta 61} &= D_{\zeta 2} + D_{\zeta 7} - D_{\zeta 38} \\
D_{\zeta 62} &= -D_{\zeta 15} + D_{\zeta 19} + D_{\zeta 26} + D_{\zeta 27},
\end{aligned}
\tag{B.9}
$$

where $f = 1 - 2M/r$ and with all other remaining coefficients vanishing.

### B.4.2 Odd Parity Perturbations: Relation between $h_0$ and other fields

In Section 3.4.1 the following relation is found between $h_0$, $h_1$, and $z_0$:

$$-i\omega h_0 = f\frac{d}{dr}\left[f\left(h_1+\frac{\left(2iMr\omega\frac{dD_{\zeta 11}}{dr}-(\ell+2)(\ell-1)D_{\zeta 21}\right)}{2C_{41}(\ell+2)(\ell-1)}z_0\right)\right] + i\omega\frac{\left(2M\left(\frac{d^2D_{\zeta 11}}{dr^2}f^2r^3-\frac{dD_{\zeta 11}}{dr}\left(4M^2-5Mr+r^2\right)\right)+(\ell+2)(\ell-1)r^2D_{\zeta 11}\right)}{2C_{41}(\ell+2)(\ell-1)r^2\sqrt{f}}z_0, \tag{B.10}$$

where $f = 1-2M/r$.

# Appendix C

## C.1 Polar Gravitational potential

The $O(a)$ correction to the potential for polar gravitational perturbations featured in eq. (5.17) is given by:

$$
\begin{aligned}
V_Z^{(1)}(r) = & \frac{F(r)^{-1}M}{729r^8\omega\ell(\ell+1)\left(6M+r\left(\ell^2+\ell-2\right)\right)^4} \\
& \times\Big(486\ell(\ell+1)\left(6M+\left(\ell^2+\ell-2\right)r\right)^4\left(\Lambda r^3+6M\right)\omega^2r^5 \\
& +9\Lambda\left(\Lambda r^3-3r+6M\right)\Big(\left(\ell^2+\ell-2\right)^3\left(5r^2\Lambda-3\right)\left(12\omega^2+\left(\ell^2+\ell+4\right)\Lambda\right)r^8 \\
& +6\left(\ell^2+\ell-2\right)^2M\left(3\ell^4+6\ell^3+\left(16\Lambda^2r^4-6\left(2\omega^2+5\Lambda\right)r^2-45\right)\ell^2\right. \\
& \left.+2\left(8\Lambda^2r^4-3\left(2\omega^2+5\Lambda\right)r^2-24\right)\ell\right. \\
& \left.+4\Big(3\Lambda^3r^6+\Lambda\left(54\omega^2+11\Lambda\right)r^4-6\left(5\omega^2+2\Lambda\right)r^2-6\Big)\right)r^5 \\
& -12\left(\ell^2+\ell-2\right)M^2\Big(6\ell^6+18\ell^5-72\ell^4-174\ell^3+3\left(-14\Lambda^2r^4\right. \\
& \left.+9\left(4\omega^2+5\Lambda\right)r^2-123\right)\ell^2+3\left(-14\Lambda^2r^4+9\left(4\omega^2+5\Lambda\right)r^2-93\right)\ell \\
& +4r^2\left(108\omega^2+\Lambda\left(81-2r^2\left(99\omega^2+\Lambda\left(13r^2\Lambda-6\right)\right)\right)\right)+708\Big)r^4 \\
& +72M^3\Big(6\ell^6+18\ell^5-381\ell^4-792\ell^3+\left(8\left(4\Lambda\left(\Lambda r^2+9\right)-9\omega^2\right)r^2+1179\right)\ell^2 \\
& +2\left(4\left(4\Lambda\left(\Lambda r^2+9\right)-9\omega^2\right)r^2+789\right)\ell \\
& +4\Big(20\Lambda^3r^6+\Lambda\left(81\omega^2-73\Lambda\right)r^4-9\left(5\omega^2+13\Lambda\right)r^2-402\Big)\Big)r^3 \\
& +432M^4\left(80\Lambda^2r^4-12(8\ell(\ell+1)-13)\Lambda r^2+3(\ell-1)(\ell+2)(37\ell(\ell+1)-144)\right)r^2 \\
& +31104M^5\left(-2\Lambda r^2+8\ell(\ell+1)-19\right)r+373248M^6\Big)r^3 \\
& -2\left(6M+\left(\ell^2+\ell-2\right)r\right)\Lambda\left(3M-r^3\Lambda\right)\left(\Lambda r^3-3r+6M\right)^3 \\
& \times\Big(-\left(\ell^2+\ell-2\right)^2\left(12\omega^2+\left(l^2+l+4\right)\Lambda\right)r^6 \\
& -3\left(\ell^2+\ell-2\right)M\left(l^4+2\ell^3+\left(4r^2\Lambda-15\right)\ell^2+4\left(r^2\Lambda-4\right)\ell\right. \\
& \left.+4\left(\Lambda^2r^4+3\left(5\omega^2+\Lambda\right)r^2-2\right)\right)r^3+6M^2\left(3\ell(\ell+1)\left(\ell^2+\ell-26\right)\right.
\end{aligned}
$$

$$
\begin{aligned}
&-4\left(5\Lambda^2 r^4-9\left(\Lambda-3\omega^2\right)r^2-36\right)\Big)r^2\\
&+432M^3\left(3\left(\ell^2+\ell-2\right)-2r^2\Lambda\right)r+2592M^4\Big)r-54\left(\Lambda r^3-3r+6M\right)\\
&\times\Big(\left(\ell^2+\ell-2\right)^3\Lambda\left(-3\left(\ell^2+\ell+2r^2\Lambda-6\right)\omega^2-\ell(\ell+1)\Lambda\left(l^2+l+r^2\Lambda-5\right)\right)\\
&\times r^{11}+\left(\ell^2+\ell-2\right)^2 M\Big(3\left(5r^2\Lambda-18\right)\ell^6+9\left(5r^2\Lambda-18\right)\ell^5\\
&-3\left(7\Lambda^2 r^4+2\left(\Lambda-6\omega^2\right)r^2+18\right)\ell^4\\
&+\left(-42\Lambda^2 r^4+\left(72\omega^2-87\Lambda\right)r^2+162\right)\ell^3-\Big(r^2\left(36\left(2\Lambda r^2+5\right)\omega^2\right.\\
&\left.+\Lambda\left(\Lambda\left(14r^2\Lambda-81\right)r^2+99\right)\right)-324\Big)\ell^2\\
&+2\left(\left(\Lambda\left(r^2\Lambda\left(51-7r^2\Lambda\right)-24\right)-36\left(\Lambda r^2+3\right)\omega^2\right)r^2+108\right)l\\
&+4r^2\left(9\left(8-3r^2\Lambda\left(r^2\Lambda-4\right)\right)\omega^2+2\Lambda\left(\Lambda\left(r^2\Lambda-3\right)r^2+9\right)\right)-432\Big)r^6\\
&+6\left(\ell^2+\ell-2\right)M^2\Big(21l^8+84l^7+3\left(9r^2\Lambda-10\right)\ell^6+\left(81r^2\Lambda-384\right)\ell^5\\
&+\left(9r^2\left(-4r^2\Lambda^2+\Lambda+16\omega^2\right)-303\right)\ell^4\\
&+3\left(44-3r^2\left(\Lambda\left(8\Lambda r^2+13\right)-32\omega^2\right)\right)\ell^3\\
&-6\left(r^2\left(4\left(8\Lambda r^2+21\right)\omega^2+\Lambda\left(r^2\Lambda-10\right)\left(r^2\Lambda-1\right)\right)-128\right)\ell^2\\
&-6\left(r^2\left(4\left(8\Lambda r^2+27\right)\omega^2+\Lambda\left(r^2\Lambda\left(r^2\Lambda-17\right)-2\right)\right)-104\right)\ell\\
&+4\Big(r^2\Big(3\left(\Lambda\left(59-8r^2\Lambda\right)r^2+60\right)\omega^2+\Lambda\left(\Lambda^3 r^6-15\Lambda r^2+12\right)\Big)-228\Big)\Big)r^5\\
&+12M^3\Big(90\ell^8+360\ell^7+\left(75r^2\Lambda-36\right)\ell^6+9\left(25r^2\Lambda-152\right)\ell^5\\
&-3\left(21\Lambda^2 r^4+8\left(5\Lambda-21\omega^2\right)r^2+162\right)\ell^4\\
&+3\left(\left(336\omega^2-\Lambda\left(42\Lambda r^2+205\right)\right)r^2+576\right)\ell^3\\
&+3\left(\left(\Lambda\left(\Lambda\left(4\Lambda r^2+57\right)r^2+27\right)-12\left(17\Lambda r^2+42\right)\omega^2\right)r^2+192\right)\ell^2\\
&+6\left(r^2\left(\Lambda\left(\Lambda\left(2\Lambda r^2+3(\ell^2+\ell-2)9\right)r^2+71\right)-6\left(17\Lambda r^2+56\right)\omega^2\right)-96\right)\ell\\
&+4\Big(r^2\Big(9\left(\Lambda\left(43-2r^2\Lambda\right)r^2+56\right)\omega^2\\
&+\Lambda\left(r^2\Lambda\left(5r^2\Lambda\left(r^2\Lambda-6\right)-27\right)-18\right)\Big)-72\Big)\Big)r^4\\
&+72M^4\Big(87\ell^6+261\ell^5+9\left(7r^2\Lambda-57\right)\ell^4+3\left(42r^2\Lambda-487\right)\ell^3\\
&+3\left(\left(72\omega^2-\Lambda\left(12\Lambda r^2+25\right)\right)r^2+516\right)\ell^2\\
&-6\left(r^2\left(\Lambda\left(6\Lambda r^2+23\right)-36\omega^2\right)-387\right)\ell+2r^2\left(2\Lambda\left(\Lambda\left(11r^2\Lambda-9\right)r^2+6\right)\right.\\
&\left.-9\left(11\Lambda r^2+24\right)\omega^2\right)-2244\Big)r^3\\
&+2592M^5\left(21\ell^4+42\ell^3+\left(2r^2\Lambda-127\right)\ell^2+2\left(r^2\Lambda-74\right)\ell\right.\\
&\left.+2\left(\Lambda^2 r^4+\left(3\omega^2+\Lambda\right)r^2+115\right)\right)r^2\\
&+5184M^6\left(-2\Lambda r^2+54\ell(\ell+1)-171\right)r+497664M^7\Big)\Big)
\end{aligned}
\tag{C.1}
$$

## C.2 Quasinormal frequency expansion coefficients

As explained in Section 5.4 and in [290], the fundamental (i.e. overtone index $n = 0$) quasinormal frequencies $\omega$ satisfying eq. (5.7) (for scalar perturbations), eq. (5.8) (for axial vector perturbations), eq. (5.14) (for axial gravitational perturbations), and for eq. (5.17) (for polar gravitational perturbations) can be expressed as a power series in inverse powers of $L = \ell + 1/2$:

$$\omega = \sum_{k=-1}^{k=\infty} \omega_k L^{-k}. \tag{C.2}$$

The expansion coefficients $\omega_k$ for each of the perturbation types (scalar, vector, or tensor), to $O(L^{-6})$, are given below. Note that, as explained in [290], the below expressions are valid only for $\Lambda \geq 0$.

### C.2.1 Scalar frequencies

The $\omega_k$ that satisfy eq. (5.7) are given by:

$$\begin{aligned}
3\sqrt{3}M\omega_{-1} &= \sqrt{1-9\Lambda M^2} \\
3\sqrt{3}M\omega_0 &= -\frac{i}{2}\sqrt{1-9\Lambda M^2} + am\sqrt{3}\left(\frac{2}{9}+\Lambda M^2\right) \\
3\sqrt{3}M\omega_1 &= \frac{81\Lambda M^4\left(61\Lambda-108\mu^2\right)+M^2\left(972\mu^2-612\Lambda\right)+7}{216\sqrt{1-9\Lambda M^2}} \\
3\sqrt{3}M\omega_2 &= -\frac{i\left(1-9\Lambda M^2\right)^{3/2}\left(45M^2\left(401\Lambda-648\mu^2\right)+137\right)}{7776} \\
&\quad -am\frac{\left(81\Lambda M^4\left(61\Lambda-108\mu^2\right)+M^2\left(972\mu^2-450\Lambda\right)-11\right)}{162\sqrt{3}} \\
3\sqrt{3}M\omega_3 &= \frac{1}{2519424}\Big(\sqrt{1-9\Lambda M^2}\Big(729\Lambda M^6\left(750851\Lambda^2-905904\Lambda\mu^2-419904\mu^4\right) \\
&\quad -1944M^4\left(53119\Lambda^2-81567\Lambda\mu^2-4374\mu^4\right) \\
&\quad +27M^2\left(146681\Lambda-245592\mu^2\right)+5230\Big)\Big) \\
&\quad -iam\frac{\left(1-9\Lambda M^2\right)}{2916\sqrt{3}}\left(405\Lambda M^4\left(401\Lambda-648\mu^2\right)\right. \\
&\quad \left.-36M^2\left(332\Lambda-567\mu^2\right)-29\right) \\
3\sqrt{3}M\omega_4 &= \frac{i\left(1-9\Lambda M^2\right)^{3/2}}{362797056}\Big(3645\Lambda M^6\left(27099013\Lambda^2-7301664\Lambda\mu^2-52907904\mu^4\right) \\
&\quad -243M^4\left(68373857\Lambda^2-101570112\Lambda\mu^2-7558272\mu^4\right) \\
&\quad +27M^2\left(12794177\Lambda-20816352\mu^2\right)+590983\Big)
\end{aligned}$$

$$
\begin{aligned}
&- am\frac{1-9\Lambda M^2}{629856\sqrt{3}}\left(27M^2\left(-11337408\Lambda\mu^4M^4\right.\right.\\
&-3888\mu^2\left(3\Lambda M^2\left(2097\Lambda M^2-437\right)+35\right)\\
&\left.\left.+\Lambda\left(9\Lambda M^2\left(2252553\Lambda M^2-357239\right)+80915\right)\right)+8137\right)\\
3\sqrt{3}M\omega_5 = &\frac{\sqrt{1-9\Lambda M^2}}{39182082048}\left(9M^2\left(22674816\mu^4M^2\left(27\Lambda M^2\left(144\Lambda M^2\left(6501\Lambda M^2-1363\right)\right.\right.\right.\\
&\left.\left.+9907\right)-427\right)-2592\mu^2\left(9\Lambda M^2\left(27\Lambda M^2\left(3\Lambda M^2\left(112055580\Lambda M^2\right.\right.\right.\\
&\left.\left.\left.-4940639\right)-7820726\right)+16693957\right)-1450348\right)\\
&+\Lambda\left(-9\Lambda M^2\left(9\Lambda M^2\left(9\Lambda M^2\left(168232451787\Lambda M^2-63977771143\right)\right.\right.\right.\\
&\left.\left.+71553627542\right)-28276533542\right)-2271718855\right)\\
&\left.+7346640384\mu^6M^4\left(36\Lambda M^2\left(198\Lambda M^2-17\right)+7\right)\right)-42573661\Big)\\
&+iam\frac{\left(1-9\Lambda M^2\right)}{68024448\sqrt{3}}\left(9M^2\left(-34012224\mu^4M^2\left(9\Lambda M^2\left(630\Lambda M^2-59\right)-2\right)\right.\right.\\
&\left.-17496\mu^2\left(3\Lambda M^2\left(9\Lambda M^2\left(56340\Lambda M^2-55807\right)+48878\right)-1721\right)\right.\\
&+\Lambda\left(27\Lambda M^2\left(3658366755\Lambda^2M^4-911149638\Lambda M^2+59613232\right)\right.\\
&\left.\left.-18218222\right)\right)+41735\Big)\\
3\sqrt{3}M\omega_6 = &\frac{i\sqrt{1-9\Lambda M^2}}{8463329722368}\left(27M^2\left(136048896\mu^4M^2\left(1-9\Lambda M^2\right)\right.\right.\\
&\times\left(243\Lambda M^2\left(15\Lambda M^2\left(217247\Lambda M^2-41079\right)+22487\right)\right.\\
&+6563\Big)+\Lambda\left(9\Lambda M^2\left(3\Lambda M^2\left(27\Lambda M^2\left(315\Lambda M^2\right.\right.\right.\\
&\left.\left.\times\left(429275206029\Lambda M^2-215443481162\right)+11851932821509\right)\\
&\left.\left.-23397470018140\right)+1898828714953\right)-84181473166\Big)\\
&-1296\mu^2\left(1-9\Lambda M^2\right)\left(9\Lambda M^2\left(135\Lambda M^2\left(43894090161\Lambda^2M^4\right.\right.\right.\\
&\left.\left.-4927747056\Lambda M^2-156842798\right)+2214937208\right)-100404965\Big)\\
&\left.-264479053824\mu^6M^4\left(9\Lambda M^2-1\right)\left(405\Lambda M^2\left(313\Lambda M^2-18\right)+37\right)\right)\\
&+11084613257\Big)\\
&+am\frac{1}{29386561536\sqrt{3}}\left(27M^2\left(120932352\mu^4M^2\left(9\Lambda M^2-1\right)\right.\right.\\
&\times\left(27\Lambda M^2\left(1485\Lambda M^2\left(197\Lambda M^2-36\right)+2047\right)+277\right)\\
&-1728\mu^2\left(9\Lambda M^2-1\right)\left(9\Lambda M^2\left(27\Lambda M^2\left(3\Lambda M^2\left(280138950\Lambda M^2-5781821\right)\right.\right.\right.\\
&\left.\left.\left.-18236525\right)+29333473\right)-1464535\right)\\
&+\Lambda\left(1551785558-9\Lambda M^2\left(3\Lambda M^2\left(27\Lambda M^2\left(45\Lambda M^2\left(56077483929\Lambda M^2\right.\right.\right.\right.\\
&\left.\left.\left.\left.-25842254398\right)+194725826099\right)-383179273148\right)
\end{aligned}
$$

$$
\begin{aligned}
&+32615632811)) - 19591041024\mu^6 M^4 \left(1-9\Lambda M^2\right) \\
&\times \left(9\Lambda M^2 \left(495\Lambda M^2 - 29\right) + 1\right)) + 18404153\Big) \qquad \text{(C.3)}
\end{aligned}
$$

### C.2.2 Axial Vector frequencies

The $\omega_k$ that satisfy eq. (5.8) are given by:

$$
\begin{aligned}
3\sqrt{3}M\omega_{-1} &= \sqrt{1-9\Lambda M^2} \\
3\sqrt{3}M\omega_0 &= -\frac{i}{2}\sqrt{1-9\Lambda M^2} + am\sqrt{3}\left(\frac{2}{9}+\Lambda M^2\right) \\
3\sqrt{3}M\omega_1 &= \frac{1}{216}\sqrt{1-9\Lambda M^2}\left(M^2\left(99\Lambda+972\mu^2\right)-65\right) \\
3\sqrt{3}M\omega_2 &= \frac{5i\left(1-9\Lambda M^2\right)^{3/2}\left(9M^2\left(31\Lambda+648\mu^2\right)+59\right)}{7776} \\
&\quad - am\frac{\left(1-9\Lambda M^2\right)}{162\sqrt{3}}\left(M^2\left(99\Lambda+972\mu^2\right)+25\right) \\
3\sqrt{3}M\omega_3 &= \frac{\sqrt{1-9\Lambda M^2}}{2519424}\left(27M^2\left(-314928\mu^4M^2\left(36\Lambda M^2-1\right)\right.\right. \\
&\quad -648\mu^2\left(9\Lambda M^2\left(6786\Lambda M^2-935\right)+19\right) \\
&\quad \left.\left.+\Lambda\left(9\Lambda M^2\left(6616-119127\Lambda M^2\right)+4121\right)\right)-71234\right) \\
&\quad + iam\frac{\left(1-9\Lambda M^2\right)}{2916\sqrt{3}}\left(9M^2\left(324\mu^2\left(90\Lambda M^2-7\right)+\Lambda\left(1395\Lambda M^2-76\right)\right)+245\right) \\
3\sqrt{3}M\omega_4 &= -\frac{i\left(1-9\Lambda M^2\right)^{3/2}}{362797056}\left(27M^2\left(68024448\mu^4M^2\left(105\Lambda M^2-1\right)\right.\right. \\
&\quad +38880\mu^2\left(27\Lambda M^2\left(10011\Lambda M^2-698\right)-415\right) \\
&\quad \left.\left.+\Lambda\left(9\Lambda M^2\left(19250805\Lambda M^2-288223\right)-585857\right)\right)-3374791\right) \\
&\quad + am\frac{\left(1-9\Lambda M^2\right)}{629856\sqrt{3}}\left(27M^2\left(11337408\Lambda\mu^4M^4\right.\right. \\
&\quad +3888\mu^2\left(3\Lambda M^2\left(3393\Lambda M^2-401\right)+11\right) \\
&\quad \left.\left.+\Lambda\left(9\Lambda M^2\left(119127\Lambda M^2-10825\right)-7043\right)\right)-21097\right) \\
3\sqrt{3}M\omega_5 &= \frac{\sqrt{1-9\Lambda M^2}}{39182082048}\left(9M^2\left(22674816\mu^4M^2\left(27\Lambda M^2\left(144\Lambda M^2\right.\right.\right.\right. \\
&\quad \left.\left.\left.\left(7689\Lambda M^2-1417\right)+8539\right)-67\right)+2592\mu^2\left(9\Lambda M^2\left(27\Lambda M^2\right.\right.\right. \\
&\quad \left.\left.\left.\left(3\Lambda M^2\left(329310180\Lambda M^2-74177569\right)+13293734\right)-1411525\right)-173540\right) \\
&\quad +\Lambda\left(9\Lambda M^2\left(63\Lambda M^2\left(9\Lambda M^2\left(1261925091\Lambda M^2-229959743\right)+55808902\right)\right.\right. \\
&\quad \left.\left.+113404646\right)+160933625\right) \\
&\quad \left.+7346640384\mu^6M^4\left(36\Lambda M^2\left(198\Lambda M^2-17\right)+7\right)\right)-342889693\Big)
\end{aligned}
$$

$$
\begin{aligned}
&+iam\frac{1}{68024448\sqrt{3}}\left(9M^2\left(34012224\mu^4M^2\left(9\Lambda M^2-1\right)\right.\right.\\
&\times\left(9\Lambda M^2\left(630\Lambda M^2-59\right)-2\right)\\
&+17496\left(3\Lambda M^2\left(600660\Lambda M^2-30323\right)-871\right)\left(1-9\Lambda M^2\right)^2\mu^2\\
&+\Lambda\left(9\Lambda M^2\left(9\Lambda M^2\left(63\Lambda M^2\left(8250345\Lambda M^2-2036507\right)+8064646\right)\right.\right.\\
&\left.\left.+424262\right)-3884077\right)\left.\left.+3233783\right)\right)\\
3\sqrt{3}M\omega_6=&\frac{i\left(1-9\Lambda M^2\right)^{3/2}}{8463329722368}\left(9M^2\left(408146688\mu^4M^2\left(243\Lambda M^2\right.\right.\right.\\
&\times\left(15\Lambda M^2\left(352463\Lambda M^2-44967\right)+13127\right)+6995\Big)\\
&+3888\mu^2\left(9\Lambda M^2\left(27\Lambda M^2\left(15\Lambda M^2\left(25239221253\Lambda M^2-3989698864\right)\right.\right.\right.\\
&\left.\left.\left.+1860754534\right)+486103048\right)+90125093\Big)\\
&+\Lambda\left(9\Lambda M^2\left(9\Lambda M^2\left(45\Lambda M^2\left(645007240719\Lambda M^2-78406459927\right)\right.\right.\right.\\
&\left.\left.\left.-380899298\right)+12521227898\right)+11148937343\Big)\\
&\left.\left.+793437161472\mu^6M^4\left(405\Lambda M^2\left(313\Lambda M^2-18\right)+37\right)\right)+74076561065\Big)\\
&+am\frac{1}{29386561536\sqrt{3}}\left(27M^2\left(120932352\mu^4M^2\left(9\Lambda M^2-1\right)\right.\right.\\
&\times\left(27\Lambda M^2\left(135\Lambda M^2\left(2563\Lambda M^2-408\right)+1777\right)+133\right)\\
&+1728\mu^2\left(9\Lambda M^2-1\right)\left(9\Lambda M^2\left(27\Lambda M^2\left(3\Lambda M^2\left(823275450\Lambda M^2\right.\right.\right.\right.\\
&\left.\left.\left.\left.-168911203\right)+27535325\right)-4529329\right)-1034153\Big)\\
&+\Lambda\left(9\Lambda M^2\left(3\Lambda M^2\left(27\Lambda M^2\left(63\Lambda M^2\left(2103208485\Lambda M^2-613717798\right)\right.\right.\right.\right.\\
&\left.\left.\left.\left.+3480361741\right)-1868367940\right)-82065323\right)-87749482\Big)\\
&\left.\left.+19591041024\mu^6M^4\left(9\Lambda M^2-1\right)\left(9\Lambda M^2\left(495\Lambda M^2-29\right)+1\right)\right)\right.\\
&-82685575\Big)
\end{aligned}
\tag{C.4}
$$

### C.2.3 Axial Gravitational frequencies

The $\omega_k$ that satisfy eq. (5.14) are given by:

$$
\begin{aligned}
3\sqrt{3}M\omega_{-1}&=\sqrt{1-9\Lambda M^2}\\
3\sqrt{3}M\omega_0&=-\frac{i}{2}\sqrt{1-9\Lambda M^2}+am\sqrt{3}\left(\frac{2}{9}+\Lambda M^2\right)\\
3\sqrt{3}M\omega_1&=\frac{1}{216}\sqrt{1-9\Lambda M^2}\left(99\Lambda M^2-281\right)\\
3\sqrt{3}M\omega_2&=\frac{i\left(1-9\Lambda M^2\right)^{3/2}\left(1395\Lambda M^2+1591\right)}{7776}-am\frac{\left(1-9\Lambda M^2\right)\left(99\Lambda M^2+133\right)}{162\sqrt{3}}
\end{aligned}
$$

$$
\begin{aligned}
3\sqrt{3}M\omega_3 = & -\frac{\sqrt{1-9\Lambda M^2}}{2519424}\left(27\Lambda M^2\left(9\Lambda M^2\left(119127\Lambda M^2+50408\right)+118999\right)\right.\\
& \left.+1420370\right)\\
& +iam\frac{\left(1-9\Lambda M^2\right)\left(279\Lambda M^2\left(45\Lambda M^2+8\right)+893\right)}{2916\sqrt{3}}\\
3\sqrt{3}M\omega_4 = & -\frac{i\left(1-9\Lambda M^2\right)^{3/2}}{362797056}\left(4677945615\Lambda^3M^6+1687260051\Lambda^2M^4\right.\\
& \left.+211769829\Lambda M^2-92347783\right)\\
& +am\frac{\left(1-9\Lambda M^2\right)}{629856\sqrt{3}}\left(27\Lambda M^2\left(9\Lambda M^2\left(119127\Lambda M^2+17687\right)-57587\right)\right.\\
& \left.+499895\right)\\
3\sqrt{3}M\omega_5 = & \frac{\sqrt{1-9\Lambda M^2}}{39182082048}\left(9\Lambda M^2\left(9\Lambda M^2\left(9\Lambda M^2\left(63\Lambda M^2\left(1261925091\Lambda M^2\right.\right.\right.\right.\\
& \left.\left.\left.\left.+181743169\right)-1078685462\right)-6276258970\right)-25334574535\right)\\
& -7827932509\Big)\\
& -iam\frac{\left(1-9\Lambda M^2\right)}{68024448\sqrt{3}}\left(9\Lambda M^2\left(27\Lambda M^2\left(3\Lambda M^2\left(57752415\Lambda M^2+5720786\right)\right.\right.\right.\\
& \left.\left.\left.-4178128\right)-42220738\right)+27500857\Big)\\
3\sqrt{3}M\omega_6 = & \frac{i\left(1-9\Lambda M^2\right)^{3/2}}{8463329722368}\left(9\Lambda M^2\left(9\Lambda M^2\left(9\Lambda M^2\left(45\Lambda M^2\left(645007240719\Lambda M^2\right.\right.\right.\right.\\
& \left.\left.\left.\left.+111206269001\right)-40406459618\right)-1321332614854\right)-1848252537217\right)\\
& -481407154423\Big)\\
& -am\frac{\left(1-9\Lambda M^2\right)}{29386561536\sqrt{3}}\left(9\Lambda M^2\left(9\Lambda M^2\left(9\Lambda M^2\left(63\Lambda M^2\left(6309625455\Lambda M^2\right.\right.\right.\right.\\
& \left.\left.\left.\left.+300876293\right)-8618549878\right)-12418517690\right)+11910847045\right)\\
& -61558283321\Big)
\end{aligned}
\tag{C.5}
$$

### C.2.4 Polar Gravitational frequencies

For the $\omega_k$ that satisfy eq. (5.17), we present the frequency coefficients in the form:

$$
\omega_k^p = \omega_k^{ax} + \Delta\omega_k, \tag{C.6}
$$

where the $\omega_k^{ax}$ are given in eq. (C.5), in order to clearly show under which circumstances isospectrality between the axial and polar gravitational sectors breaks down. The $\Delta\omega_k$ are

given by:

$$
\begin{aligned}
\Delta\omega_{-1} &= 0 \\
\Delta\omega_{0} &= 0 \\
\Delta\omega_{1} &= 0 \\
\Delta\omega_{2} &= 0 \\
\Delta\omega_{3} &= 0 \\
\Delta\omega_{4} &= \frac{am\Lambda M}{243}\left(1-9\Lambda M^2\right)\left(9\Lambda M^2\left(9\Lambda M^2\left(27\Lambda M^2-11\right)-95\right)+148\right) \\
\Delta\omega_{5} &= -\frac{iam\Lambda M}{1458}\left(1-9\Lambda M^2\right)\left(81\Lambda M^2\left(3\Lambda M^2\left(3\Lambda M^2\left(1188\Lambda M^2-487\right)-296\right)+182\right)\right. \\
&\quad \left.-152\right) \\
\Delta\omega_{6} &= -\frac{am\Lambda M}{78732}\left(1-9\Lambda M^2\right)\left(9\Lambda M^2\left(27\Lambda M^2\left(3\Lambda M^2\left(9\Lambda M^2\left(373626\Lambda M^2-158551\right)\right.\right.\right. \\
&\quad \left.\left.\left.+8158\right)+67040\right)-39581\right)-78904\Big).
\end{aligned}
\tag{C.7}
$$

The axial and polar gravitational QNMs are clearly isospectral to $O(L^{-3})$, with any difference between the two only becoming apparent in the case that both $a \neq 0$ *and* $\Lambda \neq 0$.

## C.3 QNM frequency tables

In the following tables of QNM frequency values, all numerical values will be presented to four decimal places, though relative errors were calculated using full numerical values.

Table C.1: Comparison of the $n = 0$ massless scalar QNM frequencies calculated by 6th-order WKB [293] and analytical expansion techniques for varying $\Lambda$ with $a = 0$.

| $\ell = 1$ | WKB | | L-expansion | | % error | |
|---|---|---|---|---|---|---|
| $\Lambda$ | Re($M\omega$) | -Im($M\omega$) | Re($M\omega$) | -Im($M\omega$) | Re($M\omega$) | -Im($M\omega$) |
| 0.00 | 0.2929 | 0.0978 | 0.2929 | 0.0976 | 0.0081 | -0.1555 |
| 0.04 | 0.2247 | 0.0821 | 0.2247 | 0.0821 | -0.0186 | -0.0368 |
| 0.08 | 0.1404 | 0.0542 | 0.1404 | 0.0540 | -0.0033 | -0.3689 |
| 0.10 | 0.0816 | 0.0312 | 0.08161 | 0.0312 | 0.0556 | 0.0582 |
| $\ell = 2$ | | | | | | |
| $\Lambda$ | | | | | | |
| 0.00 | 0.4836 | 0.0968 | 0.4836 | 0.0968 | 0.0007 | -0.0119 |
| 0.04 | 0.3808 | 0.0788 | 0.3808 | 0.0788 | 0.0008 | -0.0012 |
| 0.08 | 0.2475 | 0.0520 | 0.2475 | 0.0519 | -0.0002 | -0.1271 |
| 0.10 | 0.1466 | 0.0307 | 0.1466 | 0.0307 | 0.0003 | -0.0105 |

Table C.2: Comparison of the $n = 0$ electromagnetic QNM frequencies calculated by 6th-order WKB [293] and analytical expansion techniques for varying $\Lambda$ with $a = 0$.

| $\ell = 1$ | WKB | | L-expansion | | % error | |
|---|---|---|---|---|---|---|
| $\Lambda$ | Re($M\omega$) | -Im($M\omega$) | Re($M\omega$) | -Im($M\omega$) | Re($M\omega$) | -Im($M\omega$) |
| 0.00 | 0.2482 | 0.0926 | 0.2482 | 0.0925 | 0.0130 | -0.1311 |
| 0.04 | 0.2006 | 0.0748 | 0.2006 | 0.0747 | -0.0014 | -0.1036 |
| 0.08 | 0.1339 | 0.0502 | 0.1339 | 0.0502 | 0.0153 | -0.0049 |
| 0.10 | 0.0804 | 0.0303 | 0.0804 | 0.0303 | 0.0052 | -0.0278 |
| $\ell = 2$ | | | | | | |
| $\Lambda$ | | | | | | |
| 0.00 | 0.4576 | 0.0950 | 0.4576 | 0.0950 | 0.0010 | -0.0062 |
| 0.04 | 0.3672 | 0.0762 | 0.3672 | 0.0762 | -0.0006 | -0.0018 |
| 0.08 | 0.2437 | 0.0507 | 0.2436 | 0.0507 | -0.0028 | 0.0055 |
| 0.10 | 0.1458 | 0.0304 | 0.1458 | 0.0304 | -0.0015 | 0.0134 |

Table C.3: Comparison of the $n = 0$ gravitational QNM frequencies calculated by 6th-order WKB [293] and analytical expansion techniques for varying $\Lambda$ with $a = 0$.

| $\ell = 2$ | WKB | | L-expansion | | % error | |
|---|---|---|---|---|---|---|
| $\Lambda$ | Re($M\omega$) | -Im($M\omega$) | Re($M\omega$) | -Im($M\omega$) | Re($M\omega$) | -Im($M\omega$) |
| 0.00 | 0.3736 | 0.0889 | 0.3736 | 0.0887 | 0.0113 | -0.2074 |
| 0.04 | 0.2989 | 0.0733 | 0.2991 | 0.0731 | 0.0521 | -0.2165 |
| 0.08 | 0.1975 | 0.0499 | 0.1977 | 0.0498 | 0.1174 | -0.1502 |
| 0.10 | 0.1179 | 0.0302 | 0.1181 | 0.0302 | 0.1590 | -0.0368 |
| $\ell = 3$ | | | | | | |
| $\Lambda$ | | | | | | |
| 0.00 | 0.5994 | 0.0927 | 0.5994 | 0.0927 | -0.0006 | -0.0138 |
| 0.04 | 0.4801 | 0.0751 | 0.4801 | 0.0751 | 0.0024 | -0.0100 |
| 0.08 | 0.3178 | 0.0504 | 0.3178 | 0.0504 | 0.0061 | 0.0050 |
| 0.10 | 0.1900 | 0.0303 | 0.1900 | 0.0303 | 0.0081 | 0.0001 |

Table C.4: Comparison of the $n = 0$ massless scalar QNM frequencies as calculated by Leaver's continued fraction method in [47] and analytical expansion techniques for varying $a$ with $\Lambda = 0$.

| $\ell = m = 1$ | Leaver | | L-expansion | | % error | |
|---|---|---|---|---|---|---|
| $a$ | Re($M\omega$) | -Im($M\omega$) | Re($M\omega$) | -Im($M\omega$) | Re($M\omega$) | -Im($M\omega$) |
| 0.05 | 0.2969 | 0.0976 | 0.2968 | 0.0976 | -0.0363 | 0.0071 |
| 0.10 | 0.3010 | 0.0975 | 0.3006 | 0.0976 | -0.1348 | 0.0688 |
| 0.15 | 0.3054 | 0.0974 | 0.3045 | 0.0976 | -0.3029 | 0.1790 |
| 0.20 | 0.3100 | 0.0972 | 0.3084 | 0.0976 | -0.5447 | 0.3452 |
| $\ell = m = 2$ | | | | | | |
| $a$ | | | | | | |
| 0.05 | 0.4914 | 0.0967 | 0.4912 | 0.0968 | -0.0390 | 0.0190 |
| 0.10 | 0.4995 | 0.0967 | 0.4987 | 0.0967 | -0.1581 | 0.0809 |
| 0.15 | 0.5081 | 0.0966 | 0.5062 | 0.0967 | -0.3614 | 0.1920 |
| 0.20 | 0.5171 | 0.0964 | 0.5137 | 0.0967 | -0.6535 | 0.3608 |

Table C.5: Comparison of the $n = 0$ electromagnetic QNM frequencies as calculated by Leaver's continued fraction method in [47] and analytical expansion techniques for varying $a$ with $\Lambda = 0$.

| $\ell = m = 1$ | Leaver | | L-expansion | | % error | |
|---|---|---|---|---|---|---|
| $a$ | Re($M\omega$) | -Im($M\omega$) | Re($M\omega$) | -Im($M\omega$) | Re($M\omega$) | -Im($M\omega$) |
| 0.05 | 0.2516 | 0.0923 | 0.2515 | 0.0923 | -0.0499 | -0.0212 |
| 0.10 | 0.2552 | 0.0920 | 0.2541 | 0.0921 | -0.1618 | 0.0976 |
| 0.15 | 0.2590 | 0.0918 | 0.2581 | 0.0920 | -0.3526 | 0.2252 |
| 0.20 | 0.2630 | 0.0914 | 0.2614 | 0.0918 | -0.6272 | 0.4116 |
| $\ell = m = 2$ | | | | | | |
| $a$ | | | | | | |
| 0.05 | 0.4649 | 0.0949 | 0.4648 | 0.0949 | -0.0401 | 0.0206 |
| 0.10 | 0.4726 | 0.0948 | 0.4718 | 0.0949 | -0.1624 | 0.0861 |
| 0.15 | 0.4808 | 0.0946 | 0.4790 | 0.0948 | -0.3713 | 0.2030 |
| 0.20 | 0.4894 | 0.0944 | 0.4861 | 0.0947 | -0.6717 | 0.3798 |

Table C.6: Comparison of the $n = 0$ gravitational QNM frequencies as calculated by Leaver's continued fraction method in [47] and analytical expansion techniques for varying $a$ with $\Lambda = 0$.

| $\ell = m = 2$ | Leaver | | L-expansion | | % error | |
|---|---|---|---|---|---|---|
| $a$ | Re($M\omega$) | -Im($M\omega$) | Re($M\omega$) | -Im($M\omega$) | Re($M\omega$) | -Im($M\omega$) |
| 0.05 | 0.3801 | 0.0888 | 0.3799 | 0.0885 | 0.0616 | -0.3433 |
| 0.10 | 0.3870 | 0.0887 | 0.3862 | 0.0883 | -0.2163 | -0.3761 |
| 0.15 | 0.3943 | 0.0885 | 0.3924 | 0.0882 | -0.4777 | -0.3704 |
| 0.20 | 0.4021 | 0.0883 | 0.3987 | 0.0880 | -0.8522 | -0.3200 |
| $\ell = m = 3$ | | | | | | |
| $a$ | | | | | | |
| 0.05 | 0.6098 | 0.0926 | 0.6095 | 0.0926 | -0.0464 | -0.0031 |
| 0.10 | 0.6208 | 0.0924 | 0.6196 | 0.0925 | -0.1859 | 0.0511 |
| 0.15 | 0.6324 | 0.0922 | 0.6297 | 0.0924 | -0.4241 | 0.1555 |
| 0.20 | 0.6448 | 0.0920 | 0.6398 | 0.0923 | -0.7666 | 0.3183 |

Table C.7: Comparison of the $n = 0$ massive scalar QNM frequencies as calculated by Leaver's continued fraction method [305] and analytic expansion techniques for $\ell = m = 1$ for varying effective mass $\mu M$ and $a$.

| $a = 0$ | Leaver | | L-expansion | | % error | |
|---|---|---|---|---|---|---|
| $\mu M$ | Re($M\omega$) | -Im($M\omega$) | Re($M\omega$) | -Im($M\omega$) | Re($M\omega$) | -Im($M\omega$) |
| 0.1 | 0.297416 | 0.094957 | 0.297429 | 0.094935 | 0.004371 | -0.023168 |
| 0.2 | 0.310957 | 0.086593 | 0.311127 | 0.086474 | 0.054670 | 0.137613 |
| $a = 0.1$ | | | | | | |
| $\mu M$ | | | | | | |
| 0.1 | 0.305329 | 0.095029 | 0.304950 | 0.095072 | -0.124128 | 0.045249 |
| 0.2 | 0.318274 | 0.087228 | 0.318029 | 0.087108 | -0.076978 | -0.137571 |
| $a = 0.2$ | | | | | | |
| $\mu M$ | | | | | | |
| 0.1 | 0.314119 | 0.094920 | 0.312471 | 0.095209 | -0.524642 | 0.304467 |
| 0.2 | 0.326433 | 0.087709 | 0.324931 | 0.087742 | -0.460125 | 0.037624 |

Table C.8: Comparison of the $n = 0$ massive scalar QNM frequencies as calculated by Leaver's continued fraction method [298] and analytic expansion techniques for $\ell = m = 2$ for varying effective mass $\mu M$ and $a$.

| $a = 0$ | Leaver | | L-expansion | | % error | |
|---|---|---|---|---|---|---|
| $\mu M$ | Re($M\omega$) | -Im($M\omega$) | Re($M\omega$) | -Im($M\omega$) | Re($M\omega$) | -Im($M\omega$) |
| 0.1 | 0.486804 | 0.095675 | 0.486804 | 0.095674 | 0.000000 | -0.000942 |
| 0.2 | 0.496327 | 0.092389 | 0.496332 | 0.092387 | 0.001038 | -0.002358 |
| $a = 0.1$ | | | | | | |
| $\mu M$ | | | | | | |
| 0.1 | 0.502456 | 0.095674 | 0.501670 | 0.095750 | -0.156339 | 0.079541 |
| 0.2 | 0.511419 | 0.092663 | 0.510647 | 0.092731 | -0.150864 | 0.073624 |
| $a = 0.2$ | | | | | | |
| $\mu M$ | | | | | | |
| 0.1 | 0.519901 | 0.095483 | 0.516537 | 0.095826 | -0.647071 | 0.359333 |
| 0.2 | 0.528281 | 0.092755 | 0.524963 | 0.093076 | -0.628121 | 0.345666 |

# Bibliography


[1] Richard Phillips Feynman, Robert Benjamin Leighton, and Matthew Sands. *The Feynman lectures on physics; New millennium ed.* Basic Books, New York, NY, 2010. Originally published 1963-1965.

[2] Isaac Newton. *Philosophiae naturalis principia mathematica*. William Dawson & Sons Ltd., London, 1687.

[3] Kazunori Akiyama et al. First M87 Event Horizon Telescope Results. I. The Shadow of the Supermassive Black Hole. *Astrophys. J.*, 875(1):L1, 2019.

[4] Albert Einstein. The Foundation of the General Theory of Relativity. *Annalen Phys.*, 49(7):769–822, 1916. [,65(1916)].

[5] Albert Einstein. On the electrodynamics of moving bodies. *Annalen Phys.*, 17:891–921, 1905. [Annalen Phys.14,194(2005)].

[6] Edwin Hubble. A relation between distance and radial velocity among extra-galactic nebulae. *Proc. Nat. Acad. Sci.*, 15:168–173, 1929.

[7] Georges Lemaitre. A homogeneous universe of constant mass and increasing radius accounting for the radial velocity of extra-galactic nebulae. *Mon. Not. Roy. Astron. Soc.*, 91:483–490, 1931.

[8] Adam G. Riess et al. Observational evidence from supernovae for an accelerating universe and a cosmological constant. *Astron. J.*, 116:1009–1038, 1998.

[9] S. Perlmutter et al. Measurements of Omega and Lambda from 42 high redshift supernovae. *Astrophys. J.*, 517:565–586, 1999.

[10] Karl Schwarzschild. On the gravitational field of a mass point according to Einstein's theory. *Sitzungsber. Preuss. Akad. Wiss. Berlin (Math. Phys.)*, 1916:189–196, 1916.

[11] David Finkelstein. Past-Future Asymmetry of the Gravitational Field of a Point Particle. *Phys. Rev.*, 110:965–967, 1958.

[12] Roy P. Kerr. Gravitational field of a spinning mass as an example of algebraically special metrics. *Phys. Rev. Lett.*, 11:237–238, 1963.

[13] E. T. Newman, E. Couch, K. Chinnapared, A. Exton, A. Prakash, and R. Torrence. Metric of a rotating, charged mass. *Journal of Mathematical Physics*, 6(6):918–919, 1965.

[14] B. Carter. Black hole equilibrium states. In C. Dewitt and B. S. Dewitt, editors, *Black Holes (Les Astres Occlus)*, pages 57–214, 1973.

[15] S. Gillessen, F. Eisenhauer, S. Trippe, T. Alexander, R. Genzel, F. Martins, and T. Ott. Monitoring stellar orbits around the Massive Black Hole in the Galactic Center. *Astrophys. J.*, 692:1075–1109, 2009.

[16] B. P. Abbott et al. GWTC-1: A Gravitational-Wave Transient Catalog of Compact Binary Mergers Observed by LIGO and Virgo during the First and Second Observing Runs. 2018.

[17] A. Einstein. Über Gravitationswellen. *Sitzungsberichte der Königlich Preußischen Akademie der Wissenschaften (Berlin), Seite 154-167.*, 1918.

[18] Jorge L. Cervantes-Cota, S. Galindo-Uribarri, and G-F. Smoot. A Brief History of Gravitational Waves. *Universe*, 2(3):22, 2016.

[19] Andrzej Krolak and Mandar Patil. The first detection of gravitational waves. *Universe*, 3(3), 2017.

[20] Kirk T. McDonald. *http://www.hep.princeton.edu/ mcdonald/examples/stiffness.pdf.*

[21] B. P. Abbott et al. Properties of the Binary Black Hole Merger GW150914. *Phys. Rev. Lett.*, 116(24):241102, 2016.

[22] B. P. Abbott, R. Abbott, T. D. Abbott, M. R. Abernathy, F. Acernese, K. Ackley, C. Adams, T. Adams, P. Addesso, R. X. Adhikari, and et al. Observation of Gravitational Waves from a Binary Black Hole Merger. *Physical Review Letters*, 116(6):061102, February 2016.

[23] LIGO Scientific Collaboration. *Observation of Gravitational Waves from a Binary Black Hole Merger Summary*.

[24] Benjamin P. Abbott et al. GW170817: Observation of Gravitational Waves from a Binary Neutron Star Inspiral. *Phys. Rev. Lett.*, 119(16):161101, 2017.

[25] B. P. Abbott, R. Abbott, T. D. Abbott, M. R. Abernathy, F. Acernese, K. Ackley, C. Adams, T. Adams, P. Addesso, R. X. Adhikari, and et al. Tests of General Relativity with GW150914. *Physical Review Letters*, 116(22):221101, June 2016.

[26] Clifford M. Will. The Confrontation between General Relativity and Experiment. *Living Rev. Rel.*, 17:4, 2014.

[27] A Zee. *Quantum Field Theory in a Nutshell*. Nutshell handbook. Princeton Univ. Press, Princeton, NJ, 2003.

[28] V. C. Rubin, N. Thonnard, and W. K. Ford, Jr. Rotational properties of 21 SC galaxies with a large range of luminosities and radii, from NGC 4605 /R = 4kpc/ to UGC 2885 /R = 122 kpc/. *Astrophys. J.*, 238:471, 1980.

[29] Gianfranco Bertone and Dan Hooper. History of dark matter. *Rev. Mod. Phys.*, 90(4):045002, 2018.

[30] N. Aghanim et al. Planck 2018 results. VI. Cosmological parameters. 2018.

[31] R. J. Adler, B. Casey, and O. C. Jacob. Vacuum catastrophe: An Elementary exposition of the cosmological constant problem. *Am. J. Phys.*, 63:620–626, 1995.

[32] Timothy Clifton, Pedro G. Ferreira, Antonio Padilla, and Constantinos Skordis. Modified gravity and cosmology. *Physics Reports*, 513(1–3):1 – 189, 2012. Modified Gravity and Cosmology.

[33] C. Brans and R. H. Dicke. Mach's principle and a relativistic theory of gravitation. *Phys. Rev.*, 124:925–935, Nov 1961.

[34] Nicolas Yunes and Xavier Siemens. Gravitational-Wave Tests of General Relativity with Ground-Based Detectors and Pulsar Timing-Arrays. *Living Rev. Rel.*, 16:9, 2013.

[35] Jonathan R. Gair, Michele Vallisneri, Shane L. Larson, and John G. Baker. Testing general relativity with low-frequency, space-based gravitational-wave detectors. *Living Reviews in Relativity*, 16(1):7, Sep 2013.

[36] Emanuele Berti, Kent Yagi, and Nicolas Yunes. Extreme Gravity Tests with Gravitational Waves from Compact Binary Coalescences: (I) Inspiral-Merger. *Gen. Rel. Grav.*, 50(4):46, 2018.

[37] Emanuele Berti, Kent Yagi, Huan Yang, and Nicolas Yunes. Extreme Gravity Tests with Gravitational Waves from Compact Binary Coalescences: (II) Ringdown. 2018.

[38] Luc Blanchet. Gravitational Radiation from Post-Newtonian Sources and Inspiralling Compact Binaries. *Living Rev. Rel.*, 17:2, 2014.

[39] Frans Pretorius. Binary Black Hole Coalescence. 2007.

[40] Joan Centrella, John G. Baker, Bernard J. Kelly, and James R. van Meter. Black-hole binaries, gravitational waves, and numerical relativity. *Rev. Mod. Phys.*, 82:3069, 2010.

[41] Ulrich Sperhake, Emanuele Berti, and Vitor Cardoso. Numerical simulations of black-hole binaries and gravitational wave emission. *Comptes Rendus Physique*, 14:306–317, 2013.

[42] Harald P. Pfeiffer. Numerical simulations of compact object binaries. *Class. Quant. Grav.*, 29:124004, 2012.

[43] Luis Lehner and Frans Pretorius. Numerical Relativity and Astrophysics. *Ann. Rev. Astron. Astrophys.*, 52:661–694, 2014.

[44] S. Chandrasekhar. On the Equations Governing the Perturbations of the Schwarzschild Black Hole. *Proceedings of the Royal Society of London Series A*, 343:289–298, May 1975.

[45] Hans-Peter Nollert. Quasinormal modes: the characteristic 'sound' of black holes and neutron stars. *Classical and Quantum Gravity*, 16(12):R159, 1999.

[46] Kostas D. Kokkotas and Bernd G. Schmidt. Quasinormal modes of stars and black holes. *Living Rev. Rel.*, 2:2, 1999.

[47] Emanuele Berti, Vitor Cardoso, and Andrei O. Starinets. Quasinormal modes of black holes and black branes. *Class. Quant. Grav.*, 26:163001, 2009.

[48] R. A. Konoplya and A. Zhidenko. Quasinormal modes of black holes: From astrophysics to string theory. *Rev. Mod. Phys.*, 83:793–836, 2011.

[49] B. P. Abbott et al. Observation of Gravitational Waves from a Binary Black Hole Merger. *Phys. Rev. Lett.*, 116(6):061102, 2016.

[50] Werner Israel. Event horizons in static vacuum space-times. *Phys. Rev.*, 164:1776–1779, 1967.

[51] Werner Israel. Event horizons in static electrovac space-times. *Commun. Math. Phys.*, 8:245–260, 1968.

[52] B. Carter. Axisymmetric Black Hole Has Only Two Degrees of Freedom. *Phys. Rev. Lett.*, 26:331–333, 1971.

[53] S. W. Hawking. Black holes in general relativity. *Communications in Mathematical Physics*, 25:152–166, June 1972.

[54] Jacob D. Bekenstein. Nonexistence of baryon number for black holes. ii. *Phys. Rev. D*, 5:2403–2412, May 1972.

[55] Olaf Dreyer, Bernard J. Kelly, Badri Krishnan, Lee Samuel Finn, David Garrison, and Ramon Lopez-Aleman. Black hole spectroscopy: Testing general relativity through gravitational wave observations. *Class. Quant. Grav.*, 21:787–804, 2004.

[56] Emanuele Berti, Vitor Cardoso, and Clifford M. Will. On gravitational-wave spectroscopy of massive black holes with the space interferometer LISA. *Phys. Rev.*, D73:064030, 2006.

[57] S. Gossan, J. Veitch, and B. S. Sathyaprakash. Bayesian model selection for testing the no-hair theorem with black hole ringdowns. *Phys. Rev.*, D85:124056, 2012.

[58] J. Meidam, M. Agathos, C. Van Den Broeck, J. Veitch, and B. S. Sathyaprakash. Testing the no-hair theorem with black hole ringdowns using TIGER. *Phys. Rev.*, D90(6):064009, 2014.

[59] Emanuele Berti et al. Testing General Relativity with Present and Future Astrophysical Observations. *Class. Quant. Grav.*, 32:243001, 2015.

[60] Emanuele Berti, Alberto Sesana, Enrico Barausse, Vitor Cardoso, and Krzysztof Belczynski. Spectroscopy of Kerr black holes with Earth- and space-based interferometers. *Phys. Rev. Lett.*, 117(10):101102, 2016.

[61] Vishal Baibhav and Emanuele Berti. Multimode black hole spectroscopy. *Phys. Rev.*, D99(2):024005, 2019.

[62] Maximiliano Isi, Matthew Giesler, Will M. Farr, Mark A. Scheel, and Saul A. Teukolsky. Testing the no-hair theorem with GW150914. 2019.

[63] Enrico Barausse. Black holes in General Relativity and beyond. *arXiv e-prints*, page arXiv:1902.09199, Feb 2019.

[64] Jose Luis Blázquez-Salcedo, Caio F. B. Macedo, Vitor Cardoso, Valeria Ferrari, Leonardo Gualtieri, Fech Scen Khoo, Jutta Kunz, and Paolo Pani. Perturbed black holes in Einstein-dilaton-Gauss-Bonnet gravity: Stability, ringdown, and gravitational-wave emission. *Phys. Rev.*, D94(10):104024, 2016.

[65] Jose Luis Blázquez-Salcedo, Fech Scen Khoo, and Jutta Kunz. Quasinormal modes of Einstein-Gauss-Bonnet-dilaton black holes. *Phys. Rev.*, D96(6):064008, 2017.

[66] Hector O. Silva, Jeremy Sakstein, Leonardo Gualtieri, Thomas P. Sotiriou, and Emanuele Berti. Spontaneous scalarization of black holes and compact stars from a Gauss-Bonnet coupling. *Phys. Rev. Lett.*, 120(13):131104, 2018.

[67] G. Antoniou, A. Bakopoulos, and P. Kanti. Evasion of No-Hair Theorems and Novel Black-Hole Solutions in Gauss-Bonnet Theories. *Phys. Rev. Lett.*, 120(13):131102, 2018.

[68] G. Antoniou, A. Bakopoulos, and P. Kanti. Black-Hole Solutions with Scalar Hair in Einstein-Scalar-Gauss-Bonnet Theories. 2017.

[69] Athanasios Bakopoulos, Georgios Antoniou, and Panagiota Kanti. Novel Black-Hole Solutions in Einstein-Scalar-Gauss-Bonnet Theories with a Cosmological Constant. *Phys. Rev.*, D99(6):064003, 2019.

[70] Hector O. Silva, Caio F. B. Macedo, Thomas P. Sotiriou, Leonardo Gualtieri, Jeremy Sakstein, and Emanuele Berti. Stability of scalarized black hole solutions in scalar-Gauss-Bonnet gravity. *Phys. Rev.*, D99(6):064011, 2019.

[71] Masato Minamitsuji and Taishi Ikeda. Scalarized black holes in the presence of the coupling to Gauss-Bonnet gravity. *Phys. Rev.*, D99(4):044017, 2019.

[72] Andrew Sullivan, Nicolas Yunes, and Thomas P. Sotiriou. Exact Black Hole Solutions in Modified Gravity Theories: Spherical Symmetry Case. 2019.

[73] Justin Ripley and Frans Pretorius. Gravitational Collapse in Einstein Dilaton Gauss-Bonnet Gravity. 2019.

[74] Caio F. B. Macedo, Jeremy Sakstein, Emanuele Berti, Leonardo Gualtieri, Hector O. Silva, and Thomas P. Sotiriou. Self-interactions and Spontaneous Black Hole Scalarization. 2019.

[75] R. A. Konoplya. Quasinormal modes of the electrically charged dilaton black hole. *Gen. Rel. Grav.*, 34:329–335, 2002.

[76] Ruifeng Dong, Jeremy Sakstein, and Dejan Stojkovic. Quasinormal modes of black holes in scalar-tensor theories with nonminimal derivative couplings. *Phys. Rev.*, D96(6):064048, 2017.

[77] Solomon Endlich, Victor Gorbenko, Junwu Huang, and Leonardo Senatore. An effective formalism for testing extensions to General Relativity with gravitational waves. *JHEP*, 09:122, 2017.

[78] Vitor Cardoso, Masashi Kimura, Andrea Maselli, and Leonardo Senatore. Black Holes in an Effective Field Theory Extension of General Relativity. *Phys. Rev. Lett.*, 121(25):251105, 2018.

[79] Richard Brito and Costantino Pacilio. Quasinormal modes of weakly charged Einstein-Maxwell-dilaton black holes. *Phys. Rev.*, D98(10):104042, 2018.

[80] Gabriele Franciolini, Lam Hui, Riccardo Penco, Luca Santoni, and Enrico Trincherini. Effective Field Theory of Black Hole Quasinormal Modes in Scalar-Tensor Theories. *JHEP*, 02:127, 2019.

[81] Vitor Cardoso, Masashi Kimura, Andrea Maselli, Emanuele Berti, Caio F. B. Macedo, and Ryan McManus. Parametrized black hole quasinormal ringdown. I. Decoupled equations for nonrotating black holes. 2019.

[82] Ryan McManus, Emanuele Berti, Caio F. B. Macedo, Masashi Kimura, Andrea Maselli, and Vitor Cardoso. Parametrized black hole quasinormal ringdown. II. Coupled equations and quadratic corrections for nonrotating black holes. 2019.

[83] Oliver J. Tattersall, Pedro G. Ferreira, and Macarena Lagos. General theories of linear gravitational perturbations to a Schwarzschild Black Hole. *Phys. Rev.*, D97(4):044021, 2018.

[84] Oliver J. Tattersall and Pedro G. Ferreira. Quasinormal modes of black holes in Horndeski gravity. *Phys. Rev.*, D97(10):104047, 2018.

[85] Oliver J. Tattersall and Pedro G. Ferreira. Forecasts for Low Spin Black Hole Spectroscopy in Horndeski Gravity. *Phys. Rev.*, D99(10):104082, 2019.

[86] Oliver J. Tattersall, Macarena Lagos, and Pedro G. Ferreira. Covariant approach to parametrized cosmological perturbations. *Phys. Rev.*, D96(6):064011, 2017.

[87] Oliver J. Tattersall, Pedro G. Ferreira, and Macarena Lagos. Speed of gravitational waves and black hole hair. *Phys. Rev. D*, 97:084005, Apr 2018.

[88] Oliver J. Tattersall. Kerr-(anti-)de Sitter black holes: Perturbations and quasinormal modes in the slow rotation limit. *Phys. Rev.*, D98(10):104013, 2018.

[89] Macarena Lagos, Tessa Baker, Pedro G. Ferreira, and Johannes Noller. A general theory of linear cosmological perturbations: scalar-tensor and vector-tensor theories. *JCAP*, 1608(08):007, 2016.

[90] M. Lagos and P. G. Ferreira. A general theory of linear cosmological perturbations: bimetric theories. *Journal of Cosmology and Astroparticle Physics*, 1:047, January 2017.

[91] A. Friedman. Über die krümmung des raumes. *Zeitschrift für Physik*, 10(1):377–386, Dec 1922.

[92] A. Friedmann. Über die Möglichkeit einer Welt mit konstanter negativer Krümmung des Raumes. *Zeitschrift fur Physik*, 21:326–332, December 1924.

[93] G. Lemaître. L'Univers en expansion. *Annales de la Société Scientifique de Bruxelles*, 53, 1933.

[94] H. P. Robertson. Kinematics and World-Structure. *Astrophys. J.*, 82:284, November 1935.

[95] H. P. Robertson. Kinematics and World-Structure II. *Astrophys. J.*, 83:187, April 1936.

[96] H. P. Robertson. Kinematics and World-Structure III. *Astrophys. J.*, 83:257, May 1936.

[97] A. G. Walker. On Milne's Theory of World-Structure. *Proceedings of the London Mathematical Society, (Series 2) volume 42, p. 90-127*, 42:90–127, 1937.

[98] Richard L. Arnowitt, Stanley Deser, and Charles W. Misner. Dynamical Structure and Definition of Energy in General Relativity. *Phys. Rev.*, 116:1322–1330, 1959.

[99] Jerome Gleyzes, David Langlois, and Filippo Vernizzi. A unifying description of dark energy. *Int. J. Mod. Phys.*, D23(13):1443010, 2015.

[100] G. F. R. Ellis and Malcolm A. H. MacCallum. A Class of homogeneous cosmological models. *Commun. Math. Phys.*, 12:108–141, 1969.

[101] L. C. Stein and N. Yunes. Effective gravitational wave stress-energy tensor in alternative theories of gravity. *Physicsl Review D*, 83(6):064038, March 2011.

[102] Christos G. Tsagas, Anthony Challinor, and Roy Maartens. Relativistic cosmology and large-scale structure. *Phys. Rept.*, 465:61–147, 2008.

[103] Gregory Walter Horndeski. Second-order scalar-tensor field equations in a four-dimensional space. *Int. J. Theor. Phys.*, 10:363–384, 1974.

[104] C. Deffayet, Gilles Esposito-Farese, and A. Vikman. Covariant Galileon. *Phys. Rev.*, D79:084003, 2009.

[105] Emilio Bellini and Ignacy Sawicki. Maximal freedom at minimum cost: linear large-scale structure in general modifications of gravity. *JCAP*, 1407:050, 2014.

[106] Miguel Zumalacarregui, Emilio Bellini, Ignacy Sawicki, and Julien Lesgourgues. hi class: Horndeski in the Cosmic Linear Anisotropy Solving System. 2016.

[107] B. Hu, M. Raveri, N. Frusciante, and A. Silvestri. Effective field theory of cosmic acceleration: An implementation in CAMB. *Phys. Rev. D*, 89(10):103530, May 2014.

[108] E. Bellini, A. J. Cuesta, R. Jimenez, and L. Verde. Constraints on deviations from ΛCDM within Horndeski gravity. *JCAP*, 2:053, February 2016.

[109] Ted Jacobson and David Mattingly. Gravity with a dynamical preferred frame. *Phys. Rev.*, D64:024028, 2001.

[110] T. G Zlosnik, P. G Ferreira, and G. D Starkman. Modifying gravity with the Aether: An alternative to Dark Matter. *Phys. Rev.*, D75:044017, 2007.

[111] Lavinia Heisenberg. Generalization of the Proca Action. *JCAP*, 1405:015, 2014.

[112] D.G. Boulware and Stanley Deser. Can gravitation have a finite range? *Phys.Rev.*, D6:3368–3382, 1972.

[113] Claudia de Rham and Gregory Gabadadze. Generalization of the Fierz-Pauli Action. *Phys.Rev.*, D82:044020, 2010.

[114] Marco Crisostomi, Kazuya Koyama, and Gianmassimo Tasinato. Extended Scalar-Tensor Theories of Gravity. *JCAP*, 1604(04):044, 2016.

[115] Antonio De Felice, Lavinia Heisenberg, Ryotaro Kase, Shinji Mukohyama, Shinji Tsujikawa, and Ying-li Zhang. Cosmology in generalized Proca theories. *JCAP*, 1606(06):048, 2016.

[116] Antonio De Felice, Lavinia Heisenberg, Ryotaro Kase, Shinji Mukohyama, Shinji Tsujikawa, and Ying-li Zhang. Effective gravitational couplings for cosmological perturbations in generalized Proca theories. *Phys. Rev.*, D94(4):044024, 2016.

[117] Shintaro Nakamura, Ryotaro Kase, and Shinji Tsujikawa. Cosmology in beyond-generalized Proca theories. *Phys. Rev.*, D95(10):104001, 2017.

[118] Antonio de Felice, Lavinia Heisenberg, and Shinji Tsujikawa. Observational constraints on generalized Proca theories. 2017.

[119] George F. R. Ellis and Henk van Elst. Cosmological models: Cargese lectures 1998. *NATO Sci. Ser. C*, 541:1–116, 1999.

[120] K.C. Jacobs, Mathematics California Institute of Technology. Division of Physics, and Astronomy. *Bianchi Type I Cosmological Models*. CIT theses. California Institute of Technology, 1969.

[121] Edward Kasner. Geometrical theorems on Einstein's cosmological equations. *Am. J. Math.*, 43:217–221, 1921.

[122] J. M. Centrella, editor. *DYNAMICAL SPACE-TIMES AND NUMERICAL RELATIVITY. PROCEEDINGS, WORKSHOP, PHILADELPHIA, USA, OCTOBER 7-11, 1985*, 1986.

[123] Oliver Lindblad Petersen. The mode solution of the wave equation in Kasner space-times and redshift. *Math. Phys. Anal. Geom.*, 19(4):26, 2016.

[124] Norbert Wex. Testing Relativistic Gravity with Radio Pulsars. 2014.

[125] Ioannis Kamaretsos, Mark Hannam, Sascha Husa, and B. S. Sathyaprakash. Black-hole hair loss: learning about binary progenitors from ringdown signals. *Phys. Rev.*, D85:024018, 2012.

[126] Hiroyuki Nakano, Takahiro Tanaka, and Takashi Nakamura. Possible golden events for ringdown gravitational waves. *Phys. Rev.*, D92(6):064003, 2015.

[127] Vitor Cardoso and Leonardo Gualtieri. Testing the black hole no-hair hypothesis. *Class. Quant. Grav.*, 33(17):174001, 2016.

[128] Eric Thrane, Paul D. Lasky, and Yuri Levin. Challenges testing the no-hair theorem with gravitational waves. 2017.

[129] Kostas Glampedakis, George Pappas, Hector O. Silva, and Emanuele Berti. Post-Kerr black hole spectroscopy. *Phys. Rev.*, D96(6):064054, 2017.

[130] Enrico Barausse and Thomas P. Sotiriou. Perturbed Kerr Black Holes can probe deviations from General Relativity. *Phys. Rev. Lett.*, 101:099001, 2008.

[131] Emanuele Berti, Jaime Cardoso, Vitor Cardoso, and Marco Cavaglia. Matched-filtering and parameter estimation of ringdown waveforms. *Phys. Rev.*, D76:104044, 2007.

[132] Huan Yang, Kent Yagi, Jonathan Blackman, Luis Lehner, Vasileios Paschalidis, Frans Pretorius, and Nicolas Yunes. Black hole spectroscopy with coherent mode stacking. *Phys. Rev. Lett.*, 118(16):161101, 2017.

[133] Vishal Baibhav, Emanuele Berti, Vitor Cardoso, and Gaurav Khanna. Black Hole Spectroscopy: Systematic Errors and Ringdown Energy Estimates. 2017.

[134] Tomohiro Harada. Stability analysis of spherically symmetric star in scalar - tensor theories of gravity. *Prog. Theor. Phys.*, 98:359–379, 1997.

[135] O. J. Kwon, Y. D. Kim, Y. S. Myung, B. H. Cho, and Y. J. Park. Stability of the schwarzschild black hole in brans-dicke theory. *Phys. Rev. D*, 34:333–342, Jul 1986.

[136] Paul D. Lasky and Daniela D. Doneva. Stability and Quasinormal Modes of Black holes in Tensor-Vector-Scalar theory: Scalar Field Perturbations. *Phys. Rev.*, D82:124068, 2010.

[137] Vitor Cardoso and Leonardo Gualtieri. Perturbations of Schwarzschild black holes in Dynamical Chern-Simons modified gravity. *Phys. Rev.*, D80:064008, 2009. [Erratum: Phys. Rev.D81,089903(2010)].

[138] C. Molina, Paolo Pani, Vitor Cardoso, and Leonardo Gualtieri. Gravitational signature of Schwarzschild black holes in dynamical Chern-Simons gravity. *Phys. Rev.*, D81:124021, 2010.

[139] Scott Dodelson. *Modern Cosmology*. Academic Press, Amsterdam, 2003.

[140] T. P. Sotiriou and V. Faraoni. Black Holes in Scalar-Tensor Gravity. *Physical Review Letters*, 108(8):081103, February 2012.

[141] Thomas P. Sotiriou and Shuang-Yong Zhou. Black hole hair in generalized scalar-tensor gravity. *Phys. Rev. Lett.*, 112:251102, 2014.

[142] Javier Chagoya, Gustavo Niz, and Gianmassimo Tasinato. Black Holes and Abelian Symmetry Breaking. *Class. Quant. Grav.*, 33(17):175007, 2016.

[143] L. Heisenberg, R. Kase, M. Minamitsuji, and S. Tsujikawa. Black holes in vector-tensor theories. *JCAP*, 8:024, August 2017.

[144] Stephon Alexander and Nicolas Yunes. Chern-Simons Modified General Relativity. *Phys. Rept.*, 480:1–55, 2009.

[145] Tullio Regge and John A. Wheeler. Stability of a Schwarzschild singularity. *Phys. Rev.*, 108:1063–1069, 1957.

[146] Luciano Rezzolla. Gravitational waves from perturbed black holes and relativistic stars. *ICTP Lect. Notes Ser.*, 14:255–316, 2003.

[147] Karl Martel and Eric Poisson. Gravitational perturbations of the Schwarzschild spacetime: A Practical covariant and gauge-invariant formalism. *Phys. Rev.*, D71:104003, 2005.

[148] Justin L. Ripley and Kent Yagi. Black hole perturbation under a 2 + 2 decomposition in the action. *Phys. Rev.*, D97(2):024009, 2018.

[149] Eanna E. Flanagan and Tanja Hinderer. Constraining neutron star tidal Love numbers with gravitational wave detectors. *Phys. Rev.*, D77:021502, 2008.

[150] Taylor Binnington and Eric Poisson. Relativistic theory of tidal Love numbers. *Phys. Rev.*, D80:084018, 2009.

[151] Thibault Damour and Alessandro Nagar. Relativistic tidal properties of neutron stars. *Phys. Rev.*, D80:084035, 2009.

[152] Reinaldo J. Gleiser and Gustavo Dotti. Instability of the negative mass Schwarzschild naked singularity. *Class. Quant. Grav.*, 23:5063–5078, 2006.

[153] Frank J. Zerilli. Effective potential for even parity Regge-Wheeler gravitational perturbation equations. *Phys. Rev. Lett.*, 24:737–738, 1970.

[154] Apratim Ganguly, Radouane Gannouji, Manuel Gonzalez-Espinoza, and Carlos Pizarro-Moya. Black hole stability under odd-parity perturbations in Horndeski gravity. 2017.

[155] Tsutomu Kobayashi, Hayato Motohashi, and Teruaki Suyama. Black hole perturbation in the most general scalar-tensor theory with second-order field equations I: the odd-parity sector. *Phys. Rev.*, D85:084025, 2012.

[156] Tsutomu Kobayashi, Hayato Motohashi, and Teruaki Suyama. Black hole perturbation in the most general scalar-tensor theory with second-order field equations. II. The even-parity sector. *Phys. Rev.*, D89(8):084042, 2014.

[157] Paolo Creminelli and Filippo Vernizzi. Dark Energy after GW170817 and GRB170817A. *Phys. Rev. Lett.*, 119(25):251302, 2017.

[158] Y. Zhang, Y. X. Gui, and FengLin Li. Quasinormal modes of a Schwarzschild black hole surrounded by quintessence: Electromagnetic perturbations. *Gen. Rel. Grav.*, 39:1003–1010, 2007.

[159] Bobir Toshmatov, Ahmadjon Abdujabbarov, Zdenek Stuchlik, and Bobomurat Ahmedov. Quasinormal modes of test fields around regular black holes. *Phys. Rev.*, D91(8):083008, 2015.

[160] A. J. M. Medved, Damien Martin, and Matt Visser. Dirty black holes: Quasinormal modes. *Class. Quant. Grav.*, 21:1393–1406, 2004.

[161] Christopher Eling and Ted Jacobson. Black Holes in Einstein-Aether Theory. *Class. Quant. Grav.*, 23:5643–5660, 2006. [Erratum: Class. Quant. Grav.27,049802(2010)].

[162] Paolo Pani and Vitor Cardoso. Are black holes in alternative theories serious astrophysical candidates? The Case for Einstein-Dilaton-Gauss-Bonnet black holes. *Phys. Rev.*, D79:084031, 2009.

[163] P. Pani. Applications of black hole perturbation theory. *Eur. Phys. J. Plus*, 127:67, 2012.

[164] B. P. Abbott et. al. Gw170817: Observation of gravitational waves from a binary neutron star inspiral. *Phys. Rev. Lett.*, 119:161101, Oct 2017.

[165] B. P. Abbott et. al. Multi-messenger observations of a binary neutron star merger. *The Astrophysical Journal Letters*, 848(2):L12, 2017.

[166] B. P. Abbott et. al. Gravitational waves and gamma-rays from a binary neutron star merger: Gw170817 and grb 170817a. *The Astrophysical Journal Letters*, 848(2):L13, 2017.

[167] A. Goldstein et. al. An ordinary short gamma-ray burst with extraordinary implications: Fermi -gbm detection of grb 170817a. *The Astrophysical Journal Letters*, 848(2):L14, 2017.

[168] V. Savchenko et. al. Integral detection of the first prompt gamma-ray signal coincident with the gravitational-wave event gw170817. *The Astrophysical Journal Letters*, 848(2):L15, 2017.

[169] Tessa Baker, Emilio Bellini, Pedro G. Ferreira, Macarena Lagos, Johannes Noller, and Ignacy Sawicki. Strong constraints on cosmological gravity from GW170817 and GRB 170817A. 2017.

[170] Jeremy Sakstein and Bhuvnesh Jain. Implications of the Neutron Star Merger GW170817 for Cosmological Scalar-Tensor Theories. *Phys. Rev. Lett.*, 119(25):251303, 2017.

[171] Jose Maria Ezquiaga and Miguel Zumalacarregui. Dark Energy After GW170817: Dead Ends and the Road Ahead. *Phys. Rev. Lett.*, 119(25):251304, 2017.

[172] M.P. Hobson, E.G. P, G.P. Efstathiou, and A.N. Lasenby. *General Relativity: An Introduction for Physicists*. Cambridge University Press, 2006.

[173] Timothy Clifton, Pedro G. Ferreira, Antonio Padilla, and Constantinos Skordis. Modified Gravity and Cosmology. *Phys. Rept.*, 513:1–189, 2012.

[174] D. A. Coulter, R. J. Foley, C. D. Kilpatrick, M. R. Drout, A. L. Piro, B. J. Shappee, M. R. Siebert, J. D. Simon, N. Ulloa, D. Kasen, B. F. Madore, A. Murguia-Berthier, Y.-C. Pan, J. X. Prochaska, E. Ramirez-Ruiz, A. Rest, and C. Rojas-Bravo. Swope Supernova Survey 2017a (SSS17a), the optical counterpart to a gravitational wave source. *Science*, 358:1556–1558, December 2017.

[175] Lucas Lombriser and Andy Taylor. Breaking a Dark Degeneracy with Gravitational Waves. *JCAP*, 1603(03):031, 2016.

[176] Lucas Lombriser and Nelson A. Lima. Challenges to Self-Acceleration in Modified Gravity from Gravitational Waves and Large-Scale Structure. *Phys. Lett.*, B765:382–385, 2017.

[177] Tim Johannsen. Sgr A* and General Relativity. *Class. Quant. Grav.*, 33(11):113001, 2016.

[178] Clifford M. Will. Testing the general relativistic no-hair theorems using the Galactic center black hole SgrA*. *Astrophys. J.*, 674:L25–L28, 2008.

[179] Dimitrios Psaltis, Norbert Wex, and Michael Kramer. A Quantitative Test of the No-Hair Theorem with Sgr A* using stars, pulsars, and the Event Horizon Telescope. *Astrophys. J.*, 818(2):121, 2016.

[180] A. Hees et al. Testing General Relativity with stellar orbits around the supermassive black hole in our Galactic center. *Phys. Rev. Lett.*, 118(21):211101, 2017.

[181] Dimitrios Psaltis and Tim Johannsen. Sgr A*: The Optimal Testbed of Strong-Field Gravity. *J. Phys. Conf. Ser.*, 283:012030, 2011.

[182] Avery E. Broderick, Tim Johannsen, Abraham Loeb, and Dimitrios Psaltis. Testing the No-Hair Theorem with Event Horizon Telescope Observations of Sagittarius A*. *Astrophys. J.*, 784:7, 2014.

[183] Tim Johannsen, Carlos Wang, Avery E. Broderick, Sheperd S. Doeleman, Vincent L. Fish, Abraham Loeb, and Dimitrios Psaltis. Testing General Relativity with Accretion-Flow Imaging of Sgr A*. *Phys. Rev. Lett.*, 117(9):091101, 2016.

[184] Carlos A. R. Herdeiro and Eugen Radu. Asymptotically flat black holes with scalar hair: a review. *Int. J. Mod. Phys.*, D24(09):1542014, 2015.

[185] Cosimo Bambi. Black Holes: A Laboratory for Testing Strong Gravity. *Springer Singapore*, pages XV, 340, 2017.

[186] Eugeny Babichev, Christos Charmousis, and Antoine Lehébel. Asymptotically flat black holes in Horndeski theory and beyond. *JCAP*, 1704(04):027, 2017.

[187] Lavinia Heisenberg, Ryotaro Kase, Masato Minamitsuji, and Shinji Tsujikawa. Black holes in vector-tensor theories. *JCAP*, 1708(08):024, 2017.

[188] Thomas P. Sotiriou. Black Holes and Scalar Fields. *Class. Quant. Grav.*, 32(21):214002, 2015.

[189] Ted Jacobson. Primordial black hole evolution in tensor scalar cosmology. *Phys. Rev. Lett.*, 83:2699–2702, 1999.

[190] Eric W. Hirschmann, Luis Lehner, Steven L. Liebling, and Carlos Palenzuela. Black hole dynamics in einstein-maxwell-dilaton theory. *Phys. Rev. D*, 97:064032, Mar 2018.

[191] Vitor Cardoso, Sayan Chakrabarti, Paolo Pani, Emanuele Berti, and Leonardo Gualtieri. Floating and sinking: The Imprint of massive scalars around rotating black holes. *Phys. Rev. Lett.*, 107:241101, 2011.

[192] Rhondale Tso, Maximiliano Isi, Yanbei Chen, and Leo Stein. Modeling the Dispersion and Polarization Content of Gravitational Waves for Tests of General Relativity. In *Proceedings, 7th Meeting on CPT and Lorentz Symmetry (CPT 16): Bloomington, Indiana, USA, June 20-24, 2016*, pages 205–208, 2017.

[193] Antonio De Felice and Shinji Tsujikawa. Conditions for the cosmological viability of the most general scalar-tensor theories and their applications to extended Galileon dark energy models. *JCAP*, 1202:007, 2012.

[194] Pascual Jordan. The present state of Dirac's cosmological hypothesis. *Z. Phys.*, 157:112–121, 1959.

[195] C. Brans and R. H. Dicke. Mach's principle and a relativistic theory of gravitation. *Phys. Rev.*, 124:925–935, 1961.

[196] G. W. Horndeski. Second-Order Scalar-Tensor Field Equations in a Four-Dimensional Space. *International Journal of Theoretical Physics*, 10:363–384, September 1974.

[197] Jerome Gleyzes, David Langlois, Federico Piazza, and Filippo Vernizzi. Healthy theories beyond Horndeski. *Phys. Rev. Lett.*, 114(21):211101, 2015.

[198] Miguel Zumalacarregui and Juan Garcia-Bellido. Transforming gravity: from derivative couplings to matter to second-order scalar-tensor theories beyond the Horndeski Lagrangian. *Phys. Rev.*, D89:064046, 2014.

[199] David Langlois. Degenerate Higher-Order Scalar-Tensor (DHOST) theories. In *Proceedings, 52nd Rencontres de Moriond on Gravitation (Moriond Gravitation 2017): La Thuile, Italy, March 25-April 1, 2017*, pages 221–228, 2017.

[200] Claudia de Rham and Lavinia Heisenberg. Cosmology of the Galileon from Massive Gravity. *Phys. Rev.*, D84:043503, 2011.

[201] Giuseppe Papallo and Harvey S. Reall. On the local well-posedness of Lovelock and Horndeski theories. *Phys. Rev.*, D96(4):044019, 2017.

[202] Giuseppe Papallo. On the hyperbolicity of the most general Horndeski theory. *Phys. Rev.*, D96(12):124036, 2017.

[203] Thomas P. Sotiriou and Shuang-Yong Zhou. Black hole hair in generalized scalar-tensor gravity: An explicit example. *Phys. Rev.*, D90:124063, 2014.

[204] David Langlois, Ryo Saito, Daisuke Yamauchi, and Karim Noui. Scalar-tensor theories and modified gravity in the wake of GW170817. 2017.

[205] Marco Crisostomi and Kazuya Koyama. Vainshtein mechanism after GW170817. *Phys. Rev.*, D97(2):021301, 2018.

[206] Dario Bettoni and Stefano Liberati. Disformal invariance of second order scalar-tensor theories: Framing the Horndeski action. *Phys. Rev.*, D88:084020, 2013.

[207] Cedric Deffayet, Oriol Pujolas, Ignacy Sawicki, and Alexander Vikman. Imperfect Dark Energy from Kinetic Gravity Braiding. *JCAP*, 1010:026, 2010.

[208] A. A. H. Graham and R. Jha. Nonexistence of black holes with noncanonical scalar fields. *Phys. Rev. D*, 89(8):084056, April 2014.

[209] Lam Hui and Alberto Nicolis. No-Hair Theorem for the Galileon. *Phys. Rev. Lett.*, 110:241104, 2013.

[210] Andrea Maselli, Hector O. Silva, Masato Minamitsuji, and Emanuele Berti. Slowly rotating black hole solutions in Horndeski gravity. *Phys. Rev.*, D92(10):104049, 2015.

[211] Antoine Lehébel, Eugeny Babichev, and Christos Charmousis. A no-hair theorem for stars in Horndeski theories. *JCAP*, 1707(07):037, 2017.

[212] James Healy, Tanja Bode, Roland Haas, Enrique Pazos, Pablo Laguna, Deirdre M. Shoemaker, and Nicolas Yunes. Late Inspiral and Merger of Binary Black Holes in Scalar-Tensor Theories of Gravity. *Class. Quant. Grav.*, 29:232002, 2012.

[213] R. Benkel, T. P. Sotiriou, and H. Witek. Black hole hair formation in shift-symmetric generalised scalar-tensor gravity. *Classical and Quantum Gravity*, 34(6):064001, March 2017.

[214] Andrea Maselli, Leonardo Gualtieri, Paolo Pani, Luigi Stella, and Valeria Ferrari. Testing Gravity with Quasi Periodic Oscillations from accreting Black Holes: the Case of the Einstein-Dilaton-Gauss-Bonnet Theory. *Astrophys. J.*, 801(2):115, 2015.

[215] Andrea Maselli, Paolo Pani, Leonardo Gualtieri, and Valeria Ferrari. Rotating black holes in Einstein-Dilaton-Gauss-Bonnet gravity with finite coupling. *Phys. Rev.*, D92(8):083014, 2015.

[216] Burkhard Kleihaus, Jutta Kunz, and Sindy Mojica. Quadrupole Moments of Rapidly Rotating Compact Objects in Dilatonic Einstein-Gauss-Bonnet Theory. *Phys. Rev.*, D90(6):061501, 2014.

[217] Burkhard Kleihaus, Jutta Kunz, and Eugen Radu. Rotating Black Holes in Dilatonic Einstein-Gauss-Bonnet Theory. *Phys. Rev. Lett.*, 106:151104, 2011.

[218] Yungui Gong, Eleftherios Papantonopoulos, and Zhu Yi. Constraints on Scalar-Tensor Theory of Gravity by the Recent Observational Results on Gravitational Waves. 2017.

[219] L. N. Granda and D. F. Jimenez. The speed of gravitational waves and power-law solutions in a scalar-tensor model. 2018.

[220] Daniela D. Doneva and Stoytcho S. Yazadjiev. New Gauss-Bonnet Black Holes with Curvature-Induced Scalarization in Extended Scalar-Tensor Theories. *Phys. Rev. Lett.*, 120(13):131103, 2018.

[221] Kent Yagi and Leo C. Stein. Black Hole Based Tests of General Relativity. *Class. Quant. Grav.*, 33(5):054001, 2016.

[222] D. Garfinkle, F. Pretorius, and N. Yunes. Linear stability analysis and the speed of gravitational waves in dynamical Chern-Simons modified gravity. *Phys. Rev. D*, 82(4):041501, August 2010.

[223] S. Alexander and J. Martin. Birefringent gravitational waves and the consistency check of inflation. *Phys. Rev. D*, 71(6):063526, March 2005.

[224] B. L. Hu. Gravitational Waves in a Bianchi Type I Universe. *Phys. Rev.*, D18:969–982, 1978.

[225] Emory F. Bunn, Pedro Ferreira, and Joseph Silk. How anisotropic is our universe? *Phys. Rev. Lett.*, 77:2883–2886, 1996.

[226] John D. Barrow, Pedro G. Ferreira, and Joseph Silk. Constraints on a primordial magnetic field. *Phys. Rev. Lett.*, 78:3610–3613, 1997.

[227] P. A. R. Ade et al. Planck 2015 results - XVIII. Background geometry and topology of the Universe. *Astron. Astrophys.*, 594:A18, 2016.

[228] R. Bartnik and J. Mckinnon. Particle - Like Solutions of the Einstein Yang-Mills Equations. *Phys. Rev. Lett.*, 61:141–144, 1988.

[229] M. S. Volkov and D. V. Galtsov. NonAbelian Einstein Yang-Mills black holes. *JETP Lett.*, 50:346–350, 1989. [Pisma Zh. Eksp. Teor. Fiz.50,312(1989)].

[230] Noriko Shiiki and Nobuyuki Sawado. Black holes with skyrme hair. 2005.

[231] Sven Bjarke Gudnason, Muneto Nitta, and Nobuyuki Sawado. Black hole Skyrmion in a generalized Skyrme model. *JHEP*, 09:055, 2016.

[232] C. Adam, O. Kichakova, Ya. Shnir, and A. Wereszczynski. Hairy black holes in the general Skyrme model. *Phys. Rev.*, D94(2):024060, 2016.

[233] J. Zuntz, T. G Zlosnik, F. Bourliot, P. G. Ferreira, and G. D. Starkman. Vector field models of modified gravity and the dark sector. *Phys. Rev.*, D81:104015, 2010.

[234] B. Audren, D. Blas, M. M. Ivanov, J. Lesgourgues, and S. Sibiryakov. Cosmological constraints on deviations from Lorentz invariance in gravity and dark matter. *JCAP*, 1503(03):016, 2015.

[235] Ted Jacobson. Einstein-aether gravity: A Status report. *PoS*, QG-PH:020, 2007.

[236] Kent Yagi, Diego Blas, Nicolas Yunes, and Enrico Barausse. Strong Binary Pulsar Constraints on Lorentz Violation in Gravity. *Phys. Rev. Lett.*, 112(16):161101, 2014.

[237] Kent Yagi, Diego Blas, Enrico Barausse, and Nicolas Yunes. Constraints on Einstein-Aether theory and Horava gravity from binary pulsar observations. *Phys. Rev.*, D89(8):084067, 2014. [Erratum: Phys. Rev.D90,no.6,069901(2014)].

[238] Joseph A. Zuntz, P. G. Ferreira, and T. G. Zlosnik. Constraining Lorentz violation with cosmology. *Phys. Rev. Lett.*, 101:261102, 2008.

[239] Christopher Eling and Ted Jacobson. Spherical solutions in Einstein-aether theory: Static aether and stars. *Class. Quant. Grav.*, 23:5625–5642, 2006. [Erratum: Class. Quant. Grav.27,049801(2010)].

[240] R. A. Konoplya and A. Zhidenko. Gravitational spectrum of black holes in the Einstein-Aether theory. *Phys. Lett.*, B648:236–239, 2007.

[241] Enrico Barausse, Ted Jacobson, and Thomas P. Sotiriou. Black holes in Einstein-aether and Horava-Lifshitz gravity. *Phys. Rev.*, D83:124043, 2011.

[242] Enrico Barausse and Thomas P. Sotiriou. Black holes in Lorentz-violating gravity theories. *Class. Quant. Grav.*, 30:244010, 2013.

[243] Gianmassimo Tasinato. Cosmic Acceleration from Abelian Symmetry Breaking. *JHEP*, 04:067, 2014.

[244] Erwan Allys, Patrick Peter, and Yeinzon Rodriguez. Generalized Proca action for an Abelian vector field. *JCAP*, 1602(02):004, 2016.

[245] Erwan Allys, Juan P. Beltran Almeida, Patrick Peter, and Yeinzon Rodriguez. On the 4D generalized Proca action for an Abelian vector field. *JCAP*, 1609(09):026, 2016.

[246] Jose Beltran Jimenez and Lavinia Heisenberg. Derivative self-interactions for a massive vector field. *Phys. Lett.*, B757:405–411, 2016.

[247] Lavinia Heisenberg and Shinji Tsujikawa. Hairy black hole solutions in $U(1)$ gauge-invariant scalar-vector-tensor theories. 2018.

[248] Lavinia Heisenberg. Scalar-Vector-Tensor Gravity Theories. 2018.

[249] Claudia de Rham, Gregory Gabadadze, and Andrew J. Tolley. Resummation of Massive Gravity. *Phys.Rev.Lett.*, 106:231101, 2011.

[250] S.F. Hassan and Rachel A. Rosen. Bimetric Gravity from Ghost-free Massive Gravity. *JHEP*, 1202:126, 2012.

[251] Rachel A Rosen. Non-Singular Black Holes in Massive Gravity: Time-Dependent Solutions. *JHEP*, 10:206, 2017.

[252] Eugeny Babichev and Richard Brito. Black holes in massive gravity. *Class. Quant. Grav.*, 32:154001, 2015.

[253] Eugeny Babichev and Alessandro Fabbri. Rotating black holes in massive gravity. *Phys. Rev.*, D90:084019, 2014.

[254] Richard Brito, Vitor Cardoso, and Paolo Pani. Massive spin-2 fields on black hole spacetimes: Instability of the Schwarzschild and Kerr solutions and bounds on the graviton mass. *Phys. Rev.*, D88(2):023514, 2013.

[255] Richard Brito, Vitor Cardoso, and Paolo Pani. Black holes with massive graviton hair. *Phys. Rev.*, D88:064006, 2013.

[256] Nicolas Yunes and Frans Pretorius. Dynamical Chern-Simons Modified Gravity. I. Spinning Black Holes in the Slow-Rotation Approximation. *Phys. Rev.*, D79:084043, 2009.

[257] Kohkichi Konno, Toyoki Matsuyama, and Satoshi Tanda. Rotating black hole in extended Chern-Simons modified gravity. *Prog. Theor. Phys.*, 122:561–568, 2009.

[258] Kent Yagi, Nicolas Yunes, and Takahiro Tanaka. Slowly Rotating Black Holes in Dynamical Chern-Simons Gravity: Deformation Quadratic in the Spin. *Phys. Rev.*, D86:044037, 2012. [Erratum: Phys. Rev.D89,049902(2014)].

[259] Kohkichi Konno and Rohta Takahashi. Scalar field excited around a rapidly rotating black hole in Chern-Simons modified gravity. *Phys. Rev.*, D90(6):064011, 2014.

[260] Leo C. Stein. Rapidly rotating black holes in dynamical Chern-Simons gravity: Decoupling limit solutions and breakdown. *Phys. Rev.*, D90(4):044061, 2014.

[261] Robert McNees, Leo C. Stein, and Nicolas Yunes. Extremal black holes in dynamical Chern-Simons gravity. *Class. Quant. Grav.*, 33(23):235013, 2016.

[262] Clifford M. Will and Nicolas Yunes. Testing alternative theories of gravity using LISA. *Class. Quant. Grav.*, 21:4367, 2004.

[263] Saeed Mirshekari and Clifford M. Will. Compact binary systems in scalar-tensor gravity: Equations of motion to 2.5 post-Newtonian order. *Phys. Rev.*, D87(8):084070, 2013.

[264] M. W. Horbatsch and C. P. Burgess. Cosmic Black-Hole Hair Growth and Quasar OJ287. *JCAP*, 1205:010, 2012.

[265] Nicolas Yunes and Frans Pretorius. Fundamental Theoretical Bias in Gravitational Wave Astrophysics and the Parameterized Post-Einsteinian Framework. *Phys. Rev.*, D80:122003, 2009.

[266] Emanuele Berti, Alessandra Buonanno, and Clifford M. Will. Testing general relativity and probing the merger history of massive black holes with LISA. *Class. Quant. Grav.*, 22:S943–S954, 2005.

[267] Nicolas Yunes, Paolo Pani, and Vitor Cardoso. Gravitational Waves from Quasicircular Extreme Mass-Ratio Inspirals as Probes of Scalar-Tensor Theories. *Phys. Rev.*, D85:102003, 2012.

[268] Carlos F. Sopuerta and Nicolas Yunes. Extreme and Intermediate-Mass Ratio Inspirals in Dynamical Chern-Simons Modified Gravity. *Phys. Rev.*, D80:064006, 2009.

[269] A. I. Vainshtein. To the problem of nonvanishing gravitation mass. *Phys. Lett.*, 39B:393–394, 1972.

[270] Justin Khoury and Amanda Weltman. Chameleon cosmology. *Phys. Rev.*, D69:044026, 2004.

[271] Kurt Hinterbichler and Justin Khoury. Symmetron Fields: Screening Long-Range Forces Through Local Symmetry Restoration. *Phys. Rev. Lett.*, 104:231301, 2010.

[272] Lam Hui and Alberto Nicolis. Proposal for an Observational Test of the Vainshtein Mechanism. *Phys. Rev. Lett.*, 109:051304, 2012.

[273] Leor Barack et al. Black holes, gravitational waves and fundamental physics: a roadmap. 2018.

[274] Richard Brito, Alessandra Buonanno, and Vivien Raymond. Black-hole Spectroscopy by Making Full Use of Gravitational-Wave Modeling. 2018.

[275] Y. Akrami et al. Planck 2018 results. I. Overview and the cosmological legacy of Planck. 2018.

[276] Cosimo Bambi. Astrophysical Black Holes: A Review. 2019.

[277] Juan Martin Maldacena. The Large N limit of superconformal field theories and supergravity. *Int. J. Theor. Phys.*, 38:1113–1133, 1999. [Adv. Theor. Math. Phys.2,231(1998)].

[278] Alvaro Nunez and Andrei O. Starinets. AdS / CFT correspondence, quasinormal modes, and thermal correlators in N=4 SYM. *Phys. Rev.*, D67:124013, 2003.

[279] Dam T. Son and Andrei O. Starinets. Viscosity, Black Holes, and Quantum Field Theory. *Ann. Rev. Nucl. Part. Sci.*, 57:95–118, 2007.

[280] Sean A. Hartnoll. Lectures on holographic methods for condensed matter physics. *Class. Quant. Grav.*, 26:224002, 2009.

[281] Christopher P. Herzog. Lectures on Holographic Superfluidity and Superconductivity. *J. Phys.*, A42:343001, 2009.

[282] Saul A. Teukolsky. The Kerr Metric. *Class. Quant. Grav.*, 32(12):124006, 2015.

[283] S. A. Teukolsky. Perturbations of a Rotating Black Hole. I. Fundamental Equations for Gravitational, Electromagnetic, and Neutrino-Field Perturbations. *Astrophys. J.*, 185:635–648, October 1973.

[284] P. Pani, V. Cardoso, L. Gualtieri, E. Berti, and A. Ishibashi. Perturbations of slowly rotating black holes: Massive vector fields in the Kerr metric. *Phys. Rev. D*, 86(10):104017, November 2012.

[285] Paolo Pani. Advanced Methods in Black-Hole Perturbation Theory. *Int. J. Mod. Phys.*, A28:1340018, 2013.

[286] Paolo Pani, Emanuele Berti, and Leonardo Gualtieri. Scalar, Electromagnetic and Gravitational Perturbations of Kerr-Newman Black Holes in the Slow-Rotation Limit. *Phys. Rev.*, D88:064048, 2013.

[287] Vitor Cardoso and Jose P. S. Lemos. Quasinormal modes of Schwarzschild anti-de Sitter black holes: Electromagnetic and gravitational perturbations. *Phys. Rev.*, D64:084017, 2001.

[288] E. W. Leaver. An analytic representation for the quasi-normal modes of Kerr black holes. *Proceedings of the Royal Society of London Series A*, 402:285–298, December 1985.

[289] H. T. Cho, A. S. Cornell, Jason Doukas, T. R. Huang, and Wade Naylor. A New Approach to Black Hole Quasinormal Modes: A Review of the Asymptotic Iteration Method. *Adv. Math. Phys.*, 2012:281705, 2012.

[290] S. R. Dolan and A. C. Ottewill. On an expansion method for black hole quasinormal modes and Regge poles. *Classical and Quantum Gravity*, 26(22):225003, November 2009.

[291] H.-J. Blome and B. Mashhoon. Quasi-normal oscillations of a schwarzschild black hole. *Physics Letters A*, 100:231–234, January 1984.

[292] M. S. Churilova. Analytical quasinormal modes of spherically symmetric black holes in the eikonal regime. *Eur. Phys. J.*, C79(7):629, 2019.

[293] A. Zhidenko. Quasinormal modes of Schwarzschild de Sitter black holes. *Class. Quant. Grav.*, 21:273–280, 2004.

[294] Oscar J. C. Dias, Harvey S. Reall, and Jorge E. Santos. Strong cosmic censorship: taking the rough with the smooth. *JHEP*, 10:001, 2018.

[295] Steven L. Detweiler. KLEIN-GORDON EQUATION AND ROTATING BLACK HOLES. *Phys. Rev.*, D22:2323–2326, 1980.

[296] Hironobu Furuhashi and Yasusada Nambu. Instability of massive scalar fields in Kerr-Newman space-time. *Prog. Theor. Phys.*, 112:983–995, 2004.

[297] Vitor Cardoso and Shijun Yoshida. Superradiant instabilities of rotating black branes and strings. *JHEP*, 07:009, 2005.

[298] Sam R. Dolan. Instability of the massive Klein-Gordon field on the Kerr spacetime. *Phys. Rev.*, D76:084001, 2007.

[299] Shahar Hod. On the instability regime of the rotating Kerr spacetime to massive scalar perturbations. *Phys. Lett.*, B708:320–323, 2012.

[300] Shahar Hod. Stationary Scalar Clouds Around Rotating Black Holes. *Phys. Rev.*, D86:104026, 2012. [Erratum: Phys. Rev.D86,129902(2012)].

[301] Helvi Witek, Vitor Cardoso, Akihiro Ishibashi, and Ulrich Sperhake. Superradiant instabilities in astrophysical systems. *Phys. Rev.*, D87(4):043513, 2013.

[302] Aron Jansen. Overdamped modes in Schwarzschild-de Sitter and a Mathematica package for the numerical computation of quasinormal modes. *Eur. Phys. J. Plus*, 132(12):546, 2017.

[303] Vitor Cardoso, Joao L. Costa, Kyriakos Destounis, Peter Hintz, and Aron Jansen. Quasinormal modes and Strong Cosmic Censorship. *Phys. Rev. Lett.*, 120(3):031103, 2018.

[304] G. W. Gibbons and S. W. Hawking. Cosmological event horizons, thermodynamics, and particle creation. *Phys. Rev. D*, 15:2738–2751, May 1977.

[305] R. A. Konoplya and A. V. Zhidenko. Stability and quasinormal modes of the massive scalar field around Kerr black holes. *Phys. Rev. D*, 73(12):124040, June 2006.

[306] Shijun Yoshida, Nami Uchikata, and Toshifumi Futamase. Quasinormal modes of kerr–de sitter black holes. *Phys. Rev. D*, 81:044005, Feb 2010.

[307] Semyon Dyatlov. Asymptotic distribution of quasi-normal modes for Kerr-de Sitter black holes. *Annales Henri Poincare*, 13:1101–1166, 2012.

[308] Oscar J. C. Dias, Felicity C. Eperon, Harvey S. Reall, and Jorge E. Santos. Strong cosmic censorship in de sitter space. *Phys. Rev. D*, 97:104060, May 2018.

[309] E. T. Newman and A. I. Janis. Note on the kerr spinning particle metric. *Journal of Mathematical Physics*, 6(6):915–917, 1965.

[310] Vitor Cardoso and Leonardo Gualtieri. Testing the black hole no-hair hypothesis. *Classical and Quantum Gravity*, 33(17):174001, 2016.

[311] Richard Brito, Vitor Cardoso, and Paolo Pani. Superradiance. *Lect. Notes Phys.*, 906:pp.1–237, 2015.

[312] Richard Brito, Vitor Cardoso, and Paolo Pani. Partially massless gravitons do not destroy general relativity black holes. *Phys. Rev.*, D87(12):124024, 2013.

[313] Eugeny Babichev, Richard Brito, and Paolo Pani. Linear stability of nonbidiagonal black holes in massive gravity. *Phys. Rev.*, D93(4):044041, 2016.

[314] Cheng-Yong Zhang, Shao-Jun Zhang, and Bin Wang. Superradiant instability of Kerr-de Sitter black holes in scalar-tensor theory. *JHEP*, 08:011, 2014.

[315] T. Baker, E. Bellini, P. G. Ferreira, M. Lagos, J. Noller, and I. Sawicki. Strong Constraints on Cosmological Gravity from GW170817 and GRB 170817A. *Physical Review Letters*, 119(25):251301, December 2017.

[316] Helvi Witek, Leonardo Gualtieri, Paolo Pani, and Thomas P. Sotiriou. Black holes and binary mergers in scalar Gauss-Bonnet gravity: scalar field dynamics. 2018.

[317] Tsutomu Kobayashi, Masahide Yamaguchi, and Jun'ichi Yokoyama. Generalized G-inflation: Inflation with the most general second-order field equations. *Prog. Theor. Phys.*, 126:511–529, 2011.

[318] Jerome Gleyzes, David Langlois, Federico Piazza, and Filippo Vernizzi. Exploring gravitational theories beyond Horndeski. *JCAP*, 1502:018, 2015.

[319] Jibril Ben Achour, David Langlois, and Karim Noui. Degenerate higher order scalar-tensor theories beyond Horndeski and disformal transformations. *Phys. Rev.*, D93(12):124005, 2016.

[320] Bernard F. Schutz. Networks of gravitational wave detectors and three figures of merit. *Class. Quant. Grav.*, 28:125023, 2011.

[321] Emanuele Berti, Vitor Cardoso, and Marc Casals. Eigenvalues and eigenfunctions of spin-weighted spheroidal harmonics in four and higher dimensions. *Phys. Rev.*, D73:024013, 2006. [Erratum: Phys. Rev.D73,109902(2006)].

[322] *https://www2.physics.ox.ac.uk/contacts/people/tattersall*.

[323] Asimina Arvanitaki, Masha Baryakhtar, Savas Dimopoulos, Sergei Dubovsky, and Robert Lasenby. Black Hole Mergers and the QCD Axion at Advanced LIGO. *Phys. Rev.*, D95(4):043001, 2017.

[324] Richard Brito, Shrobana Ghosh, Enrico Barausse, Emanuele Berti, Vitor Cardoso, Irina Dvorkin, Antoine Klein, and Paolo Pani. Stochastic and resolvable gravitational waves from ultralight bosons. *Phys. Rev. Lett.*, 119(13):131101, 2017.

[325] Richard Brito, Shrobana Ghosh, Enrico Barausse, Emanuele Berti, Vitor Cardoso, Irina Dvorkin, Antoine Klein, and Paolo Pani. Gravitational wave searches for ultralight bosons with LIGO and LISA. *Phys. Rev.*, D96(6):064050, 2017.

[326] Vitor Cardoso, Oscar J. C. Dias, Gavin S. Hartnett, Matthew Middleton, Paolo Pani, and Jorge E. Santos. Constraining the mass of dark photons and axion-like particles through black-hole superradiance. *JCAP*, 1803(03):043, 2018.

[327] Emanuele Berti, Richard Brito, Caio F. B. Macedo, Guilherme Raposo, and Joao Luis Rosa. Ultralight boson cloud depletion in binary systems. 2019.

[328] Huan Yang, Vasileios Paschalidis, Kent Yagi, Luis Lehner, Frans Pretorius, and Nicolas Yunes. Gravitational wave spectroscopy of binary neutron star merger remnants with mode stacking. *Phys. Rev.*, D97(2):024049, 2018.

[329] C.F. Da Silva Costa, S. Tiwari, S. Klimenko, and F. Salemi. Detection of (2,2) quasinormal mode from a population of black holes with a constructive summation method. *Phys. Rev.*, D98(2):024052, 2018.

[330] Richard Brito, Alessandra Buonanno, and Vivien Raymond. Black-hole spectroscopy by making full use of gravitational-wave modeling. *Phys. Rev. D*, 98:084038, Oct 2018.

[331] Hector O. Silva, Caio F. B. Macedo, Emanuele Berti, and Luis C. B. Crispino. Slowly rotating anisotropic neutron stars in general relativity and scalar-tensor theory. *Class. Quant. Grav.*, 32:145008, 2015.

[332] Paolo Pani and Emanuele Berti. Slowly rotating neutron stars in scalar-tensor theories. *Phys. Rev.*, D90(2):024025, 2014.

[333] Andrea Maselli, Hector O. Silva, Masato Minamitsuji, and Emanuele Berti. Neutron stars in Horndeski gravity. *Phys. Rev.*, D93(12):124056, 2016.

[334] Eugeny Babichev, Christos Charmousis, and Antoine Lehebel. Black holes and stars in Horndeski theory. *Class. Quant. Grav.*, 33(15):154002, 2016.

[335] Masato Minamitsuji and Hector O. Silva. Relativistic stars in scalar-tensor theories with disformal coupling. *Phys. Rev.*, D93(12):124041, 2016.

[336] Matthew Giesler, Maximiliano Isi, Mark Scheel, and Saul Teukolsky. Black hole ringdown: the importance of overtones. 2019.

[337] Emanuele Berti and Vitor Cardoso. Quasinormal ringing of Kerr black holes. I. The Excitation factors. *Phys. Rev.*, D74:104020, 2006.

[338] Zhongyang Zhang, Emanuele Berti, and Vitor Cardoso. Quasinormal ringing of Kerr black holes. II. Excitation by particles falling radially with arbitrary energy. *Phys. Rev.*, D88:044018, 2013.

[339] Lionel London, Deirdre Shoemaker, and James Healy. Modeling ringdown: Beyond the fundamental quasinormal modes. *Phys. Rev.*, D90(12):124032, 2014. [Erratum: Phys. Rev.D94,no.6,069902(2016)].

[340] Pedro G. Ferreira, Christopher T. Hill, and Graham G. Ross. Weyl Current, Scale-Invariant Inflation and Planck Scale Generation. *Phys. Rev.*, D95(4):043507, 2017.

[341] Katy Clough, Pedro G. Ferreira, and Macarena Lagos. On the growth of massive scalar hair around a Schwarzschild black hole. 2019.

[342] Christos Charmousis, Marco Crisostomi, David Langlois, and Karim Noui. Perturbations of a rotating black hole in DHOST theories. 2019.